

**IMPACT OF PROCESSING PRIOR TO THERMOMECHANICAL
EXTRUSION OF STARCHY MATERIALS**

By

Linda Lopez

Thesis submitted to the University of Nottingham for the degree of
Doctor of Philosophy

August 2003

Division of Food Sciences
School of Biosciences
University of Nottingham
Sutton Bonington Campus
Loughborough LE12 5RD, U.K.

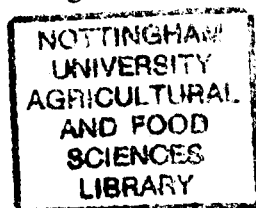


TABLE OF CONTENTS



<u>TABLE OF CONTENT</u>	1
<u>ABSTRACT</u>	6
<u>ACKNOWLEDGEMENTS</u>	8
<u>LIST OF ABBREVIATIONS</u>	9
<u>CHAPTER I</u> <u>INTRODUCTION</u>	10
<u>I.1</u> <u>PROJECT BACKGROUND</u>	10
<u>I.2</u> <u>AIM AND OBJECTIVES</u>	10
<u>I.3</u> <u>THESIS OUTLINE</u>	11
<u>CHAPTER II</u> <u>LITERATURE REVIEW</u>	12
<u>II.1</u> <u>DRY PET FOOD MANUFACTURING</u>	12
<u>II.1.1</u> <i><u>Formulation</u></i>	12
<u>II.1.2</u> <i><u>Dry pet food process</u></i>	14
<u>II.2</u> <u>PARTICLE SIZE REDUCTION</u>	16
<u>II.2.1</u> <i><u>Principles of size reduction</u></i>	16
<u>II.2.2</u> <i><u>Effect of milling on starchy foods</u></i>	20
<u>II.3</u> <u>PRECONDITIONING</u>	21
<u>II.3.1</u> <i><u>Definition and description of preconditioners</u></i>	21
<u>II.3.2</u> <i><u>Objective of preconditioning</u></i>	23
<u>II.4</u> <u>EXTRUSION COOKING</u>	25
<u>II.4.1</u> <i><u>Definition and range of application</u></i>	25
<u>II.4.2</u> <i><u>Extrusion principle</u></i>	26
<u>II.4.3</u> <i><u>Factors affecting extrusion</u></i>	30
<u>II.4.4</u> <i><u>Effect of extrusion on starch containing foods</u></i>	32
<u>II.5</u> <u>STARCH GRANULES CHARACTERISTICS: COMPOSITION AND LOCATION</u>	34
<u>II.5.1</u> <i><u>The starch granule</u></i>	34
<u>II.5.2</u> <i><u>Chemical composition</u></i>	34
<u>II.5.3</u> <i><u>Organisation of the starch granule</u></i>	36

II.6	STARCH PHYSICOCHEMICAL PROPERTIES	38
II.6.1	<i>Starch gelatinisation and gelation</i>	38
II.6.2	<i>Starch conversion</i>	39
II.6.3	<i>Glass transition</i>	42
II.7	AMYLOSE-LIPID COMPLEX: THEIR FORMATION, PHYSICOCHEMICAL PROPERTIES AND RELEVANCE TO THE EXTRUSION PROCESS	43
II.7.1	<i>Amylose-lipid complex characteristics</i>	43
II.7.2	<i>Starch-lipid interactions during extrusion cooking</i>	45
CHAPTER III	<u>MATERIALS AND METHODS</u>	47
III.1	<u>MATERIALS AND MATERIALS PROCESSING</u>	47
III.1.1	<i>Materials</i>	47
III.1.2	<i>Sample preparation technique</i>	50
III.1.3	<i>Twin screw extrusion cooking</i>	52
III.2	<u>METHODS</u>	53
III.2.1	<i>Moisture content determination</i>	53
III.2.2	<i>Expansion, bulk density and extrudates foam structure</i>	54
III.2.3	<i>Rapid Visco Analyser</i>	55
III.2.4	<i>Powder X-ray diffraction</i>	58
III.2.5	<i>Differential scanning calorimetry (DSC)</i>	61
III.2.6	<i>Texture analysis</i>	63
III.2.7	<i>¹H-NMR</i>	65
III.2.8	<i>Particle size distribution</i>	73
III.2.9	<i>Microscopic observations</i>	74
III.2.10	<i>Particle charge detection (PCD)</i>	75
III.2.11	<i>Protein solubility</i>	77
III.2.12	<i>Total soluble sugar content</i>	78
III.2.13	<i>Lipid extraction</i>	78
III.2.14	<i>Free Fatty acid content</i>	79
CHAPTER IV	<u>EFFECT OF GRINDING ON DRY PET FOOD MIX AND EXTRUDATES CHARACTERISTICS</u>	80
IV.1	<u>EXPERIMENTAL SETUP</u>	80
IV.2	<u>EFFECT OF GRINDING ON INDUSTRIAL PREMIXES AND THEIR EXTRUDATES</u> ..	83

<i>IV.2.1</i>	<i>Difference in particle size distribution</i>	83
<i>IV.2.2</i>	<i>Effect on RVA pasting curve an starch properties</i>	86
<i>IV.2.3</i>	<i>Effect on protein solubility and surface charges</i>	90
<i>IV.2.4</i>	<i>Persistence of the effect of grinding after extrusion</i>	91
IV.3	EFFECT ON INGREDIENTS	97
<i>IV.3.1</i>	<i>Comparison of energy dispersed during grinding</i>	98
<i>IV.3.2</i>	<i>Particle size distribution</i>	99
<i>IV.3.3</i>	<i>Pasting / water absorption properties</i>	102
<i>IV.3.4</i>	<i>Protein solubility</i>	106
IV.4	CONCLUSION	107
CHAPTER V	<u>EFFECT OF MODEL BATCH PRECONDITIONING ON MAIZE GRITS AND MAIZE GRITS EXTRUDATES</u>	109
V.1	INTRODUCTION	109
V.2	CHARACTERISATION OF THE TRANSFORMATIONS OF THE RAW MATERIAL OCCURRING DURING PRECONDITIONING	110
<i>V.2.1</i>	<i>Experimental set-up</i>	110
<i>V.2.2</i>	<i>Temperature increase and water absorption in batch preconditioner</i> 112	
<i>V.2.3</i>	<i>Starch conversion during preconditioning</i>	114
<i>V.2.4</i>	<i>Texture changes during preconditioning</i>	121
<i>V.2.5</i>	<i>Water mobility in preconditioned maize grits</i>	124
<i>V.2.6</i>	<i>Interaction with lipids during preconditioning</i>	132
V.3	EFFECT OF PRECONDITIONING ON EXTRUSION	136
<i>V.3.1</i>	<i>Sample preparation</i>	136
<i>V.3.2</i>	<i>Extruder operating parameters and radial die swell</i>	137
<i>V.3.3</i>	<i>RVA pasting curves</i>	137
<i>V.3.4</i>	<i>X-ray diffraction pattern and microscopic observation</i>	138
V.4	CONCLUSION	140
CHAPTER VI	<u>EFFECT OF PRECONDITIONING AND PARTICLE SIZE ON MAIZE GRITS AND MAIZE GRITS EXTRUDATES: PILOT PLANT SCALE STUDY.</u>	142
VI.1	INTRODUCTION	142

<u>VI.1.1</u>	<u>Comparison of model and pilot plant system</u>	142
<u>VI.1.2</u>	<u>Sample preparation and experimental design</u>	144
<u>VI.2</u>	<u>EFFECT OF PRECONDITIONING AND PARTICLE SIZE ON MAIZE GRITS</u>	
<u>PROPERTIES</u>		147
<u>VI.2.1</u>	<u>Moisture and temperature increase in preconditioned maize grits</u> ...	147
<u>VI.2.2</u>	<u>Effect on starch conversion</u>	149
<u>VI.2.3</u>	<u>Bulk material physical properties</u>	155
<u>VI.2.4</u>	<u>Water mobility in preconditioned maize grits</u>	157
<u>VI.3</u>	<u>EFFECT OF PRECONDITIONING AND PARTICLE SIZE ON EXTRUSION OF MAIZE</u>	
<u>GRITS</u>		158
<u>VI.3.1</u>	<u>Effect on extruder operating parameters</u>	158
<u>VI.3.2</u>	<u>Expansion of preconditioned maize grits extrudates</u>	160
<u>VI.3.3</u>	<u>Study of the state of starch in preconditioned extruded maize grits</u> ..	162
<u>VI.4</u>	<u>ANALYSIS OF CORRELATIONS</u>	167
<u>VI.4.1</u>	<u>Analysis of the raw data</u>	167
<u>VI.4.2</u>	<u>Principal component analysis</u>	170
<u>VI.5</u>	<u>CONCLUSION</u>	173
<u>CHAPTER VII</u>	<u>FORMATION OF AMYLOSE-LIPID COMPLEX IN</u>	
<u>EXTRUDED CEREAL-LIPID SYSTEMS</u>		175
<u>VII.1</u>	<u>INTRODUCTION</u>	175
<u>VI.1.1</u>	<u>Background and aim of the study</u>	175
<u>VI.1.2</u>	<u>Sample preparation</u>	176
<u>VII.2</u>	<u>EXTRUSION OF MAIZE GRITS AND LINOLEIC ACID UNDER VARIOUS</u>	
<u>CONDITIONS</u>		177
<u>VII.2.1</u>	<u>Experimental conditions</u>	177
<u>VII.2.2</u>	<u>Extrusion operating conditions and extrudates characteristics</u>	178
<u>VII.2.3</u>	<u>Effect on starch characteristics</u>	184
<u>VII.3</u>	<u>EXTRUSION OF WHEAT FLOUR AND LINOLEIC ACID</u>	192
<u>VII.3.1</u>	<u>Sample preparation</u>	192
<u>VII.3.2</u>	<u>Extruder operation characteristics and extrudates structure</u>	192
<u>VII.3.3</u>	<u>Starch characteristics</u>	196
<u>VII.4</u>	<u>EXTRUSION OF MAIZE GRITS WITH COMPLEX FATS</u>	198
<u>VII.4.1</u>	<u>Sample preparation</u>	198

<u>VII.4.2</u>	<u><i>Extruder operating parameters and extrudates characteristics</i></u>	198
<u>VII.4.3</u>	<u><i>Starch characteristics</i></u>	200
<u>VII.5</u>	<u>CONCLUSION</u>	203
<u>CHAPTER VIII</u>	<u>GENERAL DISCUSSION AND CONCLUSION</u>	204
<u>VIII.1</u>	<u>EFFECT OF PROCESSES PRIOR TO EXTRUSION</u>	204
<u>VIII.1.1</u>	<u><i>Grinding</i></u>	204
<u>VIII.1.2</u>	<u><i>Preconditioning</i></u>	206
<u>VIII.1.3</u>	<u><i>Interactions grinding – preconditioning</i></u>	207
<u>VIII.2</u>	<u>INGREDIENT EFFECTS ON EXTRUSION</u>	208
<u>VIII.3</u>	<u>COMBINED INGREDIENTS AND PROCESS EFFECTS</u>	209
<u>VIII.4</u>	<u>INDUSTRIAL SIGNIFICANCE AND FURTHER WORK</u>	211
<u>BIBLIOGRAPHY</u>	213

ABSTRACT



Dry pet foods are composed of cereal, proteins, fats, fibres and other minor components. The manufacturing process comprises a first step where the dry ingredients are ground to a suitable particle size and blended, a second step where the dry powder is mixed with water and steam in a preconditioner and then extruded and a final step where the product is dried and coated.

The aim of this work was to study the effects of the unit operations prior to thermo mechanical extrusion in the dry pet food process. The study focuses especially on the structure of the final product therefore, after studying a typical pet food recipe, a model system using cereal only or cereals and fats was considered.

The grinding process was shown to impact on the physicochemical characteristics of a pet food premix by affecting the degree of starch damage, the water absorption and water solubility properties or the total charge of the mix. The grinding method was also found to be critical as grinding ingredients together and multiple pass grinding produced more starch damage. The resulting premixes from different grinding methods were affecting the extrusion process and the extrudates characteristics. Extruded mixes with the lowest starch damage, obtained by single pass grinding presented higher expansion than mixes produced by two pass grinding.

Few studies have reported the effect of preconditioning on extrusion, therefore, a model preconditioning apparatus was first built to analyse the effect of residence time and initial moisture on maize grits physicochemical characteristics. The results of this study showed that limited precooking occurs at the preconditioner stage (0 to 80% loss in crystallinity). This precooking reduces water self diffusion coefficient in the particle, as measured by pulse field gradient NMR, decreases powder bulk density and increases powder compressibility. At the highest moisture contents (33% wb) and the highest residence time (240s), maize grits can lose its hydrated powder state and form a viscous paste. The different particle sizes used (from 240 to 476 μm modal

diameter) did not show different behaviours. The effect of preconditioning on extrusion was also studied using the model preconditioner. Results showed that pre-hydration and pre-heating increased homogeneity of the material entering the extruder and reduced the specific mechanical energy (SME). This increased in homogeneity allows a more homogeneous starch conversion in the extruder as no remnant native starch granule was found in the preconditioned sample for 240s.

The results from the model system were then partially confirmed using a pilot plant double-shafted Buhler preconditioner on maize grits of various particle size (330 to 1365 μm modal diameter). The results showed that preconditioning decreases SME but also allows a higher expansion. The SME was negatively correlated with the temperature of the mix immediately after preconditioning (at the extruder inlet) and the compressibility of the preconditioned material. The crystallinity of starch in the end product (V_h or E_h and V_h) was also dependant on the preconditioning treatment. Pre-heating reduced the E_h pattern of the extrudates.

Finally, the interactions between fats and starch during extrusion have also been studied. It has been shown that the levels of free fatty acids in fats commonly used in the dry pet food industry (sunflower oil, beef tallow and poultry fat) can affect markedly the expansion, foam structure and pasting characteristics of extrudates. This was especially correlated to the formation of crystalline complexes between amylose and free fatty acids.

ACKNOWLEDGEMENTS



I would like to thank Masterfoods, U.K., for their financial support and collaboration and Charles Speirs and Nicky Butter for their support and help during the three years of this PhD.

I would like to express my gratitude to Dr Sandra Hill for her supervision and valuable guidance throughout my PhD and Professor John Mitchell for his support and advices.

I would like to thank the Food sciences staff: Phil Glover, Val Street, Mike Chapman, Kath Brasnett, Liz Rogers and Lynn Moseley for their help.

Finally, I would also like to thank my family for their love and care, my friends for their help and support and Mollie just for being a cute cat. And last, but not least, I would like to thank Rutger for sharing his life with me.

LIST OF ABBREVIATIONS



BD	Bulk density
BT	Beef tallow
C18:2	Linoleic acid
Ctrl	Control
db	dry basis
DP	Degree of polymerisation
DSC	Differential scanning calorimetry
FFA	Free fatty acid
FID	Free induction decay
FV	Final viscosity
HC	High cereal
HP	High protein
HTST	High temperature short time
LAM	Lipid complexed amylose
MC	Moisture content
MG	Maize grits
MGL	Maize gluten
NMR	Nuclear magnetic resonance
PCD	Particle change detection
PCi	Principal component i
PF	Poultry fat
PM	poultry meal
PS	Particle size
PT	Pasting temperature
PV	Peak viscosity
RH	Relative humidity
RT	Residence time
RVA	Rapid Visco Analyser
SEI	Sectional expansion index
SME	Specific mechanical energy (kJ/kg)
SO	sunflower oil
T _g	Glass transition temperature
w/w	weight by weight
WAI	Water absorption index
wb	wet basis
WM	Whole maize
WR	Whole rice
WSI	Water solubility index
XRD _i	X-ray diffraction crystallinity index

CHAPTER I INTRODUCTION



I.1 PROJECT BACKGROUND

The pet food industry is a market that has steadily increased throughout the XXth century. The total production of pet food in the U.K. in 2001 was 1.3 million tons, which represented nearly £1.5 billion (source: PFMA).

Dry expanded pet food was first produced in the early 50s and its share of the market has been increasing ever since. Today, the dry pet food type represents a third of the total production of pet food.

Dry pet food formulation is complex but always includes protein sources, carbohydrates sources (providing starch and fibres) and lipids as well as other minor ingredients such as vitamins and minerals. These raw materials are processed by extrusion cooking. Extrusion is widely used in the food industry and has been the subject of many researches in food technology.

This PhD project was co-sponsored by the University of Nottingham and Pedigree Masterfoods to investigate process and ingredients effects on dry pet food characteristics.

I.2 AIM AND OBJECTIVES

The aim of this thesis was to provide a scientific understanding of the effect of single unit operations and ingredients on dry pet food characteristics. Two unit operations occurring before thermo mechanical extrusion have been studied: grinding and preconditioning. These unit operations have been analysed using lab-scale apparatus and industrial scale pilot plant to confirm / infirm the earlier conclusions.

Although the interactions of the different ingredients of a dry pet food mix are discussed, the focus of this thesis was mainly on the starch component and its interactions with lipids.

I.3 THESIS OUTLINE

After a short introduction, published literature in the areas of interest for this work is summarised in Chapter II. The experimental methods used in this study are detailed in Chapter III.

Chapter IV focuses on the study of the effect of particle size and grinding methods on physicochemical characteristics of dry pet food mixes and ingredients, and their effect on subsequent extrusion characteristic.

In Chapter V, the effect of preconditioning was mimicked using an orbital paddle mixer and maize grits. The effects of particle size, residence time and initial moisture content on macroscopic and molecular changes were analysed.

The conclusions drawn from the model study were tested in Chapter VI where maize grits of different particle size and different origin were extruded using various preconditioning regimes.

The following chapter focuses on the effect of added lipids on extrusion, especially on the formation of amylose-lipid complexes and their effect on expansion. This study used model systems with maize grits or wheat flour as a cereal source and linoleic acid as well as commercial fats and oil as a lipid source.

The concluding part, Chapter VIII, discusses the effect of unit operations on extrusion of dry pet food focussing especially on their effect on starch and lipids.

CHAPTER II LITERATURE REVIEW



The aim of this project was to determine, in the dry pet food process, the effect of single unit operations on the characteristics of the raw material after these operations and the overall quality of the final product. The focus was especially on the starch fraction and to a certain extent on its interactions with lipids. Therefore, it was necessary to first describe the dry pet food process (section II.1), and then understand the effect of the different unit operations we focused on, grinding (section II.2), preconditioning and extrusion (section II.3 & II.4).

As this work focused especially on starch, its origin, structure and thermo-mechanical properties are described in section II.5 & II.6 as well as the amylose-lipid complexes physicochemical properties (section II.7).

II.1 DRY PET FOOD MANUFACTURING

II.1.1 Formulation

Dry pet food is formulated in order to provide optimum nutritional balance, functional properties and organoleptic characteristics at a thermal processing cost per ton that is lower than any other processing technique (Rokey 1994).

Dry pet food raw materials include protein, starch, lipid, fibres and other minor constituents like vitamins and minerals.

Dry pet food formulation is complex. It has to take into account the nutritional requirements of the animal (cat or dog) and the processability of the mix. Furthermore, finished product usually contains different kibble types having different

recipe. Therefore, there are no typical formulation but rather an utilisation range for each ingredients / components.

Protein sources are an important constituent of dry pet food; they represent between 25 and 70% of the formulation of a finished product. These protein sources have either a plant or an animal origin. Vegetable proteins include oil seeds, wheat and corn gluten meal. They contribute both to the nutritional and functional properties of dry pet food. Animal proteins include fishmeal, meat and bone meal, blood meal and gelatine. These proteins usually do not contribute to the texture of the final product.

Starch accounts for 5 to 60% of a finished product. It is an important functional ingredient, as it will provide the binding of the different ingredients forming the pet food pellets, but is not well digested by cats and dogs. The origin of starches used in pet foods is mainly cereals (wheat, corn, rice, and barley) but also tuber (potato, manioc).

Fats are important constituents of pet feeds as they provide an excellent energy source. The fat fraction can account for up to 30% of the end product composition. Feed fat sources are animal fats (beef tallow, lard, poultry fat), vegetable and marine oils. Monoglycerides and emulsifiers are also used at low levels (less than 1%) to reduce fat migration during storage.

Fibers are a minor ingredient of dry pet food; they are incorporated especially in special diet feed.

Vitamins, although accounting for only a small part of the formulation, are an important ingredient. Their stability during the extrusion process depends on their solubility and the processing parameters. Other ingredients commonly used in dry pet feed formulation include dyes, palatability enhancer, flavours and humectants.

Table II-1: Typical formulation of dry dog food (From Ockerman (1988))

<i>Ingredients</i>	<i>Percentage (% w/w wb)</i>
Meat and bone soup	15
Animal fat	2.5
Dried skimmed milk	5
Corn, kibbled	25
Oats, rolled	20
Wheat, flakes	25
Wheat germ meal	5
Dried brewer's yeast	1
Dicalcium phosphate	1
Salt	0.5

II.1.2 Dry pet food process

The dry pet food manufacturing process can be divided into four main unit operations: raw material preparation (grinding), preconditioning, extrusion and drying. (Figure II-1).

Raw materials used in dry pet food manufacture such as whole grain cereals and frozen meat, need to be milled into a powder in order to be processed further. Grinding is an important part of the process as particle size of the raw material will affect the texture and uniformity of the final product. It is often desirable to have uniform particle size distribution to prevent segregation during transport and mixing prior to extrusion. Different grinders (often more than one) can be used to obtain the desired particle size, this will be discussed more thoroughly in Section II.2.

The preconditioner is a continuous steam cooker where product moisture and temperature are elevated prior to extrusion. It is used to reduce the amount of cooking required in the extruder itself. The characteristics of the preconditioning operation will be discussed in Section II.3.

Extrusion is the main operation of the dry pet food process; it will cook and generate the texture of the product. In the extruder, temperature, pressure and sometimes moisture as well are increased to achieve the required levels of cooking and

expansion. Extrusion of dry pet food is typically performed at higher moisture than other extrusion cooking processes (Miller 1985). This results in higher energy inputs. Furthermore, abrasive ingredients cause higher wear rate, increasing further the operating cost. Single screw extruders are more often used than twin-screw extruder for manufacturing dry pet food. The principle and effect of extrusion cooking are discussed in details in Section II.4.

The drying operation is used to reduce product moisture content to make it stable upon storage. Acceptable moisture contents for dry pet foods are 8-10%. Dry pet foods are usually processed at barrel moisture content of 22 to 33%, after water flash off this leads to a water content between 18 and 26%, the drying process is therefore necessary. Drying is usually carried out in a conventional conveyor type dryer. Heated air (95-150°C) is applied to the product. The dryer is coupled with a cooler unit to cool down the product to room temperature or below to stabilise the product and enable fat application when required.

Finally, the dried pellets are coated with a mix called baste. This solution is usually made of chicken digest and fat. The coating provides the flavour and enhances the palatability of the finished product.

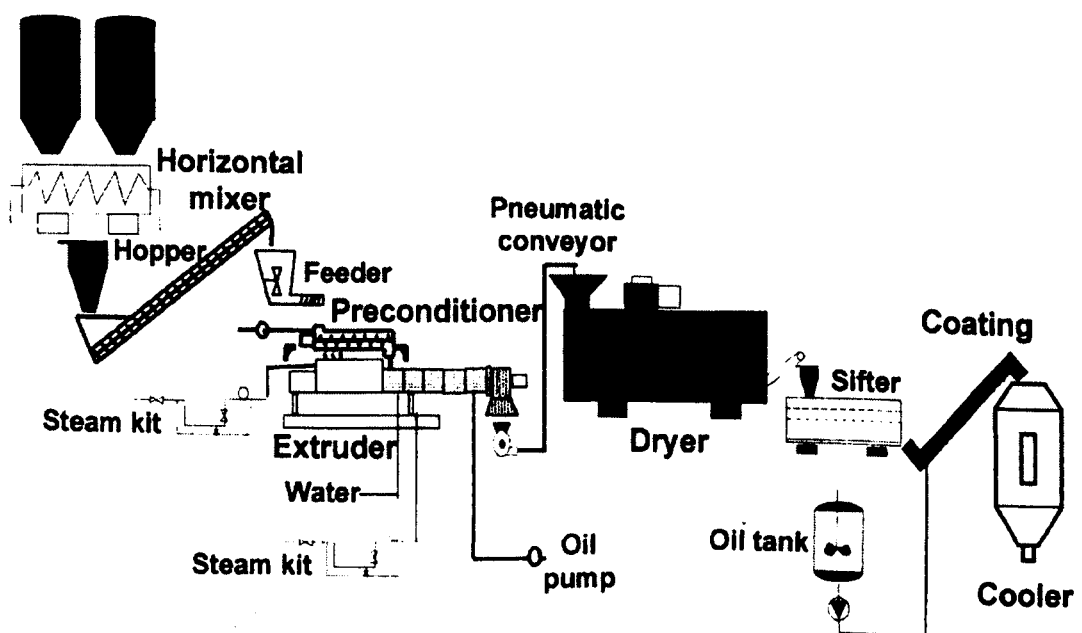


Figure II-1: Flow chart of the dry pet food process (From Bouvier 2000a)

II.2 PARTICLE SIZE REDUCTION

Comminution is the process of reducing particle size. Grinding, crushing, milling are processes used in many industries to (1) decrease the size of solid materials, (2) increase the surface area or (3) free the material from its matrices (Lowrison 1974).

In the pet food industry, grinding of raw materials is the first operation of the production process as represented in Figure II-1. This operation is used in order to reduce the size of the raw material to a powder of suitably small granulation to be extruded. As suggested by Mathew (1999a), mill type and particle size have an important effect on pet food extrudates physicochemical properties.

II.2.1 Principles of size reduction

In the grinding and milling process, the size of particles is reduced by fracturation. Although the mechanism of fracture is not yet fully understood, it is known that in this process, the material is stressed by the action of the mechanical parts of the grinding machine and initially the stress is absorbed by the material as strain energy. When the strain energy exceeds a critical level, which depends on the material, fracture occurs along lines of weakness and the stored energy is released (Figure II-2). Some of the energy is used in the creation of new surface, but most of it is dissipated as heat (Earle 1983).

The energy required in grinding depends mainly on the material's hardness and friability (i.e. its tendency to crack).

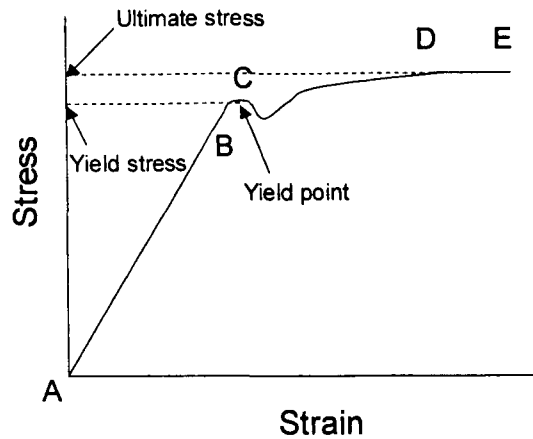


Figure II-2: Stress-strain diagram for a solid. Where AB is the elastic region, CD is the ductile region and E is the breaking point. (From Lowrison (1974)).

Breaking of larger particles will primarily occur at points of weakness such as cracks and joints of agglomeration. With smaller particles, new weakness points must be generated. Since smaller particles contain fewer fissures, their breaking strength is higher. Greater energy is required to initiate new cracks so the energy required for particle breakdown is increasing as particle size decreases.

When a solid particle is stressed below the yield stress (breaking point), elastic deformation occur, the energy stored in straining the particle is lost when the stress is released, this energy is valueless in the comminution process as no breakdown has occurred. Because of this loss of energy and inter-particle friction, the comminution process is extremely inefficient. Only a small proportion of the energy supplied to the machine is actually used in creation of new surfaces. This wasted energy is released as heat as will be discussed later.

Several attempts have been made to determine the theoretical energy required for particle size reduction. A general law suggests that the variation of energy dE required to produce a small change dx in the size of unit mass of material can be expressed as a power function of the size of the material (Equation II-1).

$$\frac{dE}{dx} = -\frac{K}{x^n}$$

Equation II-1

Kick (1885) assumed that the energy required was directly proportional to the size reduction ratio dx/x ($n=1$), whereas Von Rittinger (1887) postulated that this energy was proportional to the change in surface area ($n=2$). Experimentally, for coarse crushing where the increase in surface area per unit mass is relatively small, Kick's law provides a reasonable approximation whereas for fine grinding, Rittinger's law appeared better. Bond (1963) suggested an intermediate law where $n=3/2$. This law fits well data from a wide variety of grinding experiments.

As mentioned earlier, a great part of the energy used during comminution is released as heat. The subsequent increase in temperature of the solids can be detrimental to breaking as the solids may become more rubbery. Biopolymers physical behaviour depends on their glass transition temperature (T_g). As the temperature increases, a polymer in the amorphous glassy state will undergo a phase transition from the glassy to the rubbery state. This transition is particularly characterised by a dramatic decrease in viscosity dropping by several order of magnitudes from more than 10^{12} Pa.s at T_g . T_g depends on the nature and the composition of the material. This will be discussed with more detailed in II.6.2.

To avoid heating up the materials, some machinery use air flow to cool the material down while grinding. Liquid nitrogen can be also used prior to grinding especially in materials where volatile flavour compounds or heat sensitive vitamins are to be preserved.

There are three basic forces used in size reduction as represented in Table II-2. Most machinery will develop more than one type of forces.

Table II-2: Methods of size reduction

<i>Force</i>	<i>Principle</i>	<i>Machine</i>
Compressive	Compression (nutcracker)	Crushing rolls
Impact	Impact (hammer)	Hammer mill
Shear (attrition)	Attrition (grindstone)	Disc attrition mill

Many classifications have been given to distinguish grinding equipment. Mainly comminution machinery can be divided into crushers (where the forces are mostly in compression) and grinders (which uses shear, impact and compressive forces).

Jaw and gyratory crushers are rarely used in the food industry. Crushing rolls are mainly used in the cane-sugar industry. Hammer mills are very versatile and used in various applications such as the grinding of spices, dried milk sugar, etc ... Disc attrition mills are used when fine grinding is required such as in chocolate manufacture or in the wet milling of corn. Tumbling mills such as ball and rod mills are also used for fine grinding

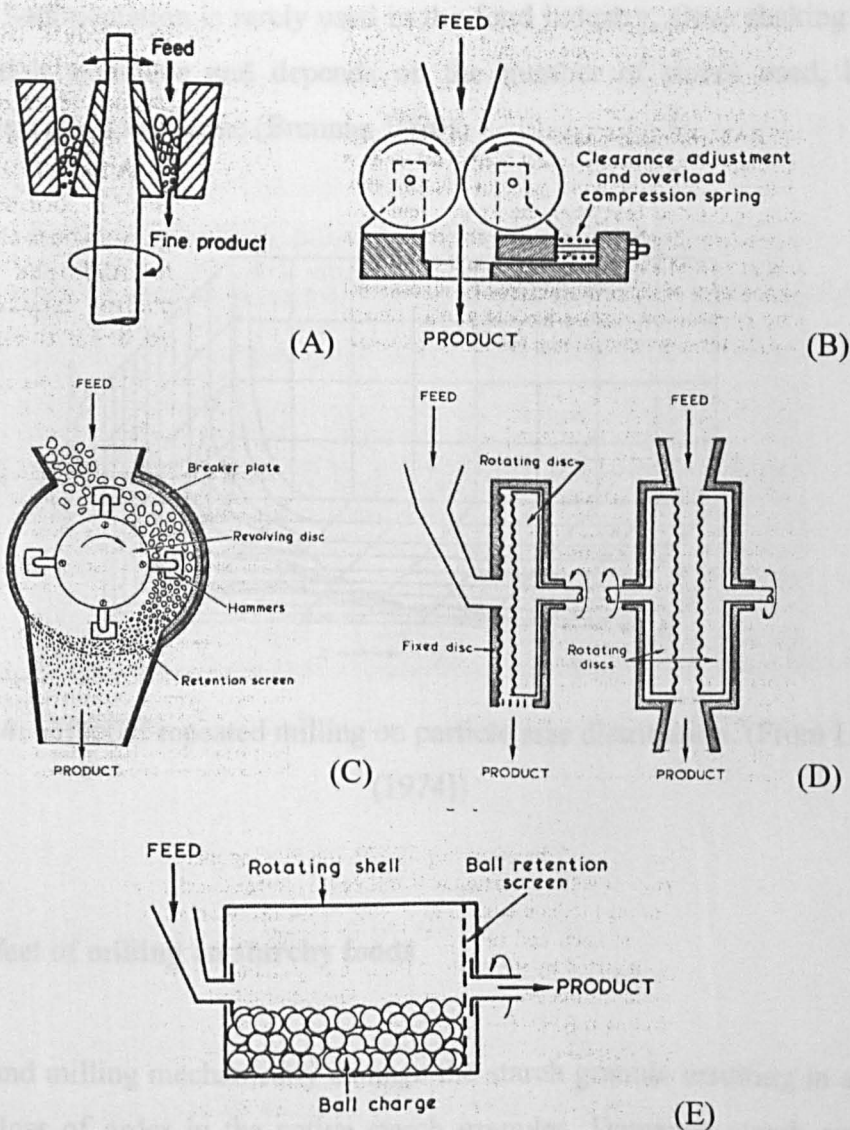


Figure II-3: Different crusher and grinders. A) gyratory crusher, B) crushing rolls, C) hammer mill, D) disc mill, E) tumbling mill (adapted from Brennan (1990) and Earle (1983)).

During the comminution process, solid material breaks into several smaller particles. The size, and to some extent the shape of the product is very much determined not only by the feed material itself but also by the type of mill (Lowrison 1974). At the inlet of the grinder, the bigger particles of the feed material are believed to be more susceptible to breaking than the smaller ones. This leads to a narrowing of the size distribution as represented in Figure II-4.

The measurement of the extent of particle size reduction can be done by sedimentation, observation under microscope, sieve shaking or small angle laser light scattering. Sedimentation is rarely used in the food industry, sieve shaking is often a low-resolution technique and depends on the number of sieves used, laser light scattering is a rapid technique (Brennan 1990).

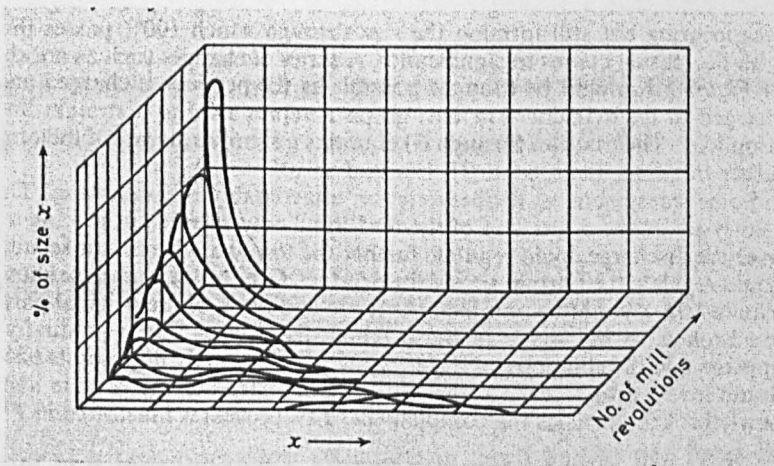


Figure II-4: Effect of repeated milling on particle size distribution. (From Lowrison, (1974))

II.2.2 Effect of milling on starchy foods

Grinding and milling mechanically damage the starch granule resulting in a complete or partial loss of order in the native starch granules. Damaged starch granules are known to absorb more water and to be more susceptible to enzyme hydrolysis. Numerous studies focused on wheat starch due to its relevance for the baking industry. Lelievre (1974) showed that the degree of starch damage was correlated to

the loss of crystallinity in wheat starch. Swelling in undamaged starch granules appears to be restricted by lipid-complexed amylose (LAM) whereas damage starch granules swelling seems unaffected by its LAM content (Tester 1993). Morrison's interpretation is that, when a granule is fractured, free amylose and amylopectin in the amorphous rings of starch are much more exposed due to the creation of fracture areas and therefore absorb water more readily. Furthermore, fracture forces seem to weaken the connections between LAM therefore making them less effective as a network. Tester (1993) also showed that low molecular weight amylopectin fragments were obtained from the soluble fraction of damaged wheat starch in excess water. Tamaki (1998) showed that loss of order, increased enzyme hydrolysis and degradation of amylose occurs during ball milling of maize. Chen (1999) showed that method of milling (wet or dry) and mill type affect the quality of rice flour. Mill type not only affects the particle size of the samples but also particle shape and pasting characteristics as reported by (Becker 2001).

The difference in particle size and mill type can subsequently affect extrusion and the characteristics of the extrudates. This will be discussed in II.4.3.

II.3 PRECONDITIONING

Preconditioning is a unit operation extensively used in the pet food industry where single screw extruders are used. This operation prepares the raw materials in order to facilitate extrusion.

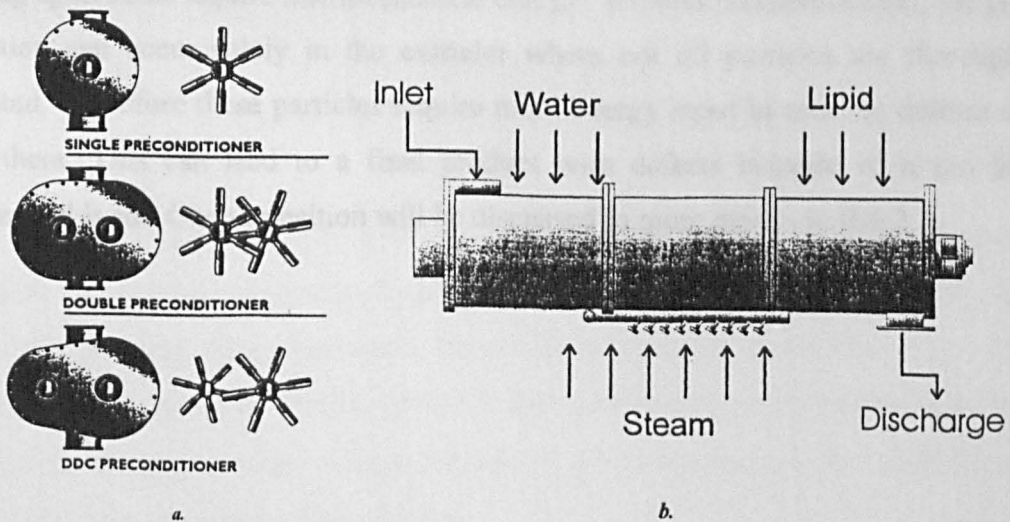
II.3.1 Definition and description of preconditioners

One simple definition of preconditioner has been given by Bouvier (1996): "Preconditioners are used to preheat and pre-humidify raw materials such as flours and grits by mixing them with steam and water".

There are different types of preconditioners. The most common are atmospheric preconditioners. They can be classified into 3 types according to the configuration of the chamber (Figure II-5). Single shaft units have generally a poor mixing and a short retention time (30s). Double shaft preconditioners have either permanently fixed or variable pitch beaters, they mix better than single shaft units and have longer retention times (up to 2 min for a similar output). Differential diameter / differential speed preconditioner are the most performing of all in terms of mixing as well as residence time 2 to 4 min). Their shaft counter-rotate usually as it is the case in the double shaft preconditioner.

Both type of preconditioners are composed of 3 parts: the chamber (or barrel), the shaft and the beaters (or paddles). The paddles can usually be adjusted to provide good conveying and mixing action.

Preconditioners are usually installed above the extruder to feed it by gravity. Water is added in the preconditioner from the top and near the inlet whereas steam should be added from the bottom in order to obtain a good mixing with the dry feed material. Lipids, if required, should be added after water and steam.



Source : Caldwell (2000)

Figure II-5: *a.* Schematic diagram of different types of preconditioners. *b.* different parts constituting a preconditioner.

Other preconditioner designs exist such as the single shafted double barrel preconditioner used in Chapter VI, but these are less common. Pressurised preconditioners have also been developed but are rarely used due to the maintenance cost. In a pressurised preconditioner, the pressure in the barrel reaches about twice the atmospheric pressure and temperatures of 120°C can be obtained. Under these conditions, substantial losses in essential amino acids, such as lysine, might occur (de Muelenaere, 1969).

II.3.2 Objective of preconditioning

The main objective of preconditioning as reported by Caldwell (2000) is to thoroughly hydrate the particles up to the centre in order to obtain a premix that will extrude with less mechanical input. In fact, as illustrated by Figure II-6, preconditioning allows the particles to hydrate therefore lowering their glass transition temperature and by heating them by steam some particles will pass into the rubbery state.

Because of the lower viscosity of polymers in the rubbery state, deformation and melting upon shear require less mechanical energy. Without preconditioning, the glass transition can occur solely in the extruder where not all particles are thoroughly hydrated. Therefore these particles require more energy input in order to deform and melt them. This can lead to a final product with defects because of a too high mechanical input. Glass transition will be discussed in more details in II.6.3.

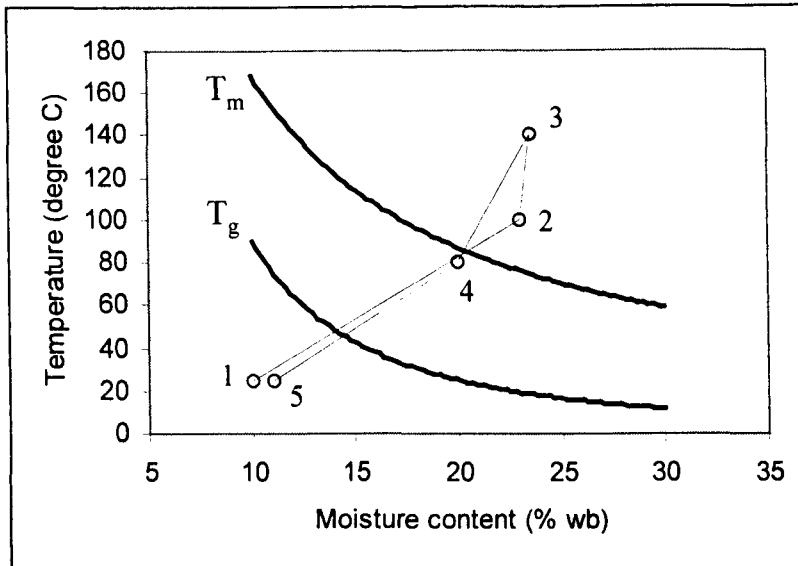


Figure II-6: Process diagram superimposed with state diagram of a pet food recipe. 1- raw mix, 2- mix after preconditioning, 3- mix inside the extruder, at the die, 4- mix at the extruder outlet, 5- extrudate after drying (Adapted from Strahm (1998))

A chemical engineering approach to preconditioning attempts to determine the flow behaviour of particles in the preconditioner as a function of different operating parameters. This approach aims at determining the efficiency of the process in pre-hydrating and pre-heating the dry mix. As has been highlighted by Levine (1995), the flow of powder material in preconditioner or paddle mixer is not simple. This complexity lies in the fact that particulates, unlike fluids, are not a continuum.

A force exerted on a fluid by a moving device is transmitted throughout until a boundary (a wall) is encountered. This results in each part of the fluid moving. Whereas, under the same conditions, only a finite region of the powder will move. The explanation given by Levine (1995) is that powders move only by failure along slip planes. These planes are defined by regions where the shear stress exerted on the powder exceeds the powder's yield stress.

A practical method to determine flow behaviour in a preconditioner is by using the method of evaluating the residence time and residence time distribution (Levine 2002; Bouvier 1996). Residence time distribution reflects both axial and radial mixing. Axial mixing is associated with water uptake of the particles but when too high, it also

results in increased spreading on the residence time distribution therefore leading to particles with different characteristics. Radial mixing provides blending (Levine 2002).

Unfortunately, there is nowhere in the literature a precise account of the transformations occurring during preconditioning and factors affecting them. Only Mathew (1999b) mentioned the effect of preconditioning in a pet food application.

II.4 EXTRUSION COOKING

II.4.1 Definition and range of application

The extrusion process may be defined as “forcing a pumpable product through a small opening to shape materials in a designed fashion” (Heldman 1997).

The first food application of the single screw extruder was the continuous pasta press in the 1930s. The screw worked to mix the semolina with water and additives and forced the dough through specific dies to obtain different shapes of pasta. A wide range of food products is produced by extrusion as shown in Table II-3.

Table II-3: Some typical food products produced by extrusion. (Source: Heldman (1997))

Pasta
Precooked and modified starch
Ready to eat (RTE cereals) <i>Puffed cereals, shredded cereals, etc.</i>
Snack products <i>Corn curls, puffed snacks, crisp breads, co-extruded products, etc.</i>
Pet foods <i>Dry, semi-moist</i>
Confectionery products <i>Liquorice, toffee, caramel, peanut brittle</i>
Texturized proteins <i>Meat analogs, fish paste (surimi)</i>

II.4.2 Extrusion principle

The residence time in the extruder is very short (5 to 10s) that is why extrusion cooking is often called a HTST process (high-temperature, short-time) as it is represented on Figure II-7.

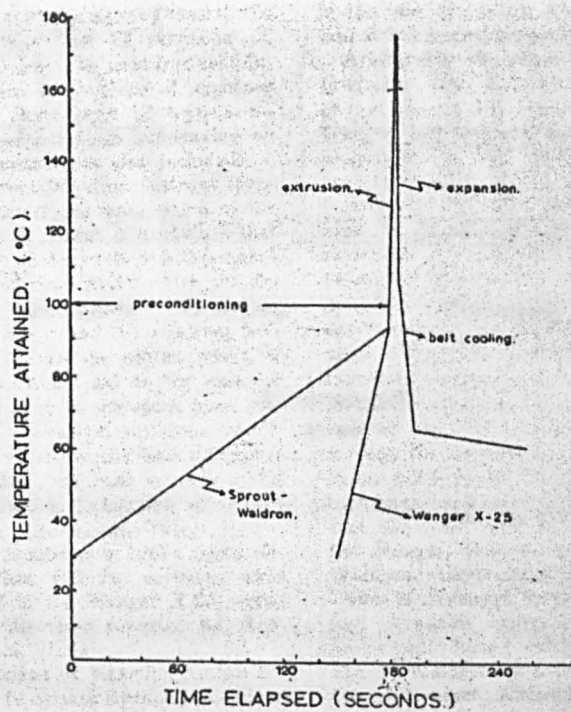


Figure II-7: Idealised time - temperature relationship for extruded degerminated corn with two types of preconditioner – extruder system (Sprout-Waldron high pressure steam preconditioner or Wenger X25 atmospheric pressure preconditioner, both systems using a single screw extruder) (From: de Muelenaere and Buzzard (1969)).

Mainly 2 types of extruders are in use in the food industry: single or twin screw extruders.

Single screw extruders are relatively inexpensive but don't offer the various possibilities of twin-screw extruders. They are often used in combination with preconditioners when more flexibility is required.

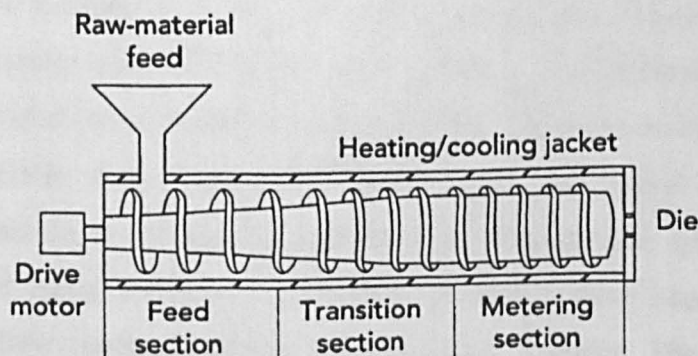


Figure II-8: Schematic diagram of a single screw extruder. (Source: Heldman (1997))

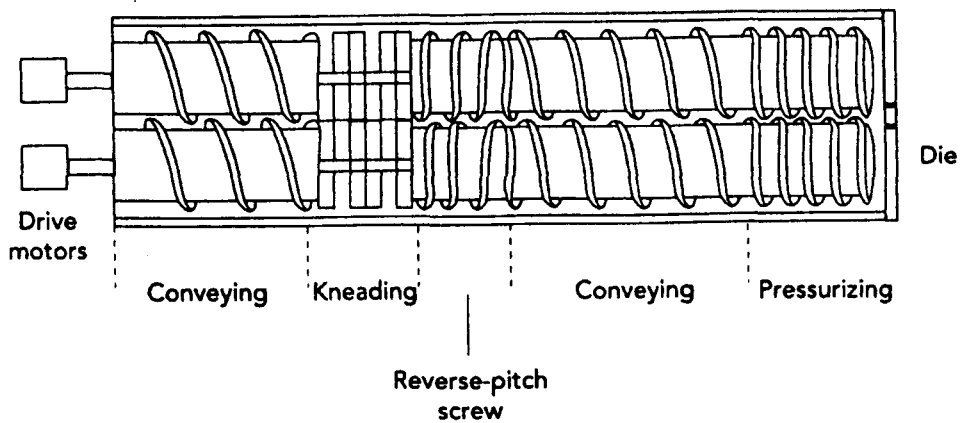


Figure II-9: Schematic diagram of a twin screw extruder (From: Heldman (1997)).

Both extruders use the same principle. The screw(s) are rotating inside a cylindrical barrel conveying the material to the end part of the extruder where it exits through a small orifice, the die. The extruder can be divided into several sections. In the first section the material is conveyed and eventually mixed with water or other ingredients. The second session is a transition between the feed section and the end section. Here, the material starts to undergo transformations: cooking occurs as well as an increase in pressure. The material, initially in a powder form starts to melt and form a viscous liquid. In the last section, the screws lead the product to the outlet die and the build-up of pressure increases.

Heat is transferred to the dough through 3 possible mechanisms: viscous dissipation of mechanical energy, heat transfer from steam or electrical heaters surrounding the barrel or direct injection of steam in the extruder barrel.

The single screw extruder is limited primarily because of its inability to transport sticky and / or gummy material (Hauck 1989). In this type of apparatus, the transport is based on frictional forces between the material and the barrel walls. For some raw materials, especially those with high lipid content, the barrel wall produces insufficient resistance to prevent the product from slipping thus spinning with the screw instead of being conveyed. A number of models have been developed to understand the flow characteristics in a single screw extruder. The flow has been described as a combination of drag and pressure flow as represented in Figure II-10.

The drag flow is due to the pumping action created as the edge of the screw forces the fluid adhering to the barrel wall and slipping freely from the root of the screw (Figure II-10). The pressure flow is in the reverse direction as it is due to the built up of pressure at the extruder die. In the extruder, the velocity profile depends on the operating conditions and primarily the extent to which the outlet is open. The throttling factor, a , is defined as the ratio of pressure to drag flow (Harper 1981). When a is zero (extruder discharge completely open), there is no pressure build-up and the pumping efficiency is high. At the opposite, when $a=1$ (extruder completely closed) there is no pumping action and the product simply mixes within the extruder.

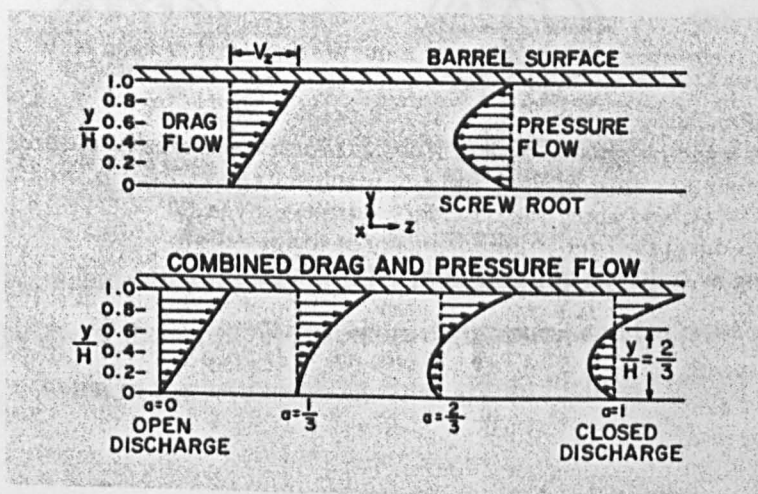


Figure II-10: Velocity profile in a single screw extruder. (From Harper (1981)).

In a twin-screw extruder various barrel and screw designs allow more option as well as more complexity in operation. The 2 screws can be counter rotating or co-rotating and either intermeshing (i.e. overlapping) or not intermeshing. The screw elements can have various configuration size and orientation of the pitch. Non-intermeshing types are rarely used in the food industry and counter-rotating intermeshing are used only for low viscosity materials such as slurries and solubilising sugars (Fichtali 1989). In co-rotating twin screw extruders, the combined flights produce a passage allowing the material to transfer from the channel of one screw to the next (Figure II-11). This prevents pressure build up and produces a self cleaning action therefore preventing material from sticking to the screw which could lead to the scorching of heat sensitive material. Co-rotating twin screw extruders also have a lower degree of positive conveying action due to significant amount of back leakage along the screw.

This also allows a better mixing capability and therefore better product homogeneity than with other extruder types. Co-rotating intermeshing twin screw extruder are the most used system in food extrusion thanks to their flexibility, good mixing characteristics, decreased wear, and high shear rates and throughput.

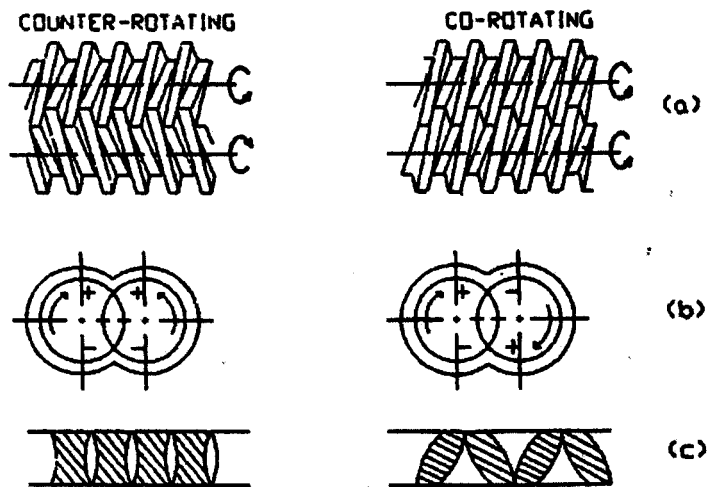


Figure II-11: Schematic diagram of fully intermeshing counter- and co-rotating extruder. (a) view of the screw, (b) pressure distribution and (c) cross section of the flights in the intermeshing zone. (From Fichtali (1989))

II.4.3 Factors affecting extrusion.

Various models have been developed to understand the heat transfers and the flow behaviour inside an extruder. However, these properties are very difficult to characterise accurately because of changing conditions in the extruder barrel. Particularly in the case of starchy material where the starch melts upon cooking and shear thus changing significantly its rheological behaviour. Different factors are affecting the extruder operations and the characteristics of the extrudates.

One of the most critical parameters affecting extruder operation and characteristics of the extrudate is the moisture level in the mix. The amount of water in the barrel will primarily influence the glass and melt transition temperature of biopolymers and therefore affects the viscosity of the melt and subsequently the amount of mechanical energy dispersed in the extruder. Moisture not only influence the conditions in the

extruder, but is also a determining factor in the degree of expansion of the material at the exit of the extruder as it has been demonstrated by Fan (1994). Finally, addition of moisture also decreases the abrasiveness of the feed material therefore decreasing the level of barrel wear (Hauck 1989).

The composition of feed is another factor influencing extruder operation. Different grains have different rheological properties. But even similar grain types might have different effect if their composition is different (Chinnaswamy 1988).

The effect of pH on extrusion has also been extensively studied. The pH might have an effect by enhancing Maillard reaction or by influencing the state of the proteins (Heldman 1997). The pH especially influences the degree at which protein can unfold and crosslink by forming disulphide bonds.

Finally, the particle size distribution is also critical and has been studied by many authors (Chen 2000; Desrumaux, 1998; Carvalho, 2001; Ryu 1988; Mathew 1999a).

Ryu (1988) found that the expansion of rice extrudates decreased as the particle size decreased and led to a more uniform internal cell distribution. Garber (1997) found that SME was lower for extrusion of maize grits of higher particle size.

Not only particle size has an effect on extrusion, but mill type also affects the characteristics of the extrudates. Mathew (1999a) showed that the volumetric expansion index (VEI) of extrudate from pin-milled samples was lower than that of extrudate from the same corn ground in a hammer mill or roller mill.

The characteristic of ingredients used in the extruder are not the only factor affecting extrusion, as the operating condition of the extruder itself might affect critically the extrusion.

Feed rate and screw speed are two parameters to take into account when determining the specific mechanical energy (SME) encountered by the melt in the extruder. SME has been correlated to increase fragmentation of starch, increased expansion (up to some limit) (Lai 1991). The screw geometry, the die configuration as well as the

barrel length are also to be taken into account as they affect critically the residence time of the melt in the extruder.

II.4.4 Effect of extrusion on starch containing foods

One of the main transformations occurring in the extruder is starch conversion. High temperature and high shear in the extruder lead to the disruption of the starch granule and the melting of starch in a limited water environment. The granular and crystalline structures of starch progressively disappear in the extruder (Colonna 1983). Although starch granule may survive extrusion under high moisture low temperature treatment, their structure is progressively disorganised, as the mechanical energy input increases (Guy 1988). The starch content does not change during extrusion as shown by Colonna (1984). But macromolecular degradation does occur and is dependent on the extruder parameters. This molecular degradation has been shown using intrinsic viscosity and gel permeation chromatography (Mercier 1979; Colonna, 1983). Fragmentation is believed to occur randomly breaking $\alpha(1-4)$ bonds in both amylose and amylopectin resulting in decrease in molecular weights (Colonna 1984). Brummer (2002) used a system analytical model to determine independently the effect of mechanical energy and thermal energy on corn extrudate molecular weight. They found that SME was solely responsible for the decrease in average molecular weight, only when temperature was increased above 180°C did the thermal energy have an influence on the reducing power of the extrudate (i.e. the formation of small molecules with DP smaller than 6).

Increase in water absorption and water solubility, cold paste viscosity and enzyme digestibility also occur during extrusion of starches (Whalen 1997; Lai 1991; Guy, 1988; Colonna 1989; Becker 2001; Carvalho, 2001).

When the melt exits the die, water vaporises (flashes off) and cools the extrudates. The melt therefore falls below the glass transition temperature and a foam-like material is formed. Different factors influence the expansion and consecutive shrinkage of the extrudate. This has been extensively studied (Alvarez-Martinez 1988; Cai 1993; Fan 1994; Padmanabhan 1989). Extrudate expansion is usually described as

a longitudinal and a sectional component. Radial die swell is a function of inertial, surface tension, wall slip, thermal effects, melt rheological properties and moisture effects. Expansion is always followed by shrinkage as the extrudate cools down (Figure II-12). Fan (1994) modelled the foaming process involved in cereal extrusion and found that T_g is an important parameter affecting expansion of puffed cereals. T_g will affect the amount of mechanical energy in the extruder but also the viscosity of the dough exiting the extruder and therefore the rate of bubble growth and shrinkage. Overall, it appears that expansion is favoured by high levels of starch conversion (high degree of fluid integrity), low viscosity (lower resistance to bubble growth) and high temperature (high driving force).

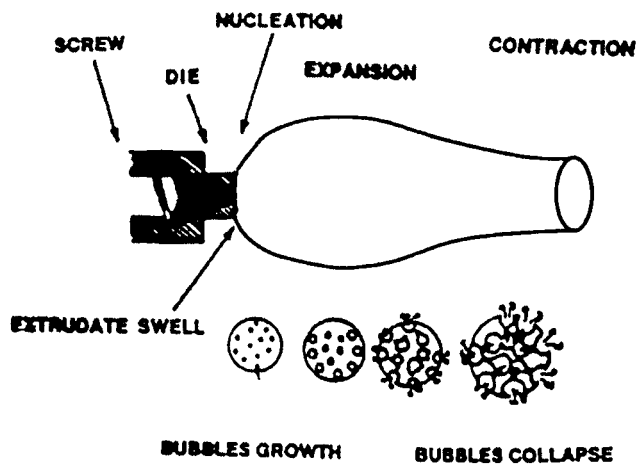


Figure II-12: Schematic diagram representing bubble growth in extrudates at the die of the extruder. (From: Fan (1994))

Another phenomenon occurring during extrusion is the formation of amylose-lipid complex. This has been thoroughly studied by several authors and will be discussed in section II.6.

II.5 STARCH GRANULES CHARACTERISTICS: COMPOSITION AND LOCATION

II.5.1 The starch granule

Starch is a form of stored energy found in amyloplasts in cereals and other higher plants (Hoseney 1994). It is synthesised in granular form and is especially abundant in grains although it can be found as well in roots, tubers, pollen, leaves and stems.

The starch granule size varies between 1 and 100 μ m and its shape varies from polygonal to almost spherical according to the species.

Table II-4: Morphological feature and amylose content of starch granules in cereals used during this study (From Buleon (1998)).

<i>Source</i>	<i>Amylose content</i> (% total starch)	<i>Size (μm)</i>	<i>Shape</i>
Maize (wild type)	25-28	30	Polyhedral and rounded
Wheat (wild type)	25-29	30	Disc
Rice		3-8	Polygonal

It was also shown that many starches such as maize, wheat, millet or sorghum have surface pores (Fannon 1993; Fannon 1992). These pores can affect the efficiency of enzymatic attacks as well as the speed of hydration of starch granules. Therefore, these pores might be of great importance for preconditioning.

II.5.2 Chemical composition

Starch is formed of two polymers of D-glucose monomers: amylose and amylopectin. Common starches contain 20 to 30% amylose and 70-80% amylopectin.

Amylose is a linear polymer formed of glucose units linked by α -1-4 bonds. Its molecular weight is around 250,000 but varies widely between as well as within species (Hoseney 1994).

Amylopectin is a branched polymer. Its backbone is formed by α -1-4 linked glucose and smaller chains of α -1-4 monomers branched by α -1-6 bond (Figure II-13). As opposed to amylose, amylopectin is a huge molecule with a molecular weight up to 10^8 . The basic organisation of the molecule is organised in A, B and C chains. A types are linear chains of α -1-4 linked glucose, B are branched chains of α -1-4 and α -1-6 linked glucose and C chains are identical to B chains but contain as well the reducing terminal group (Figure II-13).

The respective structure of amylose and amylopectin provide the molecule with different physicochemical properties. The long linear nature of amylose gives it the ability to form a helix where the central cavity is hydrophobic. This forms a perfect environment for complexation with iodine, organic alcohols or acids. Because of its linear structure, this molecule has a strong tendency to self-associate in solution and readily crystallises. Amylopectin, on the contrary, is stable in dilute solution and is less favourable to complexation.

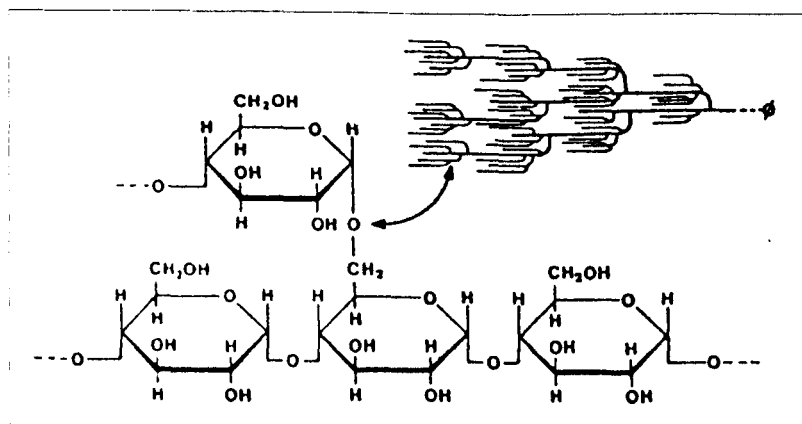


Figure II-13: Schematic representation of amylopectin (From: Zobel (1988)).

Other minor components are also present in the starch granule. They include a small amount of lipids, low levels of minerals, phosphorus and nitrogen from proteins.

II.5.3 Organisation of the starch granule

The high degree of molecular order in starch can be shown by the birefringence exhibited by the granule when observed in polarised light. All starch granules present a typical Maltese cross.

Starch is a semi-crystalline material. Native starches exhibit two types of X-ray diffraction pattern. Cereal starches mostly exhibit the A-type whereas tubers exhibit B-type. Legumes usually present a mixture of A and B sometimes referred to as C-type pattern. The A and B structure are based on 6-fold left handed amylose double helices with a pitch height of 2.08-2.38 nm (Buleon 1998) as represented in Figure II-14.

V-type crystals can be observed as well but these are not observed for the granules, they are due to the formation of amylose single helices with compounds such as iodine, alcohol or fatty acid. This structure will be discussed in section II.7.

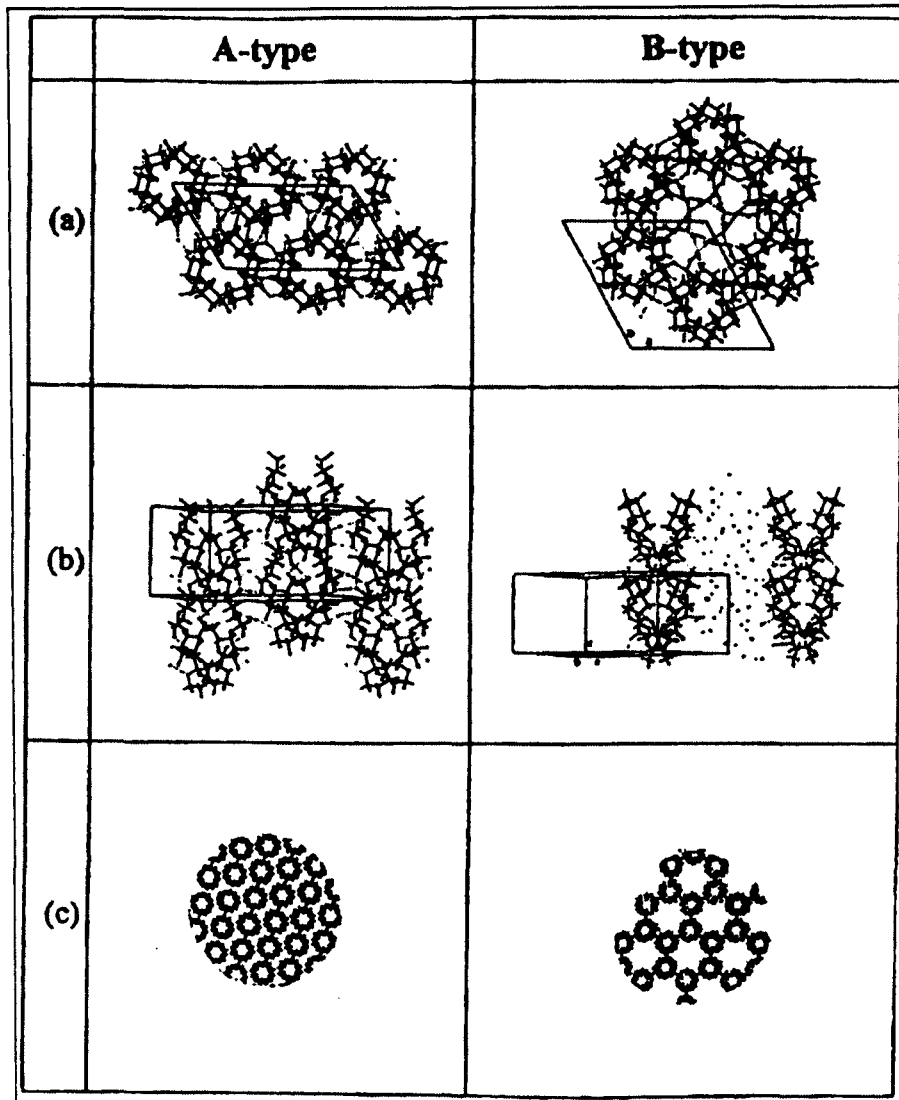


Figure II-14: Structure of the A and B starch polymorph (From Farhat (1996))

- (a) the projection onto a,b-plane. The hydrogen bonds are indicated in broken lines and the water molecules in dark circles (Imberty 1991)
- (b) as viewed along the fibre axis in c-direction (Imberty 1991)
- (c) as wider view on the projection onto a,b-plane (Grenat 1993)

The starch granule organisation is complex. It is accepted that the general orientation of the polymer chains in the granules is perpendicular to the growth rings. The ultrastructure of starch is formed by alternating amorphous and crystalline layers from 120 to 400 nm thick. The crystalline shell itself is believed to be a regular succession of amorphous and crystalline lamella (French 1984). The amylopectin is believed to support the main framework. The position of amylose in the granule is not very well known. Blanshard (1979) has shown that it can be associated to amylopectin or can

form complexes with native lipid. In the latter case, Morrison (1995) showed using solid state NMR that these complexes are native and amorphous: the chains are involved in separate inclusion compound or arrangements of a too limited extent to show the V_h -type diffraction pattern.

The distribution and dynamic state of water within starch granule are less well researched. Tang (2000) showed that beside extra granular water three intra granular water population could be observed in potato starch. Two water populations were associated with the amorphous and the crystalline growth ring respectively. Whereas the third type, not observed in A-type maize starch, was assigned to channel water corresponding to orientationally ordered water in the hexagonal channel of B-type amylopectin.

II.6 STARCH PHYSICOCHEMICAL PROPERTIES

II.6.1 Starch gelatinisation and gelation

Although, in its native state starch is a highly ordered material, most of its uses in the food industry include mechanical, hydrothermal and/or enzymatic treatment which partially or fully destroy its crystalline structure (Colonna 1992).

Starch gelatinisation is the loss of order occurring in starches when heated in excess water (Zobel 1988). When starch granules are placed in excess water and heated, swelling can be observed as the granule is absorbing water, at this stage the process is still reversible. But, when temperature is increased above the gelatinisation temperature, the swelling increases while a loss of order is observed. This stage is irreversible, a further increase in temperature leads to rupture of the granules and leaching of solubilised polymers in the solution. This phenomenon is summarised in Figure II-15.

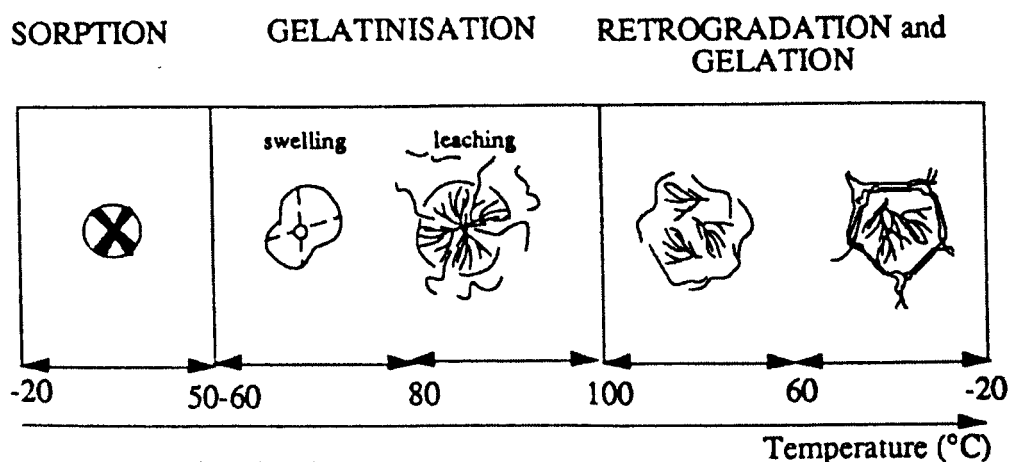


Figure II-15: Thermal transition of starch in excess water. (From Colonna (1992))

The gelatinisation transition occurs usually in the temperature range of 50-70°C Colonna (1992) and varies between species and degree of starch damage. The loss of order can be measured by birefringence, X-ray crystallinity as well as differential scanning calorimetry. At a molecular scale, the hydrogen bonds between linear segment in the crystallites are broken corresponding to the melting of crystallites and conformational changes of starch macromolecules. These events are both endothermic.

Gelatinised starches are highly unstable structures. During storage, the molecules reassociate to form a viscoelastic paste or, at sufficiently high concentration (>5%), an elastic gel. On cooling, gelation of amylose occurs first over a short time whereas amylopectin recrystallisation occurs over longer periods (days, weeks, months). This phenomenon is named retrogradation (Hoover 1995).

II.6.2 Starch conversion

Starch conversion is a term first used by Mitchell (1997) and his research team to describe the transformation occurring in starch during processing. This includes thermal and/or mechanical treatment in excess or limited water environments.

Starch conversion describes the loss of order followed by loss of granule integrity, depolymerisation of polysaccharides and complexation between amylose and lipids. Numerous studies have followed the melting of crystallites in starch at various water contents using DSC. The pioneering work by Donovan (1979) showed in potato that at water concentrations above 60%, a single endotherm was observed. However, below this water concentration, multiple endotherms were observed, suggesting that in low moisture condition the starch granules behave differently (Figure II-16). The interpretation for this behaviour is not clear (Biliaderis 1992). Evans (1982) suggested that least stable crystallites melt first (endotherm M1) and as they unfold absorb more water therefore reducing the effective solvent concentration for the remaining granules thus melting at higher temperature. Biliaderis (1992) on the contrary propose that the multiple melting is a reflection of melting and reorganisation processes occurring simultaneously.

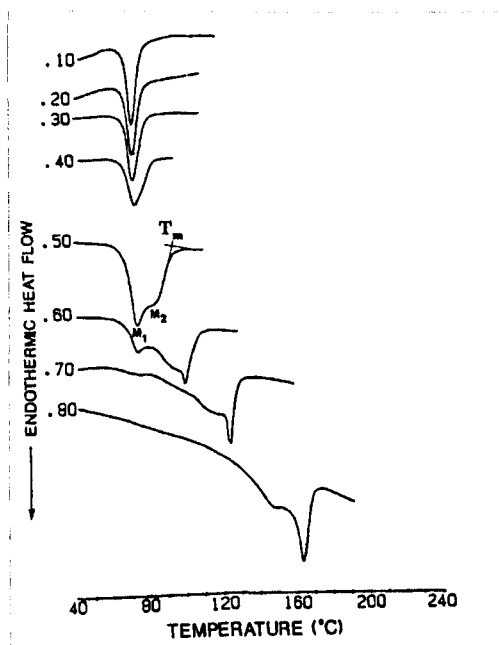
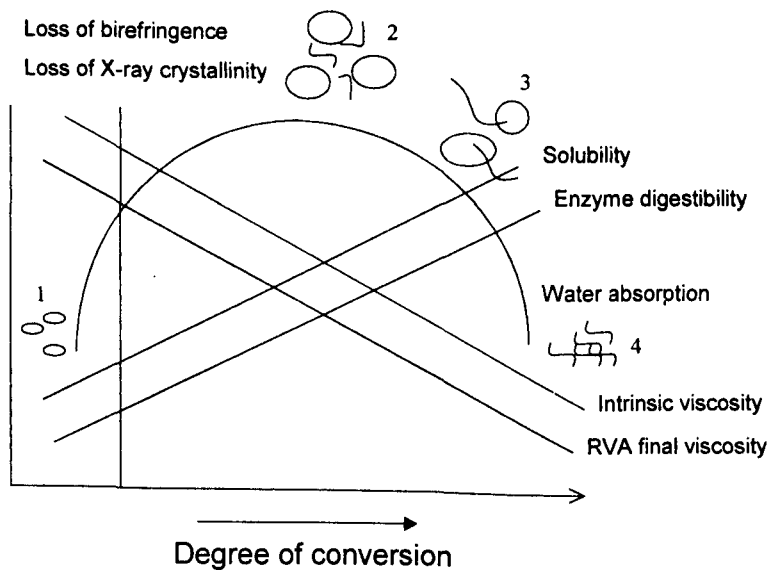


Figure II-16: Melting profiles of waxy rice starch at various weight fractions of solids.
(From: Biliaderis (1992))

Annealing represents the physical reorganisation of starch granules when heated in water at a temperature between T_g and the onset of gelatinisation, with retention of the granular structure. Annealing leads to elevation of starch gelatinisation

temperature and sharpening of the gelatinisation range (Tester 2000). The molecular transformations occurring during annealing are the subject of numerous studies (Le Bail 1999; Andreev 1999; Karkalas 1995). Tester (2000) describe the phenomenon as hydration and swelling on the amorphous regions, which facilitate ordering of the double helices in the crystalline regions hence producing “perfected” crystals.

Several techniques are commonly used to determine the degree of starch conversion. These include observation under polarised light (birefringence), X-ray diffraction and DSC. Starch conversion, however, can go beyond the loss of molecular order and other techniques are necessary to describe these changes as it is represented on Figure II-17.



- 1: Intact granule
- 2: maximally swollen granules
- 3: Swollen granules + soluble polysaccharides + granule breakdown
- 4: polymer debranching: reduction of molecular weight

Figure II-17: Simplified representation of analysis techniques commonly used to describe the degree of starch conversion (Adapted from Becker (2001)).

II.6.3 Glass transition

Slade and Levine (1991) defined the glass transition as an amorphous supercooled liquid of extremely high viscosity (between 10^{10} and 10^{13} Pa.s). The concept of glass transition comes from the synthetic polymer field and has been only recently been applied to food systems.

The glass transition behaves like a second order transition with discontinuity in the thermal and calorific properties. Different theories describe the glass transition phenomenon. According to the free volume theory, for molecules to change their conformation or motional state, they must be able to move into the free volume. As the temperature increases above T_g and into the rubbery state, the free volume increases resulting in an increase in molecular mobility (Blanshard 1993).

The glass transition temperature is very sensitive to the amount and the nature of the diluents (Karel 1993). The variation of T_g of wheat starch with moisture content is represented on Figure II-18.

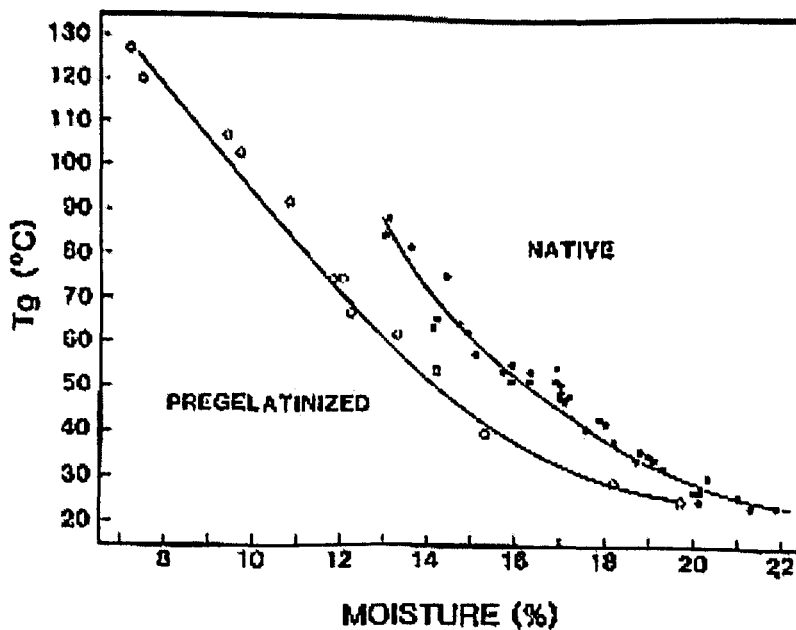


Figure II-18: Glass transition temperature of native and pre-gelatinised wheat starches as a function of moisture (Hoseney 1994).

II.7 AMYLOSE-LIPID COMPLEX: THEIR FORMATION, PHYSICOCHEMICAL PROPERTIES AND RELEVANCE TO THE EXTRUSION PROCESS

II.7.1 Amylose-lipid complex characteristics

Amylose has the property to form complexes with a large number of polar and non-polar organic compounds such as alcohol and organic acids (Takeo 1973). This phenomenon has been particularly studied with regards to lipids (monoglycerides and fatty acids) complexation with starch.

The complex consists of a left-handed single helix of amylose with 6 or sometime 7 glucose per turn. Le Bail (1999) proposed a model for a low energy conformation of fatty acid complex as represented on Figure II-19.

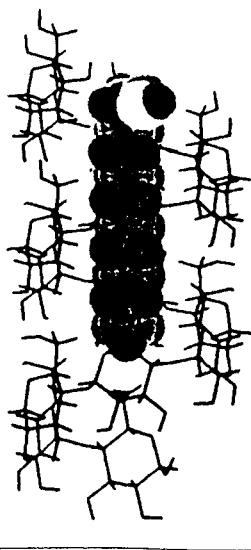


Figure II-19: Low energy conformation for the fatty acid/V-amylose complex (From: Godet (1993)).

Crystalline amylose-lipid complexes present a typical X-ray diffraction pattern characterised by two peaks at $2\theta=13^\circ$ and 19.8° . Another diffraction pattern, the E-type, can be also associated with crystalline amylose-lipid complex and is

characterised by peaks at 12° and 18.3° (Figure II-20). This form corresponds to a metastable form and can be irreversibly transformed to a V-type structure upon re-hydration (Colonna 1989).

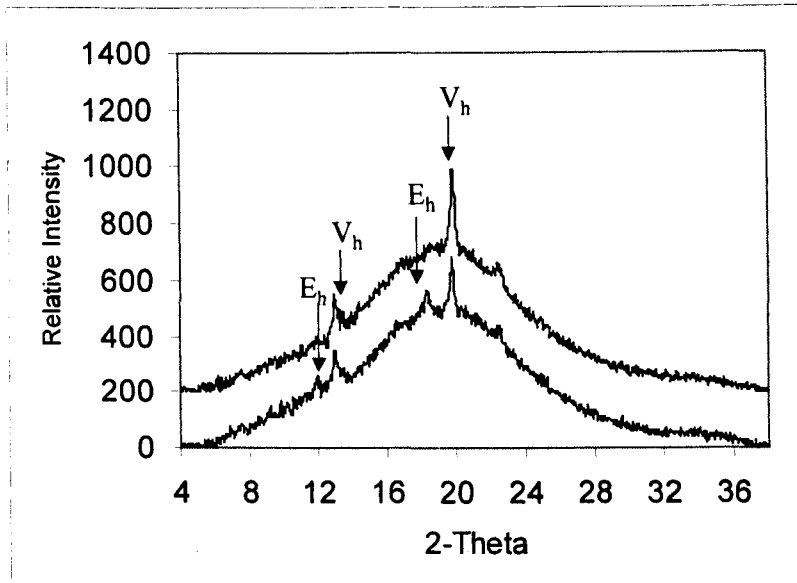


Figure II-20: X-ray diffraction pattern of extruded maize grits exhibiting both V_h and E_h pattern (own data).

Morrison (1993) showed using solid state NMR that amylose-lipid complexes were present in native maize, rice and oat starches. In this state, they did not present a crystalline structure detectable by wide angle X-ray diffraction.

The factors influencing the complexation include water and thermal conditions (Le Bail 1999), type of lipid, pH and availability of amylose (Hahn 1987).

The use of synchrotron X-ray diffraction by Le Bail (1999) showed the evolution of the complexation in maize starch with native lipids. In excess water, complexation occurs only when the gelatinisation is fully completed, whereas in limited water (19-35% wb), the appearance of the typical V_h pattern occurred before completion of the gelatinisation. At high temperatures (170°C), the V_h structure was transformed to the E form.

Numerous researches used DSC to study the dissociation of amylose-lipid complexes. (Biliaderis 1986; Jovanovich 1999; Kugimiya 1980). Karkalas (1995) showed using

amylose and fatty acids in excess water, three possible polymorphs. Type I polymorph was formed below 60°C and had a dissociation temperature in the range 96-104°C. This polymorph is non crystalline. Type IIa and IIb are both crystalline polymorphs. They are formed at higher temperature (>90°C) and have a dissociation (melting) temperature in the range 114-121°C and 121-125 respectively. Type IIb corresponds to the annealed form of type IIa.

In the food industry, complexation of amylose with monoglycerides such as emulsifiers or with fatty acids is of interest in starch containing food as it can affect their functional properties. For example, in bread making, lipids are used as modifiers to retard the staling process (Krog 1970)

II.7.2 Starch-lipid interactions during extrusion cooking

Although most studies report that complexation is impossible with bulky compounds such as triglycerides, Ho (1992) reported some evidence for some interactions with starch and proteins.

Mercier (1980) showed that no complexes were formed between manioc starch and various fats (lard, copra, palm, soya, butter, and sunflower) but were formed with fatty acids or monoglycerides. Such extrudates presented reduced water solubility and freeze thaw stability.

Addition of emulsifier to the extrusion process leads to a decrease in specific mechanical energy due to lubrication effects and increase in melt viscosity partially due to complexation (Conde-Petit 1995).

The complexation of starch with lipid during extrusion also affects the microstructure of the foam. Bhatnagar (1997) showed that pore size distribution and pore volume were affected, complexing lipids giving lower pore volume, smaller size pore and lower porosity than non complexing lipids. Donald (1993) correlated the appearance of polyhedral air cells with appearance of V_h pattern whereas spherical cells where the most dominant form associates with the metastable form E_h during extrusion of maize

grits. The E_h pattern was observed for extrudates produced under conditions of low moisture and high temperature. Donald concluded that when a high viscosity melt and a rapid cooling and moisture flash off process are combined at the exit of the die, the re-crystallisation of amylose-lipid complex is not at equilibrium and formation of the E_h form is favoured.

Bhatnagar (1994) studied the extrusion processing conditions for amylose-lipid complexation using a single screw extruder and showed that extrusion temperature was the most important factor.

The present literature survey was carried out in order to present the context of the work described hereafter.

CHAPTER III MATERIALS AND METHODS

III.1 MATERIALS AND MATERIALS PROCESSING

III.1.1 Materials

The characteristics of materials studied are given in the following section and in the relevant chapters. Maize grits have been used as a model cereal system to study the effect of processing on the characteristics of extruded dry pet food (chapter V, VI and VI). Industrial pet food premix and dry pet food pellets were studied in Chapter IV as well as some of their ingredients. Fats and their interactions with maize grits or wheat flour were studied in chapter VII. A list of the abbreviations used in this chapter and subsequently is given on p 8.

III.1.1.1 Industrial pet food premixes

Pedigree Masterfoods provided two types of industrially prepared pet-food premixes used in Chapter IV. The composition of the high cereal (HC) and the high protein (HP) content premixes is given in Table III-1.

Table III-1: Pet food premix composition

<i>High Cereal (HC)</i>	%	<i>High Protein (HP)</i>	%
Whole maize	77.4	Whole maize	17.3
Whole rice	5.1	Whole rice	20.0
Poultry meal	15.0	Poultry meal	37.9
Meat meal	2.5	Maize gluten	12.6
		Beet pulp	8.4
		Yeast	1.9
		Potassium chloride	0.9
		Dicalcium phosphate	1.0

The two types of premixes were each ground in three different ways labelled A, M and L. The following information was provided by Masterfoods, no information was given on the precise type of grinder.

- A- The cereals have been first coarsely ground then mixed and ground again with the protein meal in the same grinder.
- M- The meat meal and the cereal meal have been ground separately in two different grinders, and then blended.
- L- Cereals and meat meals have been ground by a single pass in a hammer mill.

Extruded pellets from these 6 premixes have been supplied by Masterfoods. Extrusion was performed on a single screw extruder. Masterfoods provided information on the process conditions as follow: the extruder die temperature was 105°C for HC and 60°C for HP, the barrel moisture content was 29% (wb). Pellets were then dried to a moisture content below 10%(wb).

III.1.1.2 Ingredients used in grinding trials

Grinding trials have been performed on a set of 4 ingredients commonly used in the pet food industry (see Chapter IV). Whole maize (WM), whole rice (WR), maize gluten (MGL) and poultry meal (PM) have been provided by Pedigree Masterfood.

III.1.1.3 Maize grits used in preconditioning trials

Maize grits (Maizecor Foods Ltd.) have been used as the main model system for the preconditioning experiments (Chapter V). Proximal composition is given in Table III-2.

Table III-2: Proximal composition of fine maize grits and wheat flour as given by the supplier. (*:measured)

	<i>Maize</i>	<i>Wheat</i>
Moisture (% wb)*	12.7	13.5
Amylose (g/100g (db))	20	-
Fat (% wb)	≤1	-
Protein (% wb)	8-9.5	8.5-9.5

Maize grits of different grades were provided by Maizecor and Pedigree Masterfoods for the pilot plant trials (Chapter VI). The specifications for these grades are given in Chapter VI, part VI.1.2.2.

III.1.1.4 Fats and cereals used in extrusion trials

Maize grits and wheat flour were extruded with various amounts of fats as described in Chapter VII. Maize grits (Maizecor, U.K.) and wheat flour (Spillers Milling, U.K.) composition is given in Table III-2. Linoleic acid (purity = 60%) was supplied by Acros Ltd (U.K.). Sunflower oil, beef tallow and poultry fats were supplied by Masterfoods U.K.

All fats were stored in hermetically sealed plastic containers in a cold room at -6°C except linoleic acid, which was kept at room temperature.

III.1.1.5 Chemical reagents

Chemicals were used in various experiments described in the following sections. The list of reagents used and their corresponding suppliers are given in Table III-3.

Table III-3: Chemical reagent suppliers.

<i>Chemical</i>	<i>Supplier</i>	<i>Reference in</i>
Potassium hydroxide (KOH)	1	III.2.4.3.
Sodium hydroxide (NaOH)	2	III.2.11. & III.2.14.
Sodium carbonate	1	III.2.11.
Copper sulfate	1	III.2.11
Sodium potassium tartrate	1	III.2.11
Folin-Ciocalteu reagent	2	III.2.11
Sodium chloride (NaCl)	1	III.2.4.3.
Iodine	3	III.2.2.
Potassium Iodide	1	III.2.2.
Phenol	1	III.2.12.
Sulphuric acid	1	III.2.12.
β -mercaptoethanol	2	III.2.11.
Sodiumdodecylsulfate (SDS)	1	III.2.11.
Phosphorus pentoxide	1	III.2.4.3 & III.2.13.
Ethanol	1	III.2.14.
Phenolphthalein	2	III.2.14.
Amylose from potato starch	4	V.2.6.2.
2-Propanol	1	III.2.8.1.

1. Fisher Chemicals, Ltd, Loughborough, U.K.
2. Sigma Chemicals, St Louis, USA
3. Fisons, Loughborough, U.K.
4. ICN biomedical

III.1.2 Sample preparation technique

III.1.2.1 Model preconditioner

An improved orbital paddle mixer (Kenwood *Major*) was used as a model for the batch preconditioning experiments (Figure III-1). The orbital rotation speed was 166 rpm (experimental determination). A lid was fixed on top of the mixing bowl to prevent steam loss, and a small aperture was left to allow venting.

A steam line (SteamMaster, Earlex, U.K.) was fitted at the bottom of the mixing bowl which deliver steam at a rate of 57 g / min.

Raw material (600g) was placed into the bowl together with the required amount of water and premixed for 0 to 30s before introducing the steam. The level of water added varied between 25 and 175 ml, this corresponded to initial moisture content of 16.5 to 32.6% (w/w on a wet basis, wb). Maize grits after preconditioning had the appearance of a fluffy hydrated powder.

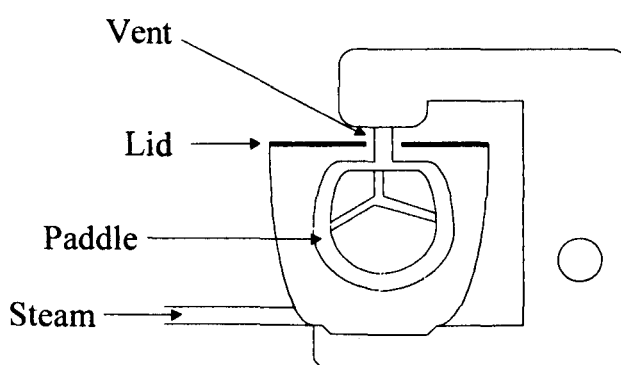


Figure III-1: Schematic diagram of the model preconditioner

III.1.2.2 Particle size reduction

The effect of using different grinding processes was tested on whole maize (WM), whole rice (WR), poultry meal (PM) and maize gluten (MG) as described in Chapter IV.

Two grinding methods were used. The mild treatment consisted of grinding the samples in a Knifetec cutting mill (Trecator U.K.) for 30s. The Knifetec mill is fitted with a cooling jacket where cold water passed through during grinding. The harsh treatment was performed on a Retch impact mill (Retch, GmbH, Germany) fitted with a screen of 2mm aperture. The samples were passed 4 times through this mill.

Current intensity was measured using an ampermeter (MX220, ITT instruments) and sample temperature increase was measured using a thermocouple thermometer at the

end of the run. The characteristics of the ground materials are discussed in Chapter IV.

In chapter V, the effect of grinding and particle size on preconditioning was tested by milling maize grits to 2 lower particle sizes. Maize grits (MG) has been milled in a lab-scale impact mill (Retch GmbH & Co) fitted with a 2mm screen (mild milling). The smaller particle size has been achieved by re-milling the maize by a second pass through the same mill fitted with a 0.75mm screen (strong milling).

The particle size has been determined by sieve shaking using an AS200 analytical sieve shaker (Retsh GmbH & Co.) fitted with 6 sieves (125 to 600 μm aperture). The results are presented in Chapter V.

III.1.3 Twin screw extrusion cooking

Extrusion is a thermomechanical way of cooking materials in a short time and using usually high temperature. The principle of extrusion cooking was discussed in Chapter II.

Various extrudates were produced using a twin-screw extruder (chapters IV, V and VII). Twin-screw extrusion was performed on a Cleextral BC21 co-rotating, intermeshing twin-screw extruder. The barrel had a useful length of 40 cm and a 16:1 length to diameter ratio. The barrel had 4 temperature zones (1 to 4 from feeder end to exit) the barrel temperature conditions are given in the relevant chapters. The die had a circular opening of 3 mm diameter and 2.5mm land length. Screw configuration is given in Figure III-2. The first section has large pitch screw elements for feeding and conveying the material, the second section has screw elements of decreasing sizes to compress the material finally in the last section (working section), the reverse pitch screw elements provide shear.

Extrudates were cut into cylinders of ca. 40 cm length and dried in a forced air oven at 105°C for 1h. Some samples were sealed in foil bags before drying to determine bulk density and extrudate diameter after cooling. Samples were then ground in a

laboratory mill (Cyclotec) for analysis and stored in plastic screw cap pots at room temperature.

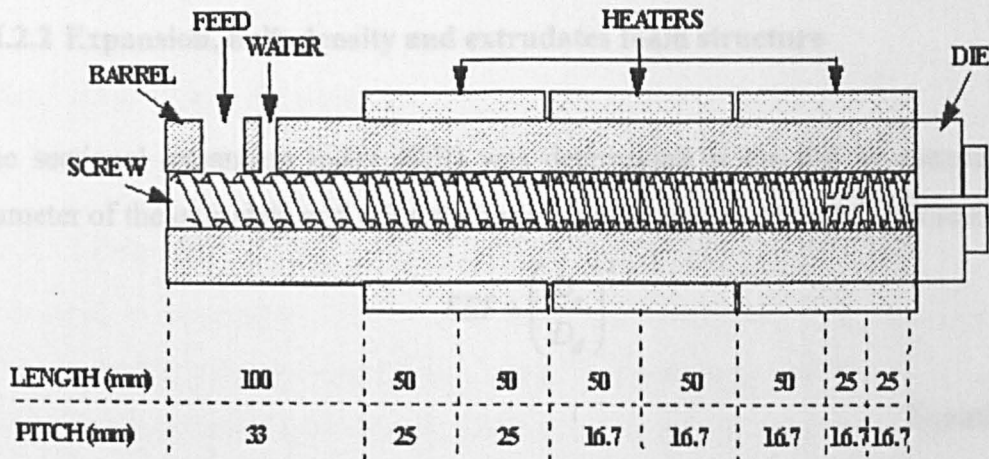


Figure III-2: BC21 screw configuration (From: Hill 2000)

III.2 METHODS

III.2.1 Moisture content determination

Unless otherwise stated, the moisture content of the materials has been determined by drying the sample (2 to 4g) in the oven at 105°C for 1 day.

$$MC = \frac{wt_w - wt_D}{wt_w} \times 100$$

Equation III-1

Where:

MC is moisture content (w/w) on a wet basis (wb)

wt_w is the sample weight wet (i.e. before drying)

wt_D is the sample weight dry.

Measurements were performed using 3 replicates. Variation coefficients were less than 2%.

III.2.2 Expansion, bulk density and extrudates foam structure

The sectional expansion index (SEI) was determined at the die by measuring the diameter of the extrudate and using the following formulae (Alvarez-Martinez 1988).

$$SEI = \left(\frac{D_e}{D_d} \right)^2$$

Equation III-2

Where D_e is the diameter of the extrudate and D_d is the diameter of the die.

The bulk density (BD) was measured on the extrudate before drying. The extrudates produced were cylinder shaped therefore the following equation was used.

$$BD = \frac{wt}{\pi \times R^2 \times L}$$

Equation III-3

Where wt is the weight of the sample, R is the radius and L is the length of the sample. The bulk density is given in g/mL.

In Chapter IV, the bulk density of extruded pet food pellets was determined using the volume displacement method with oilseed rape. A measuring cylinder was filled with 20 mL of oilseed rape and weighed. Then, two pellets were added and the displaced volume was measured as well as the weight. The bulk density was determined as the ratio of the weight of the pellet by the displaced volume. Measurements were done using 9 replicates.

In Chapter VII, the foam structure of the extrudate is shown using the method described by Angold (2000). Extrudates have been cut longitudinally and the surface has been polished using sandpaper. The extrudate surface has then been dyed by pressing the extrudate against a gelatine gel containing 1% iodine and 2% potassium

iodine. The dyed extrudates have then been scanned using an Acer Scan Prisa 640U scanner.

III.2.3 Rapid Visco Analyser

III.2.3.1 Principle

The rapid visco-analyser (RVA) is a rotational viscometer with the capacity for heating, cooling and applying variable shear. It is especially configured for analysing starch-based products. Typically, the RVA gives similar information as the Brabender viscoamylograph with the advantage of using smaller sample size and requiring less time for analysis (typically 13 min).

A dispersion of particles in an excess of water is placed into a disposable aluminium canister coupled with a paddle stirring at chosen speed. The canister temperature is varied as determined by the temperature profile and the viscosity of the sample is detected through continuous monitoring of torque on the paddle sensor throughout the test (Wrigley 1996).

A typical RVA cycle is composed of a holding time at 50°C, followed by a steady increase of temperature up to 95°C, a second holding time at 95°C, then a steady cooling ramp back to 50°C followed by a short holding time at this temperature. The rotation of the paddle begins with a high speed (960 rpm) for about 10s, in order to allow a good mixing of the particulates with water. Then the speed is lowered to a slower speed (typically 160rpm) and remains constant throughout the test.

A typical RVA pasting curve is represented on Figure III-3. At the beginning of the cycle, the native insoluble starch granules are in suspension in water. The particles present a limited swelling. The viscosity is then determined by the volume fraction of the particle and is therefore very low.

As temperature increases, swelling and starch gelatinisation occurs, this gives rise to a sudden increase in viscosity characterised by the pasting temperature and the pasting time. During this phase, progressive loss of the crystalline structure occurs and amylose starts leaching out of the granule. The peak viscosity is then reached and is related to the maximum swelling capacity of the starch particles. At this point the starch granule is believed to be completely amorphous and very shear sensitive. Therefore, particles start to rupture due to the shear of the paddle and more polymeric materials are released into solution. Subsequently, the viscosity decreases until a minimum is reached which depends on starch botanical origin and composition. Then, as the temperature starts to decrease, amylose rearrangements occur and a starch gel is formed resulting in an increase in viscosity. Its viscosity is dependent on temperature. The final viscosity is therefore determined by the volume and deformability of the particle remnants, the extent to which gelation occurs in the continuous phase and their interaction.

Various parameters typical of RVA curves are used to characterise the state of native and processed starches, they are represented in Figure III-3.

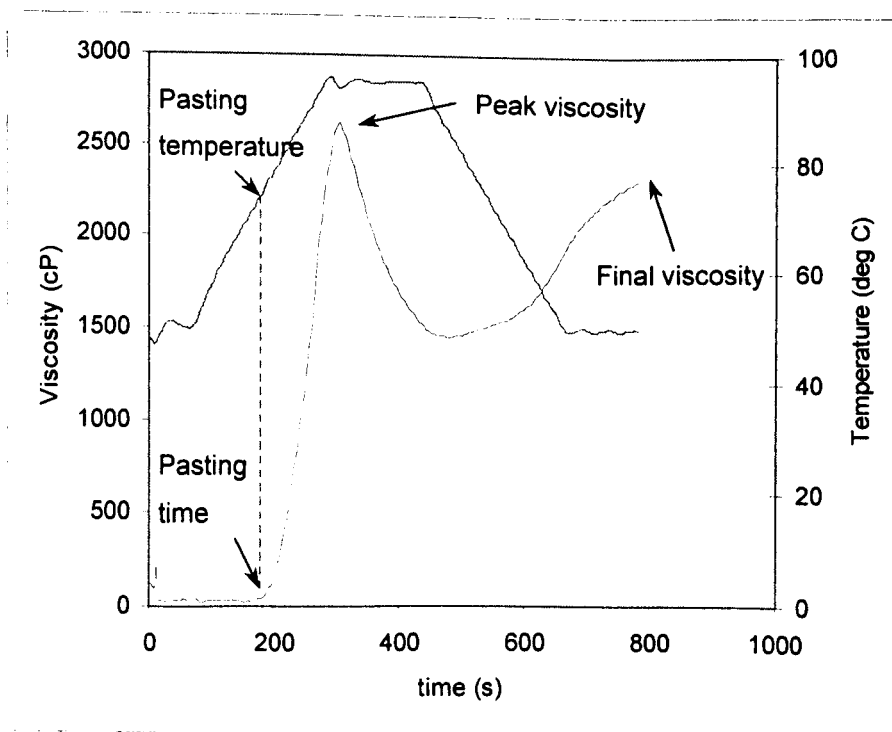


Figure III-3: RVA pasting curve of maize starch (own data).

III.2.3.2 Sample preparation

The RVA was run on a sieve fraction (250-125 μm) of the sample to avoid particle size effects.

For pure cereal mixes 3.44 g solid sample was dispersed in 25.56g water (including sample water content). For pet food premixes, 5.16g solid have been dispersed in 25.84g water to account for the lower starch content.

The standard temperature profile has been used for both raw and preconditioned materials (Table III-4). The extrusion profile has been used for extrudates (Table III-5). The extrusion profile start the temperature cycle at a lower temperature and uses a lower temperature increase rate to reach 95°C therefore allowing a better visualisation of cold swelling characteristics.

Table III-4: RVA standard temperature profile

Time (min:sec)	Paddle speed (rpm)	Temperature (°C)
00:00	960	50
00:10	160	50
01:00	160	50
04:42	160	95
07:12	160	95
11:00	160	50
13:00	160	50

Table III-5: RVA extrusion temperature profile

Time (min:sec)	Paddle speed (rpm)	Temperature (°C)
00:00	960	25
00:10	160	25
02:00	160	25
07:00	160	95
10:00	160	95
15:00	160	25
20:00	160	25

Determination of pasting temperature, peak viscosity, final viscosity and cold paste viscosity has been performed using the software provided with the RVA (TcW).

III.2.4 Powder X-ray diffraction

III.2.4.1 Principle

X-ray diffraction is a useful tool used to determine the inner structure of crystalline matter. X-rays are electromagnetic radiation of much shorter wavelength than light (Cullity 1959). X-rays used in diffraction have a range of wavelength between 0.5 and 2.5 Å.

When a beam of X-ray is sent onto a crystalline material, the different rays will be scattered when they strike the electrons in the atoms, which then become secondary emitters of X-rays. Differences in the length of the path travelled by the rays will introduce differences in phases. This depends on the scattering angle 2θ i.e. the angle of deviation of the diffracted ray from the incident ray.

Bragg (1913) first discovered that 2 rays will be scattered completely in phase if the path difference is equal to a complete number n of wavelengths as described in Equation III-4.

$$n\lambda = 2d' \sin \theta$$

Equation III-4

Where: n is the spectral order

λ is the ray wavelength

d' is the distance between adjacent planes

θ is the angle of incidence of the ray

Figure III-4 illustrates the application of the Bragg equation to X-ray diffraction. An X-ray (λ_1) strikes a layer of atom in a crystal and is diffracted. If another x-ray (λ_2) strikes the layer below the first layer, and the total distance it travels is an even number of wavelength behind the first ray, then λ_2 can add to λ_1 since they are both in phase. As this will be repeated for several layer the total intensity of the diffracted X-ray will be strong enough to be detected by a detector.

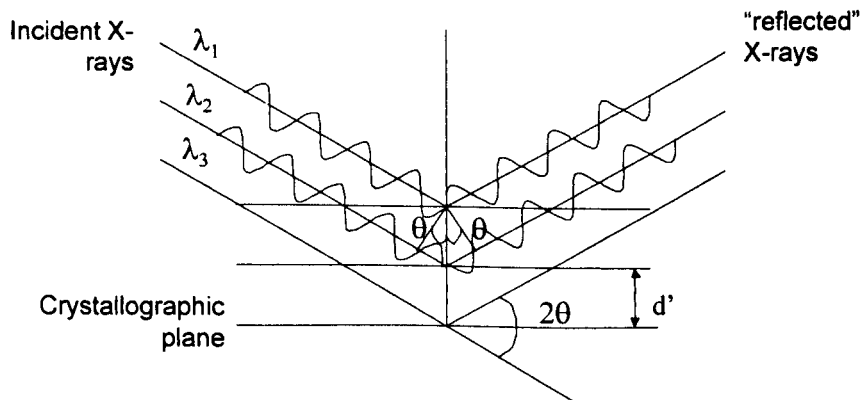


Figure III-4: Schematic representation of X-ray diffraction (Adapted from Pomeranz, (1994))

III.2.4.2 Application of x-ray diffraction to starch

Starch is a semi-crystalline material, when in a native state. Starch granules can show 2 types of X-ray diffraction pattern (A or B) depending on their origin. The A-pattern is characteristic of cereal starches, whereas the B pattern is seen for some tuber and root starches. A mixture of A and B (sometimes referred to as a C pattern), has been

•

found in pea and bean starches (Hoseney 1994). Retrograded starch may lead to A, B or C pattern.

Another important pattern related to starch crystallinity is the V-pattern. This pattern has been correlated with complexation of amylose with small molecules such as lipids, butanol, acetone or even flavour compounds (see Chapter II).

Because the diffraction pattern is a picture of the crystallinity of starch, it is possible to visualise starch conversion by the progressive disappearance of the crystalline pattern into an amorphous pattern. Different methods have been used to determine an index of crystallinity (Mizuno 1998; Farhat 1996).

III.2.4.3 Experimental methods

X-ray diffraction measurements have been performed on a Siemens D5005 X-ray diffractometer (Bruker Analytical X-ray system, Congleton, U.K.). The Kristalloflex 760 X-ray generator supplied CuK α radiation at 0.154 nm wavelength. The range of diffraction angle (2θ) used was between 4 and 38°. The step used was first 0.02° but due to the high noise of the pattern and the fact that the width of crystalline starch is larger than 1°; the use of such a high sampling rate was not justify. A step scan of 0.05° was then used and in order to increase the signal to noise ratio, the step time was set to 2.5s. The X-ray pattern obtained was first analysed by the software provided with the instrument (EVA) to remove sample holder trace. The area of the peaks was calculated using OPUS 3.0 software (Bruker Ltd.).

All samples analysed were in a powder form. As moisture content can affect crystallinity (Hartley 1996), the samples were kept in an airtight container at 20°C over a saturated solution of NaCl for one week in order to equilibrate the samples at the same relative humidity (RH=75%).

The crystallinity index was defined as follows:

$$\text{XRDi} = (A_1 + A_2 + A_3) / A_{\text{total}}$$

Where :

A_1 is the area of the first major peak ($2\theta = 15.1$ for A-type, 7.6 for V-type)

A_2 is the area of the second major peak ($2\theta = 18.2$ for A type, 13.0 for V-type)

A_3 is the area of the third major peak ($2\theta = 23.1$ for A-type, 19.9 for V-type)

A_{total} is the total area under the curve

The method is represented in Figure III-5.

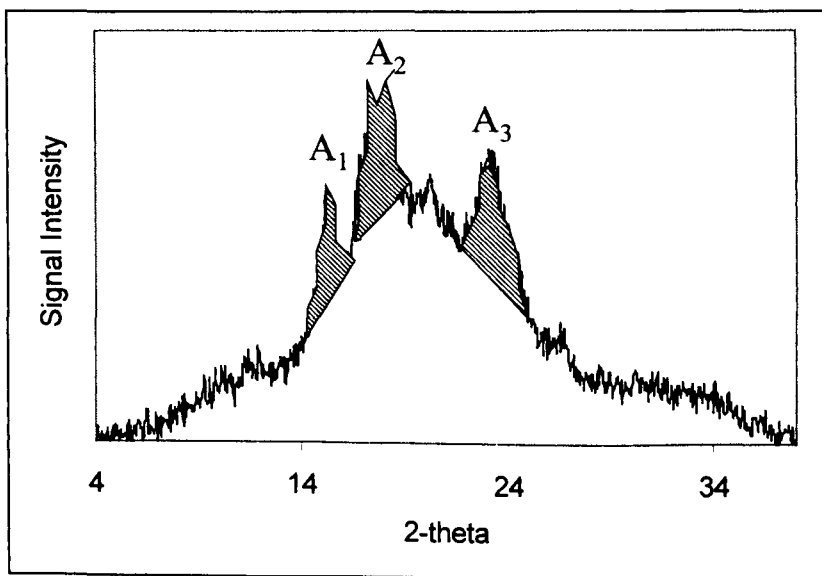


Figure III-5: Determination of areas of crystallinity peaks in maize grits. (own data)

The baseline was considered linear and defined as zero intensity at $2\theta = 4^\circ$ and $2\theta = 38^\circ$. The measurements were performed in duplicates or triplicates and variation coefficient was a maximum of 12%.

III.2.5 Differential scanning calorimetry (DSC)

III.2.5.1 Theory

Differential scanning calorimetry (DSC) is a technique in which a sample is heated at a fixed rate and the energy needed to heat is recorded. In power compensated DSC,

the technique used in this study, there are two control loops. One is for the average temperature control, so that the temperature of the sample and reference may be increased at a predetermined rate, which is recorded. The second loop ensures that if a temperature difference develops between the sample and the reference (because of exothermic or endothermic reaction) the power input is adjusted to remove this difference.

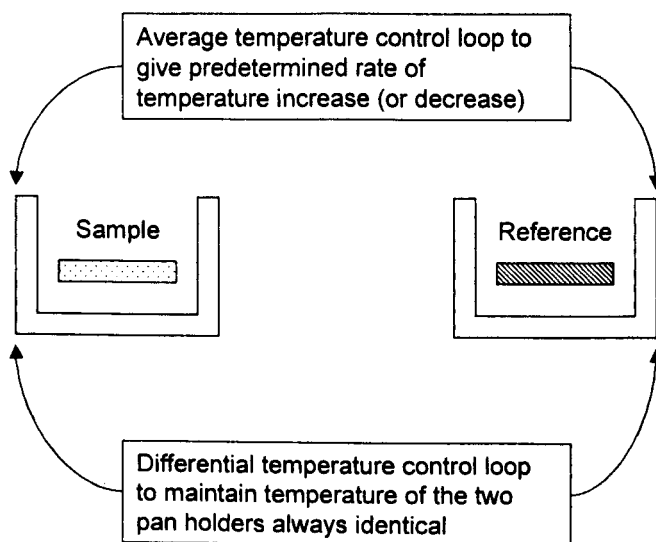


Figure III-6: Schematic representation of the DSC control loop (From McNaughton (1975))

This technique is very useful to study starch gelatinisation. As the amount of energy needed will depend on the “amount” of ungelatinised starch in the sample, and thus DSC measurement can give an indication on the amount of starch conversion in a sample.

III.2.5.2 Experimental set-up

Starch conversion has been measured by DSC on the ground pet food mixes (Chapter IV) and on precondition and extruded maize (Chapter VI)

Similarly, melting of amylose-lipid complexes can be observed and quantified by DSC (Chapter VII).

DSC experiments have been performed on a Perkin Elmer (Beaconsfield, U.K.), Pyris DSC 7 calibrated with indium. Stainless steel pans have been used. The reference used was an empty pan. Samples, preliminary ground, were mixed in the pan with water at a dry matter to water ratio of 1:3. The pans were then left in 2.5mL glass jar and shaken on a roller shaker.

The heat rate was 10°C/min. The samples were heated from 20 to 110°C for starch conversion measurements and from 30 to 130°C for amylose-lipid complex melting experiments. The pan was then cooled down to the starting temperature at the nominal rate of 180°C/min, then held at this temperature for 5 min to equilibrate and re-heated at 10°C/min.

Peak temperature (onset and end) and peak area was determined using the software provided with the DSC (Pyris). Peak area was determined in Joule per gram of dry matter or in Joule per gram of dry starch.

Measurements were performed in duplicate with a coefficient of variation smaller than 25% for enthalpy measurements.

III.2.6 Texture analysis

A method was developed to quantify the changes occurring to materials during preconditioning.

The texture analysis was performed using a TA-XT2 texture analyser (Stable Micro Systems Ltd.). The texture analyser was fitted with a 25kg load cell.

All measurements were performed when samples were cooled down to room temperature. 35.5g ± 0.5 g of preconditioned MG was inserted into a 50mm diameter cylinder and fitted onto a container holder. A 49 mm piston probe was fitted to the texture analyser. Great care was taken to have evenly packed samples and flat surfaces.

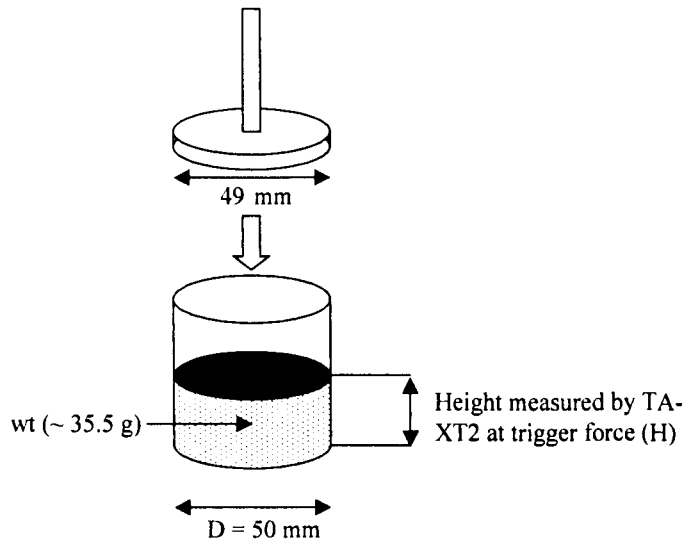


Figure III-7: Powder compression test.

A compression sequence was used with the following characteristics.

Table III-6: Compression sequence parameters (* = 2mm for raw maize grits without hydration)

Pre-test speed	2 mm/s
Test speed	1 mm/s
Post-test speed	1 mm/s
Distance	5 mm*
Trigger	Auto
Threshold	20 g

The bulk density was determined by recording the height of the sample at trigger force, then using the following equation.

$$BD = \frac{wt \times 4}{H \times D^2 \times \pi}$$

Where:

BD is the bulk density (g/mL)

H is the height of the sample at the trigger force (cm)

D is the diameter of the sample holder (5 cm)

wt is weight of sample used (g).

The hardness was recorded as the maximum force at compression.

The compressibility has been determined using the method of Peleg (1993). The compressibility is the slope of the plot of the powder bulk density in logarithm versus the logarithm of the applied normal stress (Figure III-8).

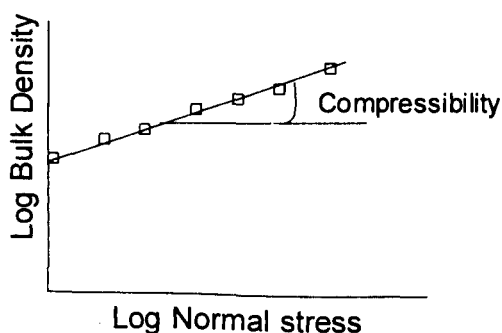


Figure III-8: Schematic representation of the relationship between normal stress and bulk density during the compaction of a powder.

III.2.7 ^1H -NMR

III.2.7.1 Principles of NMR spectroscopy (Ruan 1998; Deleanu 1997)

In order to understand nuclear magnetic resonance (NMR), it is necessary to go back to some fundamental relations describing properties of nuclei.

The nuclei active in NMR are the ones having an odd number of protons and / or neutrons. Most common nuclei have or have an isotope having this property (^1H , ^{13}C , ^{31}P ...). In the case of ^1H , the nucleus is said to have a spin $\frac{1}{2}$.

Because the nucleus of an atom is charged and spinning, it generates a magnetic field and is able to interact with other magnetic field (Ruan 1998). The magnetic field generated has a magnetic moment (μ) proportional to the angular momentum (P).

$$\mu = \gamma P$$

Equation III-7

γ is the gyromagnetic ratio ($\text{rad.kg}^{-1}.\text{s}^{-1}$), its value depends on the type of nucleus. In absence of an external magnetic field, the magnetic moments are oriented randomly resulting in no macroscopic magnetisation.

When an external magnetic field (B_0) is applied, the magnetic momentum are orientating in relation to this magnetic field (for example $\theta=54^\circ44'$ for ^1H nuclei). In this situation, the magnetic moment rotates also around the direction of the magnetic field with an angular speed ω_0 (rad.s^{-1}). The rotation frequency ω_0 is named the Larmor frequency. It corresponds to the adsorption frequency of a particular nucleus in a given magnetic field B_0 (Tesla). It has been shown that:

$$\omega_0 = -\gamma B_0$$

Equation III-8

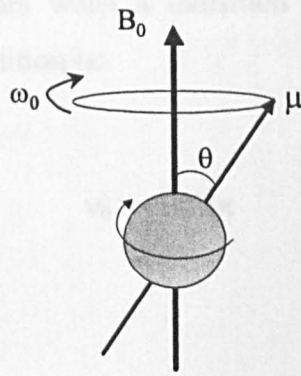


Figure III-9: Schematic representation of the different movement of a magnetic nucleus in a magnetic field B_0 . Adapted from Deleanu (1997)

For a nuclei spin $\frac{1}{2}$, only two orientations are allowed: “parallel” and “anti-parallel”. But because the energy levels associated with the two orientations are different, there are more nuclei orientated in one orientation than the other. This results in a net magnetisation (M_0) in the direction of the magnetic field B_0 .

At equilibrium, the magnetic moments are randomly distributed on the surface of a cone around the z-axis, therefore when projected on the x-y axis, their sum is zero. The macroscopic magnetisation is therefore along the z-axis only.

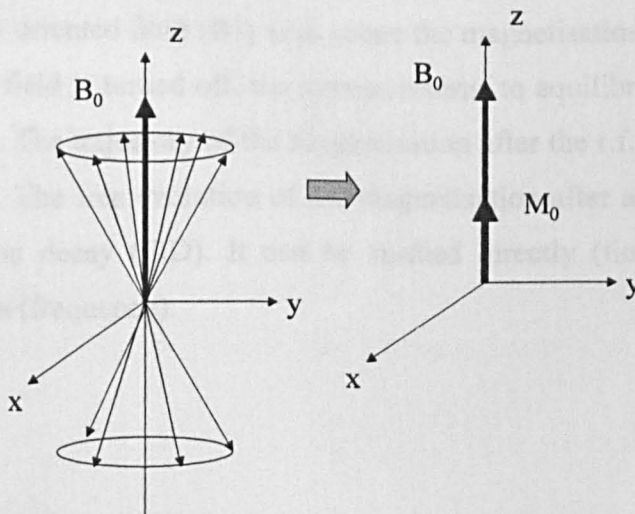


Figure III-10: Representation of the precessional cones of spin $\frac{1}{2}$ in a magnetic field B_0 . Adapted from Deleanu (1997).

The magnetic resonance occurs when a transition between two energy levels is stimulated. The resonance condition is:

$$\nu_0 = \gamma B_0 / 2\pi$$

Equation III-9

Or using $\omega_0 = 2\pi\nu_0$

$$\omega_0 = \gamma B_0$$

Equation III-10

The energy required for this transition to occur is in the radiofrequency range (i.e. 1 MHz to 800 MHz).

The ability to flip net magnetisation through rf pulse is used in pulse Fourier Transform NMR to observe and characterise the nuclei.

The magnitude of the magnetisation can be visualised by a vector model. Any magnetisation in the x-y plane will be rotating at its Larmor frequency, and thus will induce an oscillating voltage in the coil, which is detected by the NMR. The effect of a perpendicularly oriented field (B_1) is to rotate the magnetisation around it in the y-z plane. Once this field is turned off, the system returns to equilibrium. This process is called relaxation. The trajectory of the magnetisation after the r.f. pulse is represented on Figure III-11. The free evolution of the magnetisation after an r.f. pulse is called the free induction decay (FID). It can be studied directly (time domain) or after Fourier transform (frequency).

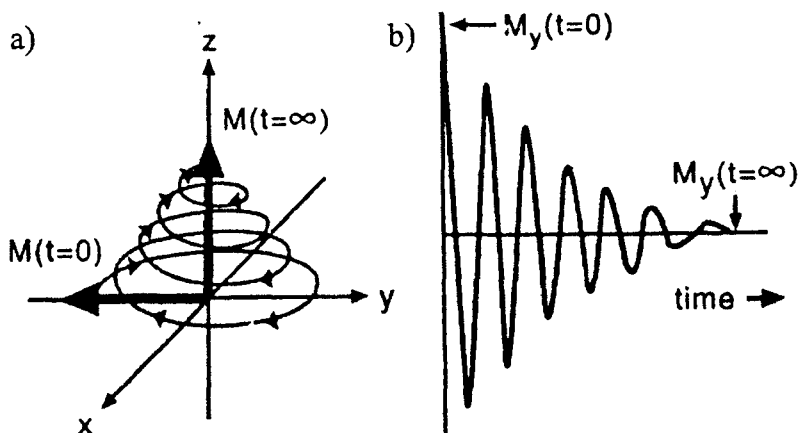


Figure III-11: Trajectory of the magnetisation after a 90° pulse (a), projection of the magnetisation on the y axis (b). (From Deleanu (1997))

While the relaxation following a 180° pulse takes place by spin-lattice mechanism, transverse relaxation is responsible for the relaxation following a 90° pulse (Equation III-11 and III-12).

$$M_z(t) - M_0 = [M_z(0) - M_0] \exp\left(-\frac{t}{T_1}\right)$$

Equation III-11

$$M_y(t) = M_0 \exp\left(-\frac{t}{T_2}\right)$$

Equation III-12

Where M_z is the magnetisation along the z-axis, M_y is the magnetisation along the y-axis, t is the time, T_1 is the spin lattice relaxation time and T_2 is the spin-spin relaxation time.

The spin-spin relaxation signal varies according to the molecule arrangement or phase state: in a solid state it is fast and T_2 is short (about 5 to 100 μs) whereas in a liquid state T_2 is greater (in the order of ms to s) indicating a higher molecular mobility. Therefore, the FID is often best fitted by a sum of components to reflect the range of mobilities, usually a sum of exponentials.

$$M_z = \sum A_i \exp\left(\frac{-t}{T_{2i}}\right)$$

Equation III-13

However, the fact that dipole-dipole interactions dominates the relaxation of solids, and because of the effect of magnetic field heterogeneity on the decay of mobile components, a gaussian lineshape usually describes better the very rapidly (rigid) and very slowly (liquid-like) decaying components (Farhat, personal communication). Thus, the following equation was used to fit the FID:

$$M_z = A_1 \exp\left(-\left(\frac{t}{T_{21}}\right)^2\right) + A_2 \exp\left(-\frac{t}{T_{22}}\right) + A_3 \exp\left(-\left(\frac{t}{T_{23}}\right)^2\right)$$

Equation III-14

Where M_z is the magnetisation along the z-axis, A_i are intensity coefficients, t is time and T_{2i} are spin-spin relaxation times of the different components.

In pulse field gradient experiments, magnetic field inhomogeneity is used to investigate the translational mobility of nuclear spins. In such experiments, the nuclei are magnetically “labelled” by applying a field gradient which phase codes the spins. The phase is then “decoded” by a second field gradient pulse equivalent to the first one in width and amplitude. The study of the resulting magnetisation echo provides information on the motional history of the nuclei between the two gradients.

In a field gradient, the frequency at which spins resonate is dependent on their position. Therefore the NMR signal will be slightly dephased due to this heterogeneity and result in an attenuated signal. The motion of spins will increase this dephasing. It was shown by Tanner (1968) that the signal attenuation is related to the diffusion constant and the strength of the magnetic field. By using a pulse field gradient sequence as is given in Figure III-12, an equation can describe the signal attenuation (Equation III-15).

$$\frac{A(G)}{A(0)} = \exp\left(-D\gamma^2 G^2 D_3^2 \left(\Delta - \frac{D_3}{3}\right)\right)$$

Equation III-15

Where $A(G)$ and $A(0)$ are the amplitudes of the signal respectively in the presence or absence of gradient, G is the magnitude of the gradient in the polarising field, D is the self diffusion coefficient, γ is the gyromagnetic ratio, D_3 is the gradient width (in μs) and Δ is the time between the first gradient and the beginning of the second one.

Therefore by recording the signal attenuation using different gradient width, the water self diffusion coefficient can be deduced (Roudaut 1998).

The spin echo technique relies on the spin-spin relaxation time T_2 and therefore is less suitable for samples with $T_2 \ll T_1$ such as systems with relatively low moisture contents. For this reason, the stimulated echo technique was used in our study. This technique uses a second 90° pulse after the first 90° - gradient sequence as represented on Figure III-13. After this second pulse the magnetisation is on the z-axis and relaxation takes place through a spin lattice process (Farhat 1996).

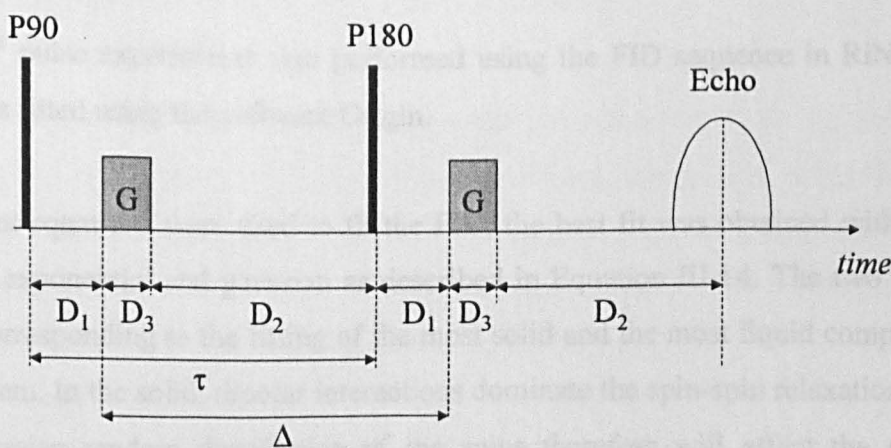


Figure III-12: Pulsed field gradient spin-echo (PFG-SE) pulse sequence (adapted from Farhat (1996))

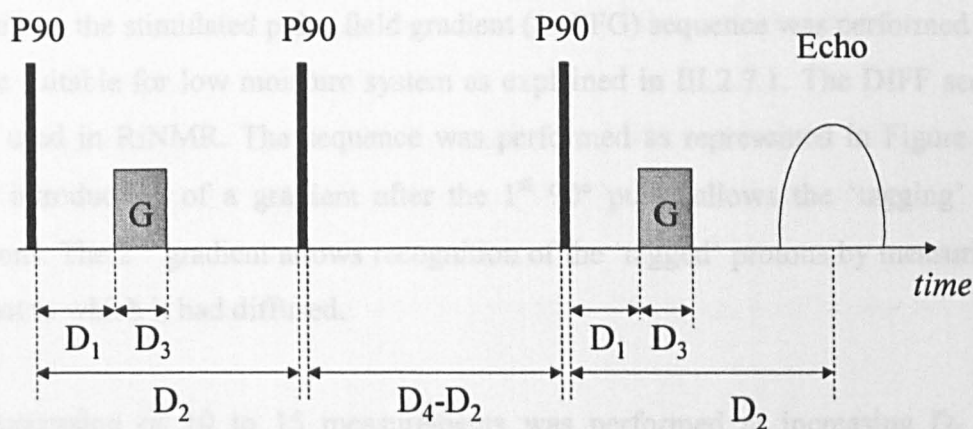


Figure III-13: St-PFG sequence (P90 is 90° pulse, G is the gradient).

III.2.7.2 Experimental method

Proton relaxation experiments were performed on a Maran spectrometer (Resonance Instruments Ltd.). The strength of the magnet was 0.5 T and the precession frequency 22.9 MHz. The signal was recorded on a PC using RiNMR software provided by Resonance Instrument.

The samples were packed in a 10 mm diameter glass tube up to a height of 1 cm. The tube was sealed by a glass rod to avoid moisture loss.

All experiments were performed at 20°C .

The 90° pulse experiments was performed using the FID sequence in RiNMR. The FID was fitted using the software Origin.

Different equations were used to fit the FID, the best fit was obtained with a mixed sum of exponential and gaussian as described in Equation III-14. The two gaussians were corresponding to the fitting of the most solid and the most liquid components of the system. In the solid, dipolar interactions dominate the spin-spin relaxation process, the gaussian random distribution of the spins therefore will affect the relaxation process. Equally in the most liquid component, field homogeneity will affect the relaxation process. Field inhomogeneity is believed to be gaussian.

Measure of water self-diffusion coefficient was first attempted using pulse field gradient experiment. Results using the pulse field gradient sequence were poor,

therefore, the stimulated pulse field gradient (St-PFG) sequence was performed as it is more suitable for low moisture system as explained in III.2.7.1. The DIFF sequence was used in RiNMR. The sequence was performed as represented in Figure III-13. The introduction of a gradient after the 1st 90° pulse allows the ‘tagging’ of the protons. The 2nd gradient allows recognition of the ‘tagged’ protons by measuring the extent to which it had diffused.

A succession of 10 to 15 measurements was performed at increasing D_3 values (increasing gradient width). The height of the echo was recorded for each value of D_3 . These values were plotted using Diffusion software in order to determine the diffusion coefficient of water in the system.

A calibration for the strength of the magnetic field was performed using distilled water at 20°C ($D = 2.3 \cdot 10^{-9} \text{ m}^2/\text{s}$).

III.2.8 Particle size distribution

III.2.8.1 Low angle laser light scattering (Mastersizer)

For food mixes with particle size below 900 μm (Chapter IV & V), particle size distribution and average diameter was determined using low angle laser light scattering. The Mastersizer S (Malvern Instrument Ltd.) measures the scattering pattern of a laser light that passes through a field of particles and uses the Mie theory to calculate the size of particles that created that pattern.

The sample ($0.20 \pm 0.05\text{g}$) was placed in a beaker with 20 ml of dispersant (distilled water or 2-propanol) and placed in a sonic bath for 2 min to disperse aggregates. The choice of the dispersant will be discussed in Chapter IV. Then the dispersion was transferred to the small sample dispersion unit connected to the Malvern Mastersizer S.

The lens was a 300RF allowing measurement of particles from 0.05 to 900 μm and the active beam length was 2.4mm.

The analysis software used a polydispersed model with a standard wet presentation 3OHD when using water as a dispersant and 3OHE when using 2-propanol.

Measurements were performed with 6 replicates. Variation coefficients were lower than 10%.

III.2.8.2 Sieve shaking

For particles with a higher particle size than 900 μm (Chapter VI), sieve shaking through a series of sieve was performed. Eleven sieves were used with the following screen size: 2000, 1500, 1000, 710, 600, 500, 425, 355, 250, 125 and 63 μm . Maize grits (60g) was added on the top sieve and the sieve stack was then shaken for 10 min on an analytical sieve shaker (Retch, GmbH, Germany). The mass of particles on top of each sieve was then weighed accurately (up to one decimal place). The particle size distribution is then given as a percentage by weight. The modal diameter was determined graphically as the diameter for which 50% of the particles are larger and 50% are smaller.

III.2.9 Microscopic observations

Processed samples were observed under polarised light in order to determine the presence or absence of native starch granules.

Small amounts of sample were suspended in distilled water and observed with an optical microscope (Leitz Diaplan, Wild Leitz GmbH, Wetzlar, Germany). A polarised filter was used to see the presence of birefringent native starch granules.

III.2.10 Particle charge detection (PCD)

The particle charge detector (PCD, Mutek, Germany) has a Teflon test cell fitted with a displacement piston. As the piston oscillates, it forces the liquid sample to flow along the wall of the cell. Under the action of van der Waals forces, high molecular charge carriers are preferentially absorbed at the surface of the test cell and the diffuse cloud of counter ions surrounding the particle is sheared, thus creating a streaming current. This potential difference is recorded by means of two electrodes.

The principle of particle charge detection is represented in Figure III-15 and Figure III-15.

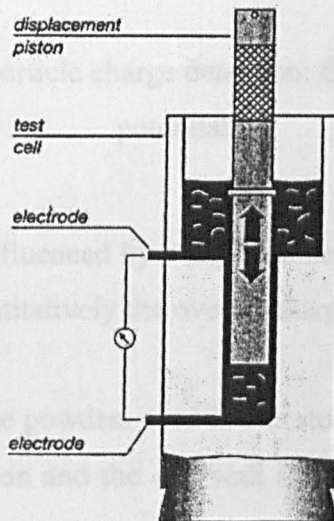


Figure III-14: Mutek cell

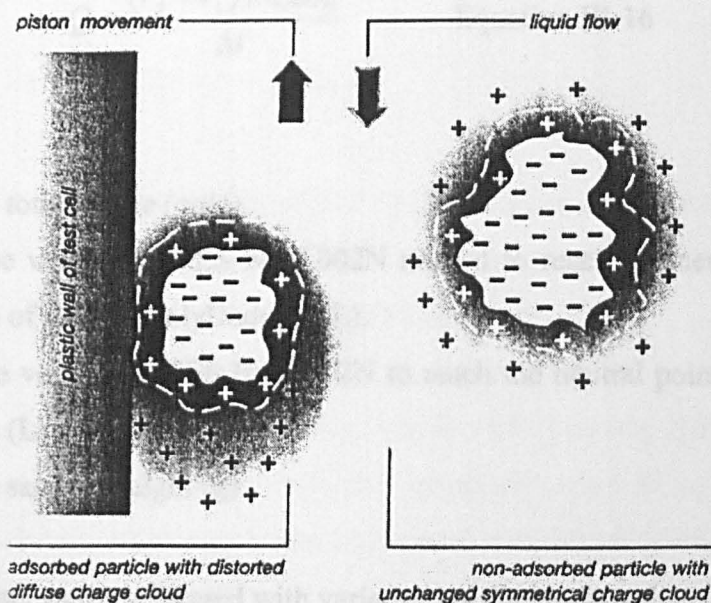


Figure III-15: Principle of particle charge detection: the formation of the streaming potential.

As the streaming current is influenced by many parameters, polyelectrolyte titration is the only way to measure quantitatively the overall charge of the system.

Because the particle size of the powders used in this study were higher than the size of the aperture between the piston and the cell wall ($300\ \mu\text{m}$), a back titration method has been chosen.

Sample ($1.00 \pm 0.01\text{g}$) was dispersed in 100ml of 0.002N Polydadmac (cationic polyelectrolyte) and stirred during 2 hours on the roller mixer. Then, the sample was centrifuged at 4000 rpm for 10 min and the sample was titrated against a solution of 0.002N PES-Na (anionic polyelectrolyte).

The total charge amount was determined according to Equation III-6.

$$Q = \frac{(V_2 - V_1) \times 0.002}{M} \quad \text{Equation III-16}$$

Where:

Q is the total charge (eq/g)

V_2 is the volume of PES-Na 0.002N needed to reach the neutral point of a solution of 0.002N PolyDadmac (L).

V_1 is the volume of PES Na 0.002N to reach the neutral point of the sample solution (L).

M is the sample weight (g)

Six measurements were performed with variation coefficient less than 3%.

III.2.11 Protein solubility

Protein solubility is discussed in Chapter IV. This method was used to determine whether protein structure was affected by the grinding process.

Protein solubility was determined using the method of Lowry (1951). A solvent was prepared containing 1% sodium dodecylsulfate (SDS) and 1% β -mercaptoethanol as the proteins were not soluble enough in water to be detected by this technique.

The sample (0.1g) was placed in a tube with 10mL solvent and shaken overnight on a roller shaker. Samples were then centrifuged for 10min at 1500g. The supernatant was then filtered through a Whatman paper No 4. An aliquot (0.4mL) of each supernatant was placed in a dry clean tube and diluted to 10mL with water. 0.5mL of this solution was mixed with 2.5mL of copper alkali solution and left for 10min. This solution was made of 49mL 0.2N sodium hydroxide, 49mL of 4% of sodium carbonate, 1mL of 1% copper sulphate and 1mL of 2% sodium potassium tartrate. 0.25mL of Folin-Ciocalteu reagent diluted to 50% was added, mixed well and left for 30 min to react. The samples were then transferred to a spectrophotometer cuvette and absorbance was read at 750nm on a Perkin Elmer double beam spectrophotometer. The blank was made of 0.5mL water mixed with the appropriate reagents. Each measurement used 5 to 10 replicates, the variation coefficient was less than 6%.

III.2.12 Total soluble sugar content

Total soluble sugar content was measured on maize grits extrudates in Chapter VI, using the method described by Dubois (1956). This was used to determine the effect of a preconditioning treatment on cereal extrudates dextrinisation.

Dry extrudates were ground in a cyclotec sample mill (Trecator U.K.) fitted with a 1mm diameter screen size. Sample weight corresponding to 60mg of starch was weighed into a 30mL screw cap bottle and mixed with 30 mL distilled water. The samples were shaken on a roller shaker overnight at room temperature. An aliquot of 10mL was then placed into centrifuge tube and centrifuged in a Multex centrifuge at 4000rpm (1500 g) for 10 min. 100 μ L aliquots of the supernatant were taken in duplicate and placed in glass test tubes. 1mL of a 2.5% phenol solution was added together with 2.5mL of concentrated sulphuric acid. The mixture was then vortexed carefully and left to stand for 30 min until it cooled down. The solution was then transferred to a disposable cuvette and the absorbance was read at 490nm.

The results were converted to equivalent glucose amounts using a calibration curve obtained using a range of glucose solutions (0 to 1000 μ g/ml). Four replicates were measured per samples, the variation coefficient was less than 6%.

III.2.13 Lipid extraction

Lipid extraction has been performed on maize grits extruded with linoleic acid (see Chapter VII). The method used was developed by Morrison (1980).

Extrudates were ground in a cyclotec sample mill fitted with a 0.5mm screen. Ground extrudates (1g) were mixed with 16mL water saturated butanol in a screw cap tube. The tubes were then transferred to a boiling water bath for 6 hours. The solvent was changed every hour. At the end of the extraction, the samples were left on a tray in the fume cupboard to evaporate the solvent overnight then transferred to a desiccator with

P_2O_5 and stored under vacuum. These lipid-extracted extrudates were then analysed for intrinsic viscosity (see Chapter VII).

III.2.14 Free Fatty acid content

The measure of fat acidity should reflect the amount of fatty acids hydrolysed from the triacylglycerols. Although acid phosphates and amino acids can also contribute to acidity, in fats and oil, fatty acids should be the prominent factors of acidity.

The method used in Chapter VII is the approved AOCS method 940.28 and why used to determine why amylose-lipid complexes were formed with some types of fats and not other.

Oil or fat (7.05g), pre-melted if necessary, were weighed in a 250ml flask. Ethanol (50mL) was mixed with 2mL of 1% phenolphthalein solution and enough 0.1N NaOH to produce a faint permanent pink colour. This solution was then added to the fat and stirred on a magnetic plate. The fat solution was titrated with 0.25N NaOH solution until a permanent pink colour appeared and persisted for more than 1 min.

The amount of 0.25N NaOH solution corresponds to the percentage of free fatty acid expressed as oleic acid. Measurements were performed in duplicates, no more than 0.1mL difference between measurements was accepted.

CHAPTER IV EFFECT OF GRINDING ON DRY PET FOOD MIX AND EXTRUDATES CHARACTERISTICS



The first operation of the dry pet food process is to transform the raw materials into a powder of suitable particle size for extrusion. This process can be done using different types of grinders and methods of grinding that will impact on the ground material characteristics. As described in chapter II, grinding can have an impact on ingredients especially starch. In this chapter, the effect of different grinding methods was evaluated first for two types of pet food recipes in order to determine if differences were perceived on commercial products. Subsequently, different types of ingredients were ground separately in order to assess the impact of grinding on the different components of the mix.

IV.1 EXPERIMENTAL SETUP

Two recipes of industrially made premixes were provided by Pedigree Masterfoods. High cereal (HC) and high protein (HP) recipe compositions are given in Chapter III. Both recipes were ground by three different methods labelled A, M and L. The three methods are described in Chapter III.

The six premixes were assessed for particle size distribution, RVA pasting properties, water solubility, water absorption indexes (WSI/WAI), protein solubility, particle charge and starch gelatinisation enthalpy (ΔH).

In order to test if the effect of grinding on the dry mix would have an effect on extrusion and the subsequent characteristics of the finish product, extrudates from the

six different mixes were produced by Pedigree Masterfoods using their pilot plant facility.

The information on processing conditions was provided by Masterfoods. The extrusion trial was done on a single screw extruder combined with preconditioner. The following throughputs were used.

Table IV-1: High cereal (HC) and high protein (HP) recipe throughputs in kg/h.

	<i>Dry mix</i>	<i>Premix water</i>	<i>Premix steam</i>	<i>Barrel water</i>
High Cereal	245	35	22	18
High Protein	245	35	12	25

Table IV-2: Extruder characteristics for HP and HC recipe from different grinding methods.

	<i>Process M</i>	<i>Process A</i>	<i>Process L</i>
<i>High Cereal</i>			
Amps drawn (A)*	26	27	27
Die Temperature (°C)	101	109	104
Die pressure (Bar)	13	11	14
Moisture exit extruder (% wb)	28.4	28.6	28.9
<i>High Protein</i>			
Amps drawn (A)*	28	28	27
Die Temperature (°C)	63	59	57
Die pressure (Bar)	10	10	10
Moisture exit extruder (% wb)	27.6	28.1	29

*: extruder engine electrical power.

The extruded pellets were then assessed for RVA pasting, total charge and protein solubility using methods described in chapter III. Bulk density of the pellets was also measured using oilseed rape. A 50 mL measuring cylinder was filled with 30 mL oilseed rape and weighed, an extruded pellet was then added and the displaced volume was recorded as well as the change in weight. This method is described in Chapter III.

The persistence of the effect of grinding after extrusion was further investigated by performing another extrusion trial on HC mixes. The extrusion was carried out in a Cleextral BC21 twin screw extruder under more controlled conditions. The feed rates were 6.9 kg/h for dry mix and 2 L/h for water. The screw speed was 125rpm and the final temperature of the barrel was 120°C.

The specific mechanical energy (SME) was determined as well as the sectional expansion index (SEI). The extrudates were cut into ropes of 15 cm length sealed under vacuum and frozen in liquid nitrogen to prevent sample retrogradation and then stored at -20°C. For RVA analysis, protein solubility and total charge, the samples were then cut into smaller pieces (~ 5 cm) and dried in an oven at 105°C for 40min. The dried pellets were then ground in a cyclotec sample mill fitted with a 1mm screen.

After assessment of the effect of grinding on full dry mix, the effect of grinding was further investigated to determine the changes in individual ingredients.

Maize, broken rice, poultry meal and maize gluten were the four ingredients studied. Two milling methods were used to mimic a mild and a strong treatment. The mild method used a Knifetec sample mill (Trecator) for 30s. Knifetec is a cutter mill with a water-cooled chamber. The harsh method used a Retch hammer mill fitted with a 2mm screen, the material was ground using 4 passes. Additionally, two “model” mixes were prepared using a mixture of 50% poultry meal and 50% whole maize. These mixes were ground either with the two ingredients together (MixT) or separately (MixS).

The energy dispersed during grinding was determined using current intensity measurement using an ampere meter (MX220, ITT instruments) and sample temperature was measured using a thermocouple at the end of the run.

The ground samples were then assessed for moisture content, particle size distribution using Mastersizer, RVA pasting properties, protein solubility and DSC. These methods are described in Chapter 3.

IV.2 EFFECT OF GRINDING ON INDUSTRIAL PREMIXES AND THEIR EXTRUDATES

The six premixes supplied were studied to see if the conditions used in their preparation caused variations in: their particle size, hydration characteristics, properties of starch (gelation) and protein (total charge and solubility).

IV.2.1 Difference in particle size distribution

When viewed by the light microscope, with or without polarised light, no clear differences could be observed between the groups of HC and HP. Therefore to get values of particle size, laser light scattering was used.

As the use of air as a dispersant was not possible using the equipment available, dry powders had to be dispersed in a solution to measure particle size distribution. As the nature of the interactions that might occur between the sample and the dispersant were not known, two dispersants have been used: water and 2-propanol (IPA). The particle size distribution is represented in Figure IV-1 and Figure IV-2.

The graphs show that the distribution of the different premixes depends on the dispersant used and the recipe but the grinding method used to produce the premixes has little effect on the overall distribution. Table IV-3 reports the modal diameters of the premixes in both water and IPA. As can be seen on the graphs, there is little significant difference between the samples having the same recipe. It is especially interesting to note that there is more difference between samples when dispersed in water than in IPA.

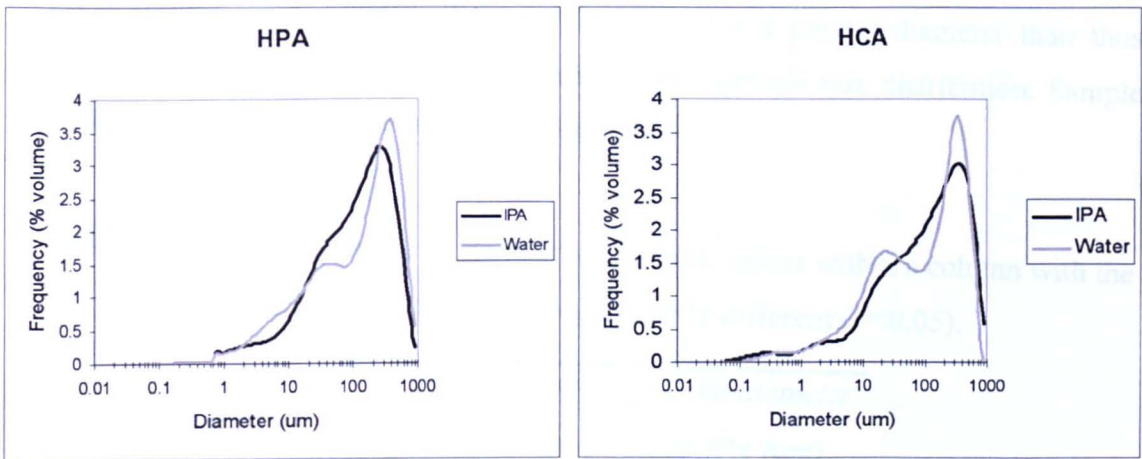


Figure IV-1: Comparison of particle size frequency distribution in two dispersants (water and IPA) for HCA and HPA mixes.

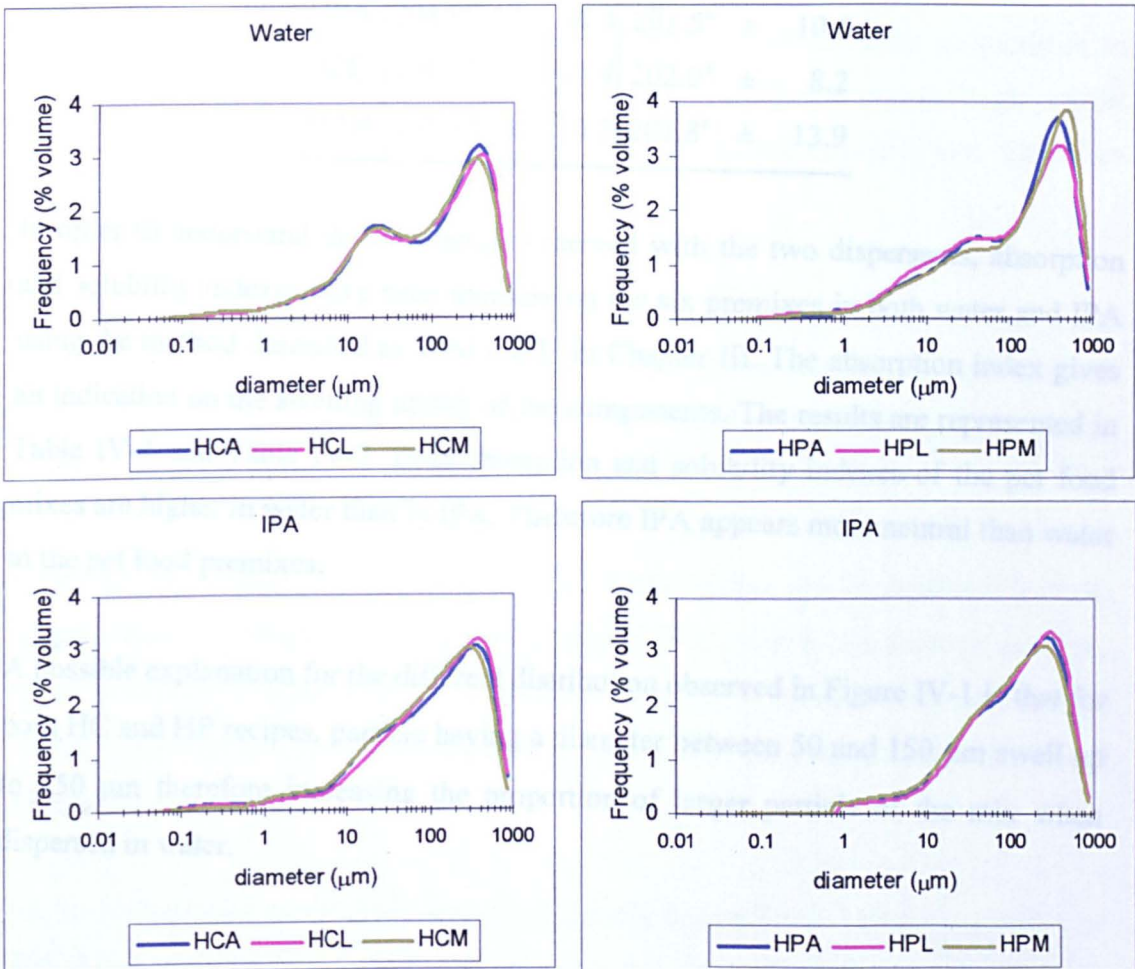


Figure IV-2: Particle size distribution of HC and HP samples dispersed in water or in IPA.

As a general trend, samples dispersed in IPA have a greater diameter than those dispersed in water and have a more homogeneous particle size distribution. Samples dispersed in water exhibit a bimodal distribution.

Table IV-3: Modal diameter (\pm standard deviation), values within a column with the same superscripts are not significantly different ($P < 0.05$).

	<i>Modal diameter in water (μm)</i>	<i>Modal diameter in IPA (μm)</i>
HCA	181.9 ^a \pm 11.0	210.9 ^a \pm 11.9
HCL	174.8 ^{ab} \pm 28.7	226.5 ^b \pm 9.4
HCM	170.6 ^b \pm 9.5	200.6 ^a \pm 12.5
HPA	201.9 ^{bc} \pm 18.4	201.5 ^a \pm 10.6
HPL	191.6 ^{ac} \pm 14.4	202.0 ^a \pm 8.2
HPM	230.4 ^d \pm 13.2	207.8 ^a \pm 13.9

In order to understand the differences observed with the two dispersants, absorption and solubility indexes have been measured on the six premixes in both water and IPA using the method described as WAI / WSI in Chapter III. The absorption index gives an indication on the swelling ability of the components. The results are represented in Table IV-4 and Table IV-7. Both absorption and solubility indexes of the pet food mixes are higher in water than in IPA. Therefore IPA appears more neutral than water to the pet food premixes.

A possible explanation for the different distribution observed in Figure IV-1 is that for both HC and HP recipes, particles having a diameter between 50 and 150 μm swell up to 350 μm therefore increasing the proportion of larger particles of the mix when dispersed in water.

Table IV-4: Absorption and solubility index of the pet food premix in IPA. Results are average of 4 measurement (\pm standard deviation).

	<i>Absorption Index (g/g dry matter)</i>			<i>Solubility Index (% dry matter)</i>		
HPA	1.05	\pm	0.00	4.87	\pm	0.85
HPL	1.05	\pm	0.00	4.36	\pm	0.74
HPM	1.06	\pm	0.02	4.01	\pm	0.77
HCA	1.04	\pm	0.02	2.91	\pm	0.62
HCL	1.05	\pm	0.01	3.32	\pm	0.53
HCM	1.05	\pm	0.00	3.33	\pm	0.11

IV.2.2 Effect on RVA pasting curve and starch properties

The two recipes exhibit very different profiles due to their different composition in starch (the high cereal recipe (HC) contained 50.2% starch whereas the high protein recipe (HP) contained only 31%). The sources of starch are also different. Therefore the 2 recipes cannot be directly compared by RVA.

Nevertheless, the effect of the grinding process might be observed in both cases (Figure IV-3 and Figure IV-4). There are significant differences between the different processes and this can be shown especially by studying the final viscosity (Table IV-5).

When the whole sample is analysed, significant differences are demonstrated for both recipes. Whereas, when only the sieved fraction 125-250 μm is analysed, to avoid the effect of different particle size, the differences seems to be less obvious in the case of the high cereal recipe. Peak viscosities were significantly different for both sieved and non sieved samples.

For the high protein recipe, HPL has a significantly higher final viscosity than HPA or HPL. Final viscosity is believed to be related to the ability of starch to form a gel and therefore to its molecular weight. Therefore, HP samples ground with the one pass process seem to be less damaged than the samples ground by two passes. For the high cereal recipe samples, there was no significant difference in final viscosity. But peak viscosity was significantly higher for HCL compared to HCM and HCA. Peak

viscosity is believed to be related to the ability of starch to absorb water; therefore HC samples processed with one pass grinding seem to have a higher water absorption capacity than sample processed with two pass grinding. This was confirmed by WAI measures (see Table IV-7).

Table IV-5: Final viscosity of the different premixes (in a standard profile analysis).

Samples with different superscripts inside one column are significantly different ($P < 0.05$). Values are average of 3 measurements, StDev is the standard deviation.

	<i>Total sample (in cP)</i>		<i>Sieve fraction 125-250 μm (in cP)</i>	
	Mean	StDev	Mean	StDev
HPA	533 ^a	34	489 ^a	57
HPL	1060 ^b	81	867 ^b	65
HPM	577 ^a	70	525 ^a	58
HCA	6359 ^c	172	5361 ^c	254
HCL	6782 ^d	135	5488 ^c	243
HCM	6435 ^{cd}	370	5095 ^c	376

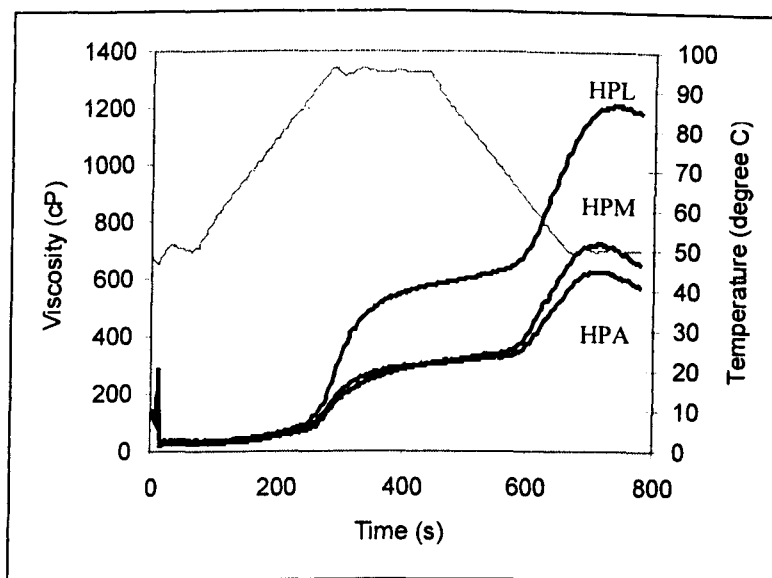


Figure IV-3: RVA standard profile, high protein recipe premix ground by 3 different processes (A, L, M). Measurements done on the whole sample.

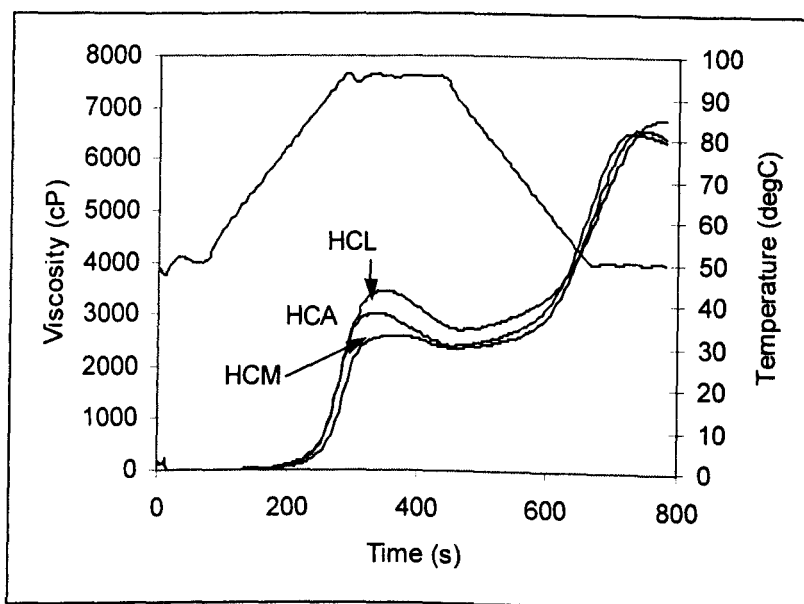


Figure IV-4: RVA standard profile of high cereal recipe premix ground by 3 different processes (A, L, M). Measurements done on the whole sample.

Correlation between final viscosity and starch conversion detected by DSC has been attempted. DSC was used to measure the starch gelatinisation enthalpy as a measure of the state of starch in the sample. The results are given in Table IV-6.

High protein recipe samples had lower and less reproducible ΔH (calculated in J per g of starch) than high cereal recipe. This could be due to the problem of sampling a representative 10mg sample or the difference in sample water repartition in the sample. Indeed, HP samples contain beet pulp, which is a fibrous material. Fibres are known to have a higher binding capacity than starch, therefore complete starch gelatinisation in the DSC pan might have been prevented due to a lack of available water.

HC samples are more reproducible. Results showed a significant difference between HCA, HCL and HCM. HCA had the lowest enthalpy variation whereas HCL had the highest. This could be due to a difference in starch content or a difference in the state of starch. There was no significant difference in starch content of the different samples for each recipe so the difference could only come from a difference in the state of starch. A lower enthalpy of gelatinisation therefore can be related to a lower amount of native starch. The results showed that the enthalpy of gelatinisation was

significantly higher for the one pass process (L) compare to the two-pass process (A). This correlate well with the RVA final viscosity values measured on the total sample (Table IV-5).

To confirm those results, water absorption / water solubility index have been measured as well.

Table IV-7 shows that the WAI of the high protein recipe is higher than the one of the high cereal recipe. As mentioned earlier this result was expected as HP contains water-binding fibbers. Due to the complexity of the recipe, it is difficult to determine if the variations in water absorption or water solubility are due to starch damage or to other factor. Especially, it can be noted that although HCL seemed to have less starch damage than HCA and HCM, it exhibits the highest WAI.

Table IV-6: Enthalpy of gelatinisation of the different recipe types at a 3:1 water to dry matter ratio (average of 2 measurements \pm standard deviation).

	ΔH (J/g starch)		
HCA	8.90	\pm	1.31
HCL	15.82	\pm	-
HCM	14.62	\pm	0.19
HPA	5.50	\pm	5.57
HPL	2.00	\pm	0.67
HPM	0.47	\pm	0.21

Table IV-7: Water absorption (WAI) and water solubility (WSI) indexes for HC and HP dry mixes. (\pm standard deviation). Values are averages of 4 measurements.

	WAI (g/g db)			WSI (% db)		
HPA	3.40	\pm	0.03	0.16	\pm	0.00
HPL	3.25	\pm	0.06	0.13	\pm	0.00
HPM	3.30	\pm	0.02	0.16	\pm	0.00
HCA	2.80	\pm	0.01	0.10	\pm	0.00
HCL	2.97	\pm	0.05	0.09	\pm	0.01
HCM	2.80	\pm	0.11	0.09	\pm	0.00

IV.2.3 Effect on protein solubility and surface charges

Results from PCD-Mutek are presented in Table IV-8. The premixes were anionic and exhibited differences according to their composition as well as the grinding conditions. On average, the high protein recipe premix had a lower total charge per gram of protein than the high cereal premix. This might be an effect of the different sources of proteins present in the 2 recipes. Finally, it can be noticed that the process L in both recipes had the highest amount of charges.

Protein solubility was measured using the Lowry method described in chapter III. The value of the absorbance at 750nm gives an indication of the solubility of the proteins. Table IV-8 shows that HP has a significantly higher absorbance due to its higher protein content, but no significant difference could be detected between the different grinding methods.

Table IV-8: Total particle charge and protein solubility (absorbance) of the 6 premixes. Values with different superscripts are significantly different ($P < 0.05$).

Values are average of six measurements.

	<i>Total negative Charge ($\mu\text{eq/g protein}$)</i>	<i>Standard Deviation</i>	<i>Absorbance at 750nm</i>	<i>Standard Deviation</i>
HCA	694 ^a	11	0.289 ^a	0.022
HCL	727 ^b	3	0.285 ^a	0.029
HCM	703 ^{ac}	29	0.285 ^a	0.032
HPA	418 ^d	17	0.366 ^b	0.056
HPL	456 ^c	9	0.363 ^b	0.012
HPM	372 ^f	5	0.368 ^b	0.019

IV.2.4 Persistence of the effect of grinding after extrusion

The results would indicate that there were differences in the samples due to their preparation methods. A and M seemed very similar, but L samples were clearly different.

IV.2.4.1 Pilot single screw extrusion

In order to know if the differences induced by the grinding process have an effect on the extrusion process and the properties of the final product, Pedigree Masterfoods produced dried extruded pellets from the 6 premixes using a pilot plant. These pellets have been analysed by the same tests as the ground raw materials.

IV.2.4.1.1 Pasting and starch properties

The energy consumption during extrusion gives an indication of the mechanical energy drawn into the system. All HC samples presented the same amount of energy consumed. This was similar for HP samples. HP had a slightly higher energy input than HC, this could be due either to the recipe difference or the slightly different preconditioning conditions used. Only die pressure was slightly different for samples ground in different ways.

For both recipes, no cold swelling peak has been detected by the RVA when the standard temperature profile was applied (Figure IV-5 and Figure IV-6). For both recipes a “hot” peak viscosity was shown. Observations under the microscope with polarised light also showed that native starch granules were still present after extrusion.

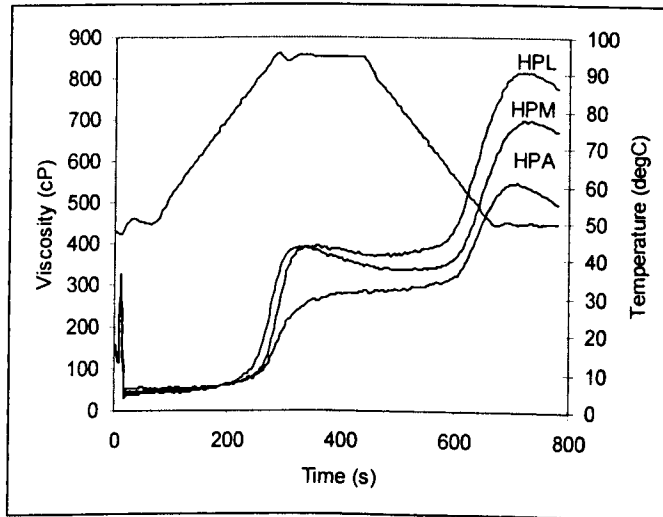


Figure IV-5: RVA profile of the high protein recipe (HP) extrudates. A, L and M are the different mixes (average of three measurements).

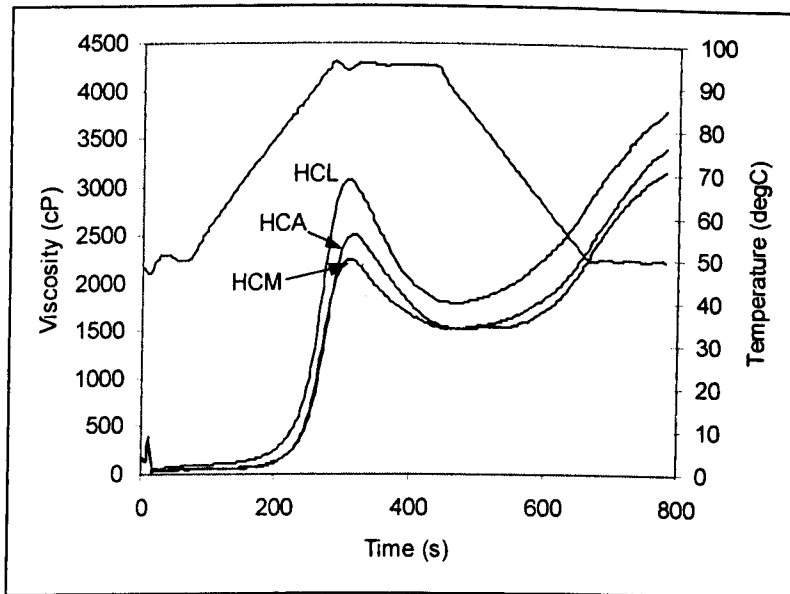


Figure IV-6: RVA profile of the high cereal recipe (HC) extrudates (average of 3 measurements).

As for the premix, values of the final viscosity have been analysed. The effect of sieving was found to be less significant for the extrudates than for the premix. This might be an effect of the greater heterogeneities in the premix than in the ground extrudates and of how representative was the sieve fraction.

Significant differences have been found between the different processing conditions for both recipes (Table IV-9). The extrudates L had the highest peak viscosity and final viscosity as for the raw premix.

Table IV-9: Final viscosity of the extrudates (average of 3 measurements, StDev is standard deviation). Samples with different superscript inside one column are significantly different ($P < 0.05$).

	<i>Total sample</i>		<i>Sieve fraction 125-250 μm</i>	
	Mean	StDev	Mean	StDev
HPA	498 ^a	18	476 ^a	27
HPL	778 ^b	19	790 ^b	33
HPM	676 ^c	20	636 ^c	29
HCA	3421 ^d	113	3375 ^d	48
HCL	3816 ^e	166	3623 ^e	18
HCM	3188 ^f	119	3005 ^f	45

IV.2.4.1.2 Particle charge analysis

Results are presented in Table IV-10. The differences between the 2 recipes were similar to that found with the raw premix, HC had higher total charge per gram protein than HP. While after extrusion HC samples exhibited lower total charge, HP samples exhibited similar or higher total charge than the ground raw materials.

Table IV-10: Total charge and protein solubility of the extruded samples after grinding. Values are average of 6 or 9 measurements. (values with different superscript within one column are not significantly different ($P < 0.005$)).

	<i>Total negative charge ($\mu\text{eq/g protein}$)</i>	<i>StDev</i>	<i>Absorbance at 750 nm</i>	<i>StDev</i>
HCA	607 ^a	7	0.241 ^a	0.071
HCL	582 ^b	8	0.193 ^a	0.040
HCM	585 ^b	9	0.166 ^a	0.035
HPA	455 ^c	11	0.296 ^b	0.033
HPL	445 ^c	10	0.302 ^{bc}	0.034
HPM	401 ^d	13	0.312 ^c	0.038

The protein solubility measurements (Table IV-10) showed reduced solubility of HC and HP extrudates compared to the raw dry mix. HC recipe still exhibited lower absorbance compared to HP. No significant difference was found between the different grinding process.

In order to check the validity of the results obtained in the pilot plant, twin screw extrusion of the high cereal recipe was performed in order to look at the differences between the different extrudates after extruding under more controlled conditions. Extrusion of high protein recipe sample with the twin-screw extruder without a preconditioning step was difficult due to the low amount of starch and produced unexpanded samples. Therefore, the analysis focused especially on high cereal recipe samples.

IV.2.4.2 Twin screw extrusion of high cereal recipe dry mixes

After extrusion and drying the twin screw extrudates HCA, HCL and HCM have been dried to a moisture content of 13.5, 10.1 and 11.0 % (w/w wb) respectively. Then extruded pellets have been ground in a cyclotec sample mill in the same way as single-screw extrudates.

The samples have been run in the RVA using a standard temperature because no cold water swelling peak was detected using an extrusion profile. This was similar to the pilot plant samples.

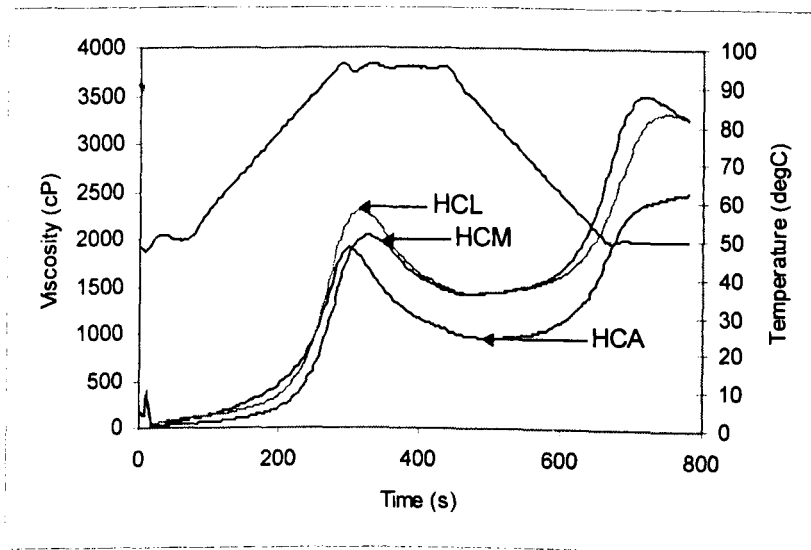


Figure IV-7: Pasting curve of twin screw extrudates from high cereal recipe (HC) premix A, L and M. (average of 3 measurements)

The profiles obtained were different from the ones obtained with the pilot plant samples. Nevertheless, the three samples exhibited different profiles and a significantly different final and peak viscosity.

IV.2.4.3 Total charge and protein solubility determination

The total charges of the three samples were also significantly different. It can be noticed that the transformations induced by the extrusion processes in term of total charges are different. While the twin-screw extrusion produced extrudates with particle charge similar or higher to the dry mix, the single screw extrusion process produced extrudates with a significantly lower particle charge.

Table IV-11: Total surface charges of HCA, HCL and HCM sample before and after both extrusion method, \pm standard deviation. SS=single screw, TS=twin screw.

Values are average of 6 measurements.

	<i>Before</i>	<i>After: SS</i>	<i>After: TS</i>
HCA	694 \pm 17	607 \pm 7	748 \pm 8
HCL	727 \pm 9	582 \pm 8	838 \pm 23
HCM	703 \pm 5	585 \pm 9	764 \pm 23

Table IV-12: Protein solubility measured by the Lowry method. Values are average of 9 measurements.

	<i>Absorbance at 750nm</i>	
HCA	0.246 \pm	0.008
HCL	0.236 \pm	0.011
HCM	0.232 \pm	0.005

Other experiments have been done to characterise further the differences induced by the grinding process on extrusion. The sectional expansion index of the twin screw extrudates have been determined. HCA, HCL and HCM had a sectional expansion index of 2.5, 3.6 and 2.5 respectively.

As the SEI of the pilot plant pellet had not been provided, the bulk density of the pellets has been determined using the rapeseed method and a comparison was made with the pellets produced using the laboratory twin screw extruder. The extrudates were dried completely prior to measurement in order to avoid difference due to moisture.

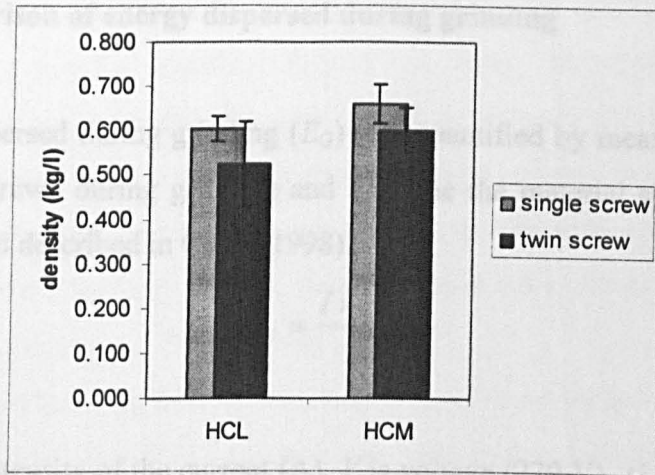


Figure IV-8: Density of single and twin-screw extrudates after complete drying. Error bars are confidence intervals.

The extrudates produced from both methods showed the same trends. HCL had a higher expansion and a lower density than HCM. The grinding process might influence the expansion of the final product.

IV.3 EFFECT OF GRINDING ON INGREDIENTS

In order to understand better the effect of grinding on single ingredients, four commonly used raw materials were supplied by Masterfoods: two cereal sources (whole maize and whole rice) and two protein source (maize gluten and poultry meal). A model mix was prepared by mixing poultry meal and whole rice in a 1:1 ratio. The mix was prepared either by grinding both ingredients together (MixT) or by grinding the ingredients separately and then mixing them (MixS). Two grinding treatments were also used labelled "harsh" and "mild". The harsh treatment was a four pass grinding process in a hammer mill whereas the mild grinding method was a single pass grinding in a cooled, cutter mill.

IV.3.1 Comparison of energy dispersed during grinding

The energy dispersed during grinding (E_G) was quantified by measuring the intensity of the current drawn during grinding and the time the material spent in the grinder using the method described in Carre (1998).

$$E_G = \frac{I \times V \times t_T}{wt_T}$$

Where I is the intensity of the current (A), V is voltage (220 V), t is the total grinding time (s) and wt_T is the total weight of material (g).

For the harsh method, the samples were passed four times into the grinder; therefore the total energy was calculated as the sum of the energy dispersed for each pass.

The variation of temperature of the sample (before and after grinding) was also recorded. All these measurements are represented in Table IV-13.

Table IV-13: Grinding energy (E_G) and variation of temperature (ΔT) of the material after grinding.

	E_G (J/g)		ΔT (°C)	
	Mild	Harsh	Mild	Harsh
Maize	557	1211	6.0	9.8
Rice	528	894	5.0	11.7
Maize gluten	543	821	9.5	11.2
Poultry meal	426	837	8.2	10.5
MixT	482	740	6.9	9.7

Table IV-14: Grinding energy and variation of temperature of the material after grinding – reproducibility test.

	E_G (J/g)		ΔT (°C)	
	Mild	Harsh	Mild	Harsh
Maize	546	483	5.3	3.5
Poultry Meal	412	524	11.1	14.3
MixT	468	673		8.65

All materials presented a higher E_G and a higher ΔT when milled with the harsh method than with the mild one. Therefore, the two methods selected give a good

segregation between harsh and mild grinding process. Maize, poultry meal and mixT were duplicated to test the reproducibility of the energy recording method. Table IV-14, shows that although for the mild grinding method, the results are fairly reproducible, for the harsh method, the reproducibility is low. Indeed, in the harsh grinding method the total grinding time is an average obtained measuring the total time needed to grind a batch of sample. This method is not accurate and influence by the irregularity of the material flow into the grinder.

Nevertheless, it can be noted that poultry meal presents a lower grinding energy than the other cereal meals, probably due to its lower particle size and hardness. ΔT for the protein meals is generally higher than for the cereals. This could be due to the difference in initial particle size of these different materials.

The energy used to grind MixT is slightly lower than the “theoretical energy” used to grind MixS corresponding to the sum of the energies dispersed to grind the same weight of maize and poultry meal.

Moisture content of the different materials was also checked before and after grinding (Table IV-15). After grinding with the milder method, the moisture content does not change significantly. But materials ground with the harsh method have a moisture content lower than the initial value.

Table IV-15: Moisture content (% wb) of the different materials before and after grinding (results are average of 3 measurements)

	<i>BEFORE</i>		<i>MILD</i>		<i>HARSH</i>	
	MC (%)	Stdev	MC (%)	Stdev	MC (%)	Stdev
Maize	14.5	0.06	14.6	0.06	12.9	0.03
Rice	12.6	0.14	12.9	0.05	12.1	0.03
Poultry Meal	2.4	0.06	2.4	0.03	2.8	0.09
Maize Gluten	11.5	0.06	10.9	0.09	9.9	0.08
MixT	-	-	8.4	0.08	7.6	0.10

IV.3.2 Particle size distribution

Particle size distribution has been determined by small angle laser light scattering using isopropanol (IPA) as a dispersant. The results are presented on Figure IV-9.

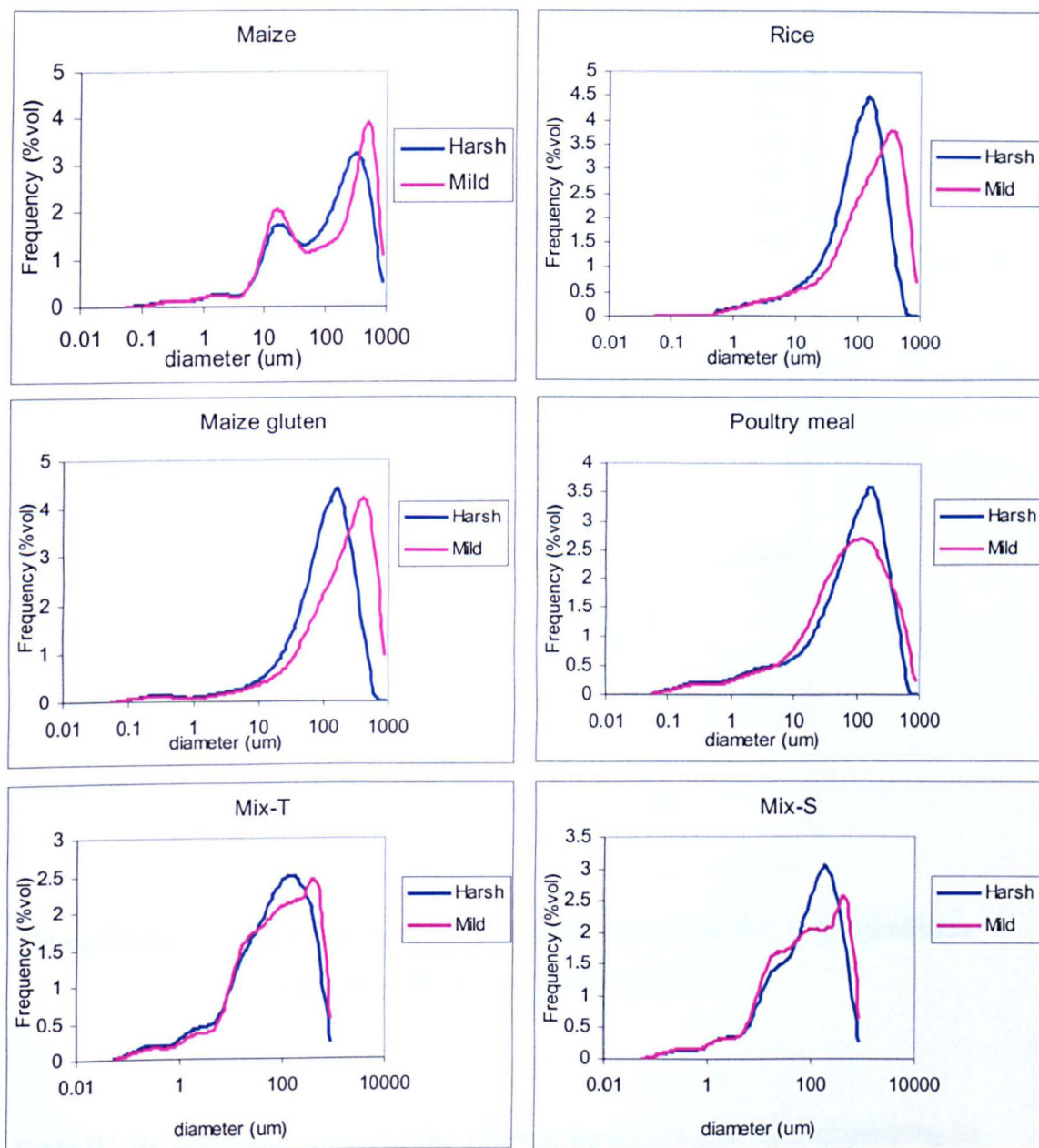


Figure IV-9: Particle size distribution of the different materials and mixes determined by small angle laser light diffraction. (average of 3 replicates).

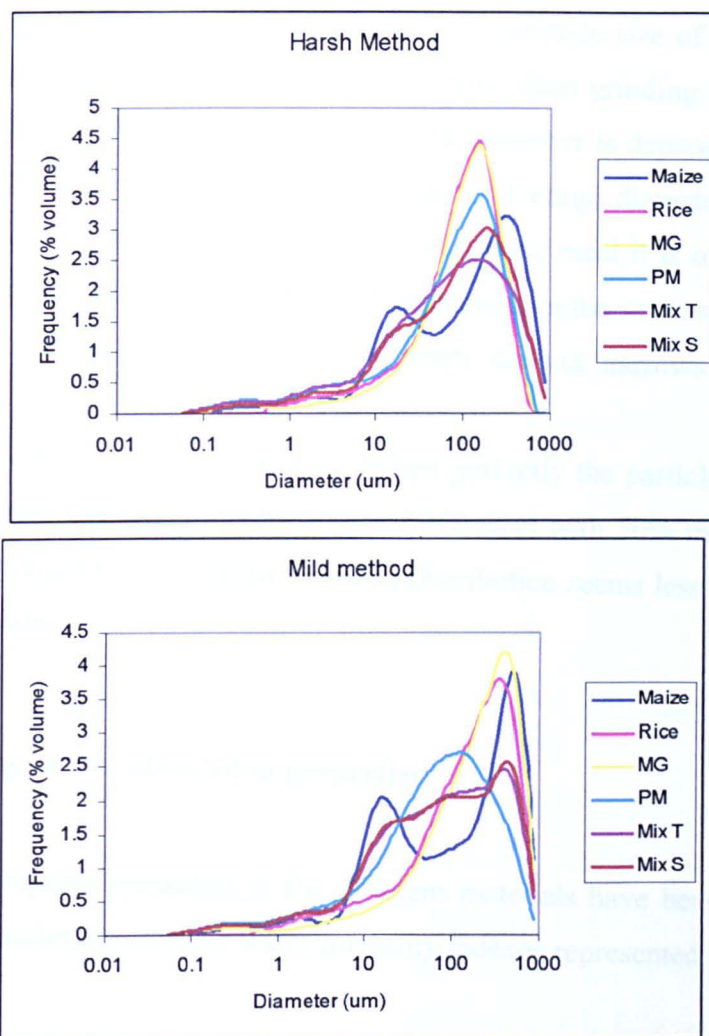


Figure IV-10: Comparison of particle size distribution of the different ingredients ground by the mild or harsh method.

Table IV-16: Average diameter of the different ingredient ground after grinding by the two methods (average of 3 measurements) and percentage of difference between the two methods for each ingredient.

<i>Sample</i>	<i>Harsh</i>	<i>Mild</i>	<i>% variation</i>
Maize	181 ± 7	220 ± 16	22.0
Rice	123 ± 2	221 ± 14	80.6
Maize Gluten	131 ± 3	249 ± 8	89.4
Poultry Meal	120 ± 6	131 ± 17	9.4
Mix-T	133 ± 3	167 ± 1	21.8
Mix-S	148 ± 2	168 ± 5	13.8

The results in Table IV-16 show that the average particle size of all the materials is lower when grinding with the harsh method than when grinding with the mild one. The difference introduced by the use of different grinder is dependent as well on the ingredient type. Rice and maize gluten have an average diameter more than 80% higher by using the mild method, whereas for poultry meal it is only 9%. Therefore the use of different mills will not affect all ingredients in the same way.

It can be noted as well that using the harsh method narrows the particle size distribution.

The particle size distribution of MixS matched perfectly the particle size distribution obtained theoretically when mixing 50% poultry meal with 50% maize. By grinding ingredient together (Mix-T), the particle size distribution seems less spread than when grinding separately.

IV.3.3 Pasting / water absorption properties

The water absorption properties of the different materials have been determined by measuring the water absorption / water solubility indexes represented in Table IV-17.

Table IV-17: Water absorption and solubility index (WAI/WSI) of the different material after grinding by the 2 methods \pm standard deviation (average of 3 measurements).

		<i>WAI (g/g dry)</i>	<i>WSI (% dry)</i>
Maize	Harsh	3.1 \pm 0.04	7.4 \pm 1.3
Maize	Mild	3.0 \pm 0.01	6.8 \pm 0.2
Rice	Harsh	3.0 \pm 0.08	5.1 \pm 2.7
Rice	Mild	2.8 \pm 0.08	4.1 \pm 0.5
Poultry meal	Harsh	3.1 \pm 0.07	19.3 \pm 0.3
Poultry meal	Mild	3.1 \pm 0.04	18.9 \pm 0.2
Mix T	Harsh	3.1 \pm 0.03	15.2 \pm 0.4
Mix T	Mild	3.1 \pm 0.04	13.2 \pm 0.9
Mix S	Harsh	3.2 \pm 0.06	14.4 \pm 0.7
Mix S	Mild	3.2 \pm 0.08	14.4 \pm 0.9
Maize Gluten	Harsh	3.4 \pm 0.07	6.5 \pm 0.2
Maize Gluten	Mild	3.3 \pm 0.13	9.6 \pm 0.8

The results show that for maize, rice and maize gluten the WAI is higher for sample processed with the harsh treatment than with the mild treatment. This could be due to an effect of particle size or the presence of more damaged starch granule. Damage starch granules are known to have a higher water binding capacity than native starch (Lelievre 1974). Maize and rice also present a higher solubility when processed with the harsh method whereas maize gluten solubility is lower with the harsh method.

MixT, MixS and poultry meal are not affected by the grinding method for their WAI and WSI. MixS appears to have a slightly higher WAI than MixT, but their solubility is similar.

Therefore the effect of the grinding method seems to be less apparent for a mixture of ingredients compare to the ingredients taken separately.

To investigate further the effect of grinding on water binding / water solubility.

Pasting experiments have been carried out using the RVA.

Figure IV-12 represents the pasting curves for rice and maize milled by the two methods. For both cereals, the results were similar. The pasting temperature was lower for the cereals ground with the harsh method than the mild. The Peak viscosity was higher for the harsh treatment and the final viscosity was higher for the mild treatment. This behaviour indicates that the amount of starch damage is higher for the harsh treatment.

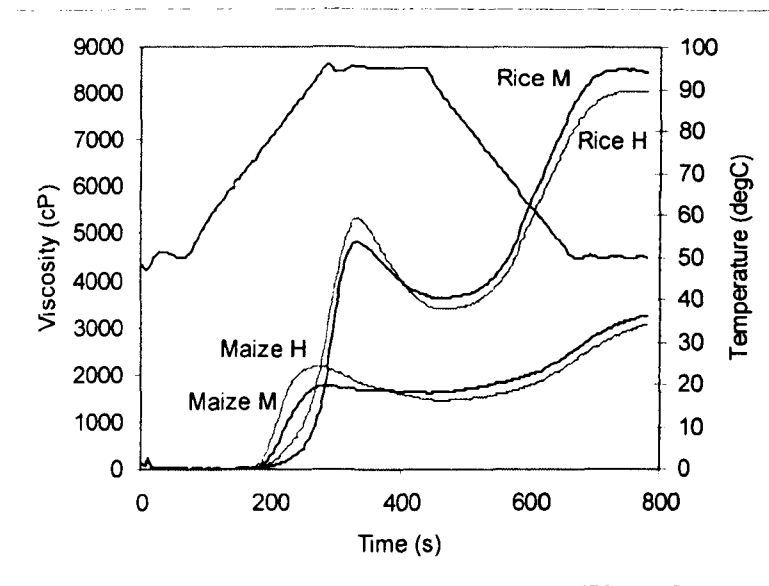


Figure IV-11: Pasting curve of sieve fraction 125 – 250 µm of rice and maize processed by the harsh (H) or mild (M) grinding method.

The RVA was also used for a suspension of poultry meal or maize gluten alone with the same concentration as the cereal meals, the viscosity recorded was nil for both type of samples, therefore it was concluded that the viscosity reading for the mixes should be the result of the effect on starch alone. Figure IV-12 represents the pasting curve for the different mixes. The effect of the different grinding methods on the mixes is different to the effect observed on individual ingredients.

There was no significant difference in pasting temperatures between the different mixes and the different grinding treatments. When the mixes were ground with the mild method, the pasting curves were similar whether the ingredients were ground together or separately. But with the harsh grinding method, a marked difference appeared between the two mixes. The peak and the final viscosity were much higher for the sample ground separately than when the samples were ground together. This highlights the interactions that can occur between ingredients during mixing.

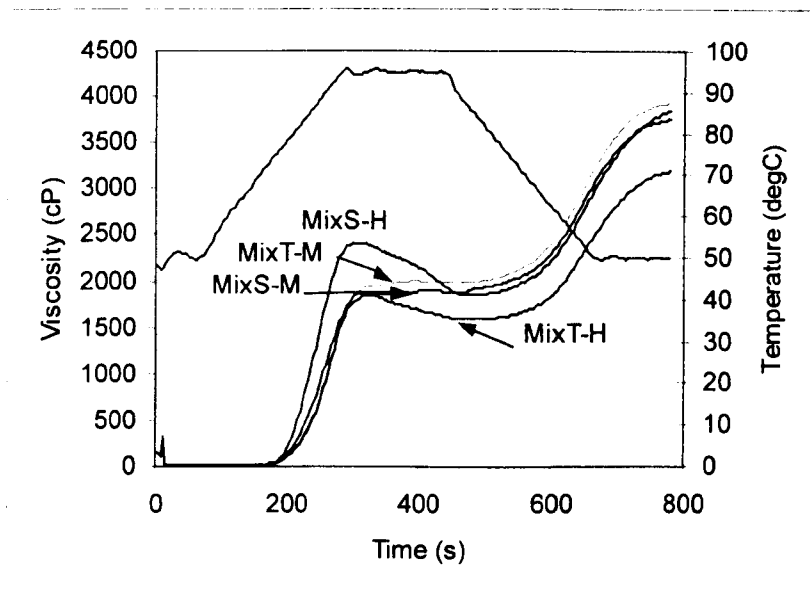


Figure IV-12: RVA pasting curve of MixS and MixT ground by the harsh (H) or mild (M) method.

DSC experiments were also performed to compare the different grinding methods and check the results obtained by RVA (Table IV-18). Maize and Mix presented a typical endotherm of gelatinisation. The onset temperature was higher for the mix than for the maize alone. This was agreeing well with the higher pasting temperature found for the mix compared to the maize alone as measured by RVA. This could be due to the presence of a high fat level in poultry meal retarding the water penetration in the starch granules. The enthalpy variation measured per gram of starch, was higher for the maize alone than for the mix. This could indicate that more starch damage occurs when the ingredients are ground together than when they are ground separately. The values of ΔH were also higher for the mild method than for the harsh method as predicted.

Table IV-18: Onset, end temperature and enthalpy variation for maize and MixT milled by two grinding methods. The results are average of two measurements performed in excess water.

	T_{onset} (°C)	T_{end} (°C)	ΔH (J/g starch)	
			Average	Standard Deviation
Maize-M	65.0	80.9	26.2	2.3
Maize-H	66.1	79.4	20.2	3.1
MixT-M	68.9	82.2	15.6	0.3
MixT-H	69.8	81.8	12.4	0.2

IV.3.4 Protein solubility

The mechanical and thermal energy exerted during grinding might not only affect starch but also protein. Especially, protein conformation might be changed or cross-linking could occur during the grinding process. To test this hypothesis, protein solubility, which would be affected by both changes was measured.

Table IV-19 shows the results of the protein solubility analysis. For poultry meal, the grinding method does not change the absorbance at 750nm, as the protein solubility is low already in the material before milling. This is probably due to the composition of the meal and the protein in poultry meal having been cooked previously to sterilise the meal.

On the contrary, maize gluten appeared affected by the grinding method. With the mild grinding method the protein solubility increased in comparison to the raw material. This could be due to an effect of particle size. But with the harsh grinding method, the protein solubility is lower than with the mild method. For Mix T and Mix S, the protein solubility is almost identical and only slightly influenced by the grinding method.

Table IV-19: Absorbance at 750 nm of samples ground by the two grinding method.

Results are the average of two measurements.

	<i>Raw</i>		<i>Mild</i>		<i>Harsh</i>	
	Average	Standard Deviation	Average	Standard Deviation	Average	Standard Deviation
Poultry Meal	0.297	0.002	0.286	0.016	0.296	0.001
Maize Gluten	0.653	0.011	0.742	0.004	0.683	0.019
MixT			0.201	0.004	0.205	0.005
MixS			0.223	0.003	0.200	0.004

IV.4 CONCLUSION

The grinding process influences the physicochemical characteristics of the dry mix by acting on the degree of starch damage and to a lesser extent, the protein characteristics. On the industrial mixes it was possible to observe the effect of the grinding process on starch characteristics. The two-pass process lead to the most starch damage as observed on pasting characteristics and water absorption indexes. The lowest starch damage was produced by the grinding process L were all the ingredients were ground together by a single pass. A slight difference was also observed on protein characteristics as shown by the particle charge measurements.

Although the extrusion process is a destructive method, the effect of the grinding process could still be observed on the characteristics of the dried pellets. Two types of extrusion were performed to make sure the difference observed on the pellet produced on a industrial scale pilot plant were still observed when using a more controlled method on a laboratory scale twin screw extruder. It was found that the characteristics of the pellets, like the bulk density, were well correlated with the state of starch determined by the grinding process. The highest expansion was obtained by the pellets produced by the process L, where the dry mix had the lowest starch damage and the highest water absorption index. These two characteristics often do not go together i.e. higher starch damage often leads to higher water absorption capacity.

Therefore, it was suspected that other components than starch were affected by grinding.

By studying the effect of grinding on the individual ingredients, it was shown that the effect of the grinding process is different depending on the ingredients. It was found that when using a harsh grinding treatment more starch damage was done when the ingredients were ground together than separately. It was noted that in this case, the temperature of the mix during grinding is also slightly higher when ingredients are ground together, therefore this could explain this difference in behaviour. Proteins seems to be also affected by the grinding process as the solubility of maize gluten meal is lowered when ground with a multi-pass grinding method compared to a single pass.

CHAPTER V EFFECT OF MODEL BATCH

PRECONDITIONING ON MAIZE GRITS AND MAIZE GRITS

EXTRUDATES



V.1 INTRODUCTION

Another unit operation used in various food industries prior to extrusion is preconditioning. A preconditioner is a closed vessel where the feed ingredients are mixed with water, steam and / or other liquid ingredients in order to increase their moisture and / or temperature (Harper 1981). Although widely used in the industry, there is little scientific understanding about this process. Previous published literature has focused mainly on the engineering aspects (Bouvier 1996; Levine 1995), but rarely on its effect on the raw materials (Caldwell 2000) or on extrusion (Mathew 1999b).

It was therefore necessary to investigate more closely the effect of preconditioning on a simple cereal matrix. In order to do so, a lab scale model batch preconditioner was developed and maize grits was chosen as a cereal matrix.

The parameters investigated were initial moisture content, residence time and particle size. The effect of these parameters on water absorption properties, starch conversion, bulk density and compressibility of the preconditioned material were studied.

The same batch preconditioner was used to characterise the effect of preconditioning on extrusion and extrudates properties.

V.2 CHARACTERISATION OF THE TRANSFORMATIONS OF THE RAW MATERIAL OCCURRING DURING PRECONDITIONING

V.2.1 Experimental set-up

V.2.1.1 Sample preparation

An orbital rotational paddle mixer fitted with a steam line was used to precondition maize grits as described in chapter III. Preconditioner residence time and initial moisture content was varied as followed:

- Residence time: 60, 120 and 240s
- Initial water level: 25, 65, 100 and 175mL, corresponding to an initial moisture content of 16.5, 21.5, 25.4 and 32.6% (w/w wb).

In order to obtain maize grits of different particle size, maize grits were milled as described in Chapter3. The modal diameters of the maize grits / flour are presented in Table V-1.

Table V-1: Particle size of milled maize grits (\pm standard derivation from 3 replications)

	Modal diameter (μm)		
Raw MG	476	\pm	1.7
Mild milling	335	\pm	0.8
Strong milling	240	\pm	4.4

Final temperature of the material was measured at the end of the run by a thermocouple. Final moisture content (FMC) was determined by drying a sample overnight in a 105°C oven (see chapter 3). FMC was between 17 and 41%, due to the absorption of the water from the steam.

H^1 -NMR measurements and texture analyses were performed on the moist material directly after preconditioning. Proton NMR measurement method is described in III.2.7. For the texture measurements the preconditioned material was sieved through a 2mm-screen sieve prior to analysis in order to remove lumps. The method used is described in III.2.6.

For RVA and X-ray diffraction, the preconditioned material was dried in a vacuum oven (Gallenkamp) at 70°C for 17h, then ground in a laboratory cutter mill (Knifetec, Tecator, U.K.) and stored in a dessicator. The method used to determine X-ray crystallinity index is described in III.2.4. For RVA analysis, the milled samples were further sieved and only the sieve fraction 125-250 μm was analysed to prevent particle size effects. Samples were then analysed using the parameters given in III.2.3.

V.2.1.2 Experimental design

A 3 \times 3 \times 3 full factorial design experimental plan was followed to study the effect of initial moisture content (iMC), residence time (RT) and particle size (PS) on preconditioned maize grits final temperature, final moisture content, RVA parameters and X-ray diffraction index. The levels of iMC were 16.5, 25.4 and 32.6% (w/w wb). RT was 60, 120 and 240s, and PS was 240, 335 and 476 μm .

To study preconditioned MG bulk density, compressibility and water mobility, particle size was not taken into account therefore a 4 \times 3 full factorial design was used, with iMC 16.5, 21.5, 25.4 and 32.6% (w/w wb) and residence time 60, 120 and 240s. Additional samples were prepared and analysed to better define the borders of the design.

Data was analysed on Design Expert (StatEase, U.K.) using a general linear model procedure. The coded factors used (-1, 0, 1) have been defined as represented in Table V-2.

Table V-2: Corresponding values for coded factors.

<i>Factor</i>	<i>-1</i>	<i>+1</i>
Residence Time (RT)	60	240
Particle Size (PS)	240	476
Initial moisture content (iMC)	16.5	32.6

V.2.2 Temperature increase and water absorption in batch preconditioner

As shown in Figure V-1, the temperature of the mix increases with the residence time. After 2 min of preconditioning, the temperature of the mix reached a plateau near 100°C.

Water from the condensing steam was absorbed by maize grits as shown by the final moisture content measurements. The quantity of moisture absorbed depends on the residence time and the initial moisture content. Figure V-2 represents the final moisture content of maize grits at different residence times and compares it with the theoretical moisture content calculated assuming complete absorption of the water added as steam. Experimental values were well below the theoretical, thus showing an estimation of the loss of steam during batch preconditioning. The rate of steam loss was calculated and varied between 18 and 44 g/min. It can be noted that with higher initial water levels, the difference between theoretical and actual value is lower.

Industrial preconditioners are continuous systems, therefore heat and mass transfers will have different characteristics.

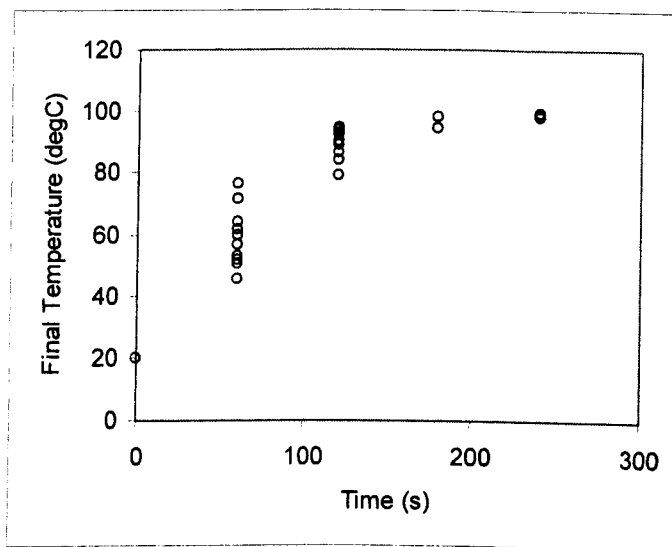


Figure V-1: Final temperature of preconditioned maize grits as a function of residence time

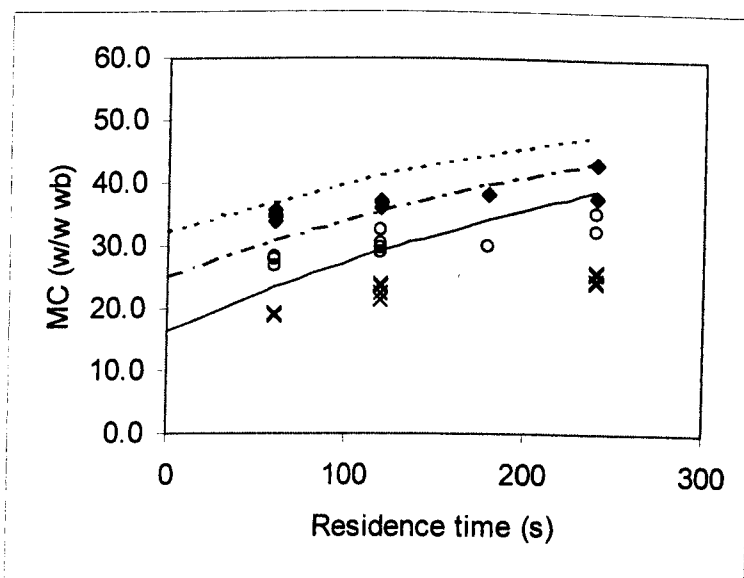


Figure V-2: Final moisture content (theoretical and actual) vs. residence time for different initial moisture content. The lines represent theoretical MC based on the initial moisture content and the absorption of all the water from the steam, where (—) iMC=16.5%, (- -) iMC=25.4% and (- - -) iMC=32.6%. The dots represent actual MC (w/w db) with (x) iMC=16.5%, (o) iMC=25.4% and (◆) iMC=32.6%.

V.2.3 Starch conversion during preconditioning

It is well known that the melting temperature of starch depends on moisture content (Colonna 1992; Biliaderis 1990; Blanshard 1979). Knowing the temperature of maize grits during preconditioning and its moisture, it should be possible to determine whether starch conversion has occurred during the process by comparing it with the glass transition and the melting temperature of maize starch.

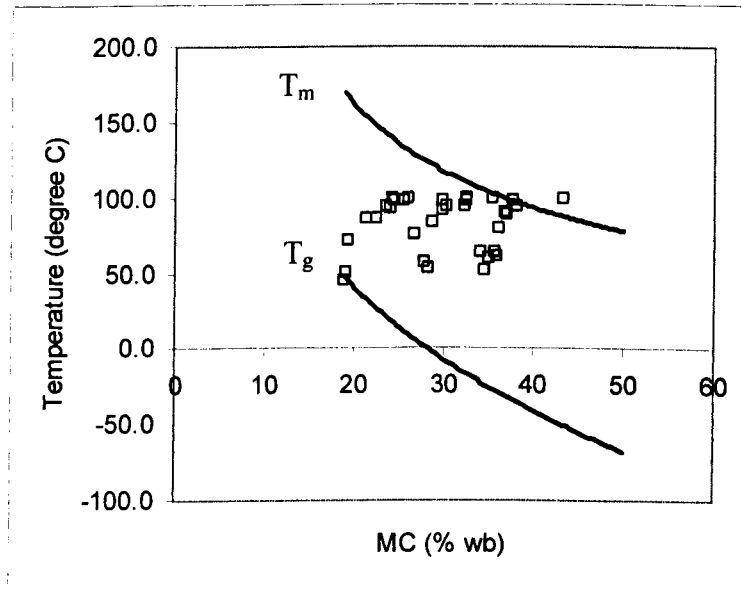


Figure V-3: Preconditioned maize grits final moisture and temperature (□). The two lines represent maize starch melting temperature (T_m) (data from Colonna (1992) and starch glass transition temperature (T_g) (calculated from Donald (1993)).

As represented on Figure V-3, all points are above the glass transition temperature. Only a few points seem to be above the melting transition curve. It should be noted that the data used only give T_m and not the onset of the melting transition. Therefore it can be assumed that more point will be above the onset of melting. Also, it should be considered that T_m for maize grits will be different from that of pure starch. Finally, in a preconditioner, conditions are very different from those used for the determination of T_m (usually done by DSC). The heating time is much shorter (30 to 240s compare to 10 to 20 min) and the mixing conditions might create localised conditions of temperature and moisture where the melting of starch can occur.

In order to determine the degree of starch conversion in preconditioned material, dried preconditioned maize grits were analysed by observation under polarised light microscope, X-ray diffraction and RVA.

V.2.3.1 X-ray diffraction and microscopic observation

Powder X-ray diffraction of raw maize grits exhibited the typical A-pattern of cereal starches characterised by diffraction peaks at $2\theta = 14, 16$ and 22° (Hoseney 1994). Upon preconditioning, the area of the peaks and their sharpness decreased indicating a decrease in crystallinity (Figure V-4). The x-ray diffraction index (XRDi) reflects this loss of long range order. The XRDi of the samples decreases with increasing moisture level and residence time. The diffraction indexes varied from 0.100 to 0.016. At low moisture content and short residence time, two samples had a crystallinity index significantly higher than that of the raw material (0.085). This might be attributed to annealing of the starch occurring during the steaming process or during drying.

By comparing values for the preconditioned samples with the XRDi of raw maize grits a percentage value for starch conversion can be obtained. The loss of long range order in preconditioned maize grits varied between 0 and 81%. Under the latter conditions, a paste was formed rather than a free flowing powder.

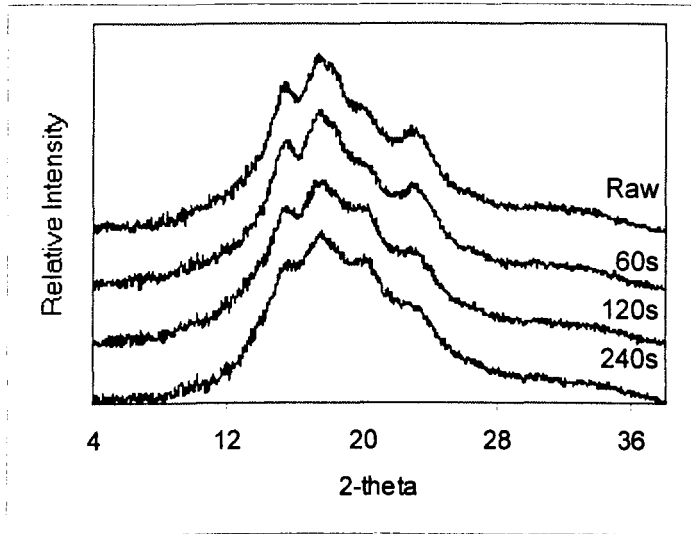
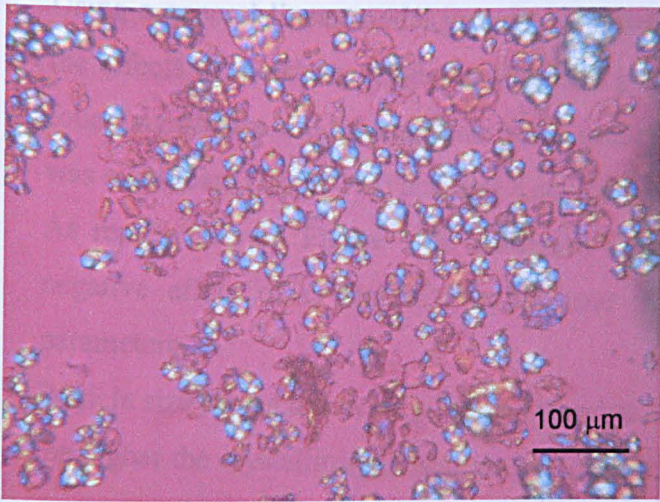
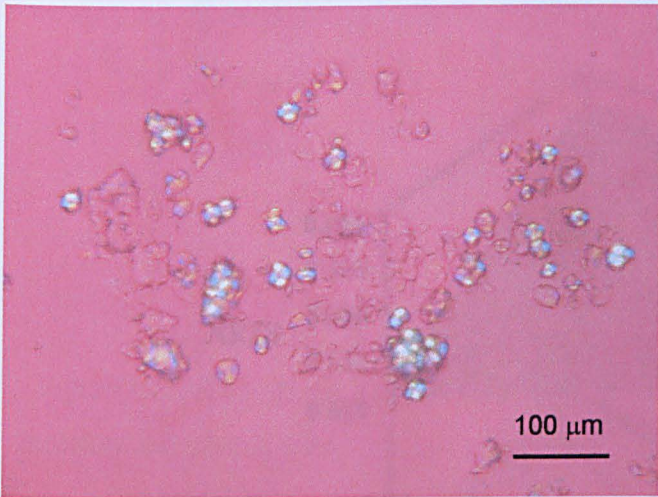


Figure V-4: Diffraction pattern of maize grits preconditioned for different times at initial moisture content 25.4% (Data are average of two curves). Comparison with raw material. All samples have been measured after equilibration at the same RH.

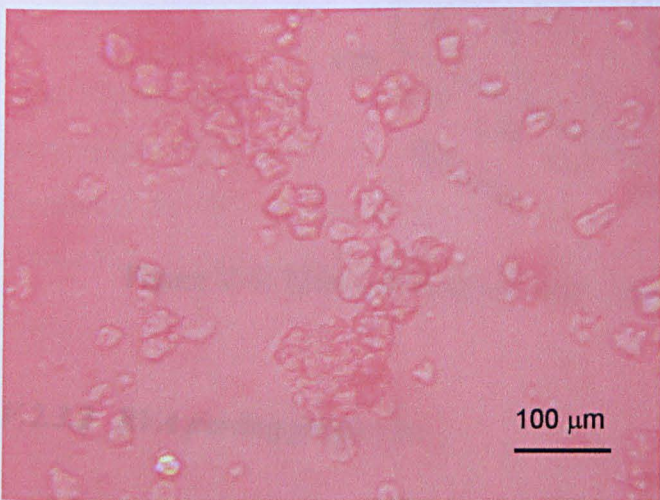
The X-ray measurements were confirmed by observation under the microscope. Samples preconditioned at 16.5% initial moisture content and for 60s presented mainly native starch granules, whereas the samples preconditioned for 240s at 32.6% showed mainly non birefringent particles. Although, starch was converted, the granular structure still remained.



A) RT = 60s



B) RT = 120s



C) RT = 240s

Figure V-5: Observation under polarised light of maize grits preconditioned for different residence time (RT) at 32.6% initial moisture content.

Using a general linear model procedure, it was possible to determine more precisely the effects of moisture, residence time and particle size on XRD_i. All 3 factors were found significant and the equation of the model is presented on Table V-3. The model was significant ($P < 0.0001$) and had a good R^2 (0.89).

As represented on Figure V-6, residence time and initial moisture content have a negative effect of crystallinity index, and there is an interaction between those parameters.

Particle size seems to have a positive effect on XRD_i, i.e. that the bigger the particles, the higher the crystallinity, therefore the lower the starch conversion.

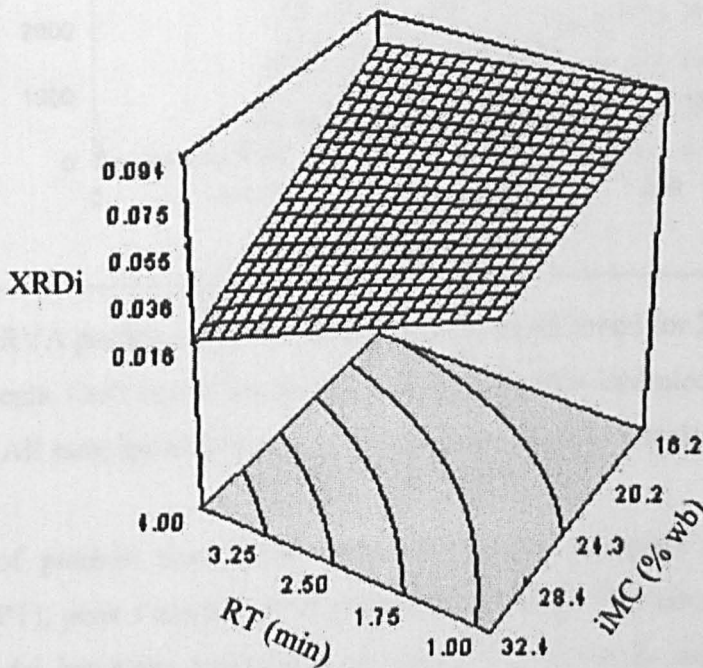


Figure V-6: Effect of residence time and moisture content on XRD_i.

V.2.3.2 RVA pasting properties

RVA is a technique used to test the pasting properties of starch heated in excess water. Although difficult to fully interpret, this method can give some information about the state of starch.

Dried, milled and sieved preconditioned maize grits have been analysed by RVA. An example of the typical pasting curves of the samples is shown on Figure V-7.

The pasting profile of preconditioned maize grits is similar to that of raw maize grits with a lower viscosity. This illustrates the mildness of the pre-cooking occurring in the preconditioner as no cold water swelling peak has been observed.

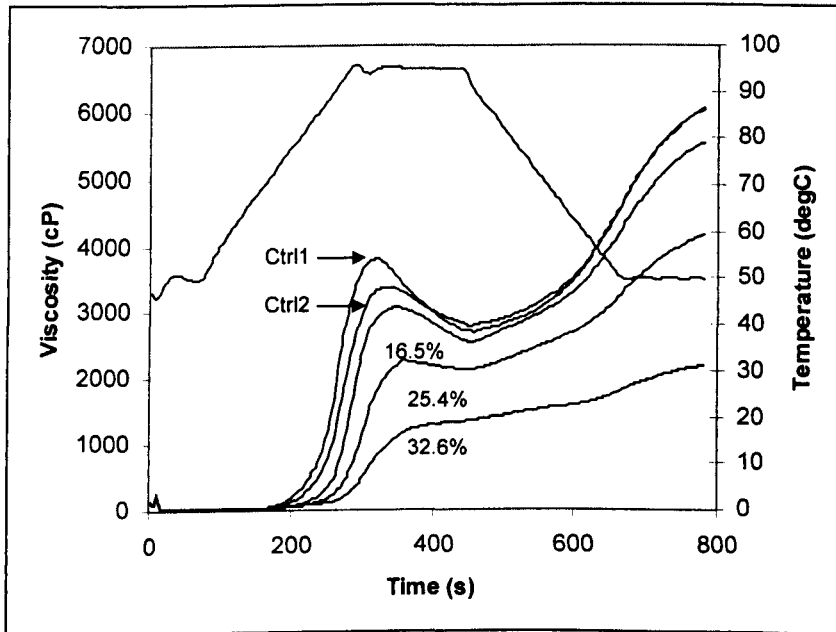


Figure V-7: RVA pasting curves of maize grits preconditioned for 240s at different moisture contents. Ctrl1 is raw maize grits and Ctrl2 is 40% hydrated raw maize grits. All samples were dried, milled and sieved before analysis.

The effects of particle size, initial water level and residence time on pasting temperature (PT), peak viscosity (PV) and final viscosity (FV) have been studied. A predictive model has been determined by analysis of variance and is presented in Table V-3. The models all present a good R^2 .

Table V-3: Equation of the predictive models and R^2 . RT is residence time, iMC is initial moisture content and PS is particle size. Equations are given in terms of coded factors (-1, +1).

<i>Parameter</i>	<i>Equation of the model</i>	R^2
PT	$87.85 + 3.81 \times RT + 5.81 \times iMC - 2.77 \times RT^2$	0.87
PV	$2149.6 - 122.5 \times PS - 437.0 \times RT - 1170.7 \times iMC - 269.0 \times RT \times iMC$	0.91
FV	$3669.5 - 374.0 \times PS - 864.9 \times RT - 2365.0 \times iMC + 283.4 \times PS^2 - 908.8 \times RT \times iMC$	0.91
XRD _i	$0.0607 + 0.0044 \times PS - 0.0192 \times RT - 0.0376 \times iMC - 0.0065 \times PS^2 - 0.0173 \times RT \times iMC$	0.89

As seen on Figure V-7, the pasting temperature (PT) is higher than that of raw maize grits. The particle size has no effect on the pasting temperature, but residence time and initial moisture content both have a positive effect. Pasting temperature gives an indication on the onset of particle swelling. Partial starch conversion generally increases the swelling ability of starch, therefore should decrease pasting temperature. On the other hand, the decrease in the amount of native starch will increase the PT to some extent as the time to reach the viscosity large enough to be recorded is delayed, but this is not enough to explain the large increase in temperature. Therefore, there is a decrease in water absorption capacity in the preconditioned material. This can be due either to the sample preparation method (drying and grinding) or to the preconditioning itself. A control sample (raw maize grits) has been hydrated (40% water (w/w, wb)), dried and ground as preconditioned samples to test the first hypothesis. The pasting temperature of this control (ctrl2) was slightly higher than that of raw maize grits (ctrl1) but far lower than most preconditioned sample (Figure V-7). Therefore, the drying was not (or only for a small part) responsible for the decrease in water absorption.

This decrease in water absorption has been already highlighted in the case of quiescent heating of maize grits and was attributed to the formation of complexes between amylose and the native lipids of maize grits (Becker 2001). X-ray diffraction did not indicate the presence of V-pattern typical of crystalline amylose-lipid complexes. The presence of amorphous amylose-lipid complexes has been shown (V.2.6), but their effect on swelling and solubility is less obvious. Other factors, such

as protein cross-linking or starch annealing could occur during preconditioning and affect the water solubility of maize grits.

The effect of initial moisture content, residence times and particle size are similar for peak viscosity and final viscosity. RT and iMC have both a negative effect on PV and FV and are in interaction as seen for XRD_i. Particle size has a much smaller effect than iMC and RT. Its effect is not the one expected and is in contradiction with the results from X-ray diffraction. Crystallinity studies showed that, the bigger the particles, the higher the crystallinity index. Whereas, lower peak and final viscosity values are found for bigger particles in the RVA, therefore suggesting higher starch conversion for those particles.

Principles in mass and heat transfer would suggest quicker transfers in small particles than bigger ones; therefore we would expect more conversion in small particles compare to bigger particles. Nevertheless, due to the limitation of the model system used here, mixing might be affected by particle size; therefore starch conversion might not be the highest for the smallest particles. The effect of particle size on starch conversion in a preconditioner will be discussed further in chapter VI.

V.2.4 Texture changes during preconditioning

It has been shown that during preconditioning, changes in water absorption and starch conversion occur. But are the macroscopic properties of the sample changed by different preconditioning conditions?

To answer this question, textural properties of preconditioned maize grits have been determined using a texture analyser (TA-XT2).

A set of samples at 4 initial moisture contents and 3 residence times has been produced. Measurements have been performed at room temperature to avoid temperature effects. Measurements of raw maize grits hydrated at 4 different moisture levels were performed as a control. Details about sample preparation can be found in chapter 3.

V.2.4.1 Change in bulk density

Bulk density of the feed material is an important parameter in extrusion as feed to the extruder is typically by volume, it will also determine partially the degree of fill of the barrel before compression and melting occurs.

The bulk density will be determined by the density of the components of the mix (water and maize grits) and by the porosity of the powder. The density of maize grits can be considered to be 1.5 g/mL (density of starch) and the density of water is 1 g/mL, therefore, as the moisture content increase, density of the system will decrease. But as can be seen in Figure V-8, the bulk density of hydrated maize grits increases as the water content increases. Therefore, it can be concluded that this decrease is due to a decrease in the porosity of the mix.

Texture analysis showed that, the bulk density of preconditioned MG was lower than for raw maize grits for the full range of moisture contents used (Figure V-8). This could be expected if the added water is associated with the native starch granules as the true density of starch granules will decrease with increasing conversion as they can swell more (Blanshard 1979). However, the general behaviour of the particulate needs to be considered along with starch granules density changes to interpret the bulk density changes.

Residence time and moisture content have a significant effect on bulk density. It appears that bulk density decreases with increasing residence time, especially between 60s and 120s. No significant difference appeared at the longer times of preconditioning between 120s and 240s for the lowest moisture content used. The moisture content seems to first decrease then slightly increase the bulk density. This effect could be the same as that observed in hydrated raw maize grits. By increasing moisture, the amounts of water bridging between particles increases therefore decreasing the pore density.

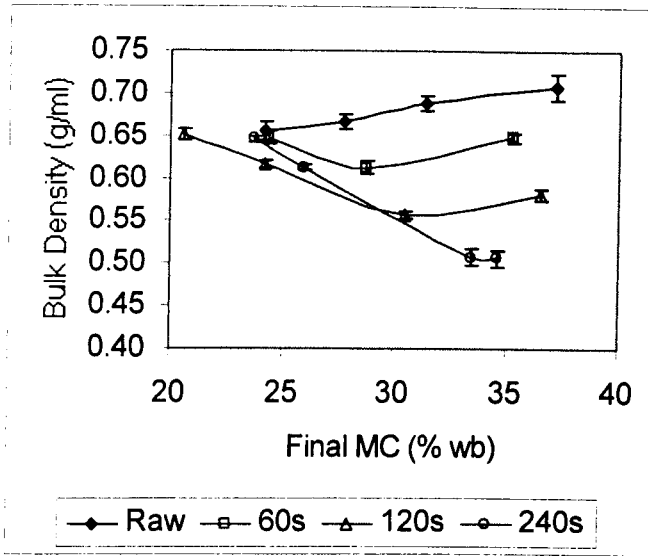


Figure V-8: Bulk density of maize grits preconditioned at different residence times with different final moisture content. Results are average of 10 measurements (Error bars are standard deviations)

There is a good correlation between bulk density of the material and XRD_i as represented on Figure V-9.

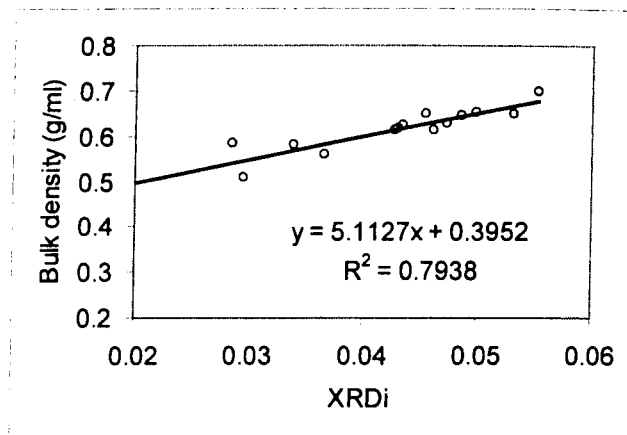


Figure V-9: Correlation between bulk density and XRD_i.

V.2.4.2 Change in compressibility

The packing capacity of the feed material is an important parameter in extrusion as highlighted by Chen (2000).

To investigate this, the compressibility of the material after preconditioning has been compared to the compressibility of raw hydrated maize grits. The method used is described in Chapter III.

As illustrated on Figure V-10, the compressibility of hydrated maize grits is low but increases slightly with moisture content (especially for moisture contents over 28%). Preconditioned maize grits compressibility is a lot higher than raw maize grits and increases significantly with moisture content but also with residence time.

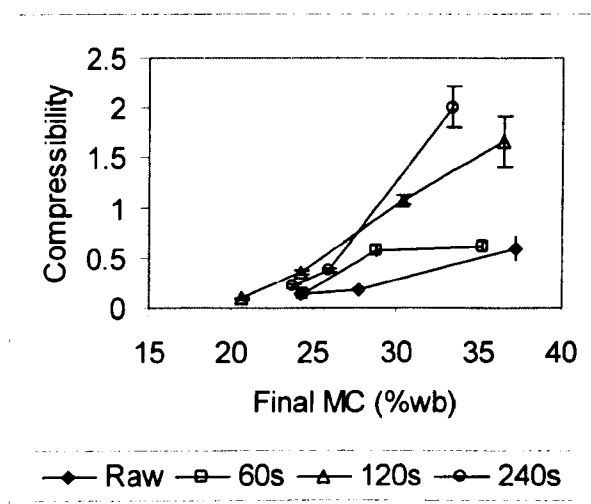


Figure V-10: Compressibility of maize grits preconditioned for different residence time with different final moisture content. Results are average of 10 measurements, error bars are standard deviation.

V.2.5 Water mobility in preconditioned maize grits

As defined by Bouvier (1996), preconditioning is used primarily to pre-humidify raw material. The quality of this pre-humidification depends on the characteristics of the solid particles (diameter, shape...) and the mixing capacity of the preconditioner. In order to study the humidification process, water mobility in preconditioned maize grits was determined using $^1\text{H-NMR}$. Two tests were performed. A stimulated pulse field gradient sequence was used to determine the self-diffusion coefficient of water. A FID sequence was also performed to determine spin-spin relaxation time

characteristics. All measurements were performed at 20°C to avoid temperature effects.

V.2.5.1 Translational mobility of water in preconditioned maize grits.

Diffusion coefficient of water in raw maize grits was used as a control. The diffusion time used (D_4) was 6 ms. It was not possible to determine water diffusivity for samples with moisture content below 22% due to their relatively fast decay.

As represented in Figure V-11, the diffusion of water is affected by the preconditioning. Diffusion of water in raw maize grits seems to increase rather steadily from 18% to 41% (w/w wb) moisture content.

For preconditioned samples with a moisture content below 30%, the diffusion of water seems to be very close to the diffusion of water in raw maize grits, although slightly higher. But for preconditioned maize grits at higher moisture content, there is a marked decrease in water diffusion coefficient compared to the raw material, especially for samples preconditioned for 240s. In general, diffusion of water in preconditioned maize grits is more restricted than in raw maize grits.

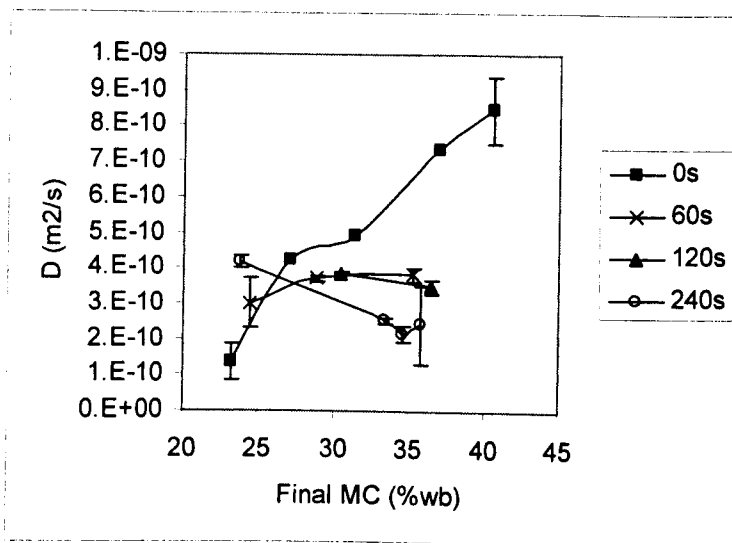


Figure V-11: Effect of time of preconditioning on self-diffusion coefficient of water in maize grits at different moisture content. Comparison with raw maize grits (0 s). Measurements are average of two measurements, error bars are standard deviation.

The absence of error bars is due to the absence of replicate.

To explain this behaviour, the distribution of moisture in the sample needs to be considered. In raw starch, when water concentration increases, there is an increase in swelling and more water is “bound” to the starch, but this is only limited. In preconditioned maize grits, as presented in the previous sections, starch conversion increases with increasing moisture content. As starch is more converted and its crystalline structure is destroyed, there are more sites for the water to form hydrogen bonds with the hydroxyl groups of amylose and amylopectin. Therefore, instead of being free, the additional water in the sample is partially bound with the food matrix and therefore has a restricted diffusion within the diffusion time of interest (6 ms). This is represented in a simplified representation in Figure V-12.

The study of relaxation times from FID experiments was therefore carried out to try to demonstrate this phenomenon.

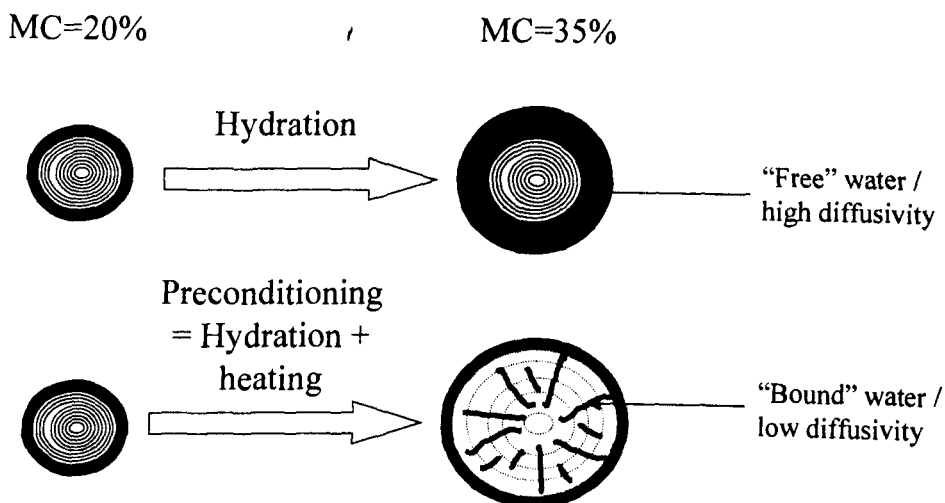


Figure V-12: Representation of the state of water in raw and preconditioned maize grits at high moisture contents (35%).

V.2.5.2 Relaxation times in preconditioned maize grits

Analysis of the free induction decay curve was performed as describe in Chapter III. To determine the spin-spin relaxation time (T_2), the FID was fitted with the equation described in Chapter III using 1, 2 or 3 components. The best fit was obtained with the 3 components equation given in III.2.7 using two gaussians (for component 1 and 3) and an exponential (for component 2). An example of the fit between raw data and the three components equation is given in Figure V-13.

The 3 components were characterised by their spin-spin relaxation times. Components 1, 2 and 3 had a relaxation time between 18-76 μs , 900-2300 μs and 1700-2800 μs respectively. The first component was associated with the rigid part of the sample whereas the 2nd and 3rd were associated with the liquid-like part. As components 2 and 3 had often very similar T_2 values, the following analysis will consider them as a single liquid component.

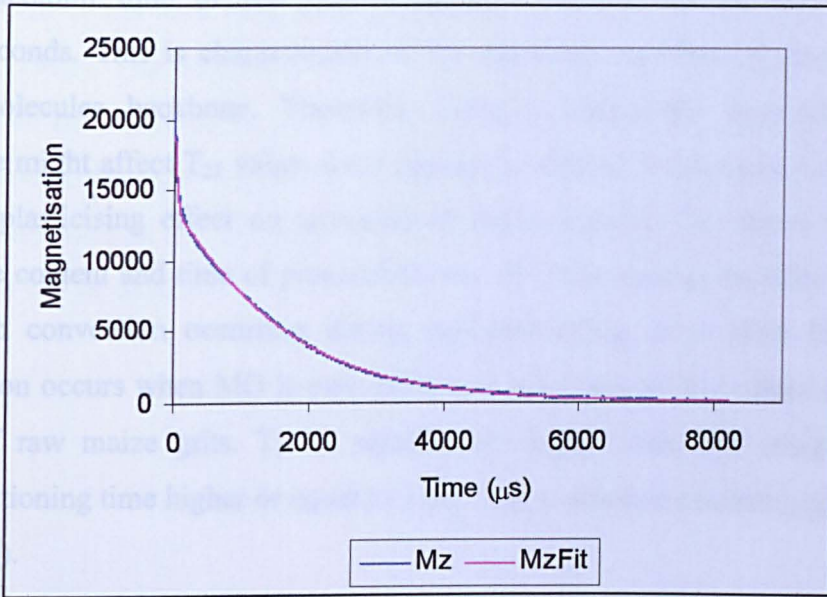


Figure V-13: Example of fitting of the FID using Equation III-14 (sample preconditioned for 240s at initial moisture 32.6%)

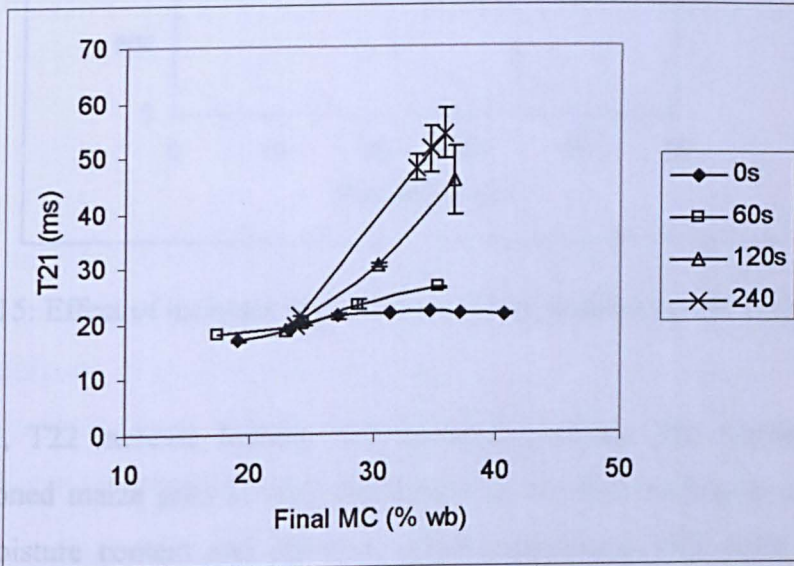


Figure V-14: Effect of moisture content and duration of preconditioning on the T_2 of the rigid component of the FID (T_{21}).

The relaxation time of the first component (T_{21}) is of the order of 10s of microseconds. This is characteristic of the rotational mobility of protons from the macromolecules backbone. Therefore, changes within the biopolymer physical structure might affect T_{21} value. As it appears on Figure V-14, water has only a very limited plasticising effect on unconverted maize matrix. T_{21} values increase with moisture content and time of preconditioning. This increase in mobility is correlated to starch conversion occurring during preconditioning. It is clear that no starch conversion occurs when MG is preconditioned for 1 min as T_{21} values are similar to those of raw maize grits. T_{21} is significantly higher than raw maize grits for a preconditioning time higher or equal to 2 min and a moisture content higher than 24% (w/w wb).

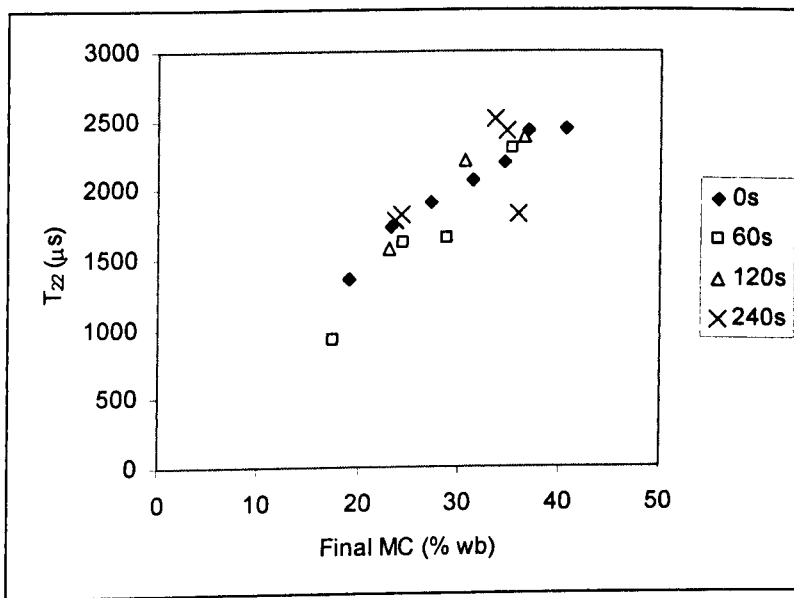


Figure V-15: Effect of moisture and duration of preconditioning on T_{22} in maize grits.

In general, T_{22} increase linearly with moisture content. The increase of T_{22} in preconditioned maize grits is very similar to that of raw maize grits except for the highest moisture content and duration of preconditioning, this point could be an outlier.

Analysis of the amplitudes related to the different T_2 might bring us further information, as the amplitude of one component to total amplitude ratio is linked to the percentage of protons in a particular state of mobility. The ratio of the solid

component to the total amplitude can be determined using the method described by Farhat (1996). The amplitude of the liquid component is proportional to the proton density of the water molecule and its weight fraction in the mixture. Similarly, the amplitude of the solid component is proportional to the proton density of the various macromolecules in the dry phase and their weight fraction. Therefore, the following equation can be used:

$$A_l = k \cdot w_w \cdot d_w$$

Equation V-1

$$A_s = k \cdot w_{MG} \cdot d_{MG}$$

Equation V-2

Where A_s and A_l are the solid and liquid component amplitude respectively, w_w and w_{MG} are the weight fractions of water and maize grits respectively and d_w and d_{MG} are the proton density of water and maize grits. Water proton density is equal to $2/18 = 0.111$. The composition of maize grits can be assumed to be 90% starch and 10% protein, therefore maize grits proton density is $0.9 \times d_s + 0.1 \times d_p$ with $d_s = 10/162$ and $d_p = 0.0665$ as given by Farhat (1996). Therefore, the following equation describes the theoretical ratio of the solid component to total amplitude.

$$\frac{A_s}{A_s + A_l} = \frac{A_s}{A_T} = \frac{w_w \cdot d_w}{w_w \cdot d_w + w_{MG} \cdot d_{MG}}$$

Equation V-3

As shown on Figure V-16, the part of the solid component in the total signal decreases with moisture content for both raw and preconditioned maize grits. For raw maize grits this decrease is parallel and higher to the calculated solid to total ratio. The difference between the two might be due to tightly bound water molecules behaving as a solid-like component. This is in agreement with Farhat (1996).

For the preconditioned material, at moisture content below 25%, the solid to total amplitude ratio follows the predicted value, but at higher moisture content, this ratio decreases more than predicted. This suggests that, for preconditioned maize grits above 25% moisture, a part of the solid component has a liquid-like behaviour. This is in agreement with our earlier observation on T_{21} measurements.

Figure V-17 confirmed this, as the participation of the liquid component to the total signal increases as the MC increase. Again, for the raw material, the increase in A_1 follows the calculated trend. For the preconditioned maize grits, the increases of the liquid to total amplitude ratio is also higher that predicted. This confirms our previous conclusions.

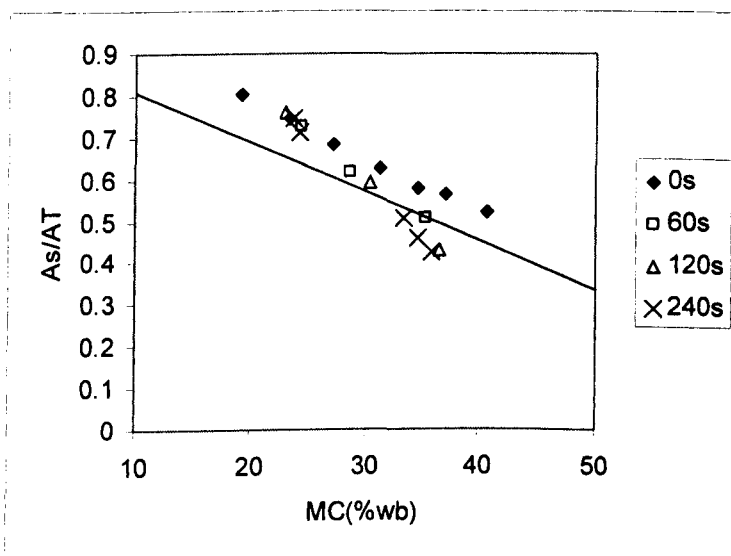


Figure V-16: First component amplitude ratio vs. MC. Effect of time of preconditioning. The line represents the theoretical solid ratio.

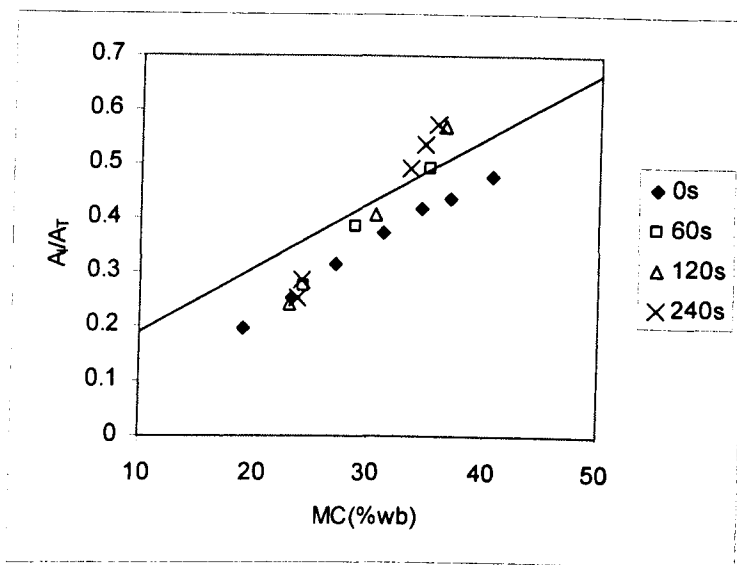


Figure V-17: Participation of the liquid component in the signal vs. MC. Effect of duration of preconditioning. The solid line represents the theoretical liquid component.

V.2.6 Interaction with lipids during preconditioning

RVA pasting curves showed a delay in pasting although starch conversion was higher in preconditioned samples. This might indicate the formation of complexes between amylose and native lipids as it has been seen in the quiescent heating of starches and maize grits (Becker 2001). X-ray diffraction have been performed on preconditioned systems with or without lipids and did not show characteristics V-pattern, therefore other methods used to determine presence of amylose lipid complexes were seek. Solid state ^{13}C -NMR was chosen as the preferred method as it is non-destructive and is able to show the presence of complexed lipids.

As the level of lipids in native maize grits is low (1%), further experiments have been performed on mixtures of maize grits and a free fatty acid, linoleic acid (C18:2).

V.2.6.1 *Experimental set-up and sample preparation*

Maize grits (600g) were preconditioned for 240s with water and 0, 2 or 4% linoleic acid (60%), the final moisture content was approximately 30% w/w wb. The samples were analysed at room temperature directly after textural assessment.

For the solid state ^{13}C -NMR experiments, amylose-linoleic acid complex was prepared using the method developed by Karkalas (1995) and used as a reference to determine the presence of amylose-lipid complex in preconditioned maize grits. Four samples were compared, raw maize grits (MC=13%), hydrated maize grits (MC=32%), preconditioned maize grits (MC=32%, RT=240s) and preconditioned maize grits with 4% linoleic acid (MC=30%, RT=240s).

V.2.6.2 *Effect of added lipids on macroscopic characteristics*

Texture studies showed that the bulk density of preconditioned maize grits with 2 or 4% linoleic acid is higher than that of maize grits preconditioned without lipids. This could indicate a restricted swelling occurring in presence of lipids.

On the other hand the compressibility of the sample is lowered by addition of lipids.

Table V-4: Macroscopic characteristics of preconditioned maize grits (240s) with different amounts of linoleic acid.

	MC (% wb)	Compressibility	Bulk Density
0%	29.76	0.565	0.597
2%	28.59	0.425	0.648
4%	29.42	0.425	0.659

V.2.6.3 *Formation of amylose-lipid complexes*

The ^{13}C -NMR spectra are represented on Figure V-18. Pure amylose-linoleic acid complex formed by the method of Karkalas (1995) was used as a control. The region

28 to 38 ppm presented a broad peak with a maximum at 31.9 ppm. A shoulder in the region of 34-36 ppm was also observed. This region corresponds to the mid chain methylene carbons $-(CH_2)_n-$. This value lies between the chemical shift found for crystalline lipids (33.2ppm for stearic acid) and solutions of fatty acids (29.7ppm) (Snape 1998). A chemical shift of 31.4 ppm has been reported for linoleic acid amylose complex prepared using the same method. This value is in accordance with those found in this study, the difference might be due to the use of a different internal reference. The shoulder observed might be due to free crystalline lipids as it has been observed by Lebail (2000).

X-ray diffraction was also performed. A V-pattern (not presented) was clearly seen on the diffractogram and confirmed the presence of amylose-lipid complex.

No peak was observed in the region 28 to 38 ppm in raw maize grits. Whereas, both hydrated and preconditioned maize grits samples exhibited a broad peak in the same region but peaking at 32.4 ppm. This seems to indicate a small shift in the value obtained compared to the pure amylose-linoleic acid complex. This might be due to the nature of the lipids forming the complex as chemical shift for lipid methylenes complexed with amylose seem to depend on the type of lipid (Lebail 2000; Snape 1998).

It is not surprising to find also a peak at 32.4 ppm for native maize grits as it has been demonstrated that raw starches also contain a certain amount of amylose lipid complex (Morrison 1993; Morrison 1995).

The spectrum of preconditioned maize grits with 4% linoleic acid confirmed the previous finding as a peak was found in the region of the methyl carbons peaking at 31.9 ppm as for the synthesised amylose-linoleic acid complex.

A rough estimate of amount of lipid complexed was determined by calculating the ratio of the area under the peak at 32.4ppm to the total area of the spectra. A value of 0.45% for processed maize grits was obtained compared to 0.33% for hydrated native maize grits. This value increased even further to 0.76% when maize grits was preconditioned in presence of linoleic acid. This seems to indicate that there is

formation of amylose-lipid complexes by preconditioning. Nevertheless, it should be noted that this is only a rough estimate used in order to compare samples and not a real attempt to be quantitative. A quantitative analysis would need to i) take into account all lipid carbons involved in the complex and ii) take into account the dynamic of the CP process which depends on the mobility of the sample.

Unfortunately, it is not possible to conclude whether the complexes are formed during the preconditioning process itself or during cooling down. Also it is not possible to conclude if the complexes are formed inside the starch granules or outside.

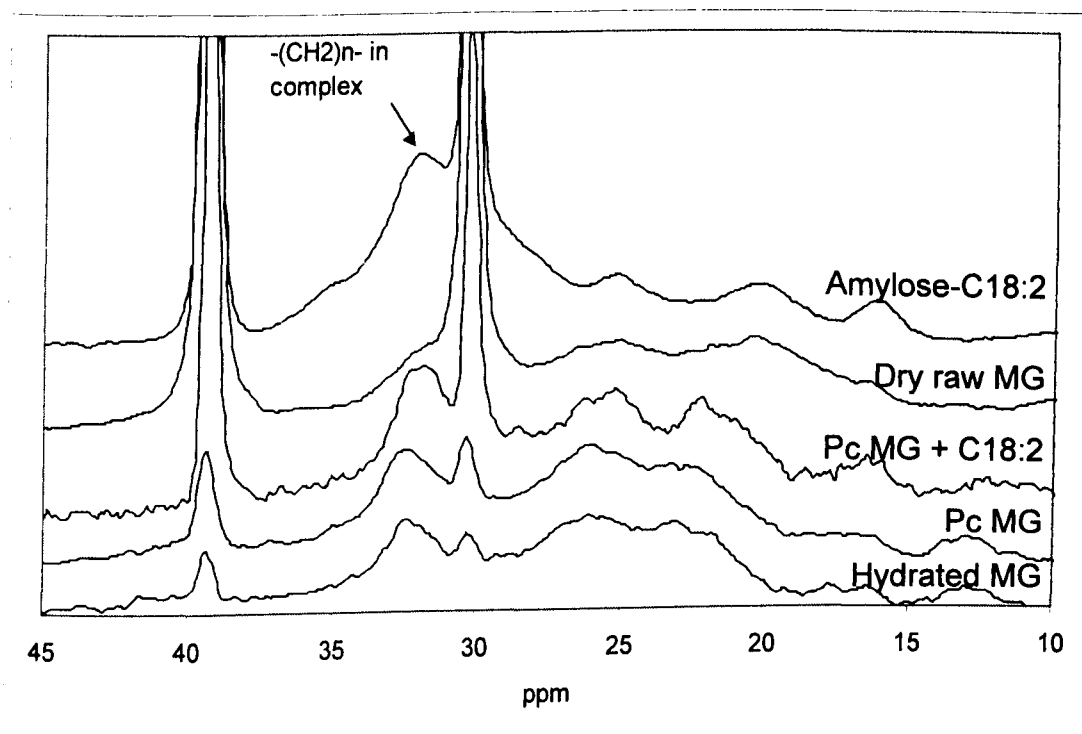


Figure V-18: ^{13}C -NMR spectra of processed maize grits and amylose-linoleic acid complex, focused on region 28-38 ppm. The peak at 30.4 and 39.4 are due to adamantane used as internal reference.

V.3 EFFECT OF PRECONDITIONING ON EXTRUSION

To test whether the small transformations involved in preconditioning have an effect on the extrusion process itself and/or the final quality of the product, an extrusion trial was performed.

V.3.1 Sample preparation

Maize grits were preconditioned for 60 or 240s (Pc60s and Pc240s) at a water level calculated to obtain a final moisture content of 30% w/w wb. The preconditioned material was then extruded in a twin screw extruder. The samples were compared with the extrudates of two controls i- raw maize grits hydrated to 30% w/w wb (CH) and ii- raw maize grits with no pre-hydration (CD), the water introduced only in the barrel of the extruder. The water feed rate was set in order to have 30% moisture in the barrel. Extruder conditions were the same for all four samples.

Table V-5 shows the conditions for the four samples. The extruder temperature zones were set at 20, 60, 75 and 100° (from the feed to the die end). The screw speed was set at 150rpm. The feed rate used was low (4.5 kg/h) due to the small capacity of the preconditioner.

Table V-5: Sample preparation and extrusion feed rates.

	CH	CD	Pc60s	Pc240s
<i>Premixing</i>				
Water	492	-	222	147
MG	2000	-	1000	1000
Steaming time (s)	0	-	60	240
<i>Extrusion</i>				
Feed Rate (kg/h)	4.5	3.5	4.5	4.5
Water feed rate (L/h)	0	1	0	0

V.3.2 Extruder operating parameters and radial die swell

When steady state was reached the extruder conditions were recorded and specific mechanical energy was determined (Table V-6). It should be noted that the feed rate was difficult to control accurately for the preconditioned samples because of the presence of lumps and the decrease in temperature of the feed mix that occurred as the extrusion proceeded. The specific mechanical energy is similar for the two preconditioned samples and significantly lower than the hydrated control. The SME of CD is lower than all the other samples; this might be an effect of the low feed rate.

Table V-6: Extruder operating characteristics and extrudates' sectional expansion index (SEI). Values with different superscript are significantly different ($P < 0.05$).

	SME (kJ/kg)	Back Pressure (bar)	SEI
CH	288.0 ^a	22.3 ^a	18.0 ^a
CD	203.5 ^b	12.7 ^b	9.0 ^b
Pc60s	257.1 ^c	21.3 ^a	18.4 ^a
Pc240s	253.7 ^c	18.7 ^c	13.8 ^c

The die swell has been recorded by measuring the sectional expansion index of the extrudates. The results are presented in Table V-6. The SEI is very dependent on the way the water is introduced in the sample. CH had the highest expansion whereas CD had the lowest. This could be related to the lower SME of CD and the heterogeneity of the melt due to a bad mixing with water in the low feeding conditions used for this trial.

Although the two preconditioned samples had a similar SME, the expansion of Pc60s was higher than the one of Pc240s. This could be due to the lower back pressure of Pc240s. Die pressure is known to have an effect on foam density (Donald 1993).

V.3.3 RVA pasting curves

All four extrudates exhibited a cold swelling peak typical of high temperature / high shear processed cereals (Whalen 1997). The final viscosity of the 4 extrudates were

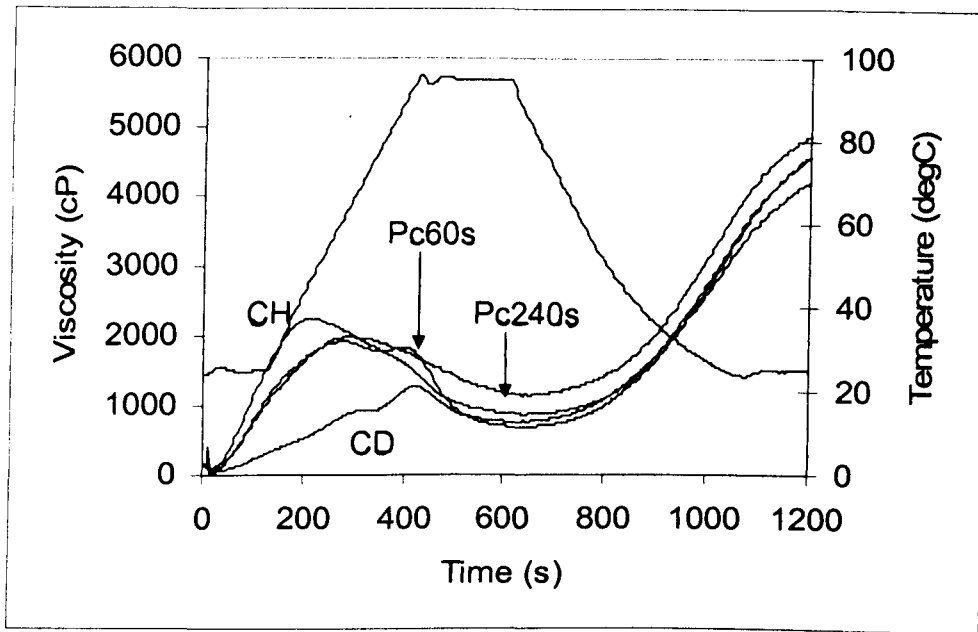


Figure V-19: RVA pasting curves of maize grits extruded under different preconditioning conditions. Average of 3 measurements.

V.3.4 X-ray diffraction pattern and microscopic observation.

The X-ray diffraction showed that all samples exhibited a V-pattern characterized by peaks at the diffraction angle $2\theta=13$ and 20° . This pattern has been observed in many studies on cereal extrudates (Bhatnagar 1994; Colonna 1989; Mercier 1979) and is related to the presence of crystalline complexes between the amylose fraction of the starch and lipids. The sharpness and area of the peaks is an indication of the amount of crystals present in the samples. From our results, it appears that CH and Pc240s have the highest amount of amylose-lipid complexes compare to the other samples. All samples had a clear amorphous background except CD and to some extent Pc60s, which exhibited remnants of peaks at the angles characteristic of the A-pattern. Observation of the sample under polarised light showed the presence of packs of native starch granules in CD and Pc60s. This consolidates the idea that the RVA might be indicating the presence of native starch (V.3.3).

starch and lipids. The sharpness and area of the peaks is an indication of the amount of crystals present in the samples. From our results, it appears that CH and Pc240s have the highest amount of amylose-lipid complexes compare to the other samples. All samples had a clear amorphous background except CD and to some extent Pc60s, which exhibited remnants of peaks at the angles characteristic of the A-pattern. Observation of the sample under polarised light showed the presence of packs of native starch granules in CD and Pc60s. This consolidates the idea that the RVA might be indicating the presence of native starch (V.3.3).

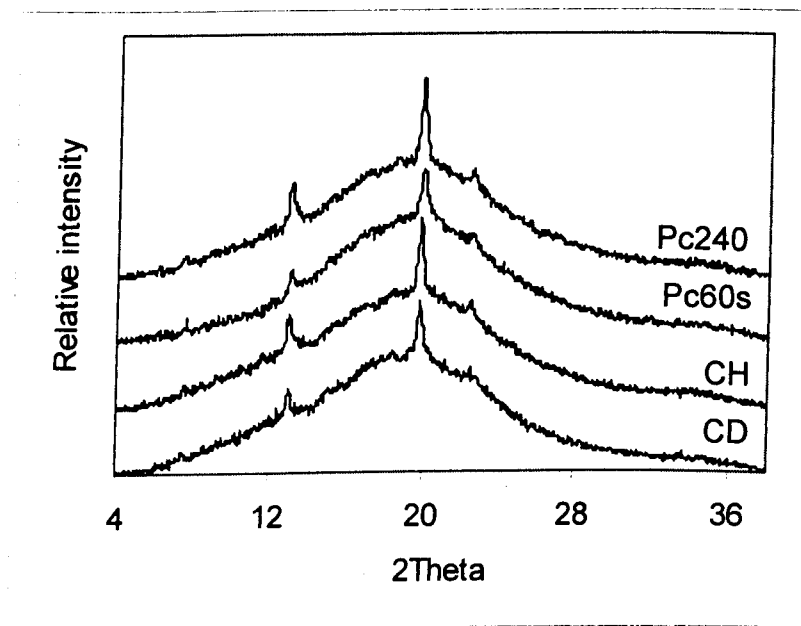


Figure V-20: X-ray diffraction pattern of maize grits extruded with different preconditioning conditions.

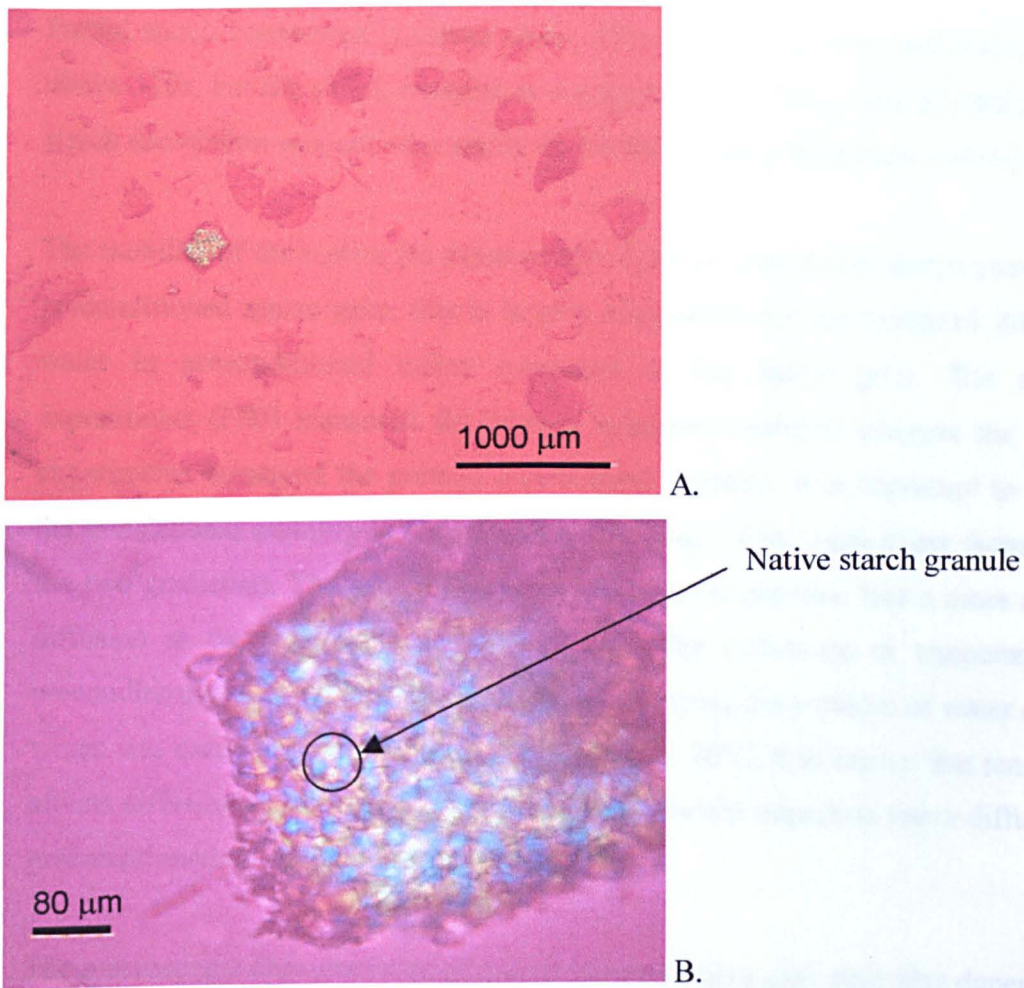


Figure V-21: Observation under polarised light of CD extrudate. A- Low magnification shows some particle with birefringence, B- Detail of a birefringent particle shows packs of native starch granules.

V.4 CONCLUSION

The use of a small-scale orbital rotational paddle mixer as a preconditioner was useful in determining the physicochemical transformations occurring during this unit operation. Both macroscopic and molecular changes occur during preconditioning and affect extrusion characteristics.

Partial starch conversion occurred above 25% moisture content and residence times above 120s, but the starch remains in a granular form. The effect of particle size on starch conversion was not clear partly due to the sample preparation technique.

The mobility of the matrix (as measured by T_2) increased due to starch conversion in preconditioned maize grits, this is largely responsible for the restricted diffusion of water in preconditioned maize compared to the native grits. The relaxation experiments (FID) measured the protons rotational mobility whereas the diffusion experiments measured the protons translational mobility. It is important to note that the translational mobility is related to the time scale of the experiment (separation of the two gradients). The samples with higher starch conversion had a more restricted diffusion at the time scale selected (6 ms). The difference in temperature post preconditioning has not been taken into account during the measure of water diffusion which was carried out after cooling the samples to 20°C. It is known that temperature affects diffusion and therefore should have an important impact on water diffusivity in preconditioned maize under process conditions.

The macroscopic characteristics of preconditioned maize grits were also dependent on initial moisture and residence time. Bulk density and compressibility were correlated with starch conversion.

There is some evidence on the formation of a small amount of amylose-lipid complexes, nevertheless, their effect on the solubility of the material in water and extrusion should be limited.

Extrusion is greatly affected by preconditioning. The quality of the final product (expansion, state of starch, crystallinity) was found to depend on the characteristics of the preconditioning. Preconditioned samples had a lower SME compare to the hydrated material. This could be an effect of temperature or starch conversion of the sample. The expansion index did not correlate with SME, therefore preconditioning had a specific effect on expansion.

**CHAPTER VI EFFECT OF PRECONDITIONING AND PARTICLE SIZE
ON MAIZE GRITS AND MAIZE GRITS EXTRUDATES: PILOT PLANT
SCALE STUDY.**



VI.1 INTRODUCTION

The use of a small orbital paddle mixer as a batch preconditioner as described in Chapter V, was useful to test many samples in small quantities and to determine some effects of preconditioning on cereal systems. Nevertheless, this system is very different from a real plant. Therefore it was necessary to perform some experiments on a real preconditioner-extruder system to confirm some of the earlier findings.

A set of experiments has been designed in order to find out whether preconditioning conditions affect extrusion parameters and the characteristics of the final product, and if so, by which mechanism.

The effect of particle size on extrusion has been extensively studied (Mathew 1999a; Desrumaux 1998; Garber 1997), but the interactions occurring between the effect of particle size and preconditioning has only been postulated by Caldwell (2000). Therefore, the effect of particle size and particle size distribution was also studied in interaction with preconditioning.

VI.1.1 Comparison of model and pilot plant system

Although the modified orbital paddle mixer was aimed at modelling a real preconditioning system, its operating characteristics differ fundamentally from a real preconditioner / extruder system.

For this study, a Buhler preconditioner was used in combination with a PX single screw extruder in Masterfoods dry pet food pilot plant in Verden (Germany). The configuration of the preconditioner is represented on Figure VI-1. The preconditioner has two chambers. In the first part the material is mixed with water and steam injected at the upper end of the barrel, the material then falls down into the second chamber where it is further mixed.

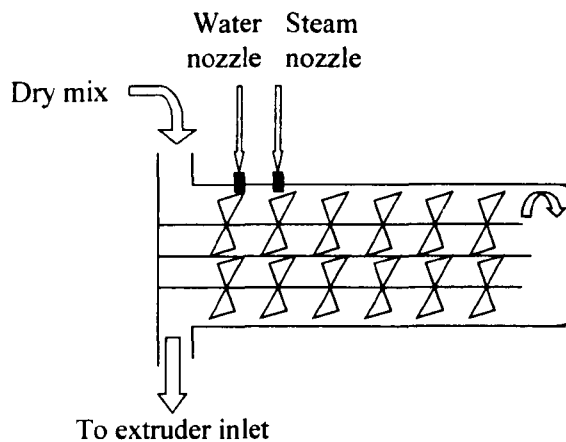


Figure VI-1: Schematic representation of Buhler preconditioner

This configuration provides different characteristics to the preconditioning process that will affect the physicochemical changes occurring in the raw material. The table below summarises the differences between the model batch preconditioner and the pilot plant.

Table VI-1: Comparison batch model system and pilot plant.

	<i>Model</i>	<i>Pilot plant</i>
Transport	Batch	Continuous
Residence time in preconditioner	60 to 240s	20 to 75s
Steam injection	Continuous for the duration of the mixing	At the inlet of the preconditioner only
Extruder feed rate	4.5 kg/h	260 kg/h
Extruder type	Twin screw	Single screw

VI.1.2 Sample preparation and experimental design

VI.1.2.1 Raw material characterisation

Maize grits of different grades and origins were preconditioned and extruded. Maizecor (U.K.) provided maize grits of 3 different particle sizes (fine, medium and coarse). A mix of coarse and fine maize has been prepared as well, to study the effect of particle size distribution on preconditioning and extrusion. The maize grits labelled Verden was provided by Masterfoods (Verden, Germany). The proximate composition of the different grades of maize is given in Table VI-2.

Particle size distribution was determined by sieve shaking on an AS200 analytical sieve shaker (Retch, GmbH). Figure VI-2 shows that fine, medium and coarse maize grits have a monomodal distribution whereas mix and Verden have a bimodal distribution. The ratio of fine to coarse grits used in the mix has been chosen in order to obtain the same modal diameter for the mix as for the medium sized grits.

Table VI-2: Composition of the different types of maize grits. Data obtained from the supplier. (*: Measured, -: not present)

	Coarse	Medium	Fine	Verden
Moisture*	14.9%	13.9%	12.6%	12.8%
Oil	<1%	<1%	<2%	-
Protein	8-9.5%	8-9.5%	6.5%	6-15%
Starch	74%	74%	75.5%	46%
Ash	-	-	0.4%	<2%

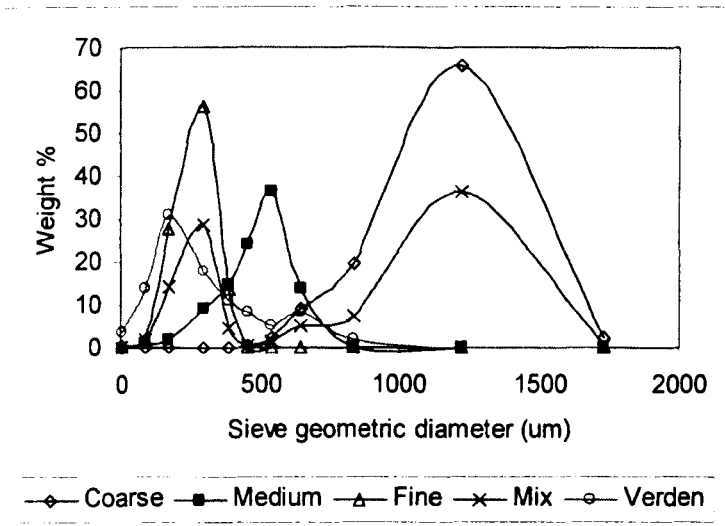


Figure VI-2: Particle size distribution of maize grits.

VI.1.2.2 Sample preparation

Each grade of maize was preconditioned in 4 different ways and extruded under similar conditions. The four preconditioning treatments (CD, CH, PcS and PcL) are described in Table VI-3.

These four preconditioning conditions correspond to those used in section V.3 but using shorter residence times (PcS and PcL correspond to Pc60s and Pc240s respectively). All samples could be extruded using those conditions except for coarse maize grits under the PcS treatment where the preconditioned mixture formed a paste-like material causing plugging of the preconditioner outlet.

Table VI-3: Preconditioner and extruder conditions. (*=12 for Verden maize grits).

	CD	CH	PcS	PcL
<i>Preconditioner</i>				
Maize feed rate (kg/min)	3.5	3.5	3.5	3.5
Water feed rate (kg/min)		0.84	0.65	0.65
Steam feed rate (kg/h)			24*	24*
Residence Time (s)	20	75	20	75
Paddle speed (rpm)	80	15	80	15
<i>Extruder</i>				
Water feed rate (kg/min)	0.84			
Temperature zone 1 (°C)	65	65	65	65
Temperature zone 2 (°C)	90	90	90	90
Temperature zone 3 (°C)	100	100	100	100
Screw speed (rpm)	281	281	281	281

Preconditioned maize grits was used “as is” for texture analysis (bulk density and compressibility). For water mobility study, the preconditioned material was snap-frozen in liquid nitrogen and stored in a -18°C freezer. The samples were sent the day after by express mail in a polystyrene container filled with dry ice. For X-ray and RVA, the samples were dried in a 105°C oven until the sample reached a moisture content equal or below 10% (wb). For the X-ray study, the powder was equilibrated in an airtight container over a saturated solution of NaCl (RH=75%) for 1 week. For RVA study, the powder was sieved and only the sieve fraction 125-250 µm was used.

Maize grits extrudates were dried in an oven until they reached a moisture content below 10%. The extrudates were then ground in a cyclotec sample mill fitted with a 1mm screen. The procedure for RVA and X-ray was similar as the one described above. Total soluble sugar content was determined using the method of Dubois (1956) as described in Chapter III.

VI.2 EFFECT OF PRECONDITIONING AND PARTICLE SIZE ON MAIZE GRITS PROPERTIES

As for the model system, the transformations of the raw material during the preconditioning process have been monitored. Changes in temperature and moisture have been recorded on the material at the exit of the preconditioner. Starch conversion was studied on the dried preconditioned material by X-ray, RVA and DSC. Texture studies of the preconditioned material showed the change in bulk density and compressibility. Water mobility was analysed using proton NMR on the frozen samples after thawing.

VI.2.1 Moisture and temperature increase in preconditioned maize grits

The temperature of the water-maize mixture directly at the exit of the preconditioner (i.e. at the extruder inlet) varied from room temperature (~22°C) to 80°C.

PcS samples have a higher temperature than PcL samples. This differs from the model system where the temperature of the mix increased with residence time. In the model system, steam injection is continuous throughout the process whereas in the Bulher preconditioner, as the sample passes the steam injection step, the mixture cools down. With longer residence time in the barrel, the sample will cool down more, therefore having a lower exit temperature. This is due to the barrel configuration: the dry mix first enters the first barrel where it is mixed with water and steam, then is conveyed to the end of the shaft and drops into the second barrel where the material is only mixed.

Preconditioned maize grits moisture content has been determined in 2 ways: on site using a Sartorius MA30 moisture analyser at 95°C or in the laboratory, on the frozen samples using a 105°C oven. This procedure has been used to check whether the targeted 30% (wb) moisture was reached.

On site determination gave moisture contents ranging from 28.2 to 31.2% (wb). The moisture content was determined at the beginning of each run, variations of more than 1% were considered unacceptable. The average moisture content was $29.8\% \pm 0.9$. Therefore, it was considered that the targeted 30% moisture was reached for all samples. No samples were re-run and preconditioner parameters were not altered.

Laboratory determination showed moisture content varying from 29.5 to 35.4% (wb). These variations were higher than those reported by on site determination. Laboratory determinations were made in a more controlled environment. The samples were taken directly out of the preconditioner, sealed in a foil bag and frozen in liquid nitrogen therefore limiting water loss and moisture absorption. Coarser samples appeared to have higher moisture content than those of finer particle size. This is probably due to different initial moisture content of the particles. A slight difference in moisture appears as well between CH and Pc samples except for the fine samples.

It is well known that moisture is a crucial factor in the extrusion process (Miller 1985; Cai 1993; Mohamed 1990). Therefore, the effect of moisture content will be taken into account in the following analysis.

Table VI-4: Moisture content of the preconditioned maize grits measured on site (1 measurement) or in the laboratory (average of 3 measurements, standard deviation in brackets). (*: sample caused blockage in the preconditioner)

		CH	PcS	PcL
Fine	On Site	29.0	30.7	29.6
	Lab	29.5 (0.1)	29.8 (0.2)	30.0 (0.2)
	Theoretical	29.5	32.7	32.7
Medium	On Site	29.5	29.2	30.9
	Lab	30.1 (0.1)	31.1 (0.2)	32.3 (0.2)
	Theoretical	30.5	33.7	33.7
Coarse	On Site	29.0	29.7*	31.2
	Lab	31.8 (0.2)	35.4 (0.7)*	33.9 (0.4)
	Theoretical	31.4	34.6*	34.6
Mix	On Site	28.2	29.9	30.5
	Lab	30.2 (0.3)	31.2 (0.4)	32.0 (0.6)
	Theoretical	30.3	33.6	33.6

As it had been done for the model system (V.2.1.), theoretical moisture content has been calculated assuming complete absorption of water from condensed steam. When a steam rate of 12 kg/h was used, the theoretical moisture contents were in agreement with the measured values. Whereas when a steam rate of 24 kg/h was used, the moisture contents of the material after preconditioning were lower than the theoretical values (calculated assuming absorption of all the water from the steam). This is due to the limited water absorption of the preconditioned material as this had been highlighted by Rokey (1994). This is in agreement with the results from the model study. One difference appeared for preconditioned coarse maize grits. In this case the moisture content of the preconditioned material (as determined by the laboratory method) matched the theoretical values. Therefore, it appears that there is more absorption of water for the coarse grits compared to the smaller particle size grits. This could be due to a higher starch conversion in this material leading to an increase in water absorption or to a difference in composition of the different grades of maize grits. It can also be due to an experimental error: the samples had to be frozen and then sent over dried ice before moisture content could be determined in the laboratory, therefore moisture could have been picked up during transport. This last hypothesis seems unlikely, as samples were heat-sealed in foiled bags before freezing to avoid moisture migration.

VI.2.2 Effect on starch conversion

VI.2.2.1 X-ray study

X-ray diffraction was used in order to determine whether starch conversion occurs during preconditioning under pilot plant conditions, and if so, whether a difference can be seen between PcS and PcL.

Crystallinity indexes (XRDi) have been derived from the diffraction pattern and reported on Figure VI-3. Crystallinity index of preconditioned maize is significantly

lower than that of pre-hydrated only (CH) or raw maize. This indicates that starch conversion occurs in the preconditioner even though the residence time is short.

PcS's crystallinity index is equal or lower than that of PcL for most grades of maize used in this study. This differs to the model system where samples with longer residence time were more converted than samples with short residence time (see paragraph VI.2.2.3).

It can be noted as well that CH has a crystallinity index marginally higher than the raw material. This could be due to experimental error or annealing of the starch during the drying of the samples.

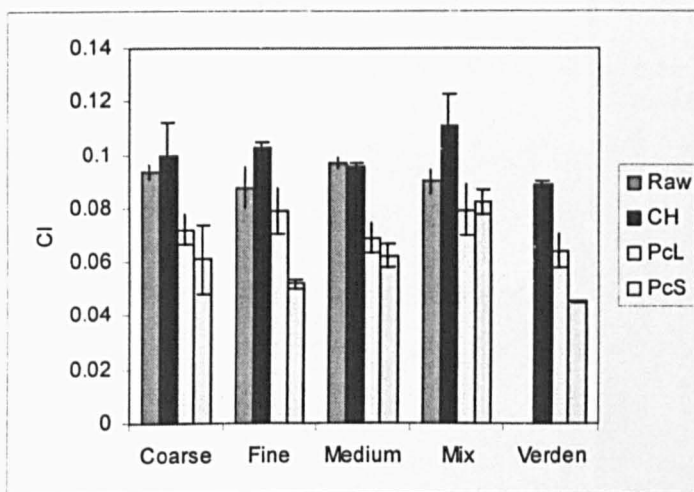


Figure VI-3: Crystallinity index (XRDi) of preconditioned maize grits under different conditions. (average of two measurements, error bars are standard deviations)

No significant difference was found between the crystallinity indexes of the different raw maize grits. The effect of particle size was not significant.

VI.2.2.2 RVA analysis

In order to verify the results of the X-ray study, RVA analysis has been performed on the dried preconditioned samples to look at the state of starch. Figure VI-4 shows the profiles for the different grades of maize and the different treatments.

All samples presented a lower peak viscosity and a higher pasting temperature than the raw sample. This is in agreement with the findings reported in chapter V. But, CH had a lower viscosity than the preconditioned samples, although X-ray studies show that starch is less converted in CH. Therefore, two hypothesis can be put forward to explain this behaviour: 1- starch in CH is more converted than in the preconditioned sample (due to the drying of the sample) or 2- another phenomenon occurs, possibly during the drying step, that prevents swelling of the granules in CH.

To test the first hypothesis, DSC has been performed on fine and coarse maize grits to test the degree of conversion. The method used is described in Chapter III.

The results are presented in Table VI-5.

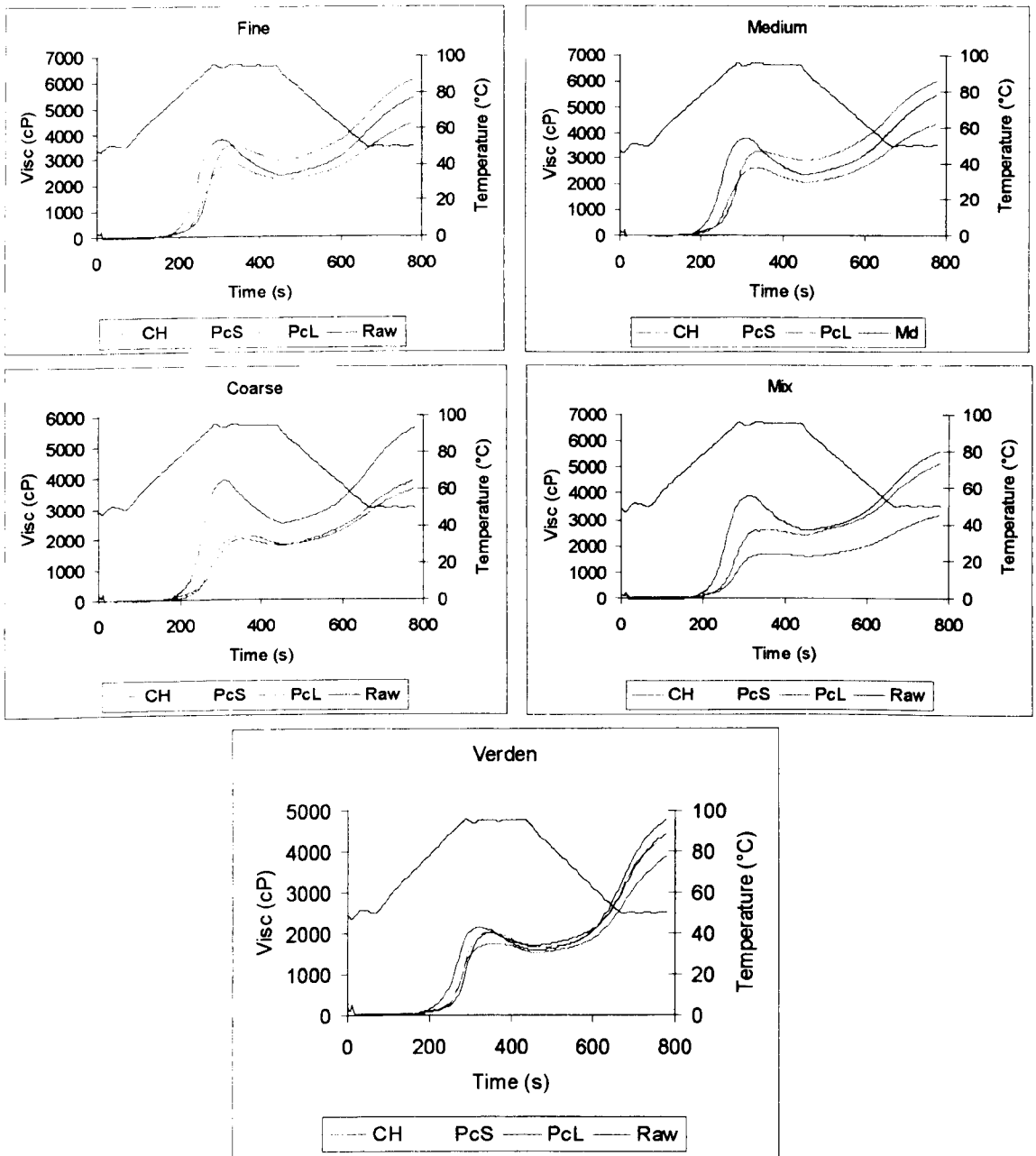


Figure VI-4: RVA profile of dried and sieved preconditioned and raw maize grits.
Results are average of two measurements.

Table VI-5: RVA characteristics of preconditioned maize. Results are average of three measurement \pm standard deviation.

Maize Grade	Treatment	Peak		Final Viscosity		Pasting Temperature	
Fine	CH	2834	\pm 36	4396	\pm 62	78.5	\pm 0.4
Fine	PcS	3252	\pm 51	5674	\pm 15	75.4	\pm 1.2
Fine	PcL	3572	\pm 19	6071	\pm 149	78.0	\pm 0.4
Medium	CH	2629	\pm 18	4379	\pm 60	79.1	\pm 0.0
Medium	PcS	2823	\pm 36	5196	\pm 92	75.6	\pm 1.3
Medium	PcL	3307	\pm 29	6024	\pm 96	75.6	\pm 0.9
Coarse	CH	2099	\pm 19	3607	\pm 18	82.0	\pm 1.0
Coarse	PcS	1941	\pm 17	3820	\pm 42	73.7	\pm 0.4
Coarse	PcL	2008	\pm 26	3876	\pm 20	78.0	\pm 0.4
Mix	CH	2577	\pm 82	5116	\pm 80	78.8	\pm 0.4
Mix	PcS	3056	\pm 32	6123	\pm 80	75.1	\pm 0.1
Mix	PcL	1690	\pm 32	3172	\pm 38	82.0	\pm 1.3
Verden	CH	1727	\pm 38	3868	\pm 25	83.5	\pm 0.5
Verden	PcS	2010	\pm 16	4348	\pm 132	85.1	\pm 1.8
Verden	PcL	2033	\pm 23	4336	\pm 119	85.1	\pm 0.6

Table VI-6: ΔH (J/g dry maize grits) values of preconditioned and raw maize grits in excess water (3:1 water : starch ratio). The results are mean of two measurements.

	Fine		Coarse	
Raw	11.28	\pm 0.95	8.95	\pm 0.00
CH	9.07	\pm 1.37	6.26	\pm 0.98
PcS	6.14	\pm 0.78	3.91	\pm 0.08
PcL	5.18	\pm 1.21	5.36	\pm 0.84

The lower values of enthalpy variation correspond to the more converted samples. PcS and PcL for both particle sizes have lower values than CH and raw maize grits. This confirms the X-ray experiments. It can also be noted that ΔH for fine maize is significantly higher than coarse maize. This in contradiction with the X-ray results where raw fine grits have a slightly lower crystallinity than coarse. This could be due to a lower hydration (in the DSC pan) for coarse grits than fine.

The DSC results point to another phenomenon than starch conversion reducing particle swelling and hence the changes in the RVA pattern occurring for CH. To check whether this phenomenon is related to drying of the sample, frozen samples have been thawed and analysed as is (without drying, grinding and sieving).

Figure VI-5 shows the RVA profiles obtained. The differences between CH, PcS and PcL are less obvious than for the dry samples. The pasting temperature of CH appears

lower than for PcS and PcL. The final viscosity of CH is still lower than the two preconditioned samples, but the difference is less than that found on the dry samples. Therefore, the sample preparation method appears responsible for the loss of solubility of CH samples.

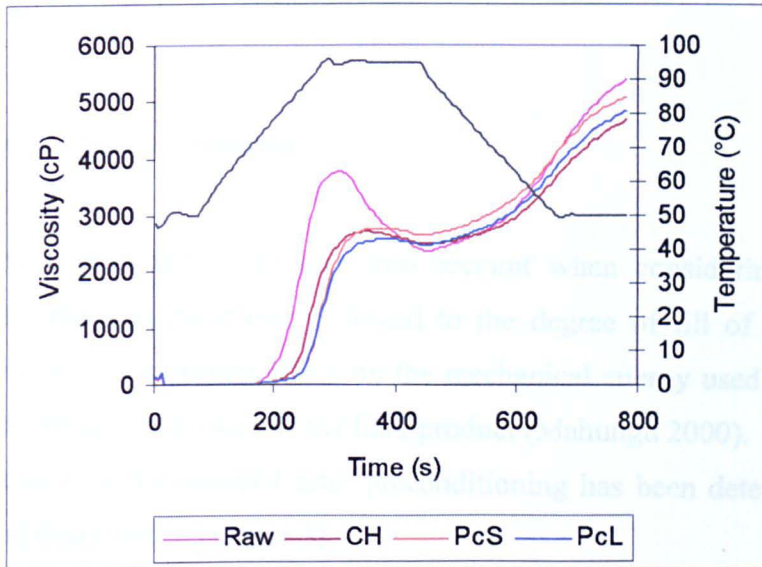


Figure VI-5: RVA profile of frozen preconditioned fine maize grits used "as is" after thawing.

VI.2.2.3 Conclusion

In order to keep the samples in a stable condition prior to analysis, the preconditioned samples had to be dried on the pilot plant site in an oven at a relatively high temperature (105°C). The drying method might have had some effects on the structure of the sample. This has been shown by the use of the RVA, which revealed a lower viscosity for CH sample. The combination of X-ray and DSC showed that this difference was not due to a higher level of starch conversion but to other factors.

This study showed that in a pilot plant preconditioner with relatively short residence times (20 to 75s), starch conversion occurs. X-ray diffraction indicated a different degree of conversion between PcS and PcL especially for lower particle size samples. This difference might be due to the different mixing efficiency of the samples. At

shorter residence time, the speed of the paddle is higher therefore providing a better mixing. Under these conditions, the steam could come in contact with more particles and thus more starch could be converted.

VI.2.3 Bulk material physical properties

VI.2.3.1 Study of the bulk density

Bulk density is a parameter to take into account when considering an extrusion process. This physical parameter is linked to the degree of fill of the barrel. The degree of fill has an important effect on the mechanical energy used in the extruder and therefore the characteristics of the final product (Mahungu 2000).

The bulk density of the material after preconditioning has been determined by TA-XT2 (method described in chapter 3).

The results are presented on Figure VI-6. Bulk density of preconditioned samples is significantly lower than the control hydrated sample (CH). No significant difference was found between PcS and PcL.

Particle size has a significant effect on the bulk density of the raw material and the control. The mix had the highest density, then density decreased as particle size decreased. The effect of particle size was less apparent on the preconditioned samples except for the coarse sample. This particular sample had a paste like appearance; therefore its density was higher than the other samples.

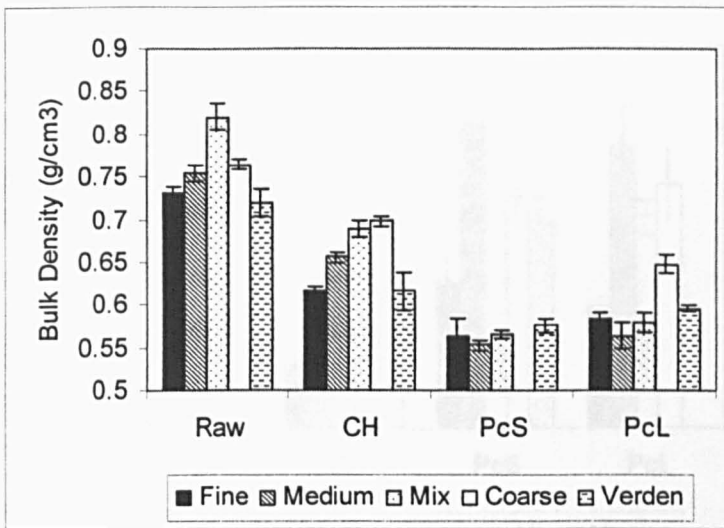


Figure VI-6: Bulk density of preconditioned maize grits (measured at room temperature). Results are average of 5 measurements, error bars are standard deviation.

VI.2.3.2 Study of the compressibility

Compressibility is also an important factor to take into account when using extrusion as it has been highlighted in chapter V.

The compressibility of the hydrated raw material depended only on the origin of the material. Preconditioning increased the compressibility of the sample. This is in agreement with Chapter V. The small variation in moisture could not explain this variation. This effect is believed to be related to starch conversion occurring during preconditioning.

The increase in compressibility depended on the particle size of the sample. Compressibility of fine grits was lower than compressibility of coarse maize and medium grits had the highest compressibility. Although mix maize had the same average particle diameter as medium maize, its compressibility was lower. Verden maize grits were far more compressible than the other types.

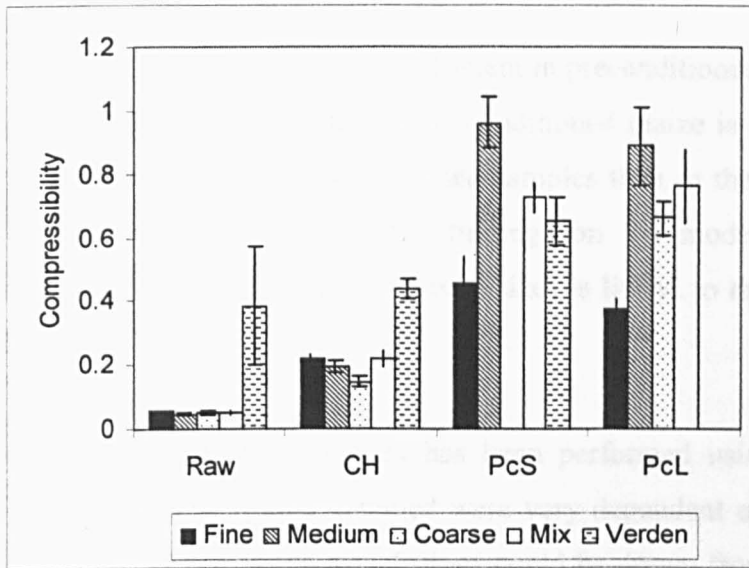


Figure VI-7: Compressibility of preconditioned maize grits.

VI.2.4 Water mobility in preconditioned maize grits

Frozen preconditioned maize grits were thawed at room temperature and analysed by H^1 -NMR at 25°C. Water self-diffusion coefficient was measured as well as free induction decay (FID). The method used is described in Chapter III.

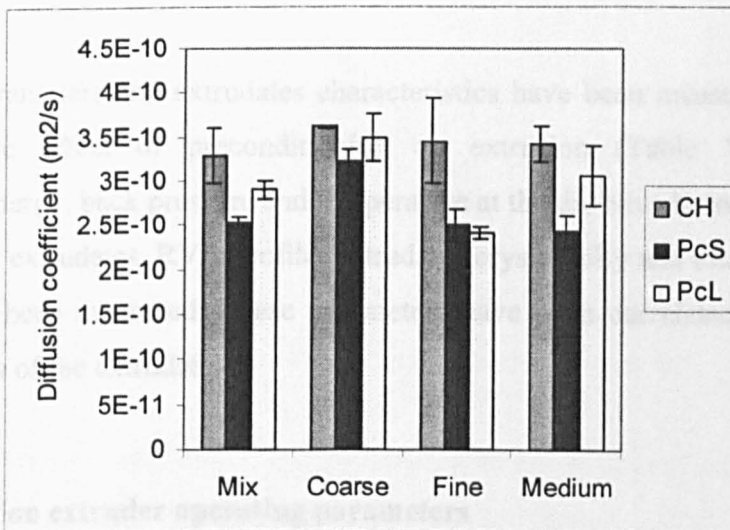


Figure VI-8: Water self-diffusion coefficient in preconditioned maize grits at 25°C.

Results are average of two measurements, error bars are standard deviation.

Figure VI-8 represents the water diffusion coefficient in preconditioned maize grits. It shows that although the moisture content in preconditioned maize is slightly higher, the diffusion is more restricted in preconditioned samples than in the hydrated only samples (CH). This confirms our previous findings on the model system. The difference observed between the different particle sizes is linked to the difference in moisture content of the samples.

Fitting of the free induction decay curves has been performed using the method described in Chapter III. The results obtained were very dependent on the moisture content of the samples, therefore few conclusions could be drawn from the analysis. Nevertheless, it was possible to compare mix and medium grits behaviour, as their moisture contents were similar. No difference was found between the FID of those samples. Therefore, the water mobility did not seem to be affected by particle size distribution.

VI.3 EFFECT OF PRECONDITIONING AND PARTICLE SIZE ON EXTRUSION OF MAIZE GRITS

Operating parameters and extrudates characteristics have been measured in order to determine the effect of preconditioning on extrusion (Table VI-7). Specific mechanical energy, back pressure and temperature at the die have been recorded. Bulk density of the extrudates, RVA profile, extrudates crystallinity and total soluble sugar content have been measured. These parameters have been correlated with different characteristics of the extrudate.

VI.3.1 Effect on extruder operating parameters

Motor power (P_M) and specific mechanical energy (SME) have been calculated using the following formulas (Bouvier, 2000b):

$$P_M = 0.9 \times 380 \times I_M \times \frac{\text{ScrewSpeed}}{398}$$

$$SME = \frac{P_M}{\text{FeedRate}}$$

Where P_M is the motor power (W), I_M is the current intensity drawn by the motor (A), screw speed is in rpm and feed rate is in kg/s. The results are represented in Figure VI-9. As it was expected, the mechanical energy decreases when the samples are preconditioned. The residence time in the preconditioner has a limited effect on SME, although, it can be noted that samples with longer residence time in the preconditioner had a slightly higher SME.

The effect of preconditioned material moisture on SME was studied. The correlation between moisture content and SME was relatively poor. This indicated that, although the variation of moisture observed in the preconditioned material can affect the SME, other factors had more impact on it. Especially, preconditioned maize temperature and compressibility have an effect on SME.

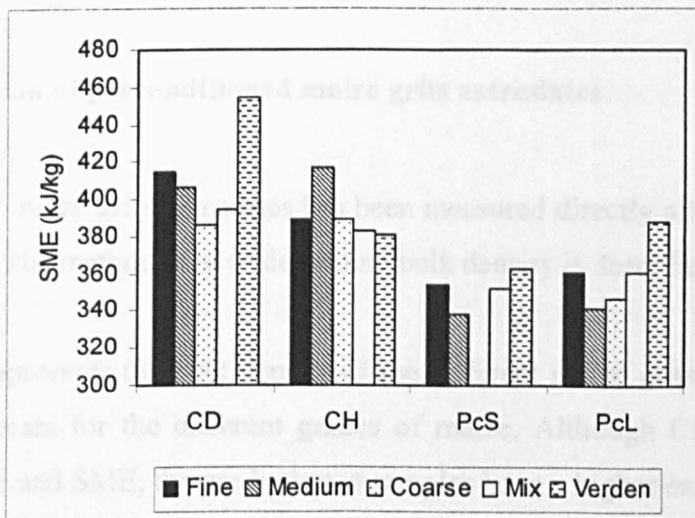


Figure VI-9: Specific mechanical energy of extruded maize grits of different grade at different preconditioning conditions.

As a general trend, back pressure tends to decrease with preconditioning and die temperature tends to increase. Nevertheless, the data for these parameters is not as

clear as it was for the SME. The back pressure is not directly correlated to preconditioned material moisture content, but die temperature is. The lower the moisture, the higher the die temperature was.

Table VI-7: Operating parameters for the different types of maize under different preconditioning treatments. (n.a.: non available)

	<i>Fine</i>	<i>Medium</i>	<i>Coarse</i>	<i>Mix</i>	<i>Verden</i>
<i>SME (kJ/kg)</i>					
CD	415	406	386	395	454
CH	389	417	389	383	380
PcS	355	338	n.a.	352	363
PcL	360	342	347	360	388
<i>Back Pressure (Bar)</i>					
CD	22	23	25	25	24
CH	25	19	24	22	19
PcS	16	19	n.a.	22	19
PcL	21	20	19	20	20
<i>Die temperature (°C)</i>					
CD	138	138	136	140	136
CH	152	141	144	151	143
PcS	155	147	n.a.	151	148
PcL	152	146	141	144	148

VI.3.2 Expansion of preconditioned maize grits extrudates

Bulk density of maize grits extrudates has been measured directly after extrusion (i.e. before drying). The method used to determine bulk density is described in chapter 3.

Figure VI-10 represents the bulk density of the different maize grits extrudates. The same trend appears for the different grades of maize. Although CH and CD have similar moisture and SME, the pre-hydrated samples have a higher expansion than the non pre-hydrated samples.

The effect of preconditioning itself (combination of pre-hydration and pre-heating) on expansion is more difficult to describe. As it has been noted in VI.3.1, preconditioning has a marked effect on SME, any change in SME will have an impact on expansion as has been highlighted by Donald (1993).

As shown on Figure VI-10, bulk density of PcS samples is very similar to CH whereas PcL samples have a slightly higher density even though the SME of PcL is higher. This could be an effect of the higher moisture in PcL samples.

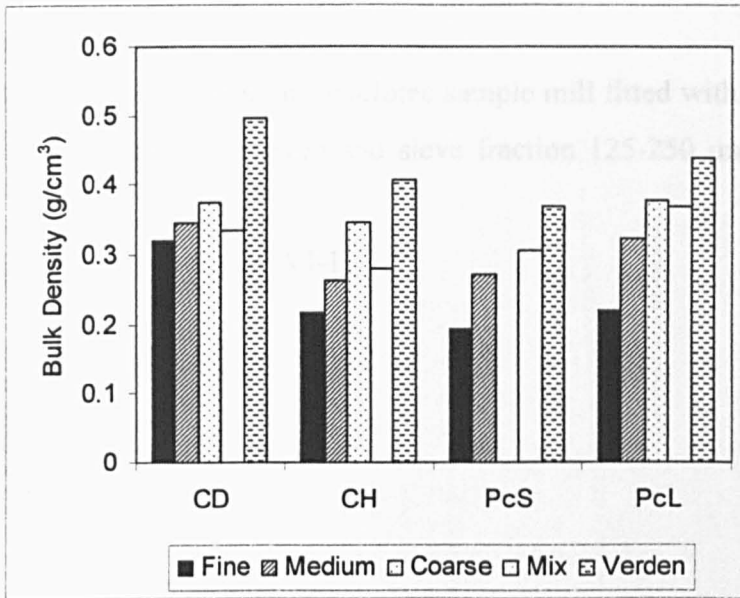


Figure VI-10: Bulk density of maize grits extrudates under different preconditioning conditions. Values are mean of 5 or more measurements.

Verden maize grits had the highest bulk density probably due to the lower starch content of the material (45%).

The effect of particle size on expansion can be clearly seen. For the non-preconditioned, non pre-hydrated samples, the effect of particle size is not significant, but when the samples are pre-hydrated and even more when pre-conditioned, the effect of particle size is marked.

The lower the particles size the higher the expansion of the sample. This effect is correlated to the moisture content of the preconditioned material. Coarser particles had higher moisture than fine ones; and their expansion is reduced. The relationships between expansion and extrusion parameters is given in more details in section VI.4.

VI.3.3 Study of the state of starch in preconditioned extruded maize grits

VI.3.3.1 RVA pasting curves

Dried extrudates have been milled in a cyclotec sample mill fitted with a 1mm screen. The powder obtained was then sieved and sieve fraction 125-250 μm was used for analysis.

The results are presented on Figure VI-11.

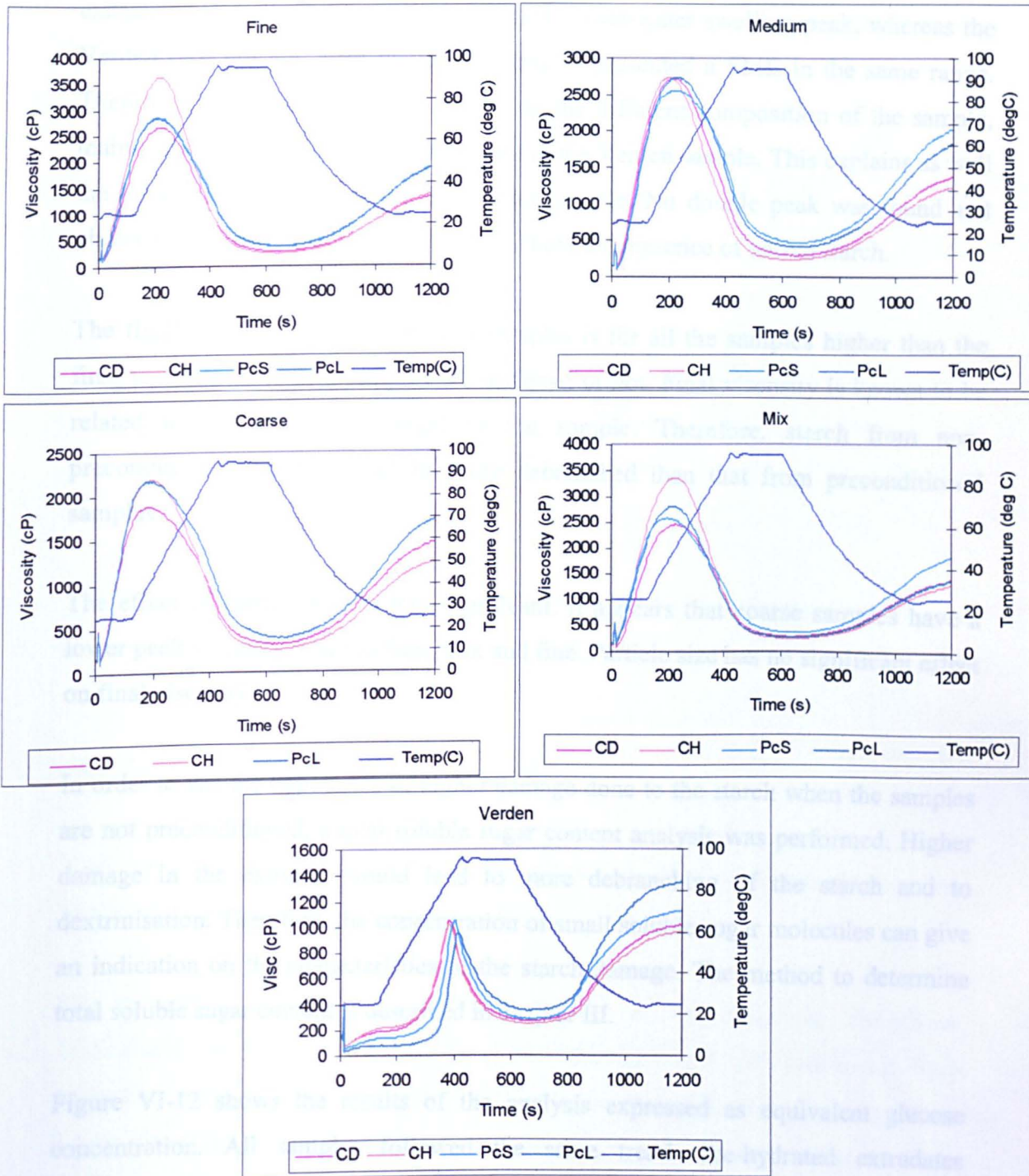


Figure VI-11: RVA pattern of extruded maize grits. Results are average of 3 measurements.

Pasting curves of maize grist of different origins are very different. All maize extrudates of grade fine to coarse presented a cold-water swelling peak, whereas the Verden type did not, even though all samples presented a SME in the same range. Therefore, this difference is mainly due to the different composition of the sample, mainly the lower amount of starch present in the Verden sample. This explains as well the lower viscosities found for the Verden sample. No double peak was found and observation under the microscope did not show the presence of native starch.

The final viscosity of preconditioned samples is for all the samples higher than the final viscosity of control samples pre-hydrated or not. Final viscosity is known to be related to the molecular weight of the sample. Therefore, starch from non-preconditioned samples could be more debranched than that from preconditioned samples.

The effect of particle size is less significant. It appears that coarse samples have a lower peak viscosity than medium, mix and fine. Particle size has no significant effect on final viscosity.

In order to test the hypothesis of higher damage done to the starch when the samples are not preconditioned, a total soluble sugar content analysis was performed. Higher damage in the extruder would lead to more debranching of the starch and to dextrinisation. Therefore, the concentration of small soluble sugar molecules can give an indication on the characteristics of the starch damage. The method to determine total soluble sugar content is described in chapter III.

Figure VI-12 shows the results of the analysis expressed as equivalent glucose concentration. All samples followed the same trend. Pre-hydrated extrudates presented higher amounts of sugar compared to the non-pre-hydrated samples. The effect of preconditioning was to decrease the total amount of soluble sugar to a level below or equal to the one found for CD. Increasing residence time in the preconditioner did not decrease further the amount of soluble sugar.

This seems to confirm the hypothesis that preconditioning reduces the amount of damage in the extruder to some extent. By pre-hydrating and pre-heating the mix

before the extruder, the mix viscosity decreases in the extruder and the amount of shear experience by the mix is lowered therefore lowering the amount of damage done to the starch.

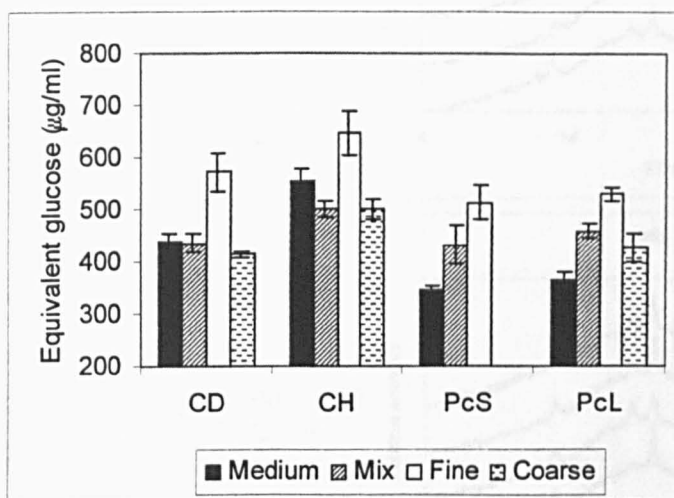


Figure VI-12: Total soluble sugar content of maize grits extrudates expressed in terms of equivalent glucose.

VI.3.3.2 X-ray analysis of extruded samples

X-ray analysis provides some information on the crystallinity of extruded samples. The results are represented on Figure VI-13.

All extrudates presented a V-pattern typical of amylose-lipid complexes. Additionally, for some samples, peaks at $2\theta = 18.4$, 11.9 and 7.0° were found. Such diffraction angles are characteristic of another type of amylose complexes known as E-type. Mercier (1979) showed that these complexes are in a metastable state. When the sample is conditioned to a moisture content of 30% (db), the E-type complexes are irreversibly converted to V-type.

This has been verified on the maize grits extrudates and confirmed the presence of the E-type complexes. When the extrudates have been equilibrated in a RH box at 95% to reach a moisture content above 30%, the diffractogram of the samples showed no traces of E-pattern, only the V-pattern was observed.

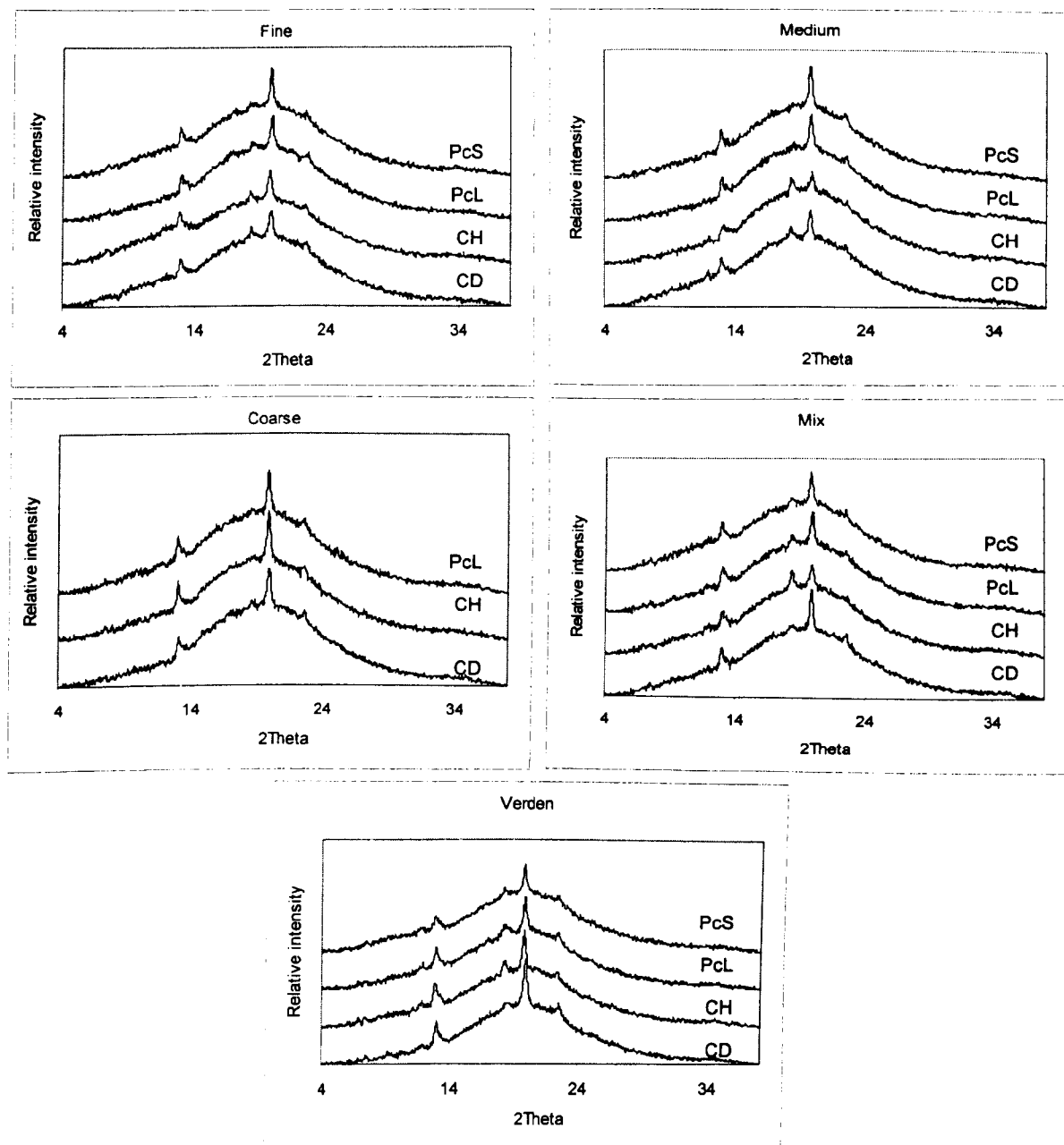


Figure VI-13: X-ray diffractogram of maize grits extrudates (average of two measurements).

The E-type crystals are also characterised by the packing of single helices of amylose, but whereas V-type crystals have an interaxial distance of 1.38nm, E-type crystals have a distance of 1.50nm (Mercier 1979). Donald (1993) found that in extrudates, this non equilibrium form is often related to higher viscosity of the melt which leads to a lower mobility of the polymer chain and therefore less possibility for the rearrangements to take place during the expansion of the extrudate.

The E-type complexes are found especially in extrudates processed under high temperature (typically above 135°C) and low moisture content (below 18%). In some cases, they can also be formed at lower temperature at higher shear rates.

In the series of preconditioned extrudates presented, the E-pattern is particularly sharp for the control samples compared to the preconditioned samples. This could be related to the lower SME of preconditioned samples.

Diffuse A-pattern characteristics appeared on most samples. Observation under polarised light microscope did not show the presence of native starch granule. DSC has been performed on the medium grits extrudates and showed some gelatinisation peaks at about 60°C, this is lower than the one found in native maize grits and therefore could be due to retrograded starch rather than native material.

VI.4 ANALYSIS OF CORRELATIONS

Many of the parameters recorded during this study are known in the literature to be correlated to each other. Especially, some of the characteristics of the preconditioned samples (degree of starch conversion, bulk density, compressibility...) have an impact on the quality of the extrudates. In order to determine this impact an analysis of correlation has been made using firstly raw data and secondly principal component analysis.

VI.4.1 Analysis of the raw data

Extrudates characteristics have been plotted against preconditioned sample characteristic in order to visualise the relations that might link one to another.

Therefore, 5 extrudates properties (SME, back pressure, die temperature, bulk density and total soluble sugar content) were plotted against 4 preconditioned material properties (XRDi, bulk density, compressibility and temperature at the extruder inlet). When a pattern was observed, a line of best fit was fitted using excel, R^2 were given as an indication of the quality of the fit.

Specific mechanical energy was negatively linearly correlated to the temperature at the inlet of the extruder. SME was also linearly correlated to the compressibility of the sample at the preconditioner exit.

Extrudates bulk density was slightly correlated to the die temperature. The higher the die temperature the lower the density.

When all the data were considered, there was no correlation between moisture content and extrudate expansion (bulk density). But when CD samples were taken out, the correlation appeared to be quite good. This showed that for the pre-hydrated samples, the small variation in moisture content was mostly responsible for the change in bulk density.

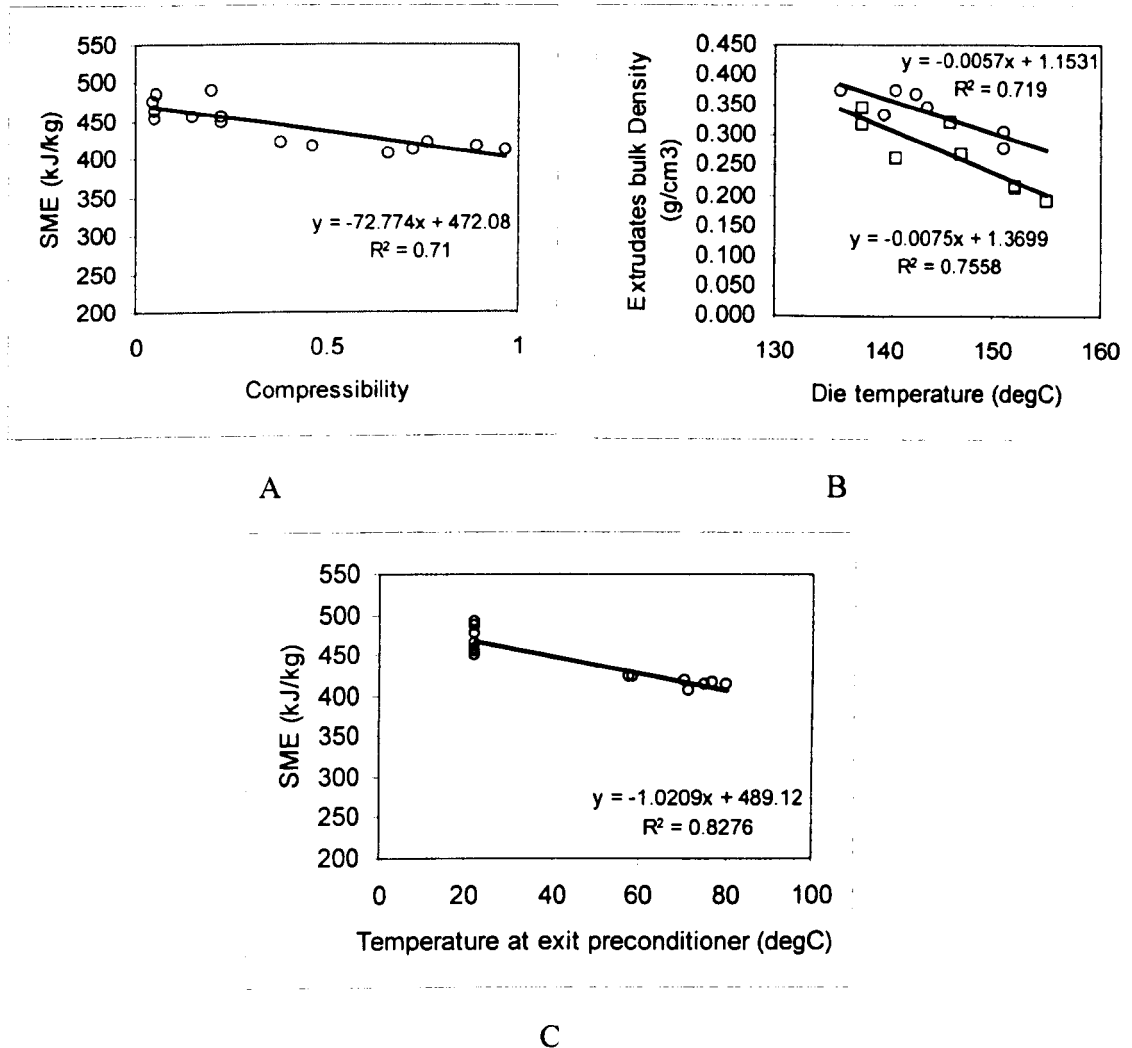


Figure VI-14: Correlation between SME and compressibility (A), correlation between die temperature and extrudates bulk density: different correlation between fine and medium grits () and coarse and mixed grits (o) (B), correlation between temperature of the mix at the exit of the preconditioner and SME (C).

No direct correlation was found between bulk density and SME or back pressure (Figure VI-15). This confirms the singular effects of preconditioning and particle size on extrudates properties. Especially preconditioning and particle size might affect the state of water in the material, this might have a durable effect during extrusion (Karathanos 1992).

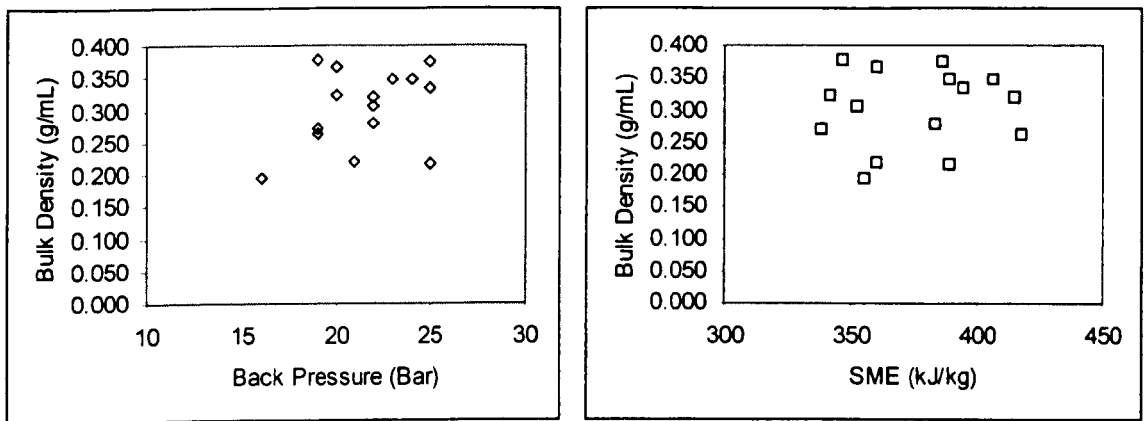


Figure VI-15: Relationship between bulk density and SME or back pressure.

VI.4.2 Principal component analysis

Principal component analysis is a descriptive method that gives a representation of the samples and the variables. This method can give a good overview of the linear interactions between variables as well as a good segregation of different groups of samples.

For the analysis, 10 variables were used:

- SME
- Back pressure (back P)
- Die temperature (die T)
- Moisture content of the preconditioned material (MC)
- Temperature at the exit of the preconditioner (T Pc)
- Compressibility (compress)
- Bulk density of preconditioned material (BlkD Pc)
- XRD_i of preconditioned material (XRD_iPc)
- Bulk density of extrudates (BlkDExt)
- Total soluble sugar in the extrudates (Sugar).

Verden samples were not included in the analysis because of their different composition and behaviour.

The results of the analysis show that principal component 1 and 2 (PC1 and PC2) explain 53% and 28% of the variance respectively. Therefore the plan described by PC1 and PC2 gives a relatively good description of the data (81% of the variation is explained by those axis).

The effect of preconditioning is clearly represented in Figure VI-16 and confirms previous observations. Three groups of samples can be distinguished according to the way the samples were preconditioned. Group 1 represents the non-hydrated samples, group 2 the hydrated samples (without heat treatment) and group 3 represents the preconditioned samples (PcS and PcL).

The effect of particle size is also seen in the representation as the coarse samples appear always on top of the group whereas the fine samples appear at the bottom.

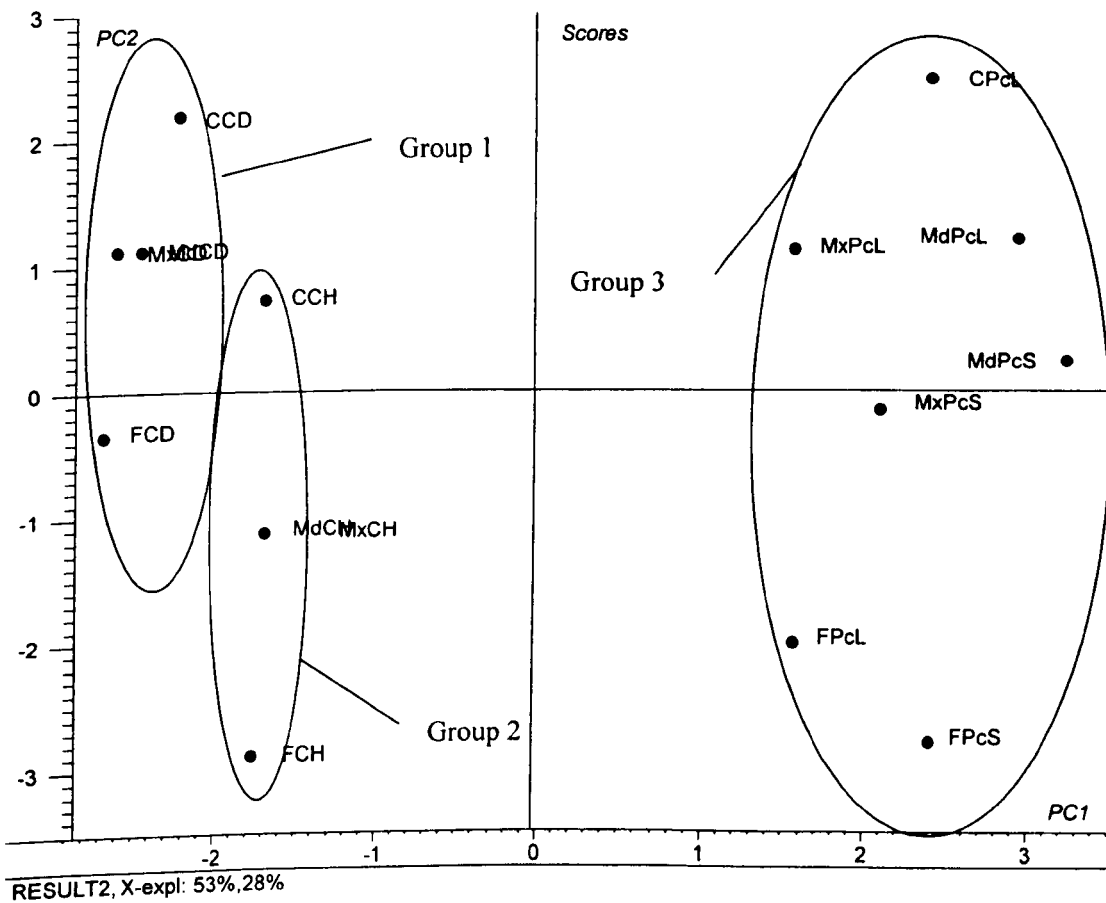


Figure VI-16: Representation of samples scoring along principal component 1 and 2.

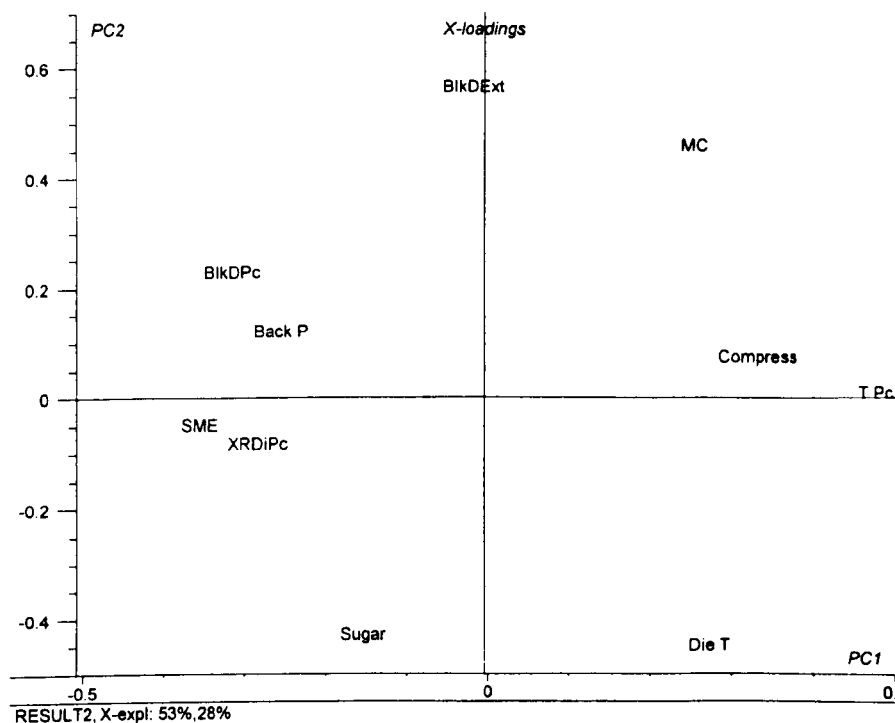


Figure VI-17: Representation of the variables loading on principal component 1 and 2.

Figure VI-17 represents the variable locations along PC1 and 2. A good correlation appears between compressibility and temperature at the extruder inlet, these 2 variables are negatively correlated to SME and XRDIPc.

Bulk density of the preconditioned material and back pressure appeared to be poorly correlated with the other variables. Moisture content appears slightly negatively correlated to the amount of soluble sugar in the extrudates.

The PCA gives a global representation of the samples and the relationships that link them. Unfortunately, the limitation in the number of samples and their variability (different particle size), doesn't allow strong correlations to be seen.

VI.5 CONCLUSION

Although experimental conditions did not allow a proper control of the moisture content of the material leaving the preconditioner, a detail analysis of the results showed the effect of preconditioning and particle size on extrusion and extrudate characteristics.

The effect of preconditioning as studied on the model preconditioning system has been confirmed with some variations due to the difference in the machine configuration.

First, there is a pre-hydration effect. Pre-hydration allows the samples to keep a similar or slightly lower SME than the non pre-hydrated, but increases the expansion of the product without changing the moisture content. Pre-hydration allows plastisation of the material before entering the extruder and therefore could lower the SME, but this was observed only for the grade of maize grits Verden in this study. This pre-hydration also allows a better homogeneity of the melt and therefore could explain the better expansion observed. A metastable form of amylose-lipid crystals also results from such a treatment, this could be due to the high viscosity of the mix and the high extrusion temperature.

The second effect of preconditioning is to heat up the material. This leads to partial starch conversion in the preconditioned material, therefore lowering its compressibility. As the compressibility decreases and the temperature of the material entering the extruder increases, the SME decreases. Although the amount of mechanical energy decreases, the expansion to that of the material produced by pre-hydration only. The amount of starch damage in the extruder is reduced as shown by the smaller amount of small sugar molecules. The extrudate crystallinity is the equilibrium form (V-type). By partially converting the starch, the viscosity of the melt in the extruder drops therefore, less mechanical energy is dispersed. As the melt viscosity decreases, there is less resistance to bubble growth when the melt exits the die even though the driving force is lower than for the non-preconditioned material.

The lower viscosity of the melt would also allow more time for the polymer chains to reorganised before reaching the glassy state, therefore allowing the more stable crystalline form of amylose-lipid complex to develop (Donald 1993).

The effect of particle size was more difficult to analyse as it was more linked to the variation in moisture of the maize grits. Particle size did not seem to affect starch conversion during preconditioning or water mobility.

The physical characteristics of the preconditioned powder were on the other hand very affected by particle size. There was also an interaction between the effect of particle size and preconditioning. The effect of particle size on bulk density was decreased and almost nullified when the grits were preconditioned whereas its effect on compressibility was magnified.

The effect of particle size on extrusion was significant. Small particle size grits were more expanded than bigger one, but as smaller particle also had lower moisture content, it was not possible to determine whether this was solely an effect of moisture or a combined effect.

The effect of particle size distribution was mainly seen on the extrudates crystallinity. The broad particle size distribution had more E-type crystallinity than the particles with a more narrow distribution.

Coarse grits could not be fed into the extruder after preconditioning with a short residence time. The mixture was then too sticky and had the appearance of a paste. X-ray and DSC analysis showed that the degree of gelatinisation was similar for coarse grits than fine grits under these conditions. Therefore, the increase stickiness of the mix in the preconditioner was not due to increase starch conversion but perhaps to localisation of the gelatinisation at the surface of the granule. Large particles are denser than small particles and therefore are more resistant to water diffusion (Caldwell 2000). When using a short residence time, the rotation speed of the paddle increases therefore increasing mixing. Under these conditions, water diffusion inside the granule is low and therefore, starch conversion could be limited only to the surface.

CHAPTER VII FORMATION OF AMYLOSE-LIPID COMPLEX IN EXTRUDED CEREAL-LIPID SYSTEMS



The three previous chapters focused mainly on the effect of the process on the characteristic of extrudates. This chapter will discuss a more complex system where lipids are added to the cereal matrix.

VII.1 INTRODUCTION

VII.1.1 Background and aim of the study

Extrusion of starch-lipid mixture has been extensively studied (Bhatnagar 1994a; Mercier 1979; Bhatnagar 1997; Desrumaux 1999). Mercier (1979) and Colonna (1989), showed the formation of amylose-lipid complexes in various extruded starches. The conditions for the formation of such complexes have also been studied (Lin 1997; Bhatnagar 1994b).

Recent studies have also showed the formation of amylose-lipid complexes during quiescent heating of various starches and their impact on pasting behaviour (Becker 2001).

The aim of this study was therefore to investigate the formation of amylose-lipid complex during extrusion cooking and what was their impact on pasting. The effect of various amounts of lipids and different extrusion conditions on extrudates characteristics was also studied.

Therefore a simple system was first analysed (maize grits with a free fatty acid) under different extrusion conditions and with various lipid content. A different type of cereal source (wheat flour) was then used with the same fatty acid to check whether the pasting behaviour of the extrudate was similar. Finally complex fats (beef tallow, poultry fat and sunflower oil) were used in combination with maize grits.

VII.1.2 Sample preparation

Maize grits was supplied by Maizecor, its characteristics are given in VI.1.2. Wheat flour was supplied by Spillers Milling. Linoleic acid (60%) was supplied by Acros Ltd.

Extrusion conditions are described in the following sections. Specific mechanical energy (SME) was calculated as described in Chapter III.

The sectional expansion index was determined by the method of Alvarez-Martinez (1988). Bulk density (BD in g/mL) was calculated approximating the shape of the extrudate to a cylinder.

$$BD = \frac{W_e \times 4}{L_e \times \pi \times D_e^2}$$

Where W_e , L_e and D_e are the extrudates weight (g), length (cm) and diameter (cm). Bulk density has been determined on the sample before drying.

After extrusion the extrudates have been dried for 1h in a forced air oven at 105°C. The moisture content of the extrudates before and after drying has been determined by drying the samples in an oven at 105°C for 1 day.

The cell structure of the extrudates has been observed using the method described in Chapter III.

Dried extrudates have been ground using a cyclotec sample mill (Trecator Ltd, U.K.) fitted with a 1mm screen. The ground powder has been left in an airtight container at

75% relative humidity to equilibrate for a week. The equilibrated samples have then been analysed by X-Ray. For RVA analysis, the ground powder was sieved, and only the sieve fraction 125-250 μm was used for analysis.

Lipid extraction was performed using the method of Morrison (1980). 1g dried extrudate ground to pass a 0.5 mm screen was mixed with 16mL water saturated butanol in a screw cap tube. The tube was left in a boiling water bath for 6 hours. The solvent was changed every hour. After extraction the sample was left on a tray in the fume cupboard to evaporate the solvent, then left in a dessicator until completely dry. Free fatty acid content was determined on the different fats used in VII.4. by the AOCS standard method 940.28 described in Chapter III.

VII.2 EXTRUSION OF MAIZE GRITS AND LINOLEIC ACID UNDER VARIOUS CONDITIONS.

VII.2.1 Experimental conditions

Maize grits were mixed with water and linoleic acid in different proportions in order to get different percentages of linoleic acid in the mix, but keeping the water / maize grits ratio constant.

Table VII-1: Composition of the mixture maize grits, water and linoleic acid.

<i>% C18:2 (wb)</i>	<i>0.0</i>	<i>0.3</i>	<i>0.6</i>	<i>0.9</i>	<i>1.2</i>
Maize Grits (g)	1500	1500	1500	1500	1500
Water (g)	368.6	368.6	368.6	368.6	368.6
C18:2 (g)	0.0	5.6	11.3	17.1	22.9

These mixes were then extruded in a Clextral BC 21 co-rotating, intermeshing twin-screw extruder. The feed rate used was 4.5 kg/h. The extruder was fitted with a 3 mm diameter circular die. Table VII-2 presents the variable extruder parameters.

It should be noted that samples extruded at 100°C and 120°C were produced on a different day.

Table VII-2: Extruder parameters.

<i>Sample</i>	<i>Temperature zone 2 (°C)</i>	<i>Temperature zone 3 (°C)</i>	<i>Temperature zone 4 (°C)</i>	<i>Screw speed (rpm)</i>
0%/100	60	75	100	150
0.3%/100	60	75	100	150
0.6%/100	60	75	100	150
0.9%/100	60	75	100	150
1.2%/100	60	75	100	150
0%/120/150	75	100	120	150
0.6%/120/150	75	100	120	150
1.2%/120/150	75	100	120	150
0%/120/250	75	100	120	250
0.6%/120/250	75	100	120	250
1.2%/120/250	75	100	120	250

Extrudates were cut into cylindrical strands of about 40 cm length as they exit the extruder, and dried. Extrudates analysis was performed according to the methods described in VII.1.2.

VII.2.2 Extrusion operating conditions and extrudates characteristics.

VII.2.2.1 Extruder operating parameters.

Specific mechanical energy and back pressure for the different extrudates are reported in Table VII-3.

Samples extruded at 120°C with a screw speed of 150 rpm had the lowest SME whereas samples extruded at 120°C with a screw speed of 250 rpm exhibited the highest SME.

For the samples extruded at 100°C, addition of linoleic acid to the water – maize mixture did not change the SME. Whereas at 120°C, samples containing 0.6 or 1.2% exhibited a slightly lower SME. This is probably due to the lubricating effect of lipids in the extruder.

The back pressure was the highest for the samples at 100°C; at 120°C the back pressure dropped significantly. When the screw speed was increased to 250 rpm, the back pressure decreased further.

The amount of linoleic acid in the sample did not significantly affect the back pressure.

Table VII-3: Extruder operating parameters (numbers in parenthesis are standard deviations).

	<i>Back P (Bar)</i>	<i>SME (kJ/kg)</i>	<i>Moisture Content (%wb)</i>
0%/100	17	258.7	22.3 (0.25)
0.3%/100	21	258.7	23.1 (0.1)
0.6%/100	15	268.8	23.4 (0.13)
0.9%/100	27	258.7	24.6 (0.11)
1.2%/100	23	266.3	25.0 (0.26)
0%/120/150	12.3 (1.2)	233.6 (6.6)	19.3 (0.43)
0.6%/120/150	12.0 (1.0)	220.2 (7.3)	21.2 (0.83)
1.2%/120/150	10.3 (2.1)	217.7 (10.2)	23.3 (0.13)
0%/120/250	6.3 (1.2)	390.8 (8.7)	20.1 (0.32)
0.6%/120/250	6.7 (0.6)	368.4 (11.1)	20.9 (0.42)
1.2%/120/250	9.3 (3.5)	368.4 (8.4)	20.9 (0.13)

VII.2.2.2 Extrudates characteristics.

The extrudates obtained after extrusion had a foam structure. The expansion was recorded in different ways. Sectional expansion index was a measure of the maximum expansion of the product, measure of the diameter and the bulk density of the extrudates after cooling down gave an indication on the shrinkage. Dyed cross sections were also observed using an office scanner using the method described in Chapter III. This gave some information on the structure of the foam.

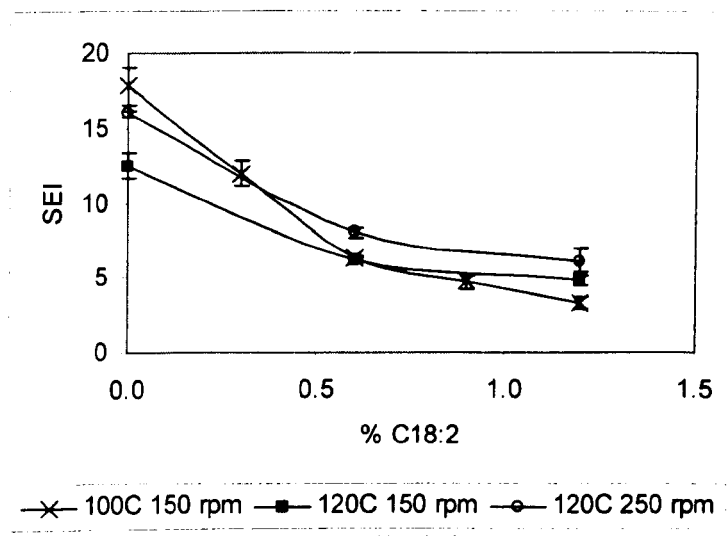


Figure VII-1: Sectional expansion index of the different maize grits extrudates (results are average of 5 replicates, error bars represent standard deviation).

The sectional expansion index decreased as the amount of lipid increased. As little as 0.3% linoleic acid decreases significantly the SEI. At 120°C, the SEI increased slightly when screw speed increased.

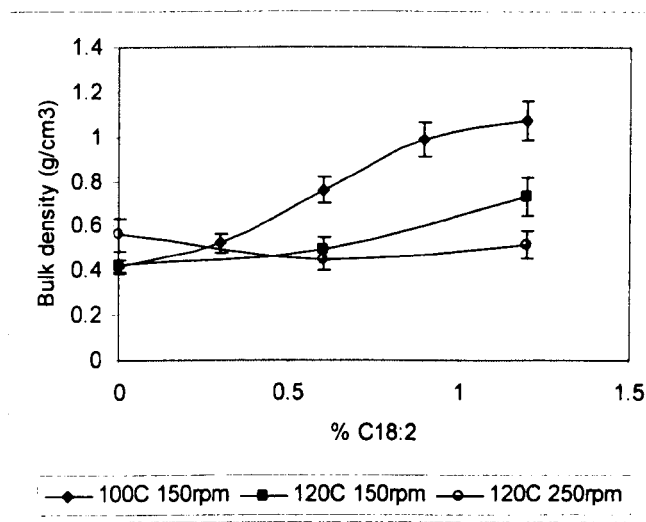


Figure VII-2: Bulk density of the different extrudates (results are average of 10 replicates, error bars are standard deviations).

The bulk density is also significantly affected by the amount of linoleic acid added to the sample but the variation in bulk density is slightly different than for SEI.

For the samples having the highest SME, the effect of lipid content is less significant. The shrinkage of the samples can be measured by recording the diameter of the extrudates at the die (when it is at its maximum) and after cooling down (Figure VII-3). As the amount of added lipid increases, the diameter of the extrudates reached a plateau and the amount of shrinkage was reduced.

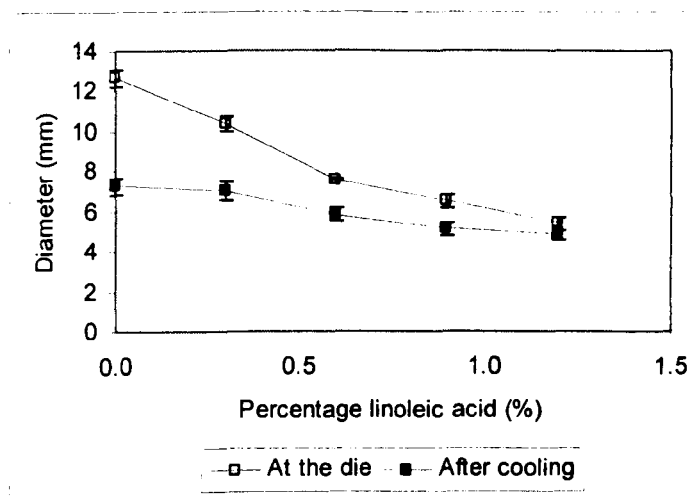


Figure VII-3: Diameter of samples extruded at 100°C at the die and after cooling down to room temperature. Results are average of 5 measurements, error bars are standard deviation.

Observation of the extrudates (Figure VII-4 to Figure VII-6) showed that, the number of cell decreased as the amount of added lipid increased, especially for the samples extruded at 100°C.

Although samples extruded at 120°C did not always show difference in bulk density, the foam structure appeared to be significantly affected by the addition of linoleic acid. It is particularly clear that the cell size is smaller for the samples with 0% linoleic acid than for the samples with 0.6 or 1.2%.

Moisture content of maize grits extrudates has been measured after the samples had cooled down. Table VII-3 shows that except for the samples extruded at 120°C and 250rpm, the moisture content of the samples is increasing as the amount of linoleic acid increases. This is well correlated with the expansion of the samples. As less water flashes off the sample at the exit of the die, the expansion is limited and the moisture content in the final extrudate is high.

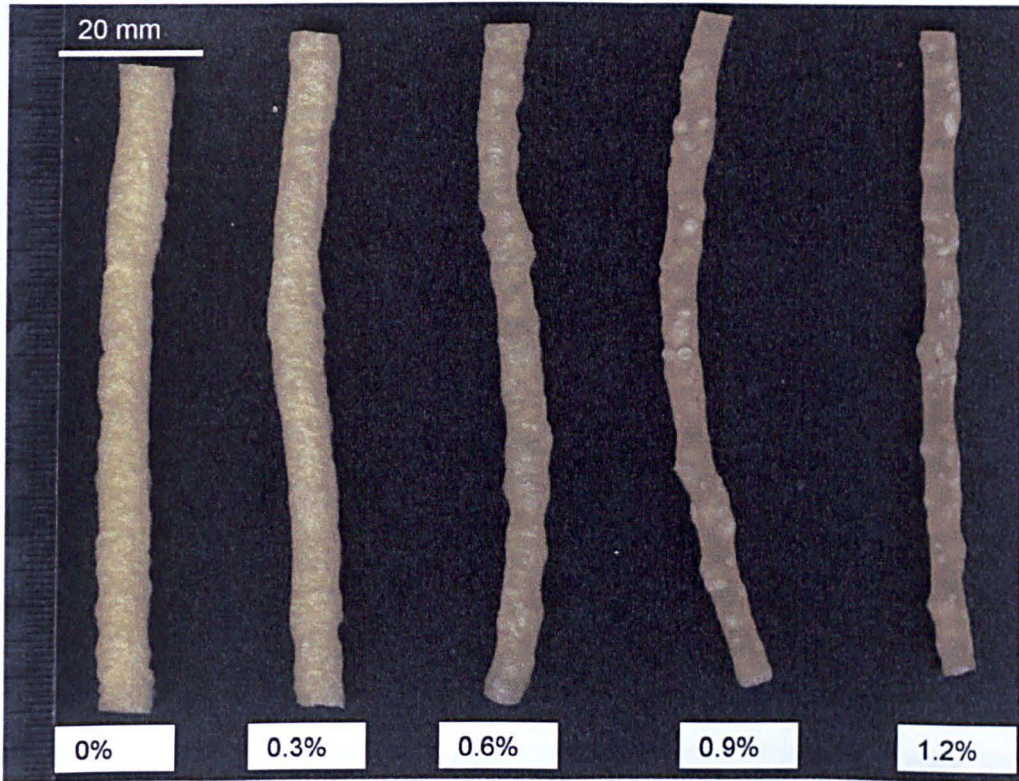


Figure VII-4: Maize grit extruded with different amount of linoleic acid at 100°C.

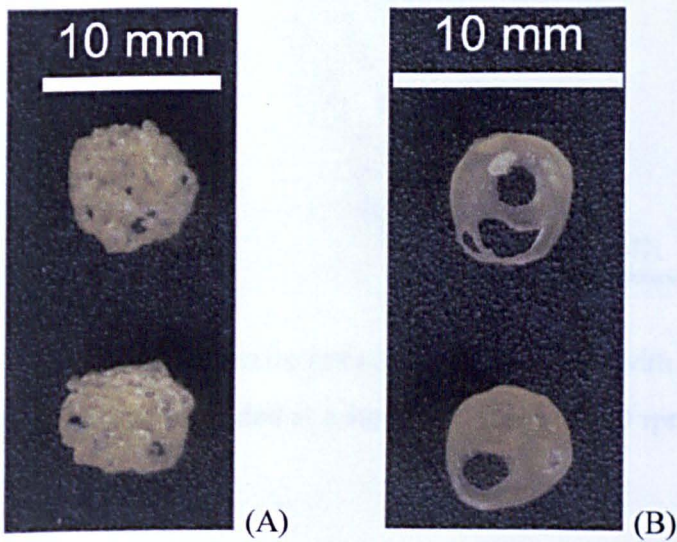


Figure VII-5: Cross section of maize grits extruded at 100°C with (A): 0% and (B): 1.2% linoleic acid

VII.3.3.1 Amylose-lipid complex formation

X-ray diffraction has been performed in order to check the presence of amylose-lipid complexes.

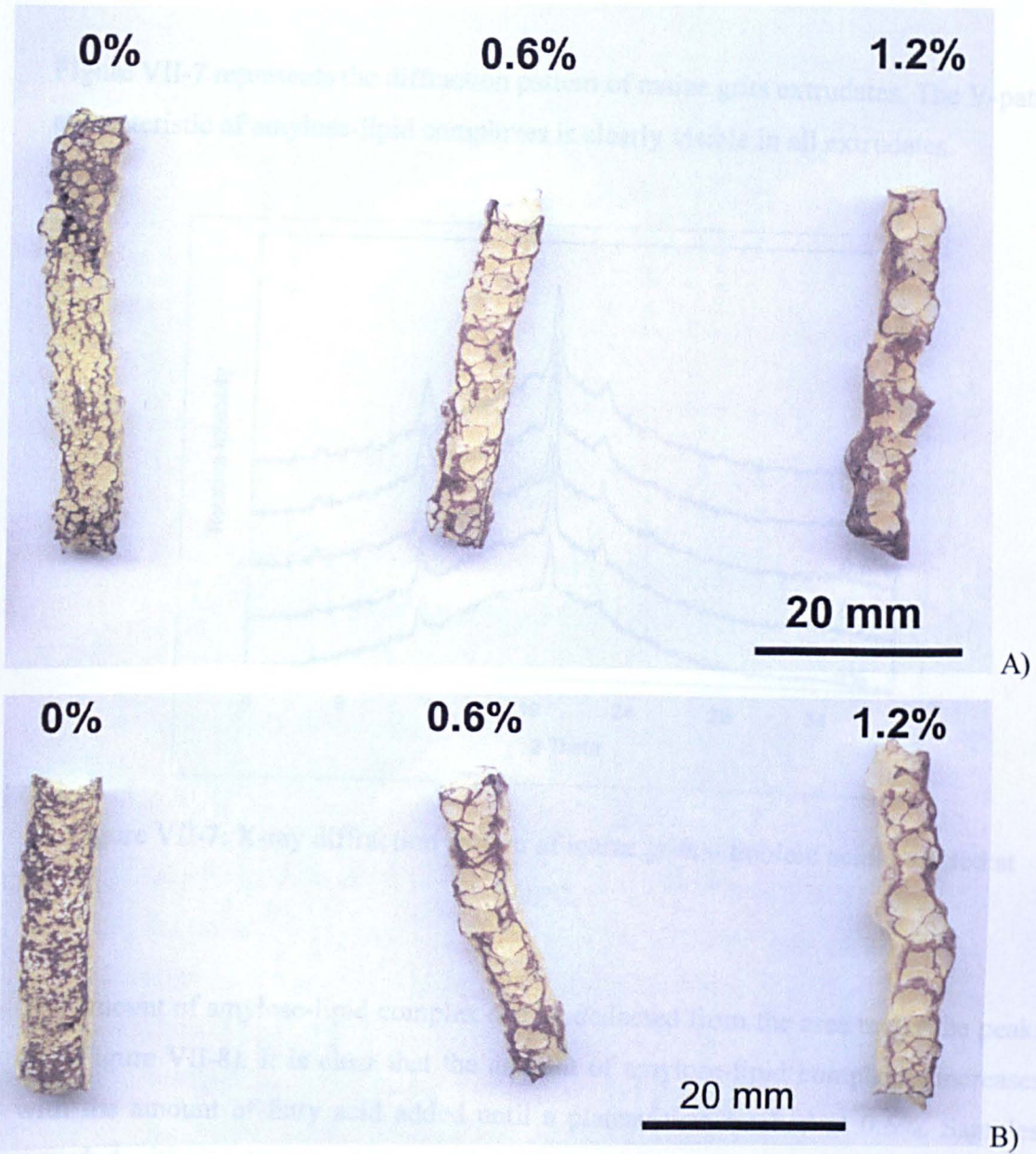


Figure VII-6: Cross sections of maize grits extruded at 120°C with different amounts of linoleic acid. Sample extruded at a screw speed of A) 150 rpm, B) 250 rpm.

VII.2.3 Effect on starch characteristics

VII.2.3.1 Amylose-lipid complex formation.

X-ray diffraction has been performed in order to check the presence of amylose-lipid complexes.

Figure VII-7 represents the diffraction pattern of maize grits extrudates. The V-pattern characteristic of amylose-lipid complexes is clearly visible in all extrudates.

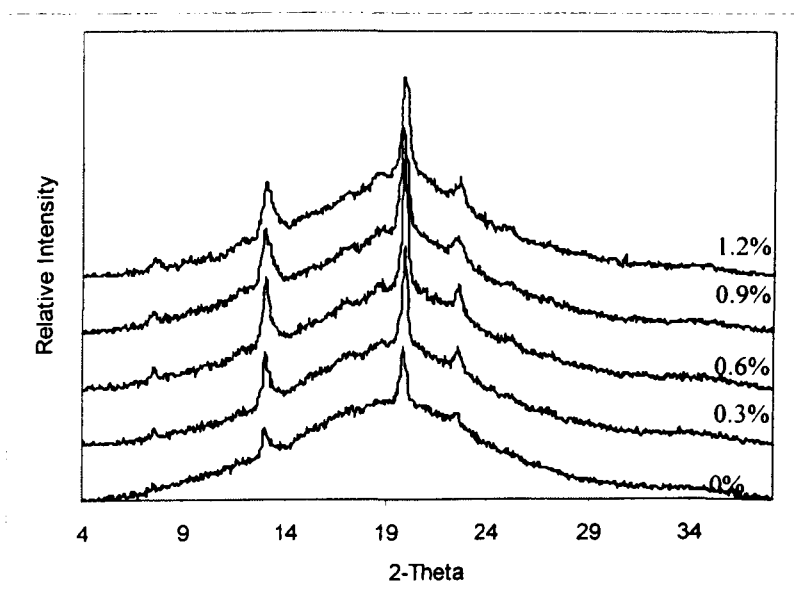


Figure VII-7: X-ray diffraction pattern of maize grits – linoleic acid extruded at 100°C.

The amount of amylose-lipid complex can be deduced from the area under the peaks (see Figure VII-8). It is clear that the amount of amylose-lipid complexes increases with the amount of fatty acid added until a plateau was reached at 0.6%. Samples extruded without addition of fatty acid exhibited a V-pattern as well. This is probably due to the formation complexes with native lipid present in the maize grits. The amount of complexes seemed to increase with the extrusion temperature. The effect of screw speed did not appear to be significant. This is in agreement with the findings of Bhatnagar (1994b).

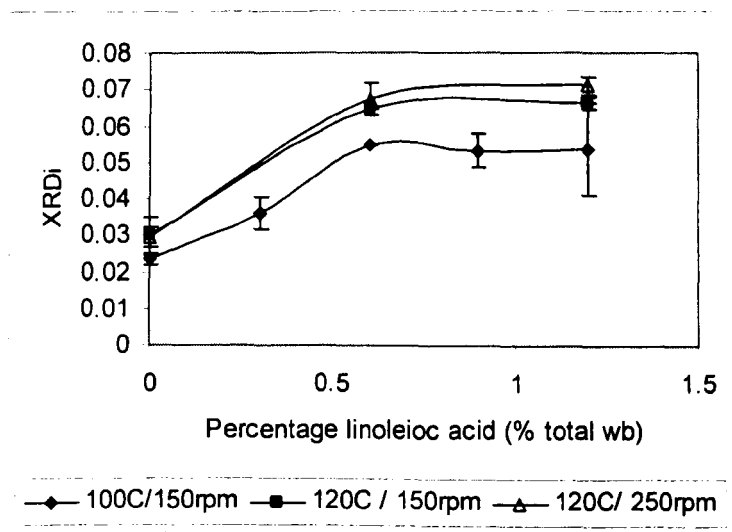


Figure VII-8: Crystallinity index (XRDi) of extruded maize grits with linoleic acid under different extruder conditions.

In order to confirm those results, DSC runs have been performed to check the presence of amylose-lipid complexes.

DSC will be able to show the endotherm of melting of the amylose-lipid complex, but it should be noted that during the heating stage, amylose-lipid complexes can be formed, therefore the results are more an indication of the maximum amount of complexes that can be form in the system rather that the precise amount of complexes present in the sample.

Figure VII-9 shows the DSC trace for maize grits extruded with linoleic acid at 100°C. Each sample presented a single peak at 112°C. After re-run, a peak was present at a lower temperature (between 90 and 95°C). A second peak was observed in the samples with higher linoleic acid content, the peak temperature was 112°C for samples at 0.3 and 0.6%. For maize grits extruded with 1.2%, this second peak seemed to appear at lower temperature and be merged with the first peak.

This behaviour is characteristic of amylose-lipid complexes formed during extrusion (Conde-Petit 1995). After melting the complexes during the first DSC run, as the sample is cooled rapidly, rearrangements can occur leading to a different form of complexes melting at a lower temperature.

It should also be noted that an exotherm seems to appear for the sample at 1.2% linoleic acid. This exotherm could be due to the formation of amylose-lipid complex.

X-ray diffraction did not show any difference between the complexes formed in the samples with 0% linoleic acid (the complexes being formed only with native lipids) and the sample with added fatty acid. DSC data shows

Analysis of the samples extruded at 120°C and 150rpm presented similar characteristics than sample extruded at 100°C (Figure VII-10). The exotherm previously observed for the sample at 1.2% linoleic acid, was again observed for most samples extruded at 120°C.

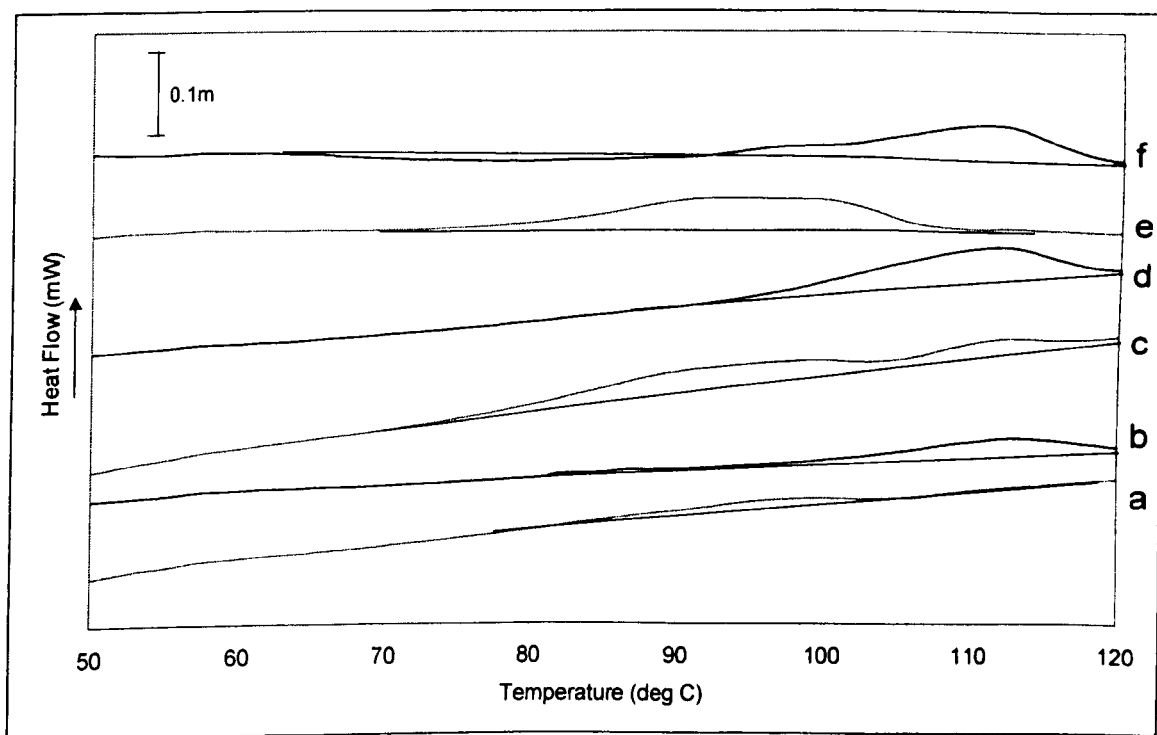


Figure VII-9: DSC endotherms of maize grits extruded at 100°C, with linoleic acid at 0% (b) and re-run (a), 0.6% (d) and re-run (c), 1.2% (f) and re-run (e). The curves were normalised to dry sample mass. The measurements were performed at a water to solid ratio 2:1.

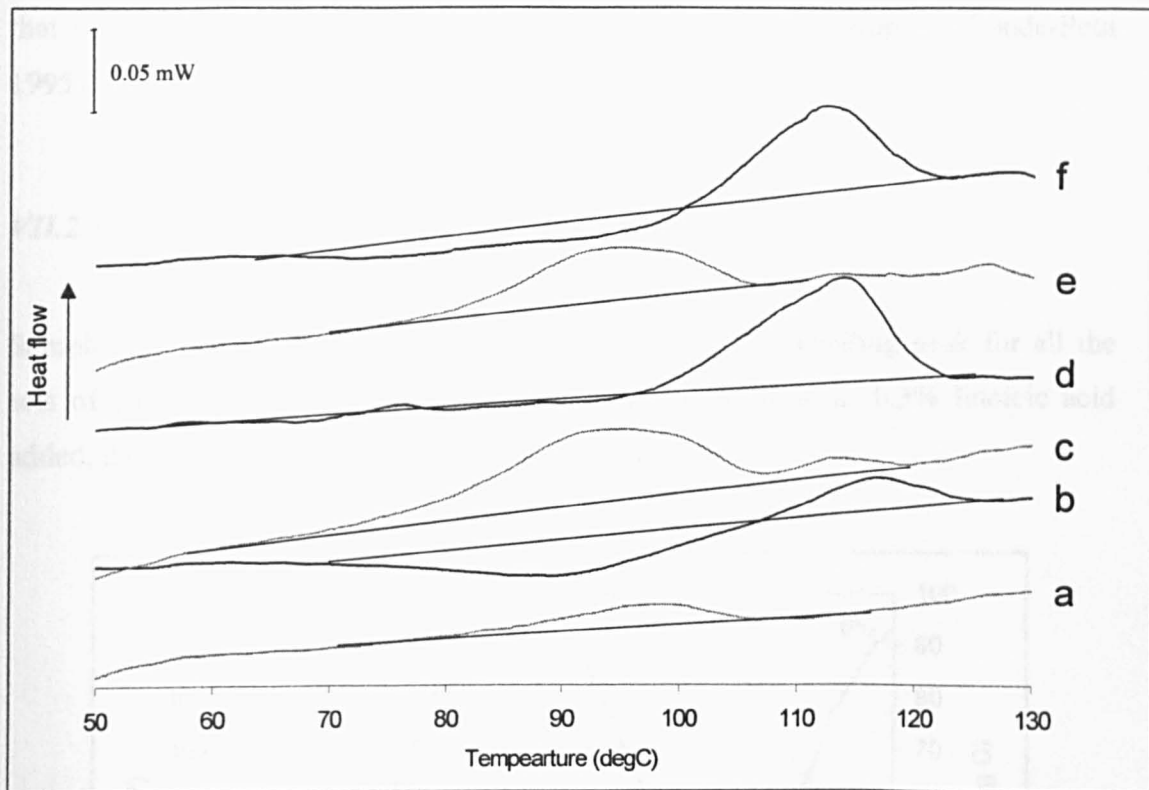


Figure VII-10: DSC endotherms of maize grits extruded at 120° and 150rpm, with 0% (b) and re-run (a), 0.6% (d) and re-run (c) and 1.2% (f) and re-run (e). All the curves have been normalised to dry sample mass. The measurements were performed at a water to solid ratio 2:1.

The DSC results did not allow us to conclude precisely on the nature of the complex. A more detailed study, for example using slower heating rates, might be required to determine more precisely the nature of the complex formed with linoleic acid.

An attempt has been made to determine whether the amylose-lipid complexes were formed in the extruder barrel as suggested by Bhatnagar (1996) or during the cooling down at the exit of the extruder as assumed by Desrumaux (1999).

Samples extruded at 100°C with 0.6% linoleic acid have been cut directly at the die of the extruder and fast frozen with liquid nitrogen in order to determine the presence of complexes at the die at different time intervals. X-ray diffraction showed that the complexes were already present therefore it was assumed that they were formed in the extruder when extruded at this temperature, which is below that of amylose-lipid complex melting. It was assumed that when extruder barrel temperature rises above

that of amylose-lipid complex melting, the complexes are disrupted (Conde-Petit 1995).

VII.2.3.2 Pasting characteristics

Samples extruded without added fatty acid showed a cold swelling peak for all the sets of conditions presented in this study. But, with as little as 0.3% linoleic acid added, the cold swelling peak virtually disappeared.

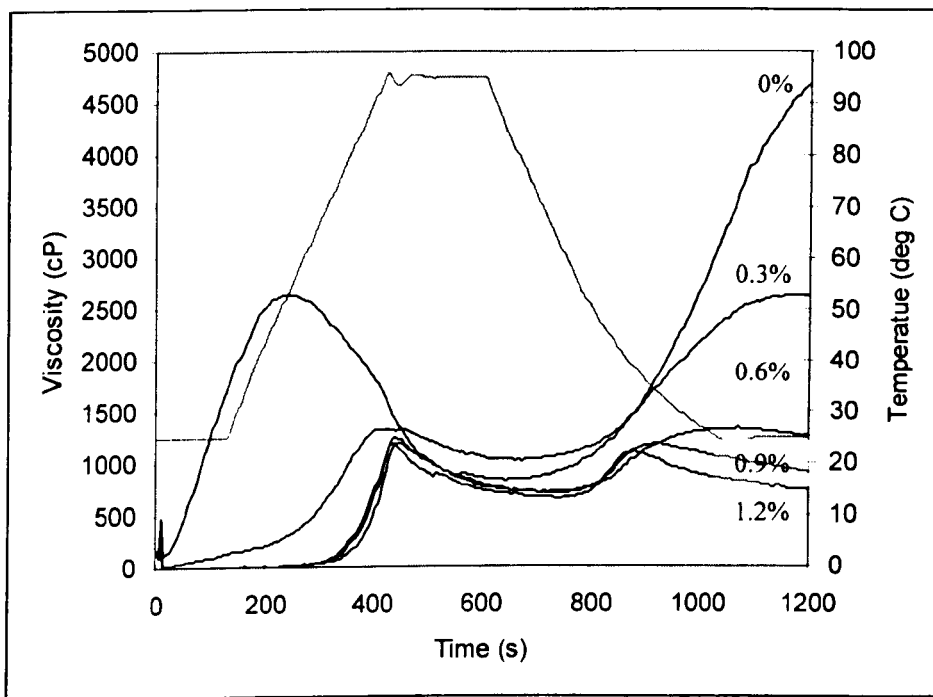


Figure VII-11: RVA pasting curves of maize grits + linoleic acid extruded at 100°C.

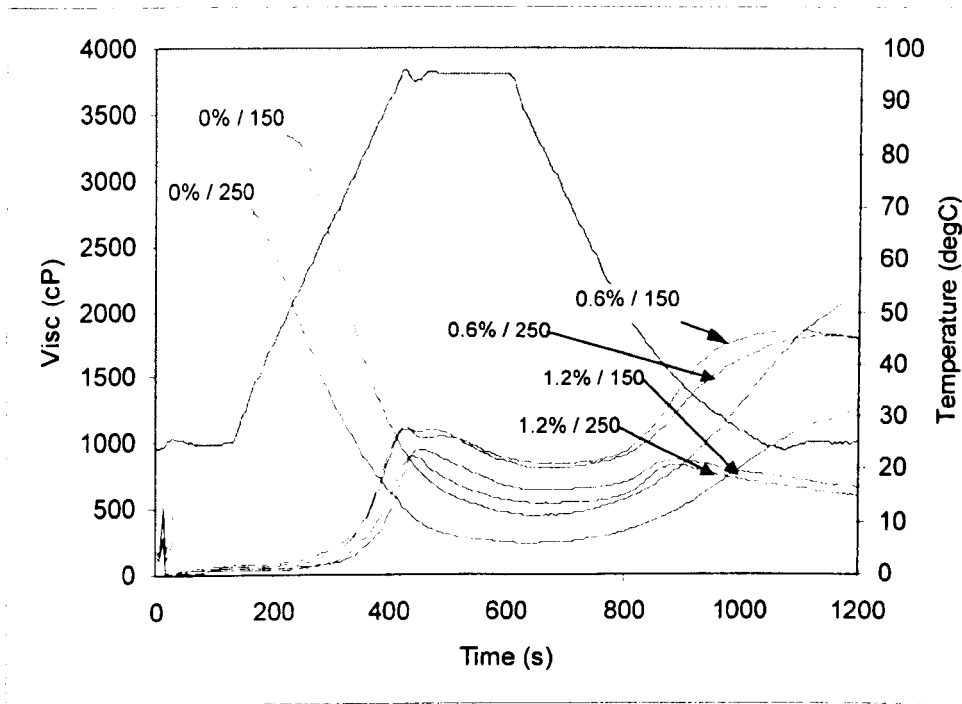


Figure VII-12: RVA pasting curves of maize grits + linoleic acid extruded at 120°C.

The presence of a cold viscosity is usually associated with high shear / high temperature extrusion. It is assumed to be related to highly swollen starch granules or high molecular weight polymers or dextrans (Whalen 1997).

Different factors could explain the absence of cold swelling peak:

1. The presence of free lipids coating the surface of the starch particles could prevent the swelling of the granules by delaying water diffusion.
2. During extrusion, the lipids could act as a lubricant and thus less damage would occur to the starch and prevent the formation of materials swelling at room temperature.
3. Formation of amylose-lipid complexes could decrease the swelling of the extrudates.

To test the first hypothesis, linoleic acid has been added to the samples extruded without added fatty acid. The pasting curve still exhibited a cold swelling peak. Therefore, linoleic acid did not prevent swelling.

Colonna (1983) has reported the lubricating role of different types of lipids, and showed that it affects the molecular structure of starch extrudates. The measure of the SME is a first indication on the amount of damage in the extruder. In this study, specific mechanical energies of the samples extruded at 150 rpm (100°C and 120°C) were not significantly different, only samples extruded at 250 rpm did show a lower SME for the samples containing linoleic acid.

Intrinsic viscosity of dilute solutions can give an indication on the molecular weight of polymers (Harding 1997). Therefore, relative viscosity measurements were performed to check if the addition of linoleic acid reduced the amount of damage done to the starch in the extruder. As lipids have an important impact on viscosity, lipids have been previously extracted using the method described in Chapter III. Samples extruded with 0, 0.3, 0.6 and 1.2% had relative viscosities of 1.175, 1.174, 1.174 and 1.170 respectively. These viscosities were not significantly different. The lubricating effect is either absent or not affecting the molecular degradation in the extruder. Therefore, the absence of cold swelling peak does not seem to be due to lower starch degradation in the extruder.

Becker (2001) showed that during quiescent heating of different starches, the absence of cold swelling peak was correlated to the presence of complexes between amylose and lipids. Such complexes are known to reduce water solubility and water absorption. In the present study, there seemed to be a correlation between the amount of complexes formed and the decrease of cold paste viscosity. Therefore, amylose-lipid complexes seem responsible, at least partially for the absence of cold swelling peak. Nevertheless, it should be noted that although amylose-lipid complexes were already formed with native lipids, cold paste viscosity was present in the sample with 0% linoleic acid. As the type of complex was similar for both samples with and without added fatty acid, this suggests that a minimum quantity of lipid must be available for complexation in order to prevent formation of cold swelling polymers.

VII.3 EXTRUSION OF WHEAT FLOUR AND LINOLEIC ACID

Wheat flour was extruded with linoleic acid to check if the same phenomenon was observed when using a different source of starch.

VII.3.1 Sample preparation

Wheat flour was mixed with linoleic acid in different proportions in order to get different percentage of linoleic acid in the mix (0.2, 0.4, 0.6, 0.8 and 1.6% of the total, including water introduced in the barrel).

These mixes were then extruded in a Cleextral BC 21 co-rotating, intermeshing twin-screw extruder. The solid feed rate was 3.6 kg/h and the water feed rate was 0.9 L/h. The screw speed was 150rpm. The temperature zones were: zone 2 = 60°C, zone 3 = 75°C and zone 4 = 100°C. The extruder was fitted with a 3 mm diameter circular die. Extruded samples were cut into strands of about 40 cm length and dried. Extrudates analysis was performed according to the methods described in VII.1.2.

VII.3.2 Extruder operation characteristics and extrudates structure.

The specific mechanical energy measurements showed that there was no significant change up to 0.8% linoleic acid added to the mixture, but with 1.6% added fatty acid, the SME was significantly lower. This showed the lubricating effect of the fatty acid.

The back pressure did not vary significantly as the amount of added lipid increased.

Table VII-4: Extruder parameters and extrudates moisture content (values in parenthesis are standard deviation). (*: Non-collapsed samples only)

	0%	0.2%	0.4%	0.8%	1.6%
<i>Moisture content (% wb)</i>	15.9 (0.23)*	17.0 (0.39)	17.0 (0.35)	17.0 (0.16)	22.1 (3.0)
<i>Back Pressure (Bar)</i>	15 (2.0)	19 (2.5)	21 (3.2)	15 (0)	16 (1.4)
<i>SME (kJ/kg)</i>	251 (4.4)	253 (5.8)	258 (16.7)	248 (10.2)	221 (10.7)

It was noted that sample extruded without added linoleic acid was unstable at the exit of the extruder. Although the radial expansion at the die appeared constant, the structure randomly collapsed. Some parts of the sample had an expanded foam-like structure whereas other lengths had a closed, collapsed structure.

Figure VII-13 represents the sectional expansion index and the bulk density of wheat flour extrudates (without data from the collapsed structures). The decrease in SEI is apparent when 0.4% linoleic acid was added, whereas, the decrease in bulk density appeared significant only after addition of more than 0.8%. This appears to be due to a higher shrinkage for the samples with higher expansion (Figure VII-14).

Figure VII-15 and Figure VII-16 are pictures of the wheat extrudates. The expanded and collapsed structures are well represented. As it has been observed for maize grits and linoleic acid, the cell size seems to increase when linoleic acid is added, but this is clearly visible only for the sample extruded with 1.6%.

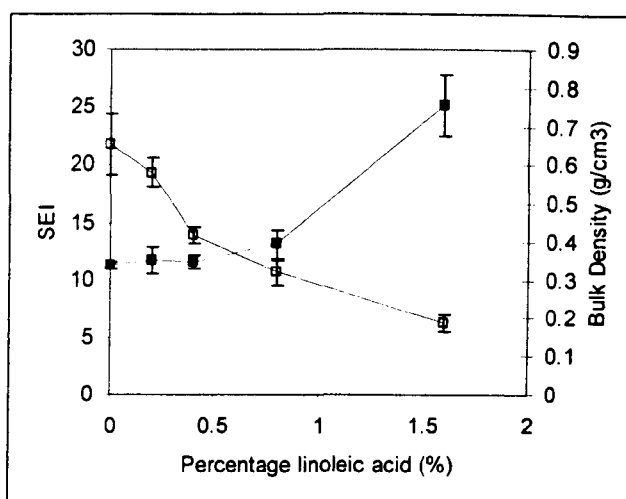


Figure VII-13: Sectional expansion index (○) and bulk density (■) of wheat flour extruded with linoleic acid. Results are average of 5 measurements. For sample at 0% linoleic acid, collapse sample diameter was not taken into account.

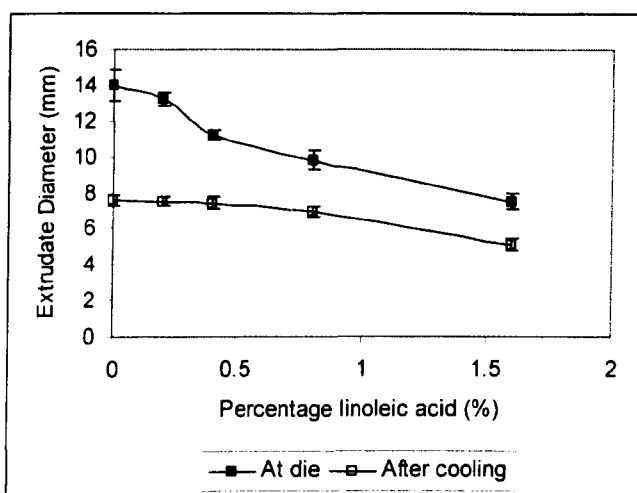


Figure VII-14: Representation of wheat flour extrudates radial shrinkage vs. percentage of linoleic acid added. Results are average of 5 measurements. For sample at 0% linoleic acid, collapsed sample diameter was not taken into account.

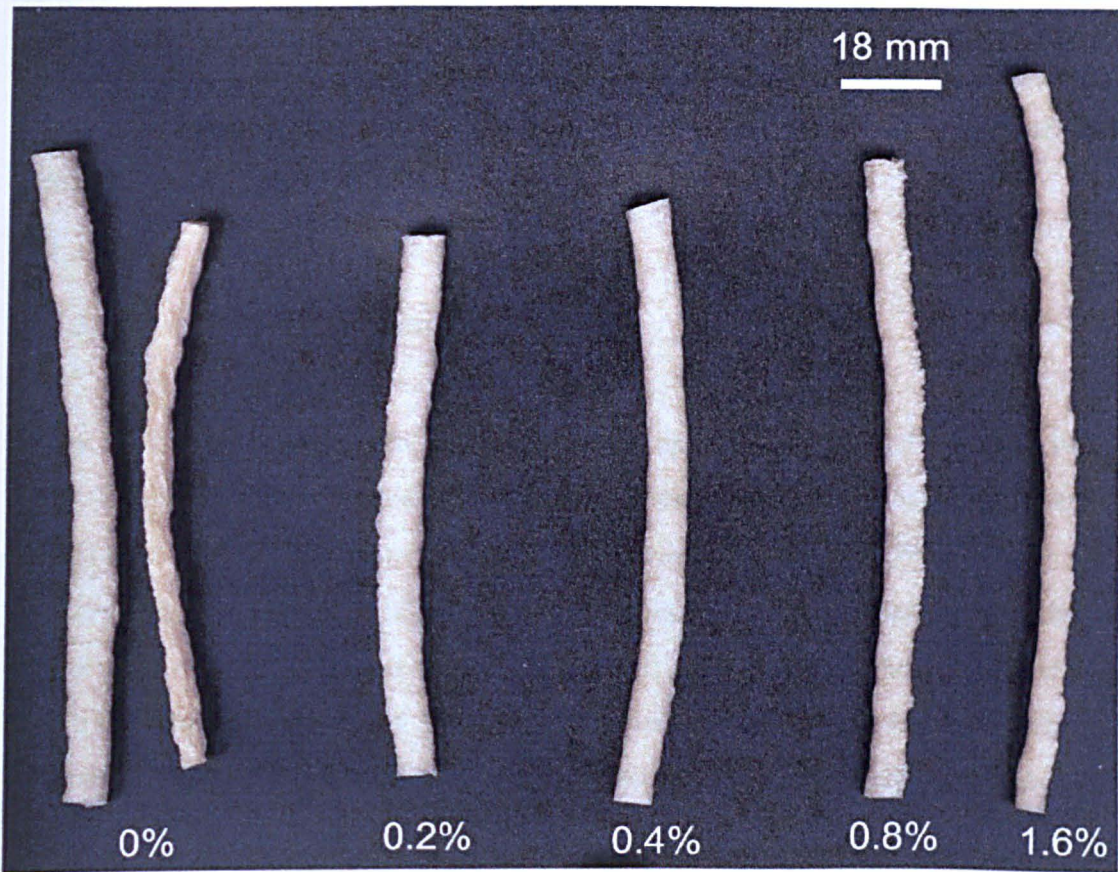


Figure VII-15: Wheat flour extruded with different amounts of linoleic acid. Samples at 0% show the 2 structures obtained after extrusion, expanded on the left and collapsed on the right.

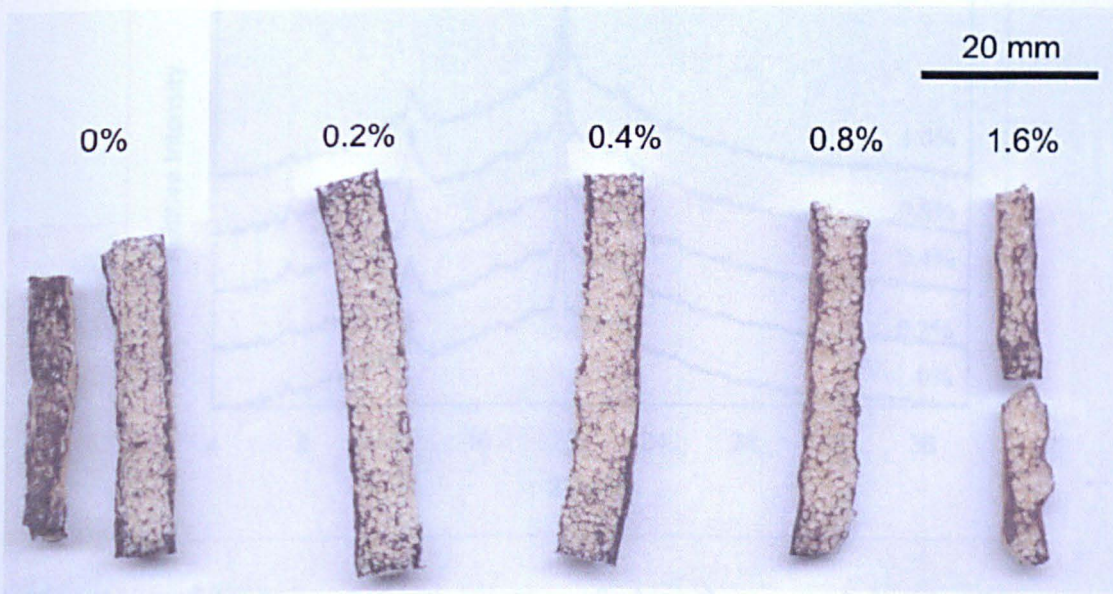


Figure VII-16: Wheat flour + linoleic acid extrudates cross-sections dyed with iodine gel.

Like maize grits extrudates, wheat flour extrudates moisture content increased when percentage linoleic acid increased (Table VII-4). This was well correlated with samples expansion.

VII.3.3 Starch characteristics

X-ray diffraction showed that amylose-lipid complexes were also formed in wheat flour (Figure VII-17). All measurements were done on samples after equilibration in an RH box at 75% humidity to obtain similar moisture content ($\pm 1.5\%$).

The crystallinity indexes of wheat flour extrudates have been compared with that of maize grits extruded under the same conditions. Figure VII-18 shows that initially XRD_i is higher for wheat flour than it is for maize grits. This might be due to a higher amount of complexes with native lipids in wheat starch as it has been highlighted by Kugimiya (1980). Like maize grits, the amount of complexes formed in wheat flour extruded with linoleic acid reached a plateau. But this plateau was reached when only 0.4% linoleic acid was added.

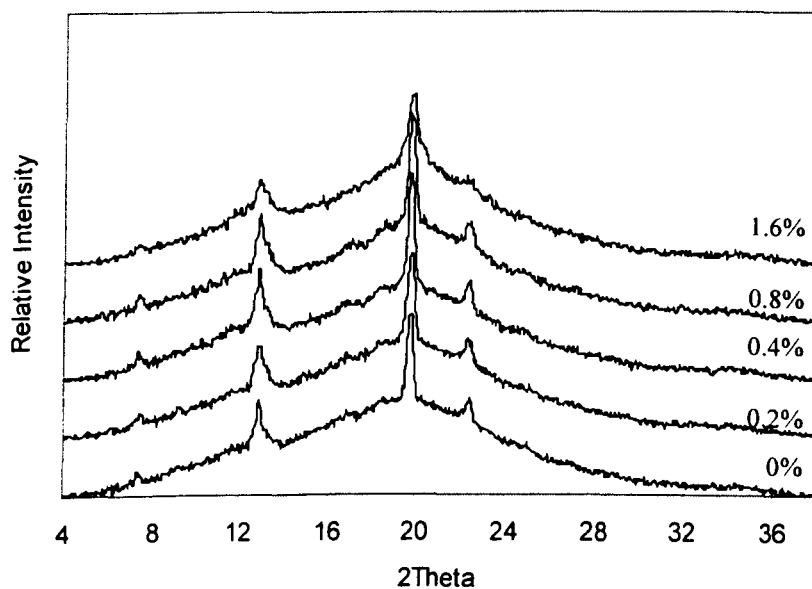


Figure VII-17: X-ray diffraction pattern of wheat flour extruded with different amounts of linoleic acid.

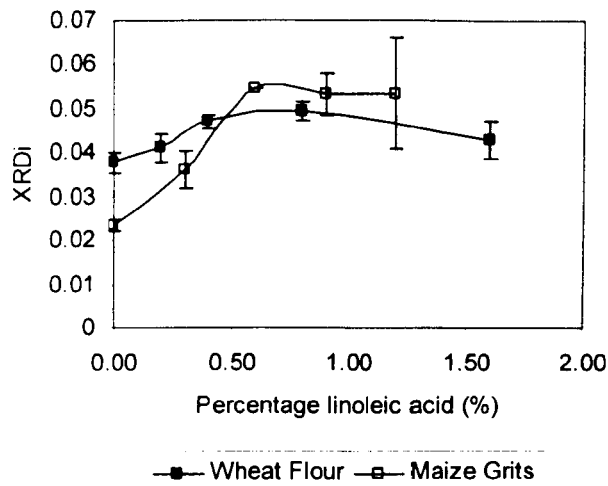


Figure VII-18: Crystallinity index of extruded wheat flour and maize grits with linoleic acid.

The pasting profiles of the wheat flour extrudates are represented in Figure VII-19. Although the pasting curves appeared more complex than those observed with maize grits extrudates, the same decrease in cold viscosity was observed.

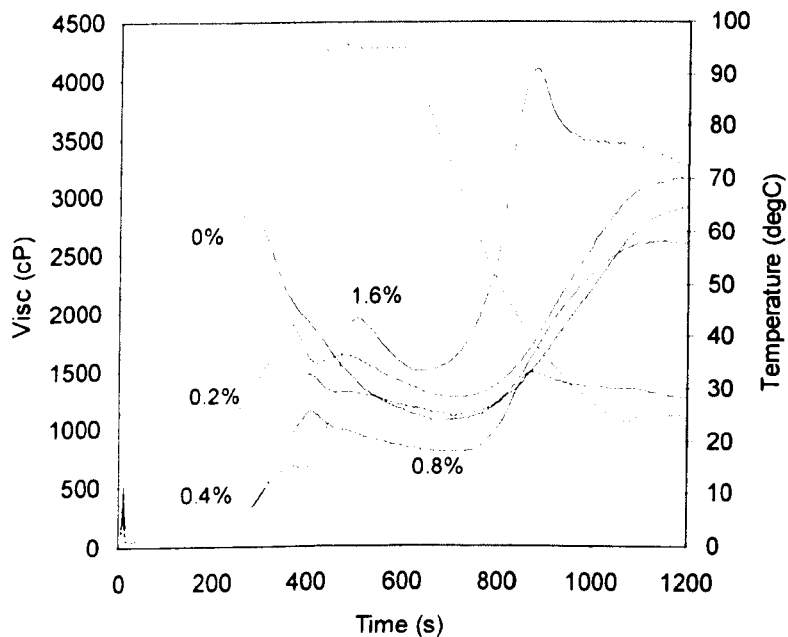


Figure VII-19: RVA pasting profile of wheat flour extruded with linoleic acid.

VII.4 EXTRUSION OF MAIZE GRITS WITH COMPLEX FATS

VII.4.1 Sample preparation

Maize grits has been extruded with three commercial fats commonly used in the pet food industry. Sunflower oil (SO), poultry fat (PF) and beef tallow (BT) have been supplied by Masterfoods U.K.

Maize grits was mixed with water and fat (at a 4% level) in a Kenwood Peerlex mixer. Poultry fat and beef tallow, being solid at room temperature, have been melted before mixing. A control sample (Ctrl) was also prepared containing no added fat. The water to maize ratio was kept constant for all samples.

The temperature zones in the extruder were: 75°C for zone 2, 100°C for zone 3 and 120°C for zone 4. The screw speed was 150 rpm and the total feed rate was 4.5 kg/h. Samples were collected in strands of about 40 cm length and dried for 1 hour in a forced air oven at 105°C. Sample analysis was performed as described in VII.1.2.

VII.4.2 Extruder operating parameters and extrudates characteristics.

Table VII-5 shows that the SME for the samples extruded with fats are lower than for the control. This was expected, as the level of fat added (4%) is higher than that used previously, therefore the lubricating effect of the lipid should be more important. The back pressure of Ctrl and BT was significantly lower than that of PF and SO.

Table VII-5: Extruder parameters and extrudates moisture content. Values in parenthesis are standard deviations.

	<i>SME (kJ/kg)</i>	<i>Back pressure (Bar)</i>	<i>Moisture content (%wb)</i>
Ctrl	248.3 (6.8)	5.7 (0.6)	18.6 (0.1)
PF	215.2 (6.3)	11.7 (1.2)	20.0 (0.1)
BT	217.1 (7.5)	6.7 (0.6)	21.3 (0.3)
SO	229.3 (1.5)	12.0 (1.0)	20.1 (0.2)

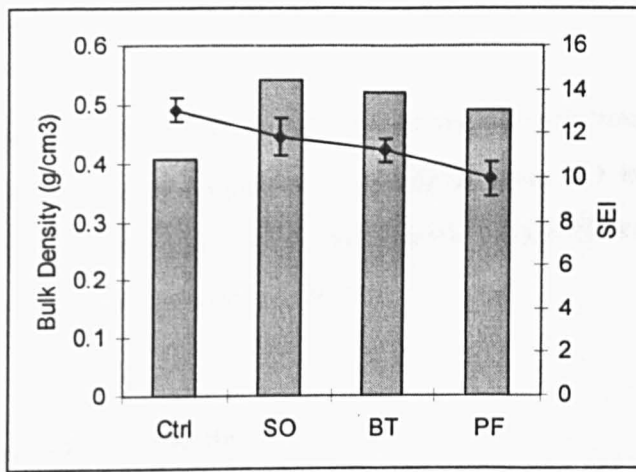


Figure VII-20: Bulk density (bars) and sectional expansion index (line) of maize grits extruded with different fats. Error bars are standard deviations. Results are average of 5 (SEI) or 10 (Bulk density) measurements.

Figure VII-20 shows the sectional expansion index and bulk density of maize grits extrudates. Both indexes showed that the expansion of the control (without added fat) is higher than the one of samples containing fat.

SEI of poultry fat sample is slightly lower than that of BT and SO, whereas bulk density of PF is lower. Therefore, either the shrinkage of PF extrudates was less than for the other fat samples or the longitudinal expansion was higher for PF.

Observation of the extrudates cross sections revealed that SO and BT presented bigger cells than the control whereas PF presented cells with an intermediate size.

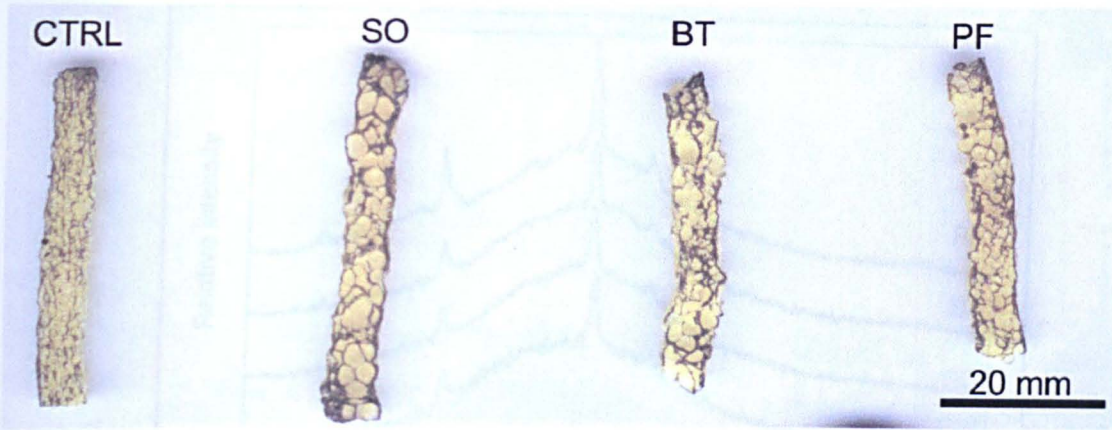


Figure VII-21: Cross section of maize grits extrudates dyed with iodine.

Moisture contents of samples extruded with 4% fat were lower than the control. BT extrudates presented a moisture content slightly higher than SO and PF extrudates although its expansion characteristics were not significantly different to that of SO. This could be due to the characteristics of the fat.

VII.4.3 Starch characteristics

VII.4.3.1 Amylose-lipid complex formation

X-ray diffractograms are represented on Figure VII-22. All patterns are similar except for the one of PF extrudates. Maize grits extruded with poultry fat presented higher peaks at 13 and 19.9°. Therefore, no additional amylose-lipid complexes seemed to be formed with beef tallow and sunflower oil (extrudates presented the same amount of complexes as found in the control), but there seem to be some complexes formed with poultry fat.

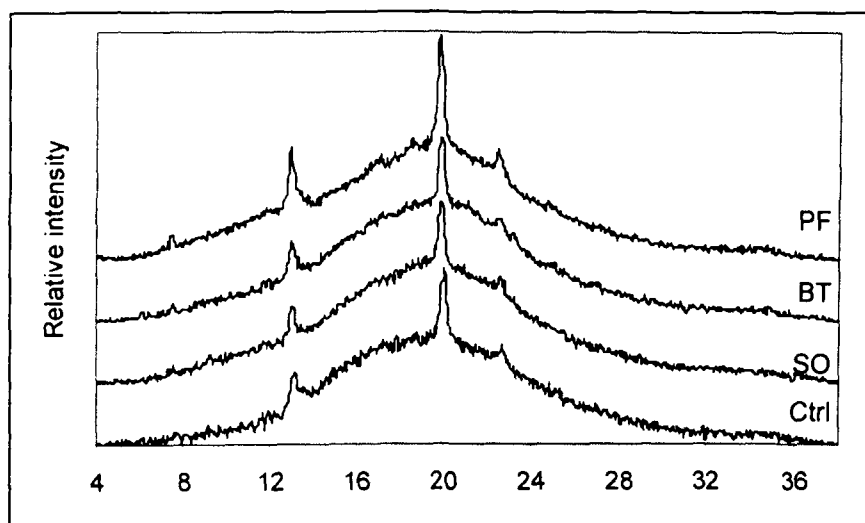


Figure VII-22: X-ray diffraction pattern of maize grits extruded with different fats.

Many authors have discussed the influence of lipid type on the formation of amylose-lipid complexes in solution or during extrusion of starchy materials. With fatty acids and monoglycerides, complexation seems to increase when carbon chain length increases according to Mercier (1980) and Hahn (1987) whereas Bhatnagar (1994a) using a single screw extruder, found that complexation was the highest with myristic acid (C14:0) and decreased when the number of carbon increased. The role of unsaturations is also unclear. Mercier (1980) found that the increasing number of unsaturation increased amylose-fatty acid complex, whereas Hahn (1987) showed that it decreased complex formation.

There is more agreement on the effect of the size of the ligand. Hahn (1987) and Ho (1992) showed that fatty acids were more complexed than di- and triglycerides. Bhatnagar (1994a & 1997) and Mercier (1980) also showed that extrusion of starch with various oils and fats failed to produce complexes due to the bulky size of the lipids.

Although animal fats and oils are mainly constituted of triglycerides, poorly refined fats or oxidative hydrolysis could lead to higher amounts of free fatty acids (FFA). FFA content was therefore measured on the different fats. Sunflower oil and beef tallow both presented low FFA content with 0.1 and 1.1% (expressed as equivalent oleic acid) respectively. However poultry fat presented a high 10.9% FFA. This could

explain why amylose-lipid complexes were formed with poultry fat and not with the other types of fats.

VII.4.3.2 *RVA pasting curves*

RVA pasting curves are presented in Figure VII-23. Ctrl, BT and SO extrudates presented a cold swelling peak. The fat containing extrudates had a lower cold viscosity than the control, this could be due to the lower mechanical energy experienced by the fat samples. PF extrudates presented virtually no cold water viscosity. This sample is the only one with a higher amount of amylose-lipid complexes. Therefore this seems to confirm our previous hypothesis.

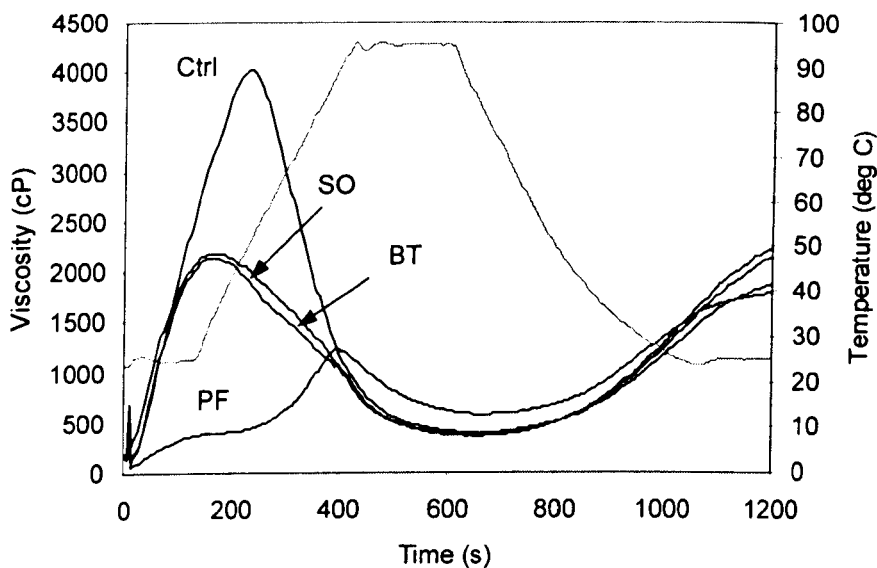


Figure VII-23: RVA pasting curves of maize grits + fat extrudates.

VII.5 CONCLUSION

Amylose-lipid complexes are formed during twin-screw extrusion of cereal and fats. These complexes have an important effect on the expansion and pasting characteristics of the extrudates.

The effect of addition of lipids on expansion is twofold. Firstly, lipids can act as a lubricant in the extruder, lowering the viscosity of the melt. The higher the amount of lipid added, the lower will be the viscosity and therefore, the lower will be the mechanical energy experienced by the material. Expansion is directly correlated to the SME as shown by Guy (1988). Up to a maximum depending both on the extruder configuration and the material, an increase in SME will increase the expansion. This has been observed for maize grist extruded with various fats and wheat flour with linoleic acid.

Lipids can also form complexes with amylose that will further decrease expansion. Although this has been Cell size seemed to increase when lipids were added to maize grits or, to some extent, to wheat flour.

Amylose-lipid complexes can also prevent the formation of a cold swelling peak in the RVA provided that there is sufficient lipids available for complexation of the cold water swelling polymers (i.e. amylose).

Amylose-lipid complexes can not form with triglycerides which are the main components of the fats used in pet food manufacture. But, due to limited fat hydrolysis, fat composition can include a significant amount of free fatty acids. It was shown that the presence of these free fatty acids can induce the formation of amylose-lipid complexes and change the structure of the extrudate. Therefore, lipid hydrolysis not only affects rancidity but also can affect structure of pet food extrudates.

CHAPTER VIII GENERAL DISCUSSION AND CONCLUSION



The major aim of the work described in this thesis was to study the impact of processes prior to extrusion and ingredients on the characteristics of starchy extrudates. The focus was primarily on starch, as it is believed to be the main provider of the final structure of dry pet food. During extrusion, the melting of starch provides a continuous phase where proteins and minor components are dispersed. When exiting the die, the water flashes off allowing expansion of the starchy melt and this provide the final structure of the material.

VIII.1 EFFECT OF PROCESSES PRIOR TO EXTRUSION

Grinding and preconditioning effects on extrusion have been investigated to understand what impact they have on the raw materials and how this will affect extrusion.

VIII.1.1 Grinding

Particle size reduction has been extensively studied and has been reported in the literature (Chen 1999; Mathew 1999; Carre 1998; Desrumaux 1998; Garber 1997). The effects of grinding on starch are well documented but the effect on other ingredients such as proteins and fat are less well known.

Dry pet food premixes are complex mixtures of ingredients; therefore the effect of grinding method was studied on a typical industrial mix and on a model mixture.

Different methods can be used to grind raw materials to a suitable size for extrusion (see Chapter II). Ingredients can be ground individually or all together and the grinding can be performed in a single pass or using multiple passes and different

grinders. In this current study it was shown that these different grinding methods impart different characteristics to a typical pet food mixture. Two pass techniques seem to give more starch damage than one pass grinding. Multiple passes also allow smaller particle size and narrower distribution. The difference between grinding ingredients in a single batch or separately was less clear. For the model system where the same grinder was used to grind ingredients together or separately, the results showed that there was more starch damage when grinding ingredients together than separately. For the industrial mixes, less starch damage was found for the process L where ingredients were ground together than when the ingredients were ground separately. But, A and M processes were double pass grinding processes.

The transformations of the raw materials due to grinding affect the extrusion process significantly. Although the industrial mixes had similar particle size, they reacted differently to extrusion leading to extrudates with different characteristics. This could be due in part to the effect on starch damage and subsequently to the water absorption capacity of the mix. It is interesting to note that the samples with less initial starch damage produced extrudates with higher pasting viscosity.

The behaviour of the differently ground material could not be explained solely from the degree of starch damage and particle size. Therefore it was suspected that other ingredients could be affected by grinding.

The effect of grinding on the protein was not clear. Protein solubility was low due to the type of proteins present in the mix and therefore, effects on solubility were difficult to analyse. Nevertheless, particle charge was different depending on the grinding method and this was suspected to be due to proteins.

It was also thought that grinding could affect fats. In particular, fats could be melted by the increase in temperature during grinding and be deposited at the surface of the particles, therefore lowering water absorption. Determinations of the kinetic of fat extraction and staining with Sudan red to locate the fat were tested but unfortunately the results were inconclusive. Therefore it was not possible to determine fat localisation and how it was altered by the grinding process.

VIII.1.2 Preconditioning

Preconditioning is a unit operation used to mix, heat and humidify raw materials prior to extrusion. This process is used mostly in combination with a single screw extruder to increase its flexibility (Caldwell 2000).

Preconditioning was studied on a model and a pilot preconditioner using maize grits of different particle size.

Precooking occurs in the preconditioner as shown by the decrease in starch crystallinity. This has an impact on the characteristics of the mixture feeding the extruder. Starch conversion increases the water absorption in the mix. It was also noted that with increase “pre-cooking” (i.e. increase initial water content and residence time) translational water diffusivity in the mix decreases. This has been attributed to the increase in starch conversion. In highly hydrated native maize grits, the absorption of water by the starch granule is limited therefore most of the water will remain outside the granule, free to diffuse. In preconditioned maize grist, where starch conversion occurred, water absorption by the starch granule is higher. Therefore, water will penetrate the granule and diffusion will be restricted.

It is believed that the state of water in the mix feeding the extruder will affect extrusion and subsequently extrudates characteristics (Karathanos 1992). Unfortunately, no direct correlation could be made between state of water in the mix and characteristics of the extrudates. More investigation should be made to understand how mixing and addition of steam affect the state of water in a cereal mix and a pet food mix. Different components such as proteins, lipids and fibres present in these mixes, have different water binding properties and therefore will affect the water distribution and the hydration characteristics of the mix.

It was also shown that hydration and starch conversion affect the macroscopic characteristics of the mix. Bulk density and compressibility were directly correlated to starch conversion.

Extrusion was affected by preconditioning in two ways. Even without adding steam, the pre-hydration function of the preconditioner provides a better homogeneity in the mix feeding the extruder. This increased homogeneity leads to an overall lower degree of starch conversion in the extruder but a better expansion. With the addition of steam in the preconditioner, increase temperature and limited starch conversion occurs and affects especially the viscosity of the mix. The crystallinity of the extrudates is affected by the preconditioning step. The metastable E-type pattern was observed mainly on extrudates produced without addition of steam in the preconditioner whereas the stable V-type was observed on material produced with addition of steam in the preconditioner.

VIII.1.3 Interactions grinding – preconditioning

The study of preconditioning from an engineering point of view does not distinguish materials of different particle size (Bouvier 1996). But, as shown in Chapter VI, particle size and particle size distribution can have a marked effect on preconditioning.

It was first observed that small differences in moisture content linked to grinding could not be distinguished using factory equipment. This difference could nevertheless affect the characteristics of the extrudates, especially expansion. Particle size also affects the water distribution during mixing. Coarse particles are more difficult to hydrate than fine particles therefore starch conversion appears to occur only at the surface and creates a cohesive mass creating blockage of the extruder inlet.

It was also noted that particle size distribution has a limited impact on preconditioning, as the characteristics of two maize grits extrudates having the same average diameter but different distribution were very close.

Degree of starch damage is also believed to affect preconditioning as this will affect hydration (Lelievre 1974).

VIII.2 INGREDIENT EFFECTS ON EXTRUSION

The effect of fats on extrusion of cereals has been investigated independently of the effect of grinding and preconditioning.

The effect of lipids on extrusion is well documented (Lin 1997; Villwock 1999; Bhatnagar, 1994a; Mercier 1979; Desrumaux 1999). Amylose-lipid complex formation was especially studied in relation with pasting characteristics of the extrudates. It was shown that cereal flours extruded with small amounts of fatty acids produced a pasting curve similar to the one obtained for raw starches. The absence of cold swelling peak and the presence of peak viscosity in extrudates are interpreted in the literature as lower mechanical energy, lower starch conversion and presence of remaining native starch (Whalen 1997 & 1999).

In all the cases studied, no native starch could be observed under polarised light microscopy and no melting endotherm characteristic of native starch were found. Furthermore it was shown that when using small amounts of fatty acids the specific mechanical energy was not decreased by the addition of lipid. It was also shown that even when adding larger amounts of fat and decreasing the SME, if the fat does not contain free fatty acids, the cold swelling peak would remain. Fats are mainly composed of triglycerides, those molecules are sterically too bulky to form complexes with amylose, only smaller molecules, such as free fatty acids can form such complexes.

Starch –lipid complexes have low water solubility and a low swelling power. Therefore the RVA peak viscosity was attributed to the presence of amylose-lipid complexes in extrudates.

It is still not clear whether there is a threshold in the amount of complexes present necessary to stop cold swelling or if the nature of amylose-lipid complexes changes depending on the nature of lipid present (fatty acids, monoglycerides, phospho- or lysophospholipids).

The impact of lipids on extrudates expansion has been studied briefly and showed that expansion was substantially lowered by addition of lipid even at a low level where no detectable change in SME were observed. The amount and the dispersion of cells in the foam were also affected by the lipid addition.

Attempts were made at determining the effect of amylose-lipid complex on the in-vitro starch digestibility of extrudates but no difference could be observed using the technique employed.

Carbohydrate-protein and protein-fat interactions have not been studied during the course of this study although it is believed that they would also have an impact on the characteristics of the extrudates. Protein could interact with fat in a similar way as starch as suggested by Ho (1992). Protein and carbohydrates could also interact by crosslinking therefore affecting the extrudates structure such as expansion, molecular weight etc...

VIII.3 COMBINED INGREDIENTS AND PROCESS EFFECTS

Interactions between unit operation and ingredients were not the focus of a systematic study, but some conclusion could be drawn from the study of grinding and preconditioning of mixed systems. This is represented on Figure VIII-1.

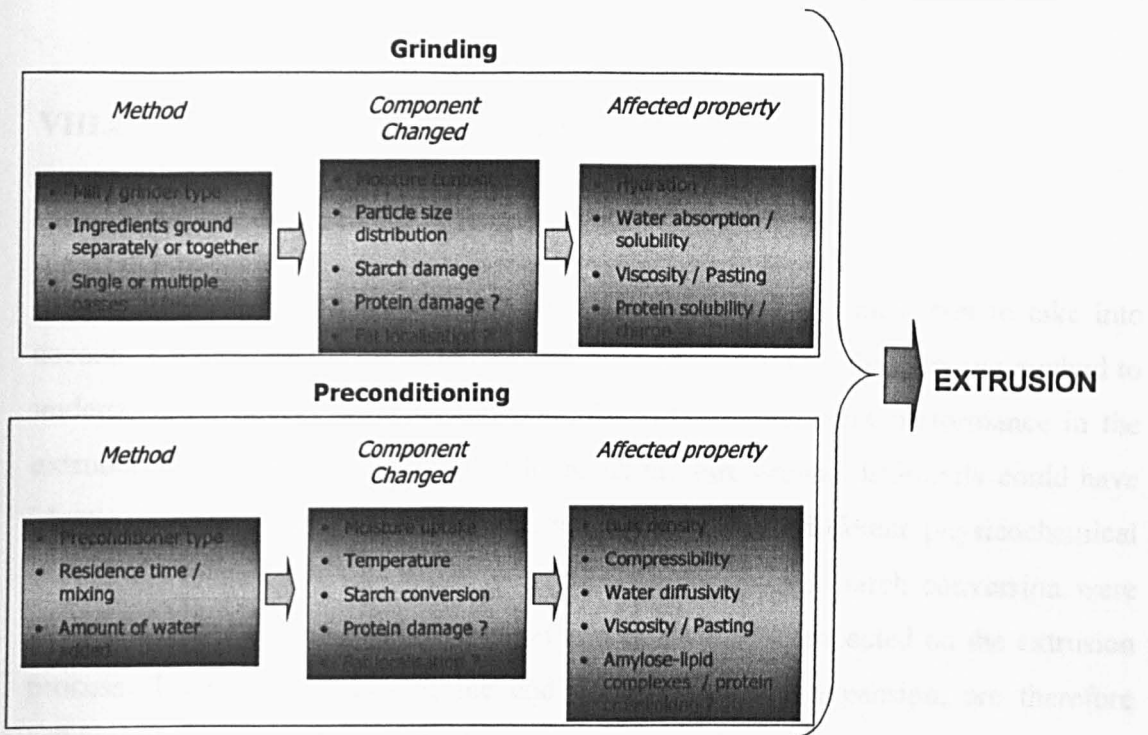


Figure VIII-1: Effect of grinding and preconditioning on extrusion

The effect of lipids on extrusion has also been studied first in combination with the analysis of the effect of preconditioning. It was first thought that interactions between starch and lipids (such as amylose-lipid complexes) during preconditioning could have an impact on extrusion and the characteristics of the extrudates. An experiment was design in order to check if the stage at which lipids were added impact on extrudates characteristics. Therefore, 1.2 or 2.4% (wb) linoleic acid was added to maize grits either in the preconditioner or in the extruder. The analysis of the extrudates did not show significant differences between extrudates. Therefore for these levels, the localisation of the addition of lipid does not seem to have an impact on extrusion.

VIII.4 INDUSTRIAL SIGNIFICANCE AND FURTHER WORK

This study investigated the role of grinding and showed it is important to take into account not only the type of grinder used in a factory but also the grinding method to understand its impact on a pet food premix and its subsequent performance in the extruder. It was also highlighted that identical mixtures ground differently could have identical particle size distributions but nevertheless have different physicochemical properties. Particularly, the water absorption properties and starch conversion were affected by the type of grinding method and subsequently impacted on the extrusion process. The characteristics of the end product, such as expansion, are therefore influenced by the grinding method.

The present work showed that protein solubility seemed to decrease when using a multi-pass grinding method on maize gluten meal. This difference in solubility is believed to be due to chemical crosslinking of the proteins. More work should be done in this area in order to confirm or not our hypothesis and determine the impact on extrusion. In high protein, textured kibbles or chunks, crosslinking is believed to occur in the extruder and generate the fibrous texture of the chunks; a difference in the nature of the protein should impact on the characteristics of the extrudates.

The use of a model system throughout this study was useful to study the preconditioning process when little information is available in the literature. The effect of particle size was particularly interesting as it was shown that large particle size could affect severely preconditioning even causing blockage depending on the residence time in the preconditioner. But this effect could be avoided by mixing the material with a similar material with smaller particle size. This behaviour was believed to be due to a slower diffusion of water in the granules leading to heterogeneous hydration and localised starch conversion at the surface of the particles. A more detailed spectroscopic study should be carried out in order to test this hypothesis.

More work would be necessary to understand the impact of preconditioning on mixed systems with a composition closer to a pet food premix. Indeed, a pet food mix contains higher quantities of fibres, proteins and fat. These different components have different water binding properties and therefore will influence water distribution during the hydration of the mix. Depending on the composition of the recipe, the proportion of water available for starch conversion will vary and so should the characteristics of the extrudates.

Finally, the study of the effect of fat and amylose-lipid complexation on extrusion showed that different fats, especially animal fat, could not be considered as interchangeable. This is of great importance industrially as those fats are sometime used as a process aid to limit expansion. For this function, our study showed that poultry fat is more efficient as it contains free fatty acids that can complex amylose and subsequently further reduce the expansion. The impact of amylose-lipid complexation is not limited to expansion; it also greatly influences the pasting behaviour of the extrudates. Many industries already use the ability of amylose to form complexes with some lipids to generate specific textures in their product. More work is required to understand how this property could be useful in pet food manufacturing.

BIBLIOGRAPHY

Alvarez-Martinez, L., Kondury, K. P. and Harper, J. M. (1988). A general model for expansion of extruded products. *Journal of Food Science* 53, 609-615.

Andreev, N. R.; Kalistratova, E. N.; Wasserman, L. A.; Yuryev, V. P. (1999). The influence of heating rate and annealing on the melting thermodynamic parameters of some cereal starches in excess water. *Starch-Starke*, 51, 422-429.

Angold, R. (2000). The microscopy of extruded products In: *Extrusion workshop, Moisture the critical variable*. 11th and 12th April 2000, Nottingham University.

Becker, A. (2001). Starch conversion and particle properties determining the Rapid Visco Analyser (RVA) profile. Thesis Food Science. University of Nottingham.

Becker, A., Hill, S. E. and Mitchell, J. R. (2001). Milling - A further parameter affecting the rapid visco analyser (RVA) profile. *Cereal Chemistry* 78, 2, 166-172.

Becker, A.; Hill, S. E.; Mitchell, J. R. (2001). Relevance of amylose-lipid complexes to the behaviour of thermally processed starches. *Starch-Starke*, 53, 121-130.

Bhatnagar, S.; Hanna, M. A. (1994a). Amylose Lipid Complex-Formation During Single-Screw Extrusion of Various Corn Starches. *Cereal Chemistry*, 71, 582-587.

Bhatnagar, S.; Hanna, M. A. (1994b). Extrusion Processing Conditions For Amylose Lipid Complexing. *Cereal Chemistry*, 71, 587-593.

Bhatnagar, S.; Hanna, M. A. (1996). Starch-Stearic Acid Complex Development within Single and Twin Screw Extruders. *Journal of Food Science*, 61, 778-782.

Bhatnagar, S.; Hanna, M. A. (1997). Modification of microstructure of starch extruded with selected lipids. *Starch-Starke*, 49, 12-20.

Biliaderis, C. G. (1990). Thermal analysis of food carbohydrates. In *Thermal analysis of foods*; V. R. Harwalkar and C.-Y. Ma ed.; Elsevier applied science: London and New York, p 168-220.

Biliaderis, C. G. (1992). Structures and Phase-Transitions of Starch in Food Systems. *Food Technology* 46, 6, 98-109.

Biliaderis, C. G.; Page, C. M.; Maurice, T. J. (1986). Non-equilibrium melting of amylose-V complexes. *Carbohydrate Polymers*, 6, 269-288.

Blanshard, J. M. V. (1979). Physicochemical aspects of starch gelatinisation In: *Polysaccharides in food*, J. M. V. Blanshard and J. R. Mitchell ed, Butterworth, London, p 139-152.

Blanshard, J. M. V.; Lillford, P. J. (1993). *The glassy state in foods*, Nottingham University Press; Nottingham.

Bond, F. C. (1963). Some recent advances in grinding theory and practice. *British Chemical Engineering* 8, 631-634.

Bouvier, J. M. (1996). Engineering analysis of preconditioning in the extrusion-cooking process. *Cereal Foods World* 41, 9, 737-740.

Bouvier, J. M. (2000a). Case studies in Food and feed extrusion In: *Extrusion workshop, Moisture the critical variable*. 11th and 12th April 2000, Nottingham University.

Bouvier, J. M. (2000b). Fundamentals and evaluation of food and feed extrusion In: *Extrusion workshop, Moisture the critical variable*. 11th and 12th April 2000, Nottingham University.

Bragg, W. L. (1913). The diffraction of short electromagnetic waves by a crystal. *Proceedings of the Cambridge Philosophical Society*, 17, 43-47.

Brennan, J. G., Butters, J. R., Cowell, N. D. and Lilley, A. E. V. (1990). Size reduction and screening of solids In: *Food Engineering Operation*, J. G. Brennan, J. R. Butters, N. D. Cowell and A. E. V. Lilley ed, Elsevier applied science, London and New York, p 67-90.

Brummer, T., Meuser, F., van Lengerich, B. and Niemann, C. (2002). Effect of extrusion cooking on molecular parameters of corn starch. *Starch-Starke* 54, 1, 1-8.

Buleon, A., Colonna, P., Planchot, V. and Ball, S. (1998). Starch granule: structure and biosynthesis. *International Journal of Biological Macromolecules* 23, 85-112.

Cai, W.; Diosady, L. L. (1993). Modeling of Expansion and Water Solubility Index of Wheat- Starch During Extrusion-Cooking. *Acta Alimentaria*, 22, 181-192.

Caldwell, E. F., Fast, R. B., Ievolella, J., Lauhoff, C., Levine, H., Miller, R. C., Slade, L., Strahm, B. S. and Whalen, P. J. (2000). Cooking of ready-to-eat breakfast cereals. *Cereal Foods World* 45, 6, 244-252.

Carre, B.; Melcion, J. P.; Widiez, J. L.; Biot, P. (1998). Effects of various processes of fractionation, grinding and storage of peas on the digestibility of pea starch in chickens. *Animal Feed Science and Technology*, 71, 19-33.

Carvalho, C. W. P. (2001). Effect of sugar on the extrusion of maize and wheat. Thesis Food Science. University of Nottingham.

Chen, J. J., Lu, S. and Lii, C. Y. (1999). Effects of milling on the physicochemical characteristics of waxy rice in Taiwan. *Cereal Chemistry* 76, 5, 796-799.

Chen, Z. C., Ikeda, K., Murakami, T. and Takeda, T. (2000). Effect of particle packing on extrusion behavior of pastes. *Journal of Materials Science* 35, 21, 5301-5307.

Chinnaswamy, R. and Hanna, M. A. (1988). Relationship Between Amylose Content and Extrusion Properties of Corn Starches. *Cereal Chemistry* 65, 2, 138-143.

Colonna, P. and Mercier, C. (1983). Macromolecular Modifications of Manioc Starch Components by Extrusion-Cooking with and without Lipids. *Carbohydrate Polymers* 3, 87-198.

Colonna, P., Doublier, J. L., Melcion, J. P., de Monredon, F. and Mercier, C. (1984). Extrusion Cooking and Drum Drying of Wheat Starch. I. Physical and Macromolecular Modification. *Cereal Chemistry* 61, 6, 538-543.

Colonna, P., Leloup, V. and Buleon, A. (1992). Limiting Factors of Starch Hydrolysis. *European Journal of Clinical Nutrition* 46, S17-S32.

Colonna, P., Tayeb, J. and Mercier, C. (1989). Extrusion cooking of starch and starchy products In: *Extrusion cooking*, C. Mercier, P. Linko and J. M. Harper Eds, American association of cereal chemists, St Paul (MN), p 247-319.

Conde-Petit, B.; Escher, F. (1995). Complexation induced changes of rheological properties of starch systems at different moisture levels. *Journal of Rheology*, 39, 1497-1518.

Cullity, B. D. (1959). *X-ray diffraction*, Addison-Wesley publishing company, inc.; Reading Massachusetts, USA.

de Muelenaere, H. J. H. and Buzzard, J. L. (1969). Cooker extruders in service of world feeding. *Food Technology* 23, 345.

Deleanu, C.; Pare, J. R. J. (1997). Nuclear magnetic resonance spectroscopy (NMR): Principles and applications. In *Instrumental methods in food analysis*; J. R. J. Pare and J. M. R. Belanger, Eds.; Elsevier: Amsterdam; pp 179-237.

Desrumaux, A., Bouvier, J. M. and Burri, J. (1998). Corn grits particle size and distribution effects on the characteristics of expanded extrudates. *Journal of Food Science* 63, 5, 857-863.

Desrumaux, A.; Bouvier, J. M.; Burri, J. (1999). Effect of free fatty acids addition on corn grits extrusion cooking. *Cereal Chemistry*, 76, 699-704.

Donald, A. M.; Warburton, S. C.; Smith, A. C. (1993). Physical changes consequent on the extrusion of starch. In *The glassy state in foods*; J. M. V. Blanshard and P. J. Lillford, Eds.; Nottingham University press: Nottingham; pp 375-394.

Donovan, J. W. (1979). Phase transition of the starch water system. *Biopolymers*, 18, 263-275.

Dubois, M.; Gilles, K. A.; Hamilton, J. K.; Rebers, P. A.; Smith, F. (1956). Colorimetric method for the determination of sugars and related substances. *Analytical Chemistry*, 28, 350.

Earle, R. L. (1983). Chapter 11: Size reduction In: *Unit Operation in Food Processing*, R. L. Earle ed, Pergamon Press, Oxford, p 159-163.

Evans, I. D.; Haisman, D. R. (1982). The effect of solutes on the gelatinization temperature-range of potatoe starch. *Starke*, 34, 7, 224-231.

Fan, J. (1994). Bubble growth and starch conversion in extruded and baked cereal systems. PhD Thesis, Food Science. University of Nottingham.

Fannon, J. E., Hauber, R. J. and BeMiller, J. N. (1992). Surface pores of starch granules. *Cereal Chemistry* 69, 3, 284-288.

Fannon, J. E., Shull, J. M. and BeMiller, J. N. (1993). Interior channels of starch granules. *Cereal Chemistry* 70, 5, 611-613.

Farhat, I. A. (1996). Molecular Mobility and Interactions in Biopolymer-Sugar-Water Systems. PhD Thesis, Food Science, University of Nottingham.

Farhat, I. A.; Mitchell, J. R.; Blanshard, J. M. V.; Derbyshire, W. (1996). A pulsed ^1H NMR study of the hydration properties of extruded maize-sucrose mixtures. *Carbohydrate Polymers*, 30, 219-227.

Fichtali, J. and Van de Voort, F. R. (1989). Fundamental and practical aspects of twin screw extrusion. *Cereal Foods World* 34, 11, 921-929.

French, D. (1984). Organisation of starch granule In: *Starch Chemistry and Technology*, R. L. B. Whistler, J. N.; Paschall, E. F. ed, Academic Press, Inc., Orlando, p 183-247.

Garber, B. W.; Hsieh, F.; Huff, H. E. (1997). Influence of particle size on the twin-screw extrusion of corn meal. *Cereal Chemistry*, 74, 656-661.

Godet, M. C.; Tran, V.; Delage, M. M.; Buleon, A. (1993). Molecular modelling of specific interactions involved in the amylose complexation by fatty acids. *International Journal of Biological Macromolecules*, 15, 11-16.

Grenat, C., Radosta, S., Anger, H. and Damaschun, G. (1993). Crystalline parts of three different conformations detected in native and enzymatically degraded starches. *Starch-Starke* 45, 9, 309-314.

Guy, R. C. E. and Horne, A. W. (1988). Extrusion and co-extrusion of cereals In: *Food Structure - Its creation and evaluation*, J. M. V. B. a. J. R. Mitchell ed, Butterworths, London, p 331-349.

Hahn, D. E.; Hood, L. F. (1987). Factors influencing corn starch-lipid complexing. *Cereal Chemistry*, 64, 81-85.

Harding, S. E. (1997). The intrinsic viscosity of biological macromolecules. Progress in measurement, interpretation and application to structure in dilute solution. Progress in Biophysics & Molecular Biology, 68, 207-262.

Harper, J. M. (1981). Extrusion of foods. CRC Press, Boca Raton (Florida), pp. 174.

Hauck, B. W. and Huber, G. R. (1989). Single screw vs. twin screw extrusion. Cereal Foods World 34, 11, 930-939.

Harris, R. K. (1983). Nuclear Magnetic Resonance Spectroscopy, A physicochemical View. Pitman Books, London.

Hartley L.P (1996), Hydration of biopolymers to low water content, PhD Thesis, University of Nottingham – UK

Heldman, D. R. and Hartel, R. W. (1997). Food Extrusion In: Principles of Food Processing, ed, Chapman & Hall, p 253-283.

Hill, S. E. (2000). Moisture and Biopolymer conversion in the extruder. In: Extrusion workshop, Moisture the critical variable. 11th and 12th April 2000, Nottingham University.

Ho, C.-T.; Izzo, M. T. (1992). Lipid-protein and lipid-carbohydrate interaction during extrusion. In Food extrusion science and technology; J. L. Kokini; C.-T. Ho and M. V. Karwe, Eds.; Marcel Dekker, Inc.: New York-Basel-Hong-Kong; pp 415-425.

Hoover, R. (1995). Starch retrogradation. Food Reviews International 11, 331-346.

Hoseney, R. C. (1994). Principle of cereal science, The American Association of Cereal Chemists.

Imberty, A.; Buleon A.; Tran V. and Perez, S. (1991). Recent advances in knowledge of starch structure. Starch-Starke 43, 10, 375-384.

Jovanovich, G.; Anon, M. C. (1999). Amylose-lipid complex dissociation. A study of the kinetic parameters. Biopolymers, 49, 81-89.

Karathanos, V. T. S., G.D. (1992). Water diffusivity in extrusion cooking of starch material. In Food extrusion science and technology; J. L. Kokini; C. T. Ho and M. V. Karwe, Eds.; Marcel Dekker: Hong Kong; pp 177-199.

Karel, M.; Buera, M. P.; Roos, Y. (1993). Effect of glass transitions on processing and storage. In The glassy state in foods; J. M. V. Blanshard and P. J. Lillford, Eds.; Nottingham University Press: Nottingham; p 13-34.

Karkalas, J.; Ma, S.; Morrison, W. R.; Pethrick, R. A. (1995). Some Factors Determining the Thermal-Properties of Amylose Inclusion Complexes With Fatty-Acids. Carbohydrate Research, 268, 233-247.

Kick, F. (1885). Das Gesetz der proportionalem widerstand und anwendung. Felix, Leipzig.

Krog, N.; Jensen, B. N. (1970). Interaction of monoglycerides in different physical state with amylose and their anti-firming effect in bread. Journal of Food Technology, 5, 77-82.

Kugimiya, M.; Donovan, J. W.; Wong, R. Y. (1980). Phase transitions of amylose-lipid complexes in starches: a calorimetric study. Starch-Starke, 32, 265-270.

Lai, L. S. and Kokini, J. L. (1991). Physicochemical changes and rheological properties of starch during extrusion (A review). Biotechnology Progress 7, 251-266.

Le Bail, P.; Bizot, H.; Ollivon, M.; Keller, G.; Bourgaux, C.; Buleon, A. (1999). Monitoring the crystallization of amylose-lipid complexes during maize starch melting by synchrotron x-ray diffraction. Biopolymers, 50, 99-110.

Lebail, P.; Buleon, A.; Shiftan, D.; Marchessault, R. H. (2000). Mobility of lipid in complexes of amylose-fatty acids by deuterium and C-13 solid state NMR. Carbohydrate Polymers, 43, 317-326.

Lelievre, J. (1974). Starch damage. *Starch-Starke*, 26, 85-88.

Levine, L. (1995). Of Paddle Mixers and Preconditioners. *Cereal Foods World* 40, 6, 452-453.

Levine, L., Bouvier, J. M., Brent, J. L. and Miller, R. C. (2002). An analysis of preconditioner residence time and residence time distribution. *Cereal Foods World* 47, 4, 142-148.

Lin, S.; Hsieh, F.; Huff, H. E. (1997). Effects of lipids and processing conditions on degree of starch gelatinization of extruded dry pet food [Full text delivery]. *Food Science and Technology-Lebensmittel-Wissenschaft & Technologie*, 30, 754-761.

Lowrison, G. C. (1974). *Crushing and Grinding, The size reduction of solid materials*. Butterworths, London.

Lowry, O. H.; Rosebrough, N. J.; Farr, A. L.; Randall, R. J. (1951). Protein measurement with the Folin phenol reagent. *Journal of Biological Chemistry*, 193, 265-275.

Mahungu, S. M.; Drozdek, K. A.; Artz, W. E.; Faller, J. F. (2000). Residence time distribution and barrel fill in pet food twin-screw extrusion. *Cereal Chemistry*, 77, 220-222.

Mathew, J. M., Hosney, R. C. and Faubion, J. M. (1999a). Effects of corn sample, mill type, and particle size on corn curl and pet food extrudates. *Cereal Chemistry* 76, 5, 621-624.

Mathew, J. M., Hosney, R. C. and Faubion, J. M. (1999b). Effect of corn moisture on the properties of pet food extrudates. *Cereal Chemistry* 76, 6, 953-956.

McNaughton, J. L.; Mortimer, C. T. (1975). Differential scanning calorimetry. In *Physical chemistry*; IRS, Ed. Butterworths: London.

Mercier, C., Charbonniere, R., Gallant, D. and Guilbot, A. (1979). Structural modification of various starches by extrusion cooking with a twin-screw french extruder In: Polysaccharides in Food, J. M. V. Blanshard and J. R. Mitchell ed, Butterworth, London, p 153-170.

Mercier, C.; Charbonniere, R.; Grebaut, J.; de la Gueriviere, J. F. (1980). Formation of Amylose-Lipid Complexes by Twin-Screw Extrusion Cooking of Manioc Starch. *Cereal Chemistry*, 57, 4-9.

Miller, R. C. (1985). Extrusion Cooking of Pet Foods. *Cereal Foods World* 30, 5, 323-324.

Miller, R. C. (1985). Low Moisture Extrusion - Effects of Cooking Moisture On Product Characteristics. *Journal of Food Science*, 50, 249-253.

Mitchell, J. R., Hill, S. E., Paterson, L., Valles, B., Barclay, F. and Blanshard, J. M. V. (1997). The role of molecular weight in the conversion of starch In: Starch - Structure and functionality, P. J. Farzier, A. M. Donald and P. Richmond ed, The Royal Society of Chemistry, Cambridge, p 68-76.

Mizuno, A.; Mitsuiki, M.; Motoki, M. (1998). Effect of crystallinity on the glass transition temperature of starch. *Journal of Agricultural and Food Chemistry*, 46, 98-103.

Mohamed, S. (1990). Factors Affecting Extrusion Characteristics of Expanded Starch-Based Products. *Journal of Food Processing and Preservation*, 14, 437-452.

Morrison, W. R. (1995). Starch Lipids and How They Relate to Starch Granule Structure and Functionality. *Cereal Foods World*, 40, 437-445.

Morrison, W. R.; Law, R. V.; Snape, C. E. (1993). Evidence for inclusion complexes of lipids with V-amylose in maize, rice and oat starches. *Journal of Cereal Science*, 18, 107-109.

Morrison, W. R.; Tan, S. L.; Hargin, K. D. (1980). Methods for the quantitative analysis of lipids in cereal grains and similar tissues. *Journal of the Science of Food and Agriculture*, 31, 329-340.

Ockerman, H. W. and Hansen, C. L. (1988). Pet or exotic animal food In: *Animal By-Product Processing*, H. W. Ockerman and C. L. Hansen ed, VCH, p 256-278.

P.F.M.A. (Pet food manufacturer association) web site, www.pfma.com

Padmanabhan, M. and Bhattacharya, M. (1989). Extrudate Expansion During Extrusion Cooking of Foods. *Cereal Foods World* 34, 11, 945-949.

Peleg, M. (1993). Glass transitions and physical stability of food powders. In *The glassy state in foods*; J. M. V. Blanshard and P. J. Lillford Eds; Nottingham University press: Nottingham; p 435-451.

Pomeranz, Y.; Meloan, C. E. (1994). *Food analysis: Theory and Practice*, Chapman & Hall; New York.

Rokey, G. J. (1994). Petfood and fishfood extrusion In: *The technology of extrusion cooking*, N. D. Frame Eds, Blackie academic & professional, London, p 144-189.

Roudaut, G.; van Dusschoten, D.; Van As, H.; Hemminga, M. A.; Le Meste, M. (1998). Mobility of lipids in low moisture bread as studied by NMR. *Journal of Cereal Science*, 28, 147-155.

Ruan, R. R.; Chen, P. L. (1998). *Water in foods and biological materials – A nuclear magnetic resonance approach*. Technomic; Lancaster – Basel.

Ryu, G. H., Neumann, P. E. and Walker, C. E. (1988). Effect of moisture content and particle size of rice flour on the physical properties of extrudates. *Korean Journal of Food Science and Technology* 20, 463-469.

Slade, L.; Levine, H. (1993). The glassy state phenomenon in food molecules. In *The glassy state in foods*; J. M. V. Blanshard and P. J. Lillford Eds; Nottingham University press: Nottingham; p 35-101.

Snape, C. E.; Morrison, W. R.; Maroto-Valer, M. M.; Karkalas, J.; Pethrick, R. A. (1998). Solid state C-13 NMR investigation of lipid ligands in V- amylose inclusion complexes. *Carbohydrate Polymers*, 36, 225-237.

Strahm, B. (1998). Fundamentals of polymer science as an applied extrusion tool. *Cereal Foods World* 43, 8, 621-625.

Takeo, K.; Tokumura, A.; Kuge, T. (1973). Complexes of starch and its related materials with organic compounds. *Starch-Starke*, 25, 357-362.

Tamaki, S., Hisamatsu, M., Teranishi, K., Adachi, T. and Yamada, T. (1998). Structural change of maize starch granules by ball-mill treatment. *Starch-Starke* 50, 8, 342-348.

Tang, H. R., Godward, J. and Hills, B. (2000). The distribution of water in native starch granules - a multinuclear NMR study. *Carbohydrate Polymers* 43, 375-387.

Tanner, J. E.; Stejskal, E. O. (1968). *Journal of Chemical Physics*, 49, 1768-1777.

Tester, R. F. and Morrison, W. R. (1993). Properties of damage starch granules. V. Composition and swelling of fractions of wheat starch in water at various temperatures. *Journal of Cereal Science* 20, 175-181.

Tester, R. F.; Debon, S. J. J. (2000). Annealing of starch - A review. *International Journal of Biological Macromolecules*, 27, 1-12.

Villwock, V. K.; Eliasson, A. C.; Silverio, J.; BeMiller, J. N. (1999). Starch-lipid interactions in common, waxy, ae du, and ae su2 maize starches examined by differential scanning calorimetry. *Cereal Chemistry*, 76, 292-298.

Von Rittinger, P. R. (1887). Lehrbuch der Aufbereitung Kunde. Ernst and Korn, Berlin.

Whalen, P. J.; Bason, M. L.; Booth, R. I.; Walker, C. E.; Williams, P. J. (1997). Measurement of extrusion effects by viscosity profile using the rapid ViscoAnalyser. Cereal Foods World, 42, 469-475.

Wrigley, C. W.; Booth, R. I.; Bason, M. L.; Walker, C. E. (1996). Rapid Visco Analyser: Progress from concept to adoption. Cereal Foods World, 41, 6-11.

Zobel, H. F. (1988). Molecules to granules: A comprehensive starch review. Starch-Starke 40, 2, 44-50.